ELUCIDATING THE FUNCTION AND DYNAMICS OF RESIDENT AND RECRUITED MACROPHAGE POPULATIONS IN THE LUNG

by
H.A. Daniel Lagassé

A dissertation submitted to Johns Hopkins University in conformity with the requirements for the degree of Doctor of Philosophy

Baltimore, Maryland
July 2014

ABSTRACT

Acute lung injury and chronic lung inflammation are major causes of morbidity and mortality in the US and worldwide. The cellular and molecular factors that function to limit the extent of acute and chronic inflammation in order to preserve the physiological roles of the lungs have not been fully defined. Here we use two sources of pulmonary inflammation – severe malaria infection resulting in acute lung injury and elastase-induced lung damage leading to chronic emphysema – to investigate the mechanisms that govern the nature and extent of lung injury. Employing the *P. berghei*-C57BL/6 mouse model, we demonstrate that sequestration of infected erythrocytes on post-capillary endothelial surfaces results in lung injury and the rapid recruitment of inflammatory monocytes from the circulation; which were instrumental in phagocytic clearance of adherent parasitized cells. However, in contrast, alveolar macrophages did not contribute to clearance of malaria-infected cells. Infection of $CCR2^{-/-}$ animals, which exhibited impaired monocyte recruitment and parasite clearance, resulted in elevated parasite burden and exacerbated lung injury. Results from $CD36^{-/-}$ and CD36 bone marrow chimeric mice demonstrated that parasite sequestration in the absence of CD36-mediated phagocytic clearance by monocytes results in exaggerated lung pathology. Hence, the data suggest a model in which the level of malaria-induced lung pathology is proportional to steady-state levels of parasite adherence and monocyte-driven phagocytic clearance. Employing the elastase mouse model of emphysema, we demonstrated that, unlike the malaria system, lung-resident alveolar macrophages, not recruited monocytes, play a dominant role in the inflammatory response. Upon elastase-induced lung damage, alveolar macrophages proliferated and dynamically changed their morphology, surface phenotype, gene expression profile and adopted a mixed M1/M2 activation phenotype. These results suggest upon initial tissue damage, resident alveolar macrophages could contribute significantly to the regulation of progressive emphysematous lung injury. These two studies have clarified our understanding of the dynamic properties and functional roles that resident alveolar macrophages and recruited monocyte-derived macrophages adopt to regulate the degree of acute and chronic pulmonary inflammation. Thus, these studies may contribute toward the development of future therapeutic approaches protecting from severe inflammatory lung diseases.

THESIS READERS

Advisor:

Dr. Alan L. Scott — Professor

Department of Molecular Microbiology and Immunology

Johns Hopkins Bloomberg School of Public Health

Thesis Committee:

Dr. Noel R. Rose — Professor

Department of Molecular Microbiology and Immunology

Johns Hopkins Bloomberg School of Public Health

Dr. Wayne A. Mitzner — Professor

Department of Environmental Health Science

Johns Hopkins Bloomberg School of Public Health

Dr. David J. Sullivan — Associate Professor

Department of Molecular Microbiology and Immunology

Johns Hopkins Bloomberg School of Public Health

Dr. Nicola M. Heller — Assistant Professor

Department of Anesthesia and Critical Care Medicine

Johns Hopkins School of Medicine

Alternate:

Dr. Michael J. Matunis — Professor

Department of Biochemistry and Molecular Biology

Johns Hopkins Bloomberg School of Public Health

ACKNOWLEDGEMENTS

Just as tissue macrophage function should not be considered in isolation, but as the end product of a myriad of factors within the local microenvironment, the process of pursing (and completing) a doctoral degree demands the contributions of many supportive and influential inter-personal relationships. Luckily, I am blessed in that arena, as many people have supported me throughout my time at Johns Hopkins. So, in order to more fully understand my perspective in the coming pages, one must appreciate the context in which it took place…

I'd like to thank Dr. Alan Scott for all of his guidance, advice and support. I couldn't have asked for a better mentor. I really appreciate his dedication to mentorship, scholarship and teaching. I have learned a great deal from him and am quite thankful for his enthusiasm and even temperament. It's an added benefit that Dr. Scott and I share many interests outside of the lab, especially because you can't talk shop all the time!

I'd like to thank Dr. Matt Craig and Dr. Ifeanyi Anidi, two men with which I have spent countless hours with in the lab. We definitely surpassed the lab mate status; we were friends that happened to work together. While we certainly tossed around many scientific ideas, helped each other with numerous experiments, and learned from one another, we still managed to find time to discuss all things sports and music. The collegial atmosphere found within the Scott Lab cannot be recreated and has been the envy of many… I'd also like to thank Dr. Mark Siracusa and Dr. Kiwon Park, former graduate students within the Scott Lab, for their hands-on training and scientific insights during my earlier days within the lab.

I'd like to thank all my thesis readers and committee members including Dr. Noel Rose, Dr. Wayne Mitzner, Dr. David Sullivan, Dr. Nicola Heller and Dr. Michael Matunis for their willingness to help, read this document, and for all of their guidance. In addition, I'd like to thank the members of my graduate board orals and comprehensive exam committees including Dr. Val Culotta, Dr. Anna Durbin, Dr. Jay Bream, Dr. Nirbhay Kumar, and Dr. Richard Markham for their time and consideration. Additionally, I'd

like to thank Dr. Richard Markham and Dr. Diane Griffin for allowing me to rotate through their laboratories during my first year, providing me with interesting projects, and their patience, as I was just learning to navigate graduate school. I'd also like to thank all of the Department of Molecular Microbiology and Immunology staff for all of their support over the years, especially Gail O'Connor, Thom Hitzelberger, Debbie Bradley, Nancy Lanse, Konstantin Milman, and Leonid Shats.

Everyone in the 4th floor East Wing labs deserves many thanks! Anne Jedlicka and Amanda Dziedzic in the Gene Array and Sequencing Core; Kate, Cathy, and Leah in the Scott Lab; Daniel and Christine in the Sinnis Lab; Teegan, Krista, and Alfredo in the Prigge Lab; Andrea, Diego, and Eva in the Zavala Lab. All of you have made our little corner of the building a great place to work because of your smiling faces and amazing attitudes.

A big thank you to my friends Kirk, Tiff, Nick, Tara, Eileen, and everyone at Baltibrew for lots of fun times!

Family support has been paramount during my time in graduate school. Everyone on the Lagasse/Suarez side of the family: Cristina, Alden, Cooper, Meme, Pepe, Nena, Luis, and Abuelito; as well as everyone on the Prokop side: Bob, Diane, and Anna have all been instrumental and have supported me tremendously. Of course my parents, Philip and Maria, have been supporting me long before graduate school…and like they have done for everything in my life, they have backed me completely and been my biggest cheering squad! I am eternally grateful for all that they have sacrificed for me.

I'd like to thank my daughter, Alexandra for always bringing a smile to my face and constantly reminding me of the wonder of life!

Of course none of this would have been possible without my lovely wife, Lisa. She has been my motivator, a commiserator, a cheerleader, and most of all, a partner throughout this process. We've certainly had quite a ride… and there is no one I'd rather share it with than you. Thank you! 143!

TABLE OF CONTENTS

ABSTRACT ..... **ii**

ACKNOWLEDGEMENTS ..... **iv**

TABLE OF CONTENTS ..... **vi**

LIST OF FIGURES ..... **xii**

LIST OF TABLES ..... **xvi**

CHAPTER 1: GENERAL INTRODUCTION **1**

1.1 PREFACE 2

1.2 LUNG MACROPHAGES 2

1.2.1 Historical Perspective *3*

1.2.2 Mononuclear phagocyte system (MPS) *4*

1.2.3 Tissue macrophages *4*

1.2.4 General lung function *7*

1.2.5 Lung as regulatory mucosal surface *7*

1.2.6 Lung organization *8*

1.2.7 Alveolar organization *10*

1.2.8 Alveolar leukocytes *10*

1.2.9 General properties of lung macrophages *10*

1.2.10 Phenotypic characteristics of LMs *11*

1.2.11 LM as sentinels *13*

1.2.12 LM Phagocytosis *14*

1.2.13 LM Opsonic phagocytosis *14*

1.2.14 LM non-opsonic phagocytosis *15*

1.2.15 LM Efferocytosis *16*

1.2.16 LM microbial killing *17*

1.2.17 LM antigen presentation *18*

1.2.18 LM Activation *19*

1.2.19 LM metabolism *21*

1.2.20 Pulmonary environment and immunomodulation *22*

1.2.21 Soluble factor-dependent immunomodulation *23*

1.2.22 Contact-dependent interactions *25*

1.2.23 LM-mediated suppression *26*

1.2.24 Dynamics of mononuclear phagocytes *26*

1.2.25 Migration to draining lymph nodes *27*

1.2.26 Blood monocyte recruitment *27*

1.2.27 A challenge to the MPS paradigm *28*

1.2.28 Tissue macrophage niches are seeded embryonically. *29*

1.2.29 Lung macrophage origins *30*

1.2.30 Implications of embryonic tissue mac seeding *31*

1.2.31 Tissue macrophages self-maintain *31*

1.2.32 Macrophage proliferation in general *33*

1.2.33 Lung macrophage proliferation *33*

1.2.34 Summary *34*

1.3 MALARIA 34

1.3.1 Public health significance *34*

1.3.2 Plasmodium life cycle *35*

1.3.3 Severe malaria and pulmonary pathology *36*

1.3.4 Parasite sequestration *38*

1.3.5 Innate immune responses to malaria *40*

1.3.6 Outstanding questions *41*

1.3.7 Hypothesis *42*

1.3.8 Approach *42*

1.4 EMPHYSEMA 44

1.4.1 Public health significance....44
1.4.2 COPD definitions....45
1.4.3 Clinical features of COPD....45
1.4.4 Risk factors....47
1.4.5 Pathogenesis/pathophysiology....48
1.4.6 Innate immune responses: role of neutrophils....49
1.4.7 Innate immune responses: role of macrophages/monocytes....49
1.4.8 Adaptive immune responses: role of DCs and T cells....51
1.4.9 Imbalances contributing to emphysema....52
1.4.10 Outstanding questions....54
1.4.11 Hypothesis....56
1.4.12 Approach....56
1.5 THESIS AIMS....59
1.5.1 SPECIFIC AIMS MALARIA:....60
1.5.2 SPECIFIC AIMS EMPHYSEMA:....60

CHAPTER 2: RECRUITED MONOCYTES ARE RESPONSIBLE FOR LIMITING MALARIA-INDUCED LUNG INJURY THROUGH CD36-MEDIATED CLEARANCE OF SEQUESTERED INFECTED ERYTHROCYTES....62
2.1 ABSTRACT....63
2.2 INTRODUCTION....64
2.3 MATERIALS AND METHODS....66
2.3.1 Mice....66
2.3.2 Parasites and infection....67
2.3.3 Antibodies....67
2.3.4 Flow cytometry....67
2.3.5 Bronchoalveolar lavage (BAL)....68
2.3.6 Histology....69

2.3.7 Evans Blue extravasation....69

2.3.8 Hemozoin quantification....70

2.3.9 Adoptive transfer of monocytes....70

2.3.10 Pulmonary Edema....71

2.3.11 Nucleic acid isolation and gene expression analysis....71

2.3.12 Statistical analysis....72

2.4 RESULTS....72

2.4.1 Plasmodium berghei infection results in acute lung injury (ALI)....72

2.4.2 Dynamics of lung-resident macrophages and recruited inflammatory monocytes....74

2.4.3 Recruited monocytes are responsible for parasite clearance in the lungs....79

2.4.4 Activation status of AM and MDM following P. berghei infection....79

2.4.5 CCR2-deficiency impairs monocyte recruitment and parasite clearance from the lungs....86

2.4.6 CCR2-deficiency results in increased parasite burden, elevated pro-inflammatory cytokine expression and exacerbated lung damage.....88

2.4.7 Adoptive transfer of monocytes into CCR2$^{-/-}$ lungs is protective.....88

2.4.8 CD36 is necessary for efficient clearance of sequestered infected erythrocytes by recruited monocytes....92

2.5 DISCUSSION....96

2.6 ACKNOWLEDGMENTS....100

CHAPTER 3: DYNAMIC CHANGES TO CELLULAR MORPHOLOGY, SURFACE PHENOTYPE AND ACTIVATION STATE ACCOMPANY ALVEOLAR MACROPHAGE PROLIFERATION FOLLOWING ELASTASE-INDUCED LUNG DAMAGE....102

3.1 ABSTRACT....103

3.2 INTRODUCTION....104

3.3 MATERIAL AND METHODS....106

3.3.1 Mice....106

3.3.2 Elastase challenge....107

3.3.3 Antibodies *107*

3.3.4 Flow cytometry *107*

3.3.5 Bronchoalveolar lavage (BAL) *108*

3.3.6 In vivo labeling of resident lung macrophages *108*

3.3.7 Lung macrophage depletion *109*

3.3.8 Neutrophil depletion *109*

3.3.9 Bead selection of lung macrophages *109*

3.3.10 Nucleic acid isolation and gene expression analysis *110*

3.3.11 Histology *110*

3.3.12 Immunofluorescence microscopy *111*

3.3.13 Statistical analysis *111*

3.4 RESULTS 111

3.4.1 Preliminary data in the PPE model *112*

3.4.2 Dynamics of myeloid cells in the lungs following PPE challenge *112*

3.4.3 Examining the role of inflammatory monocytes on the progression of elastase-induced emphysema *119*

3.4.4 In vivo lung-resident macrophage staining and cell fate tracking following elastase challenge *123*

3.4.5 Dynamics of elastase-induced lung-resident macrophage phenotypic changes *130*

3.4.6 Lung-resident macrophage dynamics following elastase-challenge to the lung *133*

3.4.7 Gene expression dynamics in CD11c^{+} cells following elastase-challenge to the lung. *140*

3.4.8 Effect of lung macrophage depletion on the progression of elastase-induced emphysema *144*

3.4.9 Effect of neutrophil macrophage depletion on dynamics of lung-resident macrophage population *146*

3.5 DISCUSSION 151

3.6 ACKNOWLEDGMENTS 162

CHAPTER 4: GENERAL DISCUSSION 164

4.1 MACROPHAGE BIOLOGY: LOOKING AHEAD 165
4.2 MACROPHAGES IN MALARIA 166
4.3 MACROPHAGES IN EMPHYSEMA 172
4.4 FINAL THOUGHTS 175

APPENDIX I: CHAPTER 2 SUPPLEMENTAL MATERIAL 178

AI.1 MATERIALS AND METHODS 179
AI.1.1 Mice 179
AI.1.2 Parasites and infection 179
AI.1.3 Bone marrow chimeras 179
AI.1.4 Antibodies 180
AI.1.5 Bronchoalveolar lavage (BAL) 180
AI.1.6 Histology 181
AI.1.7 Lung injury scores 181
AI.1.8 Statistical analysis 181
AI.2 RESULTS 182
AI.2.1 CD36 and malaria-induced ALI 182

REFERENCES 186

CURRICULUM VITAE 230

LIST OF FIGURES

FIGURE 1.1 MONONUCLEAR PHAGOCYTE SYSTEM (MPS) AND DISTRIBUTION OF TISSUE MACROPHAGE SUBSETS 5

FIGURE 1.2 RESPIRATORY TREE ORGANIZATION AND ALVEOLAR STRUCTURE 9

FIGURE 1.3 CHALLENGE TO THE MPS: TISSUE MACROPHAGE ORIGINS AND MAINTENANCE 32

FIGURE 1.4 *PLASMODIUM* LIFE CYCLE 37

FIGURE 1.5 INTRODUCTION TO THE *PLASMODIUM BERGHEI* MOUSE MODEL OF SEVERE MALARIA 43

FIGURE 1.6 MAJOR PHASES AND CELLULAR PLAYERS IN PATHOGENESIS OF EMPHYSEMA 46

FIGURE 1.7 INTRODUCTION TO THE PORCINE PANCREATIC ELASTASE (PPE) MURINE MODEL OF EMPHYSEMA 57

FIGURE 2.1 PARASITE BURDEN IN THE LUNGS OF *PLASMODIUM BERGHEI*-INFECTED MICE. 73

FIGURE 2.2 PLASMODIUM BERGHEI INFECTION LEADS TO ACUTE LUNG INJURY 75

FIGURE 2.3 CELLULAR DYNAMICS IN THE AIRWAYS DURING *P. BERGHEI* INFECTION 76

FIGURE 2.4 DYNAMICS OF CYTOKINE EXPRESSION IN THE LUNGS OF C57BL/6 MICE DURING THE COURSE OF *P. BERGHEI* INFECTION 77

FIGURE 2.5 DYNAMICS OF MONONUCLEAR CELLS IN THE LUNGS DURING *P. BERGHEI* INFECTION 78

FIGURE 2.6 DYNAMICS OF PARASITE PHAGOCYTOSIS IN THE LUNGS DURING *P. BERGHEI* INFECTION 80

FIGURE 2.7 VISUALIZATION OF *P. BERGHEI* PHAGOCYTOSIS 81

FIGURE 2.8 ACTIVATION OF ALVEOLAR MACROPHAGES (AM) AND MONOCYTE-DERIVED MACROPHAGE (MDM) POPULATIONS FOLLOWING MALARIA INFECTION 83

FIGURE 2.9 RELATIONSHIP BETWEEN PARASITE UPTAKE AND ACTIVATION STATE FOLLOWING MALARIA INFECTION 84

FIGURE 2.10 CCR2-DEFICIENCY RESULTS IN ALTERED CELL TRAFFICKING AND PARASITE UPTAKE 85

FIGURE 2.11 ACTIVATION OF CCR2-DEFICIENT ALVEOLAR MACROPHAGES (AM) AND MONOCYTE-DERIVED MACROPHAGE (MDM) POPULATIONS FOLLOWING MALARIA INFECTION 87

FIGURE 2.12 CCR2-DEFICIENCY RESULTS IN INCREASED PARASITE BURDEN 89

FIGURE 2.13 CCR2-DEFICIENCY RESULTS IN ELEVATED PRO-INFLAMMATORY CYTOKINE EXPRESSION 90

FIGURE 2.14 CCR2-DEFICIENCY RESULTS IN EXACERBATION OF LUNG INJURY 91

FIGURE 2.15 ADOPTIVE TRANSFER OF $CCR2^{+}$ MONOCYTES REDUCES LUNG INJURY IN INFECTED CCR2-DEFICIENT MICE 93

FIGURE 2.16 DYNAMICS OF MONONUCLEAR CELLS AND PARASITE CLEARANCE IN THE LUNGS OF $CD36^{-/-}$ MICE.....94

FIGURE 2.17 ACTIVATION OF CD36-DEFICIENT ALVEOLAR MACROPHAGES (AM) AND MONOCYTE-DERIVED MACROPHAGE (MDM) POPULATIONS FOLLOWING MALARIA INFECTION.....95

FIGURE 3.1 IDENTIFICATION OF MYELOID CELL POPULATIONS IN THE LUNGS 113

FIGURE 3.2 DYNAMICS OF MYELOID CELLS IN THE LUNGS FOLLOWING PPE CHALLENGE.....116

FIGURE 3.3 DYNAMICS OF MYELOID CELL POPULATIONS IN THE LUNGS FOLLOWING PPE CHALLENGE.....117

FIGURE 3.4 DYNAMICS OF LUNG $CD11c^{+}SiglecF^{+}$ POPULATION'S SURFACE PHENOTYPE FOLLOWING PPE CHALLENGE 118

FIGURE 3.5 CCR2 SURFACE EXPRESSION ON $CD11b^{+}Ly6C^{+}$ CELLS IN THE LUNGS FOLLOWING PPE CHALLENGE 120

FIGURE 3.6 EFFECT OF CCR2-DEFICIENCY ON MONOCYTE AND LUNG MACROPHAGE DYNAMICS FOLLOWING PPE CHALLENGE.....121

FIGURE 3.7 EFFECT OF CCR2-DEFICIENCY ON $CD11c^{+}SiglecF^{+}$ PHENOTYPIC CHANGES FOLLOWING PPE CHALLENGE 122

FIGURE 3.8 EFFECT OF CCR2-DEFICIENCY ON THE PROGRESSION OF EMPHYSEMA FOLLOWING PPE CHALLENGE 124

FIGURE 3.9 *IN VIVO* LABELING OF LUNG-RESIDENT PHAGOCYTIC CELLS WITH PKH26-PCL 125

FIGURE 3.10 VISUALIZATION OF *IN VIVO* LUNG-RESIDENT PHAGOCYTIC CELL PKH26-PCL STAINING SPECIFICITY 127

FIGURE 3.11 DYNAMICS OF LUNG-RESIDENT $PKH26\text{-}PCL^{+}CD11c^{+}$ CELLS GRANULARITY AND SURFACE PHENOTYPE FOLLOWING PPE CHALLENGE 128

FIGURE 3.12 VISUAL EVIDENCE FOR LUNG-RESIDENT MACROPHAGE MORPHOLOGICAL CHANGES FOLLOWING ELASTASE CHALLENGE....129

FIGURE 3.13 DYNAMICS OF PKH26-PCL^{+}CD11C^{+} POPULATION'S SURFACE CD11B LEVELS FOLLOWING PPE CHALLENGE....131

FIGURE 3.14 DYNAMICS OF PKH26-PCL^{+}CD11C^{+} POPULATION'S SURFACE CD200R LEVELS FOLLOWING PPE CHALLENGE....132

FIGURE 3.15 DYNAMICS OF CD11C^{+}SIGLECF^{+} POPULATION'S SURFACE ST2 LEVELS FOLLOWING PPE CHALLENGE....134

FIGURE 3.16 EXPERIMENTAL DESIGN FOR MONITORING PKH26-PCL^{+}CD11C^{+} LRM POPULATION FOLLOWING PPE CHALLENGE....135

FIGURE 3.17 DYNAMICS OF LUNG-RESIDENT PKH26-PCL^{+}CD11C^{+} POPULATION NUMBERS FOLLOWING PPE CHALLENGE....136

FIGURE 3.18 DYNAMICS OF KI-67 POSITIVITY IN PKH26-PCL^{+} AND PKH26-PCL^{-} POPULATIONS FOLLOWING PPE CHALLENGE....137

FIGURE 3.19 DYNAMICS OF PKH26-PCL FLUORESCENCE INTENSITY ON A PER CELL BASIS FOLLOWING PPE CHALLENGE....139

FIGURE 3.20 DYNAMICS OF MACROPHAGE ACTIVATION (INNATE /M1) GENE EXPRESSION IN CD11C^{+} CELLS FOLLOWING PPE CHALLENGE....141

FIGURE 3.21 DYNAMICS OF MACROPHAGE ACTIVATION (M1/MMP) GENE EXPRESSION IN CD11C^{+} CELLS FOLLOWING PPE CHALLENGE....142

FIGURE 3.22 DYNAMICS OF MACROPHAGE ACTIVATION (M2A/M2C) GENE EXPRESSION IN CD11C^{+} CELLS FOLLOWING PPE CHALLENGE....143

FIGURE 3.23 EFFECT OF LUNG MACROPHAGE DEPLETION ON THE PROGRESSION OF EMPHYSEMA FOLLOWING PPE CHALLENGE....145

FIGURE 3.24 EFFICACY OF LUNG MACROPHAGE DEPLETION FOLLOWING PPE CHALLENGE....147

FIGURE 3.25 EFFECT OF LUNG NEUTROPHIL DEPLETION ON LUNG-RESIDENT PKH26-PCL^{+} POPULATION'S SURFACE PHENOTYPE FOLLOWING PPE CHALLENGE....148

FIGURE 3.26 EFFECT OF NEUTROPHIL DEPLETION ON LUNG-RESIDENT PKH26-PCL^{+} POPULATION NUMBERS FOLLOWING PPE CHALLENGE.....150

FIGURE 4.1 CURRENT WORKING MODEL: MALARIA.....167

FIGURE 4.2 CURRENT WORKING MODEL: MALARIA.....169

FIGURE 4.3 CURRENT WORKING MODEL: MALARIA.....170

FIGURE 4.4 CURRENT WORKING MODEL: EMPHYSEMA.....173

LIST OF TABLES

TABLE 1.1 LOCATION AND FUNCTION OF TISSUE MACROPHAGE SUBSETS....6

TABLE 1.2 PHENOTYPIC CHARACTERISTICS OF MURINE LUNG MACROPHAGES AT STEADY STATE....12

TABLE 1.3 ACTIVATION STATES OF MACROPHAGES....20

TABLE 1.4 OFFICIAL WHO CLINICAL MANIFESTATIONS/FEATURES OF SEVERE *P. FALCIPARUM* MALARIA INFECTIONS....36

TABLE 1.5 MACROPHAGE EFFECTOR MOLECULES INVOLVED IN THE PATHOPHYSIOLOGY OF EMPHYSEMA 50

TABLE 1.6 IMBALANCES CONTRIBUTING TO PATHOGENESIS OF EMPHYSEMA....54

TABLE 1.7 MEASURES USED TO ASSESS EMPHYSEMA PROGRESSION IN PPE MODEL....58

TABLE 3.1 MYELOID CELLS SUBSETS IN THE MURINE LUNG....114

CHAPTER 1

GENERAL INTRODUCTION

1.1 PREFACE

Inflammation within the pulmonary environment requires highly regulated control processes, as the central function of the lungs, gas exchange, must be preserved. Failure to properly control pulmonary inflammation can lead to loss of lung function and death. Lung macrophages are innate immune cells that are perfectly situated to respond to inflammatory insults originating from either the respiratory or circulatory systems. These highly phagocytic cells function to rid the lung environment of possibly harmful non-self substances such as bacteria, viruses, parasites, fungi and particulate matter. In addition to their role in clearing unwanted material from the parenchyma and airspaces, lung macrophages also play a role in maintaining lung homeostasis and in tissue repair processes via the secretion of a variety of effector cytokines.

The over-arching goal of my thesis research is to elucidate the underlying mechanisms that control the dynamics and function of lung resident macrophage and recruited monocyte/macrophage populations following pulmonary insults. The majority of this study will focus on two sources of pulmonary inflammation: *Plasmodium* infection and intra-tracheal liquid elastase challenge. While both insults result in lung inflammation, the nature of these insults differs, as the *Plasmodium* infection results in a crescendo of parasite burden and lung injury originating from a pathogenic source (antigen driven process), while the liquid elastase challenge model of emphysema results in a non-infectious point insult (protease activity) resulting in sterile inflammation and progressive alveolar wall destruction. The goal of this work is to elucidate similarities as well as differences in the cellular players and their role in regulating the pathogenesis of these inflammatory states of the lung.

1.2 LUNG MACROPHAGES

1.2.1 Historical Perspective

Macrophages were first described by the Russian comparative zoologist Ilya Mechnikov (Elie Metchnikoff) in the late 19th century during his studies of splinter-pricked *Bipinnaria* starfish larvae and *Daphniae* water fleas that had ingested needle-like spores [1]. Mechnikov noticed masses of motile cells with moving extensions surrounding, devouring, and destroying foreign insults. He termed these cells *macrophages* due to their distinctive role as "big-eaters" stemming from the Greek roots *makros* or "large" and *phagein* or "eat" [2]. Through his studies of macrophages and phagocytosis, Mechnikov developed his phagocyte theory of immunity, in which he posited that phagocytes were the main defense mechanism against all infectious agents. In his 1908 Nobel Prize lecture, Ilya Mechnikov stated that to understand immunity, first one must understand the nature of phagocytosis [1].

> *Whenever the organism enjoys immunity, the introduction of infectious microbes is followed by the accumulation of mobile cells, of white corpuscles of the blood in particular which absorb the microbes and destroy them. The white corpuscles and the other cells capable of doing this have been designated "phagocytes" i.e. devouring cells, and the whole function that ensures immunity has been given the name of "phagocytosis".*
> *It has been established as a general rule that in all cases of immunity, natural or acquired, either by preventative vaccination or following an attack of infectious illness, phagocytosis takes place to a marked degree, whereas in fatal or very dangerous diseases, this phenomenon does not exist at all or is attenuated.[1]*

Mechnikov envisioned the role of phagocytes as the first line of defense and the key to effective immune responses. While macrophages and other phagocytes are certainly important players in the innate immune response, as well as shaping the adaptive immune response, we now know that Mechnikov's phagocyte theory was important in promoting the role of innate immunity. Unknowingly Mechnikov was one of the grandfathers of the innate immunity. Mechnikov, a cellularist, shared the 1908 Nobel Prize in Physiology or Medicine with Paul Ehrlich, a humoralist, who, through his Side Chain Theory, laid the foundation for understanding humoral immunity; what we know now consider an important facet of adaptive immunity. At the time, their views were considered in opposition and mutually exclusive, however, we now know that both were describing different aspects of the immune response. In fact, Mechnikov's and Ehrlich's competing theories of immunity nicely complemented one another. Remarkably, many of the insights that Mechnikov and Ehrlich made over a century ago still stand as pillars of modern immunology.

1.2.2 Mononuclear phagocyte system (MPS)

Macrophages are just one subset of cells belonging to a vast family of myeloid cells collectively known as the mononuclear phagocyte system (MPS) [3]. The MPS has been considered the central doctrine of the myeloid cell compartment since its conception in the late 1960s by Ralph van Furth and Zanvil Cohn [4]. The MPS is a conceptual framework that encompasses a direct lineage of cells originating from stem cells in the bone marrow to mature circulating erythrocytes, platelets, granulocytes, and peripheral mononuclear phagocytes (Figure 1.1A) [5, 6]. Within the bone marrow, hematopoietic stem cells (HSCs) give rise to common myeloid progenitors (CMPs) as well as common lymphoid progenitors (CLPs). Multipotent CMPs are antecedents to a large number of distinct cell types including platelets, erythrocytes, mast cells, and granulocytes (neutrophils, basophils, eosinophils), as well as macrophage/dendritic cell precursor (MDP) cells. In the bone marrow, MDPs give rise to peripheral mononuclear phagocytes: monocytes and pre-dendritic cells [6]. Traditionally, monocytes have been considered to be the origin of tissue dendritic cell and macrophage populations; however, recent findings suggest that the origins of some tissue macrophage populations may fall outside the purview of the linear MPS conceptual framework [these issues will be discussed in more detail later]. While phagocytic capacity is a common trait connecting monocyte, DC, and tissue macrophage populations, the overall function of these cell types can vary greatly. Even between macrophages of different tissue origin, there is considerable heterogeneity in the function, origin, and nature of these related cell populations.

1.2.3 Tissue macrophages

Generally, macrophages are described as large and granular cells with many pseudopodia, or “false feet” used to engulf material. However, macrophages are quite dynamic and can alter their function and morphology quite dramatically depending upon their local environment and activation state [7]. As a whole, tissue macrophages are long-lived cells that function at the confluence of innate and adaptive immune responses and play major roles in phagocytosis, immune surveillance, wound repair, tissue homeostasis, and metabolism [8, 9]. Tissue macrophages are distributed in a variety of organ systems throughout the mammalian body (Figure 1.1B) and are as functionally distinct as their anatomical location [10]. While all related, the functional heterogeneity between tissue macrophage subsets is astounding:

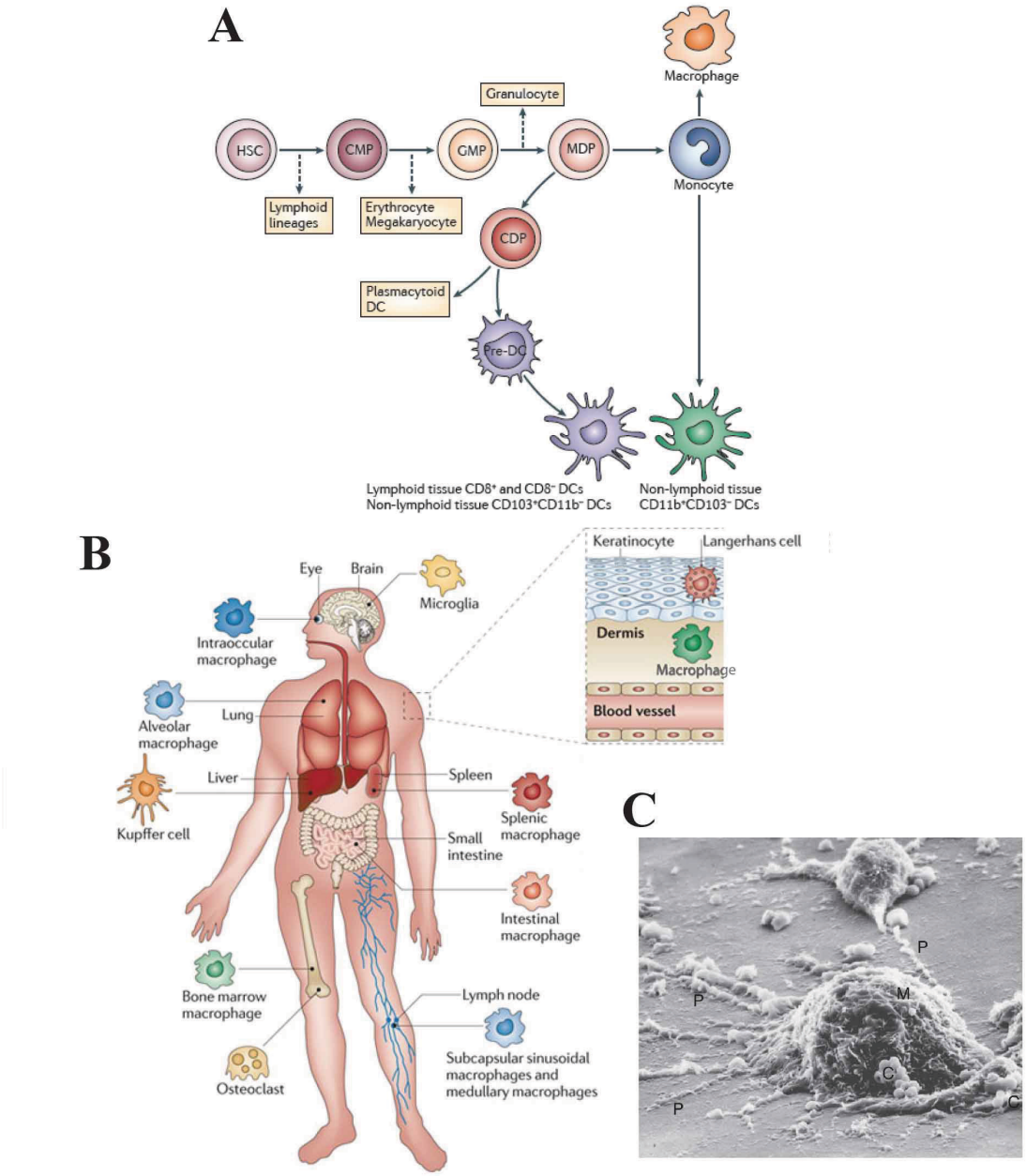

Figure 1.1 Mononuclear phagocyte system (MPS) and distribution of tissue macrophage subsets. (A) Cartoon depicting the MPS conceptual framework. Reprinted by permission from Macmillan Publishers Ltd: Nature Reviews Immunology. Chow A, Brown BD, Merad M: **Studying the mononuclear phagocyte system in the molecular age**. Nature Reviews Immunology 2011, 11(11):788-798., copyright 2011. (B) Cartoon depicting the heterogeneity and distribution of tissue macrophages. Reprinted by permission from Macmillan Publishers Ltd: Nature Reviews Immunology. Murray PJ, Wynn TA: **Protective and pathogenic functions of macrophage subsets**. Nature Reviews Immunology 2011, 11(11):723-737., copyright 2011. (C) Scanning electron micrograph (SEM) image of macrophage [M] with pseudopodia [P] engulfing cocci [C]. Reproduced with permission from Swartz R, Holmes C: **Macrophages**. New England Journal of Medicine 1995, 333(23):1546-1546., Copyright Massachusetts Medical Society.

Kupffer cells in the liver, microglia in the central nervous system (CNS), osteoclasts in the bones, Langerhans cells in the dermis, and alveolar macrophages in the lungs; all possess unique qualities suited for immune surveillance and maintenance of homeostasis within specialized compartments. The microenvironment largely dictates the function of a particular tissue macrophage subset. Recently, gene expression profiling studies have demonstrated that tissue macrophage subsets maintain a 'core' signature, but can also be distinguished based on their specialized tissue-specific phenotype [11]. Many tissue macrophage subsets have been well characterized; Table 1.1 provides a brief overview of some of the most prominent tissue macrophage subsets including some of their key features.

Table 1.1 Location and function of tissue macrophage subsets

Tissue Macrophage Subset	Anatomical Location	Major Function
Alveolar macrophages	Lungs	Phagocytose inhaled particles (dust; allergens) and microorganisms; immune surveillance; maintain lung homeostasis; regulate DC activation [12-16]
Kupffer cells	Liver	Immune surveillance; iron homeostasis; clearance of damaged or senescent erythrocytes, cellular debris and microorganisms from the blood [17]
Langerhans cells	Skin	Present antigen to T cells in draining lymph node [18]
Microglia	Central nervous system	CNS immune surveillance; promote neuronal survival [19]
Osteoclasts	Bone	Resorb bone and support erythropoiesis [20, 21]
Red pulp macrophages	Spleen	Immune surveillance; clearance of damaged or senescent erythrocytes and iron homeostasis [22]
Marginal zone macrophages	Spleen	Trapping of blood-borne particulate antigen; clearance of apoptotic cells; minimize autoimmune responses [23, 24]
Subcapsular sinus ($CD169^+$) macrophages	Lymph nodes	Immune surveillance; prevent systemic dissemination from lymphatics to bloodstream; present antigen to B cells [25]

In order to more fully understand the function and role of tissue macrophages, one must appreciate the anatomical context in which they reside.

1.2.4 General lung function

Maintaining lung homeostasis and function is paramount to an individual's survival during inflammatory insults, whether systemic, localized to distal tissues, but especially when concentrated within the lungs. The consequences of impaired lung function are numerous and devastating as the lung serves as the site of gas exchange for the bloodstream. Gas exchange is accomplished through the act of respiration where deoxygenated venous blood is pumped into the lungs from the heart via the pulmonary artery. Within the airways, carbon dioxide is exchanged across the respiratory epithelial surface for atmospheric oxygen brought into the lungs upon inspiration. The newly oxygenated erythrocytes return to the heart via the pulmonary veins and are pumped out into the systemic circulation. The lung environment is certainly unique as it serves as a scaffold for the delicate interface between the largest vascular bed of the closed circulatory system and the respiratory tract, a vast mucosal surface that is in constant contact with the external environment.

1.2.5 Lung as regulatory mucosal surface

Mucosal surfaces act as a physical barrier to protect the body from the environment. The lungs of an average adult male have a surface area of approximately 100 m^2 and come in contact with approximately 11,000 liters of air a day [26]. In comparison to other mucosal surfaces, the surface area of the lungs is much greater than the skin (2 m^2) and rivals that of the gastrointestinal tract (300 m^2) [27, 28]. Upon each inspiration, the airways are assaulted with a myriad of foreign substances, largely innocuous, but generally comprised of highly immunogenic antigens, and potentially including pathogenic bacteria, viruses, parasites and fungi, as well as harmful particulate matter, noxious chemicals, and allergens. These potentially dangerous substances are only a few micrometers away from entering the systemic circulation via capillaries that surround the airways, so the body must respond appropriately to harmful insults, while limiting damage inflicted upon the lungs. Therefore, in order to maintain lung function, even in the face of

an inflammatory insult, many regulatory immune mechanisms must be in place to prevent the elicitation of robust inflammatory responses against the numerous foreign and highly immunogenic antigens that are continuously introduced to the system. Through highly-regulated immune mechanisms the body avoids immune activation in response to all foreign substances entering the airways, as doing so would certainly lead to chronic inflammation and impair normal lung function. In order to appreciate how lung homeostasis is maintained through immune regulation, it is necessary to understand the anatomy (structure/organization) and physiology (function) of the lung tissue.

1.2.6 Lung organization

The lungs can be divided into two main functional areas, the conducting zone and the respiratory zone. Upon inspiration, the diaphragm contracts leading to a reduction in intra-thoracic pressure that results in lung expansion. This change in lung pressure causes atmospheric oxygen to be drawn in via the oral and nasal cavities. Air then enters conducting zone at the trachea. The conducting zone's main feature is to facilitate the movement of air from the upper airways (nose, pharynx and larynx) into the lower airways and to the respiratory zone, the site of gas exchange. The conducting zone is a branched tree of progressively smaller and more narrow air-conducting tubes largely comprised of cartilage and smooth muscle tissue overlaid with mucosal tissue including ciliated cells and mucous-secreting goblet cells [29]. In humans, this highly organized structure may consist of a respiratory tree that branches as many as 23 generations from the trachea down to the alveolus [30], while murine lungs can branch 13-17 times [31]. Distal to the trachea is the first bifurcation point leading to the left and right (primary) bronchi, which divide further into lobar (secondary) and segmental (tertiary) bronchi eventually leading to conducting bronchioles (Figure 1.2A). Once in the respiratory zone, the respiratory tree continues to branch into respiratory bronchioles, leading to alveolar ducts and to alveolar sacs, which finally branch into an individual alveolus, where the majority of blood re-oxygenation occurs [29](Figure 1.2B). Intact alveolar structure maintains the delicate interface between the respiratory tract and the circulatory system.

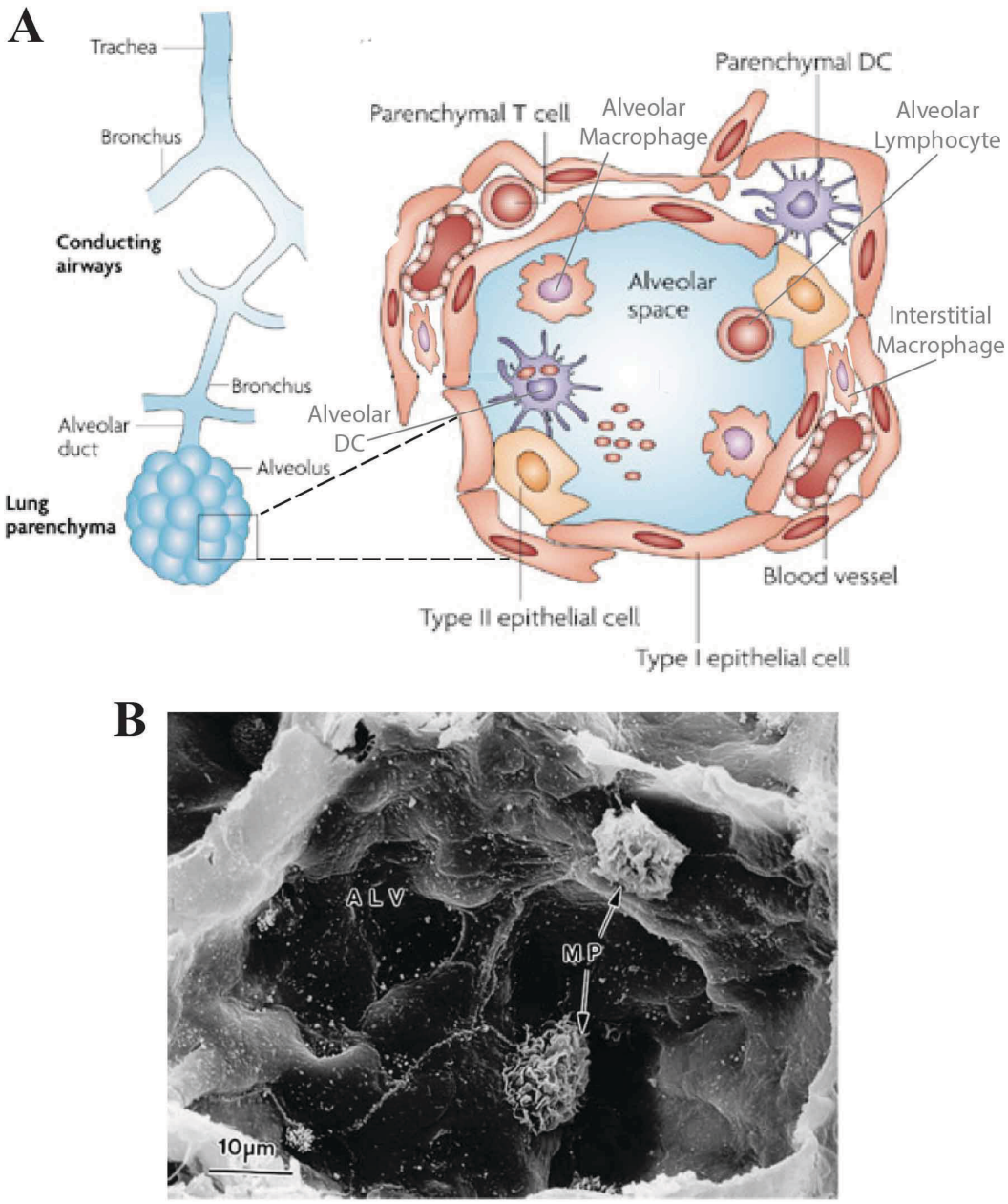

Figure 1.2 Respiratory tree organization and alveolar structure.
(A) Cartoons illustrating the organization of the respiratory tree from the trachea to the alveolus (not to scale) and alveolar structure highlighting structural, alveolar and parenchymal cell populations. Adapted by permission from Macmillan Publishers Ltd: Nature Reviews Immunology. Holt PG, Strickland DH, Wikstrom ME, Jahnsen FL: **Regulation of immunological homeostasis in the respiratory tract**. Nature Reviews Immunology 2008, 8(2):142-152., copyright 2008. (B) The alveolar environment in the lungs. Scanning electron micrograph of a rat lung showing the images of erythrocytes in the alveolar wall capillaries and two ruffled alveolar macrophages (MP) in the alveolar space (ALV). Reprinted with permission of the American Thoracic Society. Copyright © 2014 American Thoracic Society. Martin TR, Frevert CW. (2005) Innate immunity in the lungs. Proceedings of the American Thoracic Society 2(5):403-411. Official Journal of the American Thoracic Society.

1.2.7 Alveolar organization

Alveolar epithelial cells (AECs) are specialized cells that provide the alveolar walls with structure and are responsible for gas exchange and lung flexibility. Type I AECs or type I pneumocytes are thin elongated cells that facilitate the exchange of oxygen and carbon dioxide across its membrane surface [32]. Type I AECs make up approximately ~40% of the total AECs, but cover ~97% of the surface area of the lung tissue [32]. Type II AECs or type II pneumocytes are cuboidal epithelial cells that serve two main functions, they replenish type I AECs in addition to generating large amounts of pulmonary surfactant. Type II pneumocytes comprise ~60% of the total AECs, however they only account for ~3% of the alveolar surface area [33]. Pulmonary surfactants are lipoproteins primarily produced by type II AECs that relieve surface tension and allow the lungs to expand and contract with ease while also playing a key immunomodulatory role [34]. In addition to their main functions, type I and II pneumocytes also maintain immune homeostasis directly through physical interactions with lung-resident leukocytes and indirectly through the release of immune modulatory effectors. The microanatomical organization of the alveolar epithelial surface facilitates the maintenance of normal lung function as well as immune surveillance.

1.2.8 Alveolar leukocytes

Several highly specialized immune cell types reside within the alveolar space in order to maintain lung homeostasis. Alveolar macrophages are the predominant cell-type residing within the airspace, comprising approximately 90% of leukocytes in the airways, with dendritic cells and T cells making up the remaining airway leukocytes [35] (Figure 1.2). In addition to leukocytes directly situated within the airways, there are populations of macrophages, DCs, T cells, and mast cells that reside within the lung parenchyma, the thin layer of interstitial tissue that contains the pulmonary capillaries and keeps them in close contact with the airspaces. Understanding how these lung-resident leukocytes function is key to understanding the maintenance of lung function under normal and inflammatory conditions.

1.2.9 General properties of lung macrophages

Lung macrophages (LMs) are key cells of the innate immune system well positioned within the

parenchyma and alveolar spaces to serve as a first line of defense against a wide variety of foreign substances entering the pulmonary space via the airways or the bloodstream [36, 37]. The localization of LMs at the interface between respiratory surfaces and the circulatory system necessitates that these cells play an active role in a variety of homeostatic functions. These highly specialized phagocytic cells are most noted for their ability to take up particulate matter as well as infectious agents and clearing these potentially harmful substances without compromising pulmonary function [38]. For example, LMs are key in defending against environmental insults such as tobacco smoke [39, 40], asbestos [41], and particulate matter [42]. LMs also play key roles in immunity to infectious agents including influenza [43], *Streptococcus pneumoniae* [44], *Mycobacterium tuberculosis* [12], *Aspergillis fumigatus* [45], and *Nippostrongylus brasiliensis* [13, 46]. In addition to host defense, LMs maintain homeostasis [29, 47], contribute to tissue remodeling [48] and the resolution of inflammatory responses [49]. It is clear that under normal conditions LMs are central to limiting pulmonary inflammation and maintaining lung function, however, upon dysregulation LMs can contribute to the pathogenesis of pulmonary inflammation as they are mediators of inflammatory lung diseases including sarcoidosis [50], idiopathic pulmonary fibrosis (IPF) [51], asthma [52, 53], allergy [54], and COPD [55]. Given their pleiotropic functions, LMs play an important role in shaping the nature and the extent of pulmonary inflammation.

1.2.10 Phenotypic characteristics of LMs

Just as all tissue macrophages should not be considered equivalent, LMs can be further sub-classified based on their micro-locale: alveolar macrophages (AMs) reside within the airspaces, while interstitial lung macrophages (IMs) occupy the lung parenchyma [56]. Although only separated by a thin epithelial cell layer, these distinct lung macrophage populations can take on very different roles largely driven by lung architecture and influence of the pulmonary environment. Therefore, we must identify some of the phenotypic characteristics that are used to define, isolate, and characterize murine LMs under experimental conditions. LMs are generally characterized by their large, granular, and auto-fluorescent physical properties. Lung macrophages differ greatly from other tissue macrophage subsets as they exhibit low levels of surface F4/80, the classic macrophage marker [57, 58]. AMs possess an atypical macrophage surface marker phenotype: $CD11c^{+}$ $CD11b^{-/low}$ $F4/80^{low}$ $CD64^{+}$ $MHCII^{low}$ $SiglecF^{+}$ [14]. In particular, AMs

express high levels of the integrin CD11c, typically associated with dendritic cells, while expressing low levels of the integrin CD11b, a common myeloid cell marker [59]. Interestingly, AMs are the only known SiglecF-expressing tissue macrophage subset [14, 60, 61]. While a much smaller macrophage population, IMs have a more typical tissue macrophage surface marker phenotype ($CD11c^{-/low}$ $CD11b^{+}$ $F4/80^{low}$ $CD64^{+}$ $MHCII^{mid}$ $SiglecF^{-}$), however during inflammatory conditions, IMs can be difficult to discriminate from recruited inflammatory monocytes. While the possible number of markers used to define LMs are limitless, several key phenotypic markers have been identified and are outlined in **Table 1.2**. Many of the phenotypic markers used to define LMs directly contribute to the major functions of these lung-resident myeloid cells.

Table 1.2 Phenotypic characteristics of murine lung macrophages at steady state

Characteristic	Interstitial Macrophages (IMs)	Alveolar Macrophages (AMs)
Physical Properties	FSC^{high}; SSC^{high}; auto-fluorescence^{high}	FSC^{high}; SSC^{high}; auto-fluorescence^{high}
Integrins and Adhesion Molecules	$CD11b^{+}$; $CD11c^{-/low}$; ICAM-1^{+}	$CD11b^{-}$; $CD11c^{+}$; ICAM-1^{+}
Antigen Presentation	$MHCII^{mid}$; $CD80^{low}$; $CD86^{-}$	$MHCII^{low}$; $CD80^{low}$; $CD86^{-}$
Lectins/Scavenger/Fc Receptors	$SiglecF^{-}$; $CD36^{+}$; Mannose receptor^{mid} (CD206); $CD68^{low}$ (binds low density lipoproteins; $CD16^{+}$; $CD32^{+}$; $CD64^{+}$	$SiglecF^{+}$ [14]; $CD36^{+}$; Mannose receptor^{high} (CD206); $CD68^{high}$ (binds low density lipoproteins); Galectin-3^{+} (binds B-glycosides); Dectin-1^{+}; $MARCO^{+}$; DEC-205^{+} [62] ; $CD16^{+}$; $CD32^{+}$; $CD64^{+}$
Transcription Factors	PU.1^{+}; PPAR-γ^{+}; Mafb^{+}	PU.1^{+}; PPAR-γ^{+}; Mafb^{+}
Growth Factor Receptor	CSF-2Rb^{+} (GM-CSF receptor, unlike other mac pops which are CSF1R^{+} and respond to M-	CSF-2Rb^{+} (GM-CSF receptor, unlike other mac pops which are CSF1R^{+} and respond to M-

	CSF); F4/80^{low} [63]	CSF); F4/80^{low} [63]
Signaling Molecule and Other Markers	CD45^{+}; CD14^{mid}; Ly6C$^{-/low;}$ Ly6G^{-}; CD200R^{mid}; CD103^{-}	CD45^{+}; CD14^{low}; Ly6C$^{-/low}$; Ly6G^{-}; CD200R^{high}; CD103^{-}

**these characteristics are highly plastic so may not apply to LMs during inflammatory conditions* [56-58]*

1.2.11 LM as sentinels

Lung macrophages serve as sentinels of the innate immune system and serve as the first line of defense against pathogens and other potentially harmful insults. LMs interface with the vast array of foreign substances within the lung environment through a myriad of cell surface and intracellular receptors specially adapted to detect foreign and potentially harmful substances through the recognition of pathogen associated molecular patterns (PAMPs) and damage/danger associated molecular patterns (DAMPs) [64]. The idea of the innate immune system's role in recognizing patterns and danger signals were championed by theories devised in the late-1980s and mid-1990s by Charles Janeway [65] and Polly Matzinger [66] respectively. These semi-specific receptors allow LMs to set the lung's danger threshold, as the consequences of uncontrolled inflammation within the pulmonary environment are deleterious to the entire organism. The most well-characterized of these receptors are the Toll-like receptors (TLRs), a family of 10 surface and endosomal receptors recognizing the presence of a variety of PAMP structures such as lipopolysaccharide (LPS) on the surface of Gram negative bacteria (TLR4), bacterial flagellin (TLR5), double-stranded RNA (TLR3), and unmethylated CpG containing DNA (TLR9) [67]. The outcome of TLR engagement is the induction of proinflammatory cytokines through MyD88 and/or TRIF signaling. LMs deploy these and many other surface and cytosolic pattern recognition receptors (PRRs) such as nucleotide-binding oligomerization domain (NOD)-like receptors (NLRs) or inflammasomes [68, 69], RIG-like helicases (RLHs) [70], lectins [71], and scavenger receptors [72] in order to fulfill their role as cells responsible for immune surveillance within the lungs. While the nature of the PAMPs and DAMPs recognized by this cadre of innate immune receptors varies wildly, PRR signaling invariably leads to the activation of pro-inflammatory cytokine and chemokine production [73, 74]. The downstream signaling pathways generally converge on activation of several transcriptional cascades including nuclear factor

kappa-light-chain-enhancer of activated B cells (NF-κB), mitogen-activated protein kinase (MAPK), and interferon response factor (IRF) pathways. The downstream effector molecules generated by these diverse innate immune signaling pathways set the stage and influence the nature and magnitude of adaptive immune responses.

1.2.12 LM Phagocytosis

In alignment with initial Mechnikov's discovery, the most prominent feature of lung macrophages in their role as innate immune cells is their ability to phagocytose foreign material that enters the lungs. Through the action of phagocytosis, lung macrophages clear inhaled particulate matter and potential pathogens or allergens that have bypassed the mucus-lined bronchial epithelium and entered the respiratory zone, which does not contain mucus-secreting goblet cells [75]. The primary objective of alveolar macrophage phagocytosis is to sequester antigen emanating from environmental challenge or pathogens from the rest of the immune system, thereby shielding the lungs from local specific immune responses [76]. There are several mechanisms by which lung macrophages are able to phagocytose foreign material including opsonic, non-opsonic and triggered non-specific phagocytosis [77]. The context in which the foreign material is initially recognized by LMs dictates the type of phagocytic clearance and immune response (or lack thereof) that follows. In order to recognize the variety of self and foreign material requiring clearance from the lungs, LMs deploy an array of cell surface receptors to facilitate triggered non-specific, opsonic, and non-opsonic phagocytosis.

1.2.13 LM Opsonic phagocytosis

Lung macrophages deploy a variety of surface complement and immunoglobulin subclass-specific Fc-receptors in order to perform opsonic phagocytosis. During innate immune responses, the majority of opsonic phagocytosis is carried out through complement receptors on the surface of alveolar macrophages. LMs express several complement receptors (CR) including CR1 (CD35), CR3 (CD11b/CD18), and CR4 (CD11c/CD18) [78]. The CRs on the surface of the lung macrophages allow them to recognize a variety of serum proteins involved in the classical and alternative complement pathways decorating pathogen

surfaces. For example, CR1 binds C3b with high affinity, but iC3b and C4b with low affinity; CR3 binds iC3b and β-glucan on bacterial and fungal cell walls with high affinity, however binds to factors C3dg and C3d with low affinity; CR4 exclusively binds iC3b [78]. During adaptive immune responses or secondary challenge, immunoglobulin receptors on the LM cell surface are also involved in opsonic phagocytosis. There are several receptors specific for binding IgG Fc regions (FcγR) found on the LM surface including: FcγRI (CD64), the high affinity receptor for monomeric IgG; FcγRII (CD32), the low affinity receptor for IgG and aggregated IgG; FcγRIII (CD16), the low affinity receptor for aggregated IgG [79]. Engagement of FcγR can result in different outcomes based on downstream signaling events, with FcγRI, FcγRIIA, and FcγRIII functioning as activating receptors and signaling through cytoplasmic immunoreceptor tyrosine-based activation motifs (ITAM) while FcγRIIB functions as an inhibitory receptor signaling through a cytoplasmic immunoreceptor tyrosine-based inhibitory motif (ITIM) [79]. Despite the fact that LMs reside near mucosal surfaces, the majority of LMs bind IgG through FcγR (90%), while fewer have FcεR (17%) or FcαR (14%) receptors specific for IgE or IgA respectively [80]. In addition to complement and immunoglobulin Fc receptors, LMs can recognize and phagocytose foreign material containing PAMPs by deploying non-opsonic cell surface receptors.

1.2.14 LM non-opsonic phagocytosis

Non-opsonic phagocytosis is accomplished using a variety of lectins and scavenger receptors found on the LM cell surface. Notably, AMs express the C-type (calcium-dependent) lectin mannose receptor (CD206), macrophage receptor with collagenous structure (MARCO), the class B scavenger receptor CD36, and SiglecF on their surface. Mannose receptor (MR) binds to terminal mannose residues common on a variety of pathogens such as *Mycobacterium tuberculosis*, *Francisella tularensis*, and *Streptococcus pneumoniae* via its c-type carbohydrate recognition domains (CRDs) [81]. Due to its lack of a cytoplasmic signaling domain, MR requires association with other PRRs or recognition of opsonized bacteria in order for a productive inflammatory response to be elicited [82]. Otherwise, recognition via MR leads to suppression of alveolar macrophage inflammatory responses [56]. Macrophage receptor with collagenous structure (MARCO) is a class A scavenger receptor (SR-A) that binds to acetylated low density lipoproteins (LDL) as well as bacteria, non-opsonized environmental particles, and apoptotic cells [56]. Similar to MR,

MARCO acts as an inhibitory receptor on the surface of LMs; in fact MARCO$^{-/-}$ mice show enhanced inflammation during influenza infection [83]. CD36 is a lipid-binding class B scavenger receptor (SR-B) family member that can bind to an array of ligands including oxidized LDL (oxLDL), collagen, non-opsonized bacteria, β-amyloid, *Plasmodium*-infected erythrocytes and apoptotic bodies [84, 85]. CD36 is expressed on the surface of a variety of cell-types including endothelial cells, platelets, monocytes, and macrophages [85]. Similar to the nature of MR- and MARCO-mediated phagocytosis, CD36-mediated non-opsonic phagocytosis can lead to pro-inflammatory as well as non-inflammatory signaling cascades, depending on concurrent engagement of TLRs [84]. Lastly, SiglecF is a member of the CD33-related Siglecs (sialic-acid-binding immunoglobulin-like lectins) family in mice [86]. SiglecF is a 569 amino-acid single-pass transmembrane protein with four extracellular Ig-like domains, the first containing a V-set domain necessary for sialic acid binding, and two intracellular immunoreceptor tyrosine-based inhibitory motif (ITIM)-like domains on the cytoplasmic tail [87]. SiglecF binds specifically to the glycan ligand 6'-sulfated sialyl Lewis X (6'-sulfo-sLex) [88]. This glycan ligand and the enzymes responsible for its synthesis are expressed by airway epithelial cells in the lungs of mice [89]. In mice, SiglecF is predominantly expressed on the surface of eosinophils, but is also expressed on AMs and myeloid cell precursors in the bone marrow [61, 90]. The cytoplasmic ITIM motifs suggest that SiglecF may act as an inhibitory receptor [86], and have been implicated in the induction of apoptosis of eosinophils in order to regulate the pathogenesis of allergic responses [90]. Therefore, it has been suggested that SiglecF has regulatory properties on the surface of cells.

1.2.15 LM Efferocytosis

In addition to their role in immune surveillance and phagocytosis of foreign material, lung macrophages play an important role in the maintenance of lung homeostasis through the clearance of apoptotic bodies and cellular debris. Apoptotic bodies arise as part of normal cellular turnover as well as during and following inflammatory reactions. Without proper clearance mechanisms, apoptotic bodies can undergo secondary necrosis and inflammatory responses can persist [91]. Efferocytosis, or the clearance of apoptotic bodies, is mediated through a wide array of cell surface scavenger receptors including, but not limited to CD36, receptor for advanced glycation end products (RAGE), T cell immunoglobulin mucin 4

(TIM4), and $\alpha_v\beta_{3/5}$ integrins that bind phosphatidylserine (PS) or its oxidized form directly or via bridge molecules [92]. PS binding allows for discrimination from healthy-viable cells, as PS is a normally localized to the plasma membrane inner-leaflet, however PS becomes cell-surface-associated during apoptosis [93]. Following pulmonary insults, lung macrophages are responsible for the clearance of apoptotic epithelial cells, stromal cells and leukocytes (neutrophils, lymphocytes) via efferocytosis. The act of efferocytosis does not elicit pro-inflammatory cytokine or chemokine production, in fact, anti-inflammatory responses generally follow efferocytosis, thereby allowing for the resolution of inflammation [91]. Another receptor involved in efferocytosis, MER tyrosine kinase (MERTK), a transmembrane receptor on the surface of LMs and member of the TAM receptor family with TYRO3 and AXL [94-96] indirectly recognizes PS through binding to its ligand growth-arrest-specific-6 (GAS6) [96]. The role of MerTK in efferocytosis is central to the function of tissue macrophages. It has been demonstrated that MerTK deficient mice displayed normal Fc-mediated opsonic phagocytosis, but exhibited deficits in the clearance of apoptotic cells and were associated with elevated anti-nuclear autoantibodies [97]. In fact, MerTK, in addition to CD64 (FcγRI), were recently reported to be expressed by all tissue macrophage populations [11]. While there are several mechanisms by which LMs can accomplish engulfment of particulate matter, pathogens, or apoptotic bodies, in order to limit inflammatory responses in the lungs, the act of phagocytosis is not complete until the final steps of degradation take place within the phagosome thereby ensuring proper clearance.

1.2.16 LM microbial killing

Following recognition and phagocytosis of foreign or self matter, ingested material enters the endocytic pathway, where the phagolysosome is formed and degradation, the final step of the phagocytic process, is carried out. The goal of phagocytosis is to eliminate material through physical clearance and ultimately destroy/degrade the foreign material. In LMs, microbicidal activity is largely due to the production of reactive oxygen species (ROS) generated by phagocyte nicotinamide adenine dinucleotide phosphate (NADPH) oxidase (Phox) [98, 99], a six subunit enzyme complex that assembles along the phagosomal membrane upon initiation of a respiratory burst [100, 101]. The Phox enzyme complex converts molecular oxygen into reactive superoxide anion ($O2^{\bullet -}$), which serves as a precursor to other ROS such as hydrogen

peroxide (H_2O_2, generated by superoxide dismutase (SOD), and hydroxyl radicals ($OH^{\bullet}$) produced in the presence of iron [100, 101]. Through its antimicrobial activity NADPH oxidase activity limits inflammation [100]. In fact, humans with a defect in an NADPH oxidase enzyme subunit develop chronic granulomatous disease (CGD), a heterogeneous immunodeficiency, characterized by severe bacterial and filamentous fungal infections due to dysfunctional phagocytic respiratory burst [102]. In addition to its importance in the clearance of pathogens and particulate matter, phagocytosis can also promote adaptive immune responses.

1.2.17 LM antigen presentation

In addition to their key role in innate immune responses, LMs can also contribute to the initiation of adaptive immune responses as antigen presenting cells (APCs). Exogenous protein antigens can be introduced into the endocytic trafficking pathways upon phagocytosis. Within the phagolysosome, protein antigens are exposed to a myriad of active lysosomal cysteine proteases, such as cathepsin S [103], that cleave protein antigens into smaller peptides. These peptides (15-25 amino acids) are loaded into the binding clefts of major histocompatibility complex type II (MHCII) molecules and presented on the cell surface to $CD4^+$ T lymphocytes in order to elicit antigen-specific adaptive immune responses. Although technically an APC, LMs play a relatively minor role in antigen presentation in comparison to lung dendritic cells [104]. LMs are generally considered poor APCs partially due to low B7 costimulatory molecule expression (B7-1/CD80 and B7-2/CD86) [105]. Low CD80/CD86 expression may drive anergic T cell responses and promote peripheral tolerance to the large number of foreign antigens that enter the lungs during respiration [105]. In allergic asthmatics, LMs have been shown to up-regulate CD80 and CD86 surface expression, present antigen, and promote pro-inflammatory cytokine production in effector T cells within the lungs [106]. While generally restricted to the lung, under certain conditions, LMs have been shown to migrate to draining lymph nodes and present antigen [14]. Although their role in antigen presentation may be limited, LMs can significantly influence the function of other immune cells and the lung environment as a whole upon activation.

While these highly-specialized phagocytic cells are most recognized for their ability to take up and clear particulate matter as well as infectious agents without compromising pulmonary function [38], LMs play an active role in a variety of functions including host defense, maintaining lung homeostasis, tissue remodeling and wound repair [29] through the production of effector molecules such as enzymes, cytokines and chemokines following activation.

1.2.18 LM Activation

Lung macrophages, similar to other tissue macrophages exhibit phenotypic plasticity and flexibility; they can change from one activation state to another depending on the local environmental cues [10, 107, 108]. George Mackaness first described macrophage activation in 1962. Mackaness identified macrophages with enhanced non-specific microbicidal activity following infection with *Listeria monocytogenes* [109]. Later, macrophage activation (now termed 'classical activation') was found to be antigen-dependent and linked to interferon gamma (IFNγ) production and T_H1 responses [110]. Thirty years following Mackaness' initial description, Siamon Gordon reported macrophages up-regulating mannose receptor in response to interleukin 4 (IL-4) signaling, and termed this phenotype 'alternative activation' [111]. These are but two examples of how cytokine signaling can elicit particular responses within tissue macrophages, however, it is now evident that these activation states are merely conceptual frameworks by which researchers group together similar responses to an infinite number of stimuli. To that end, in addition to taking on classically activated (CAM; M1) and alternatively activated (AAM; M2) phenotypes [112, 113], there is growing evidence that LMs play other important roles in shaping the nature and the extent of pulmonary inflammation [112], as other cytokines and signaling molecules that elicit M2-like phenotypes have been identified. For example, macrophage activation induced by Fc receptors and immune complexes has been termed type II activated or M2b [114], while activation induced by IL-10 and glucocorticoids has been termed deactivated or M2c [115]. As the signals and sources for each activation state differ, so do the effector molecules produced. Not surprisingly, each functional macrophage phenotype has been associated with promoting distinct immune responses. For a more complete overview of the signals, effector molecules, and downstream consequences of these broad macrophage activation phenotypes, refer to Table 1.3

Table 1.3 Activation states of macrophages

Activation State	Signals (source)	Effector Molecules	Consequences
Classical [CAM] (M1)	IFNγ (NK; T_H1; some macrophages) + LPS (bacteria) or TNFα (APC);	IL-12; iNOS (NO); ROS; many chemokines (xx)	Intracellular pathogen microbicidal activity; T_H1 response; delayed-type hypersensitivity
Alternative [AAM] (M2a)	IL-4 (T_H2; basophil; ILC2); IL-13 (T_H2; ILC2); IL-33 (epithelial)	Arg1; Ym1; Fizz1	Wound healing/tissue repair; T_H2 response; allergy; parasite killing
Type II (M2b)	immune complexes (ICs) + LPS (TLR ligands); Fc receptors	IL-10; TNFα; IL-1β; IL-6	Immunoregulatory activity; promote T_{reg} response
Deactivated (M2c)	IL-10 (T_{reg}) + glucocorticoids (adrenal cells)	IL-10; TGF-β	Immunoregulatory activity; promote T_{reg} response

While functional macrophage phenotypes are associated with a unique transcriptional networks controlling gene expression and production of effector molecules [107], no master transcriptional regulators have been identified as in $CD4^+$ helper T cell subsets [116]. Instead, many transcription factors play roles in macrophage activation. Generally, M1 and M2 macrophage polarization is controlled through the nuclear translocation of interferon response factors (IRFs). The transcription factors IRF5 and signal transducer and activator of transcription 1 (STAT1) are among those that drive M1 macrophage polarization [117-119],

while NF-kB p50 has been shown to inhibit M1 macrophage polarization [120]. Similarly, the transcription factors IRF4, STAT6, peroxisome proliferator-activated receptor-γ (PPAR-γ) and CCAAT/enhancer-binding protein β (C/EBPβ) control M2 macrophage polarization [13, 121-123]. At rest, tissue macrophages are typically polarized towards a type 2-like phenotype as they maintain tissue homeostasis [8, 10, 124]. There are several transcription factors including PPAR-γ/retinoid X receptor (RXR) [125, 126], PU.1 [127, 128], and MafB [129] that have been shown to act as the primary LM global transcriptional regulators; responsible for controlling many aspects of LM function. As a consequence of macrophage activation, effector molecules are produced in order to direct macrophage metabolism as well as eliciting responses in other macrophages or other cell types.

1.2.19 LM metabolism

The polarization of macrophages can have a profound impact on several metabolic pathways. For example, metabolism of L-arginine, an essential amino acid, is central to M1 and M2 polarized macrophage effector functions. Upon activation, M1 macrophages elevate production of inducible nitric oxide synthase (iNOS), an enzyme that metabolizes L-arginine into L-citrulline and nitric oxide (NO) [130]. By damaging proteins, lipids, and DNA, NO is a key mediator of M1 induced microbicidal activity. In fact, iNOS competes with arginase 1 (Arg1), an effector of M2 polarized macrophages, for L-arginine substrate [131, 132]. Upon M2 polarization, Arg1 metabolizes L-arginine into urea and L-ornithine, a precursor of L-proline that promotes tissue repair through collagen synthesis [132]. Similarly, metabolism of arachidonic acid, a source of effector lipid mediators, differs between M1 and M2 polarized macrophages [133]. Arachidonic acid metabolism through the cyclo-oxygenase pathway driven by cyclooxygenase 2 (COX-2) enzymatic activity produces of thromboxanes and prostaglandins [134]. COX-2 products (thromboxane B2 (TxA2); prostaglandin E2 (PGE2); PGD2; PGF2a), also known as prostanoids, are released by LMs upon LPS stimulation and M1 polarization and can mediate inflammatory responses and vasoconstriction [135]. Alternatively, arachidonic acid metabolism via the lipoxygenase pathway produces leukotrienes and hydroxyeicosatetraenoic acids, such as leukotriene B4 and 5-hydroxyicosatetraeonic acid (5-HETE) upon M2 macrophage polarization and activation of 5/12/15-lipoxygenases [133]. These lipid mediators are released from LMs upon M2 polarization and can sustain inflammatory responses, however can also

contribute to the pathogenesis of allergy and asthma [135]. M1 and M2 polarized macrophages also have differing metabolic requirements in relation to glucose, cholesterol and iron metabolism [134]. In fact, mechanistic target of rapamycin (mTOR), a serine/threonine kinase, is a key nutrient, growth factor, and energy sensor that recently has been implicated in the regulation of macrophage polarization. mTOR is the catalytic subunit of two different multi-protein signaling complexes, mTORC1 and mTORC2 that phosphorylate and regulate a number of other intracellular signaling pathways involved in cellular growth processes [136]. Interestingly, mTORC1 signaling has been associated with M1 macrophage effector function, while mTORC2 signaling has been associated with M2 activation [137, 138]. While the initial conceptual frameworks described M1 and M2 macrophage activation as dichotomous outcomes, recent studies have demonstrated that macrophage polarization should be considered spectral in nature [107, 112]. This evolution is similar what has taken place with regards to the differentiation of $CD4^+$ helper T cell subsets; as that field moved from the original monolithic view to a more flexible and plastic view [116]. In fact, macrophage activation responses depend on the particular milieu of signals that individual cells are exposed to within their tissue environment. In addition to location and environmental factors, timing must also be taken into account, as macrophage functional states are not static, but highly dynamic in nature. Therefore, understanding how these many factors influence the activation state of lung macrophages will inform us and continue to elucidate their nature and roles in a variety of biological situations.

1.2.20 Pulmonary environment and immunomodulation

Many of the immune-modulatory factors that shape the pulmonary environment and LM function are produced by AECs. The relationship between AECs and lung macrophages should not be overlooked as these cell populations reside within close proximity of one another and together maintain homeostasis at the mucosal interface between the environment and the host. Understanding the multitude of soluble factors and cell-to-cell contacts responsible for controlling the lung macrophage population under steady state conditions is key when studying their function upon inflammatory insult. The alveolar epithelium is a major source of cytokines and chemokines that can greatly influence the LM population and the lung environment as a whole.

1.2.21 Soluble factor-dependent immunomodulation

Type II pneumocytes produce large amounts of surfactant proteins and lipids [34]. In addition to their major role in relieving surface tension within the airspaces, surfactant proteins A and D are members of the collectin family of anti-microbial peptides. These collectins can aid in phagocytosis of microorganisms and apoptotic bodies through opsonization [34, 139, 140]. For example, surfactant protein A (SP-A) has been shown to stimulate the phagocytosis of apoptotic neutrophils (PMNs) by normal alveolar macrophages [139], while surfactant protein D can influence integrin CD11b and CD11c expression (subunits of complement receptors) on the surface of lung macrophages, thus impacting their phagocytic abilities [140]. By directing material for phagocytosis, the AECs can indirectly influence the function and activation state of the LM pool.

AECs are major producers of the pleotropic cytokine granulocyte macrophage colony stimulating factor (GM-CSF or CSF2) [37]. In addition to its role as a growth factor implicated in macrophage recruitment and proliferation, GM-CSF also enhances antigen presentation, opsonic phagocytosis, microbicidal capacity, chemotaxis, and adhesion [127](refs). More specifically, GM-CSF stimulates the up-regulation of integrin CD11c (integrin α x) expression on the surface of lung macrophages [63, 141, 142]. The constant exposure of LMs to GM-CSF in the lung environment imparts a unique feature of lung macrophages compared to other tissue macrophages subsets, they express CD11c at high levels on the cell surface [37], an uncommon phenotype for tissue macrophages and more common feature of dendritic cell populations [143]. GM-CSF signaling regulates the function of lung macrophages through the transcription factor PU.1 [127] and promotes M1 macrophage polarization via NF-kB and IRF5 nuclear translocation [117]. In GM-CSF deficient mice, the alveolar macrophage population does not develop properly and has deficits in functional capabilities such as phagocytosis and TNFα production [144, 145]. In fact, GM-CSF deficient mice develop a condition similar to human pulmonary alveolar proteinosis (PAP) due to deficits in alveolar macrophage surfactant catabolism [127, 144, 146]. While exposure to GM-CSF greatly impacts normal LM function in a variety of ways, there are other immunomodulatory signals present in the lung environment that also influence LM function.

IL-10, an inhibitory cytokine, is constitutively secreted by AECs while it's receptor, IL-10R, is normally expressed on the LM surface [147]. IL-10 has many inhibitory effects upon macrophages and DCs including the inhibition of pro-inflammatory cytokine production (decreased TNFα, IL-1β, and IL-6) and decreased MHCII and costimulatory molecule expression (decreased CD40, CD80 and CD86) preventing efficient antigen presentation to antigen-specific T cells resulting in anergic $CD4^+$ T cells [147, 148]. Despite constitutive IL-10 production in the lungs, LMs can circumvent this inhibitory mechanism upon engagement of toll-like receptors (TLRs) by PAMP ligands [147].

Transforming growth factor β1 (TGFβ), is a multifunctional growth factor secreted by a variety of cell types, including macrophages [149, 150]. TGFβ has profound regulatory effects by inhibiting leukocyte activation via SMAD-dependent and SMAD-independent pathways [151]. TGFβ-deficient mice develop diffuse mononuclear cell infiltrates and succumb to chronic inflammation a few weeks after birth [149]. TGFβ is secreted as a latent procytokine (protein complex of TGFβ-homodimer and latency-associated peptide (LAP)) requiring proteolytic cleavage or a conformational change to be maintained in its active, non-latent form and bind with its receptor [152]. Within the alveolar space active TGFβ is held by the αvβ6 integrin on the surface airway epithelial cells [152, 153]. When AMs adhere to the airway epithelium, active TGFβ contributes to maintaining AMs in a quiescent state through engagement of TGFβR and SMAD3-dependent down-regulation of macrophage activity [153, 154].

As a result of cellular or tissue stress, AECs can release danger/damage signals to alert the immune system. These functionally related molecules are collectively referred to as alarmins and include several family members such as IL-25, IL-33, and thymic stromal lymphopoietin (TSLP) [64]. There are a variety of non-pathogenic insults that can lead alarmin release including physical trauma, excessive heat or cold, exposure to radiation or chemicals, and insufficient oxygen or nutrients [64]. Similar to PAMPs, these epithelial-derived cytokines can initiate nonspecific broad-spectrum inflammatory responses; however, alarmins are endogenous molecules. For example, IL-33, an IL-1 member cytokine, is released upon cellular stress and signals through its receptor ST2/IL1RL1 on the surface of several different cell types including macrophages, mast cells and type 2 innate lymphoid cells (ILC2s) [155-158]. A non-membrane bound

alternate splicing variant of ST2 is believed to act as a decoy receptor. Similar to TGFβ, IL-33 is released as an inactive propeptide requiring protease cleavage in order to release the bioactive form [159]. IL-33 signaling results in the activation of the NF-κB and MAPK pathways [158]. IL-33 has been shown to promote wound-healing T_H2 responses through the promotion of downstream factors such as IL-4, IL-5 and IL-13 [155]. AECs can also influence LM function through the release of IL-33, thereby inducing macrophage alternative activation [155]. The effects of soluble immunomodulatory factors on the LM population must not be considered in isolation, as together they shape the pulmonary immune environment and dictate the immune homeostatic setpoint of LMs.

1.2.22 Contact-dependent interactions

In addition to soluble factors, AECs can also modulate lung macrophage function through non-phagocytic contact-dependent interactions [160, 161]. CD200 (also known as OX2) is a molecule expressed on the surface of a wide array of cell types including, but not limited to AECs, T cells, B cells, and neurons [161-163]. CD200R is a transmembrane receptor almost exclusively expressed by myeloid cells, but can also be expressed by T cells [162, 164]. Of note, CD200R is expressed at high levels on the surface of lung macrophages [47, 163]. Ligation of the receptor inhibits macrophage activation through recruitment of Dok2 and subsequent RasGAP activation, which mediates inhibition of the Erk, Jnk, and p38 MAPK pathways [164-166]. Engagement of CD200R on the surface of lung macrophages negatively regulates the level of pro-inflammatory activation and maintains lung homeostasis [47], however, failure to engage the inhibitory CD200R can lead to myeloid cell activation.

Recently, another role for AECs has been reported; AECs serve as a conduit for inter-lung macrophage communications via calcium ion flux [167]. Recently, multiple studies have illustrated the importance of direct interaction between lung macrophages and AECs [47, 154, 167]. In fact, a recent study demonstrated that lung epithelial cells act as a conduit and scaffold for inter-macrophage communications [167]. Lung macrophages bind to AECs via the gap junction protein connexin 43 and utilize Ca^{2+} fluxes to communicate with distal lung macrophages via AECs [167]. The importance of the relationship of LMs with the pulmonary environment and AECs in particular cannot be stressed enough. LM function is tightly

controlled by a myriad of local environmental factors. Likewise, LMs can exert control over and regulate the function of other leukocytes in the lungs.

1.2.23 LM-mediated suppression

LMs enact a suppressive role onto dendritic cells, T cells, and neutrophils in the lungs through the secretion of soluble immunomodulatory factors as well as through cell-dependent mechanisms. LMs can suppress the function of activated T cells through secreted mediators such as NO, prostaglandins, TGF-β and IL-10 [112, 168-170]. LMs can also induce anergic T cell responses (functionally inactivated) by limiting B7 costimulatory signals (B7-1/CD80 and B7-2/CD86) [171]. Instead, programmed death ligand 1 (PDL-1; B7-H1) and 2 (PDL-2; B7-DC) are expressed on the surface of LMs [46]. These ligands interact with programmed cell death 1 (PD1), an immune checkpoint receptor and negative regulator of immune function, on the surface of activated T lymphocytes [172]. PD1/PDL-1 engagement inhibits effector T cell activation in the lungs [173, 174]. Under M1 polarization, macrophages have been shown to greatly elevate PDL-1 surface expression, while under M2 polarization macrophages only slightly up-regulate PDL-1 levels, but robustly elevate PDL-2 on the surface [175, 176]. Interestingly, hypoxia induced factor 1-α (HIF-1α) elevates PDL-1 surface expression under hypoxic conditions [177]. This is of particular importance as variety of inflammatory lung insults result in hypoxic conditions and the elicitation of pro-inflammatory responses [178]. LM-derived soluble factors such as TGF-β, IL-1, PGE2, and NO that influence the maturation, function, and migration of lung DCs [62, 179]. LMs also suppress lung DC antigen presentation function [15, 62] and migration to draining lymph node (dLN) [62]. Through regulation of lung DCs, LMs can control the initiation of adaptive inflammatory responses [63] and set the immune threshold.

1.2.24 Dynamics of mononuclear phagocytes

As is evident from APC migration to lung draining lymph nodes, mononuclear phagocyte populations are in flux, moving in and out of the lung environment during inflammatory conditions. These dynamic processes are relevant to the maintenance of homeostasis within the lungs and overall health by preserving

gas exchange. In addition to LMs and lung DCs trafficking antigen to draining lymph nodes, myeloid cells are recruited from the periphery to the lungs. These recruited cells respond to local factors and can differentiate upon exposure to the lung environment. In addition, myeloid cell populations can expand and contract upon inflammatory insult. Elucidating the underlying mechanisms behind these dynamic processes and their contribution to the maintenance of lung homeostasis is key to understanding pulmonary immunity.

1.2.25 Migration to draining lymph nodes

Upon inflammatory insults that exceed the pulmonary immune threshold, antigen loaded APCs migrate to the lung draining lymph nodes (dLNs) to present antigen to naïve T cells and elicit adaptive immune responses. As immuno-regulatory cells, AMs do not readily migrate to the secondary lymphoid tissue and have minimal role in antigen presentation [180]. The role of professional APC is largely carried out by migratory lung DCs [143]. However, under certain pulmonary insults such as *Streptococcus pneumonia* infection, $CD11c^{+}SiglecF^{+}$ AMs migrate to the B cell zone of dLNs [14]. It is proposed that migrating AMs may interact with B cells in a similar fashion to $CD169^{+}$ subcapsular sinus (SCS) macrophages, however the exact mechanisms have not been identified [25]. Interestingly, unlike lung DCs, AM migration to the dLN is independent of CCR7 signaling [14, 62].

1.2.26 Blood monocyte recruitment

Typically, pathogen exposure results in the production of chemokines such as CCL2 (MCP-1), CCL3 (MIP-1α), CCL7 (MCP-3), CXCL10 (IP-10) and CX_3CL1 (fractalkine) [181-183], which induce a rapid influx of large numbers of mononuclear phagocytes to the lungs [184-186]. These infiltrating cells typically display a wide spectrum of activation phenotypes and have been documented during influenza [185], *Mycobacterium tuberculosis* [12, 184] and *Nippostrongylus brasiliensis* [13, 46] infections. There are two major circulating monocyte populations, first, “classical” or inflammatory monocytes and second, the “patrolling” or steady state monocytes. In the mouse, the classical inflammatory monocytes are defined as $CD11b^{+}Ly6C^{high}CCR2^{hig}CX_3CR1^{int}$ [187]. These monocytes are largely driven to emigrate from the bone

marrow to sites of inflammation through the CCL2/CCR2 chemokine axis [188, 189]. In fact, alveolar CCL2 secretion is sufficient to recruit inflammatory monocytes to the lungs [190]. There are many cellular sources of CCL2, also known as monocyte chemotactic protein 1 (MCP-1), including endothelial cells, epithelial cells, monocytes, dendritic cells, and macrophages, which produce CCL2 upon activation by pro-inflammatory cytokines or engagement of PRRs [191]. Inflammatory monocytes have a very short half-life in circulation (~19 hours) [192, 193], only neutrophils have a shorter circulating half-life (estimated at 11.4 hours) [194]. CCR2 is required for $Ly6C^+$ monocyte exit from the bone marrow and the generation of $Ly6C^-CX_3CR1^+$ monocytes [191, 195]; as in the absence of inflammation, inflammatory monocytes traffic back to the bone marrow and serve as an obligate intermediate for "patrolling" monocytes as they differentiate into $Ly6C^-CX_3CR1^{hi}$ cells [196]. The murine "inflammatory" monocyte population corresponds to the $CD14^+CD16^+$ and $CD14^+CD16^-$ monocyte populations described in humans [187]. The "patrolling" monocytes are defined as $CD11b^+Ly6C^-CCR2^-CX_3CR1^{high}$ cells that migrate to the lungs and other tissues at steady state as they survey endothelial integrity by adhering and crawling along the luminal side of endothelial cells [197]. These monocytes have a half-life of 2 days in circulation [196, 198], are responsive to the chemokine CX_3CL1 (fractalkine), and correspond to the $CD14^{lo}CD16^+$ monocyte population described in humans [187]. Within the MPS conceptual framework, these $Ly6C^+$ "inflammatory" and $Ly6C^-$ "patrolling" bone marrow monocyte subsets are directly responsible for seeding tissue macrophage populations.

1.2.27 A challenge to the MPS paradigm

The current conceptual framework, MPS, characterizes monocytes as precursors to tissue macrophage populations, as they arise from the same developmental spectrum [5]. However, there were some inconsistencies that arose that lead some investigators to challenge the MPS. For example, monocytopenic animals have normal tissue macrophage densities [199], an unexpected outcome if monocytes do seed tissue macrophage populations. Similarly, in human populations, congenital monocytopenias such as reticular dysgenesis [200] and IRF8 null mutations [201] do not lead to global deficits in tissue macrophage subsets. Also, macrophages have been detected in tissues prior to the development of monocytes, making it

difficult to explain the origin of these early tissue macrophages and their relationship to putative bone marrow monocyte precursors [202-205].

Recent studies have challenged the MPS and the idea that monocytes invariably give rise to tissue macrophages. Amidst the development of new technologies and experimental methods allowing for advanced cell fate mapping, the macrophage biology field is in the midst of a paradigm shift. The latest studies contradict earlier experiments using radiolabeling [4], irradiation chimeras [206], parabiosis [207], and replacement after depletion [186] that supported the notion that monocyte populations seeded tissues as macrophage precursors and tissue macrophages maintained their population size through continual renewal from blood monocyte stocks. In recent parabiosis experiments, there is discordance between monocyte and macrophage chimerism: monocytes reach measurable chimerism levels while tissue macrophages do not; even at one year post-parabiosis [208]. Due to recent advancements, there are two major areas of investigation within the macrophage biology field that are contributing to the evolving paradigm shift: first, regarding the origin or seeding of tissue macrophages, and second, local tissue macrophage proliferation.

1.2.28 Tissue macrophage niches are seeded embryonically.

In the late 1990s, it was postulated that microglia are seeded from yolk sac progenitors and are able to proliferate and self-maintain within the brain [209]. However, this notion did not take hold for very long. Recently, the field at large has begun to appreciate that many tissue macrophage subsets are not continuously being replenished from blood monocyte stocks; in fact, the tissue macrophage niches are seeded even before birth and are able to maintain the local population levels through longevity and limited self-renewal capabilities [196, 208, 210]. However, just as tissue macrophage function largely depends on the local tissue environment and requires individual evaluation, the same considerations must be applied to understanding the origins and maintenance of these cell populations. For example, recent studies have revealed that microglia are seeded from primitive yolk sac macrophages (embryonic day 8) [203, 211] while Langerhans cells, splenic, hepatic, pancreatic, and cardiac macrophages are seeded prior to birth from fetal liver monocytes (embryonic day 11.5-12.5) [204, 205, 212, 213]. These studies have revealed that adult tissue macrophages arise from two independent hematopoietic waves: first is the “primitive”, arising

from yolk sac-derived macrophages (E8.5-9; PU.1 dependent), and second, is the "definitive" arising from the fetal liver monocytes (E11.5-12.5; MYB dependent) [214]. While embryonic seeding appears to be a common feature of most tissue macrophage populations [196, 210], this is not a universal truth, as intestinal macrophages are constantly being reseeded by $Ly6C^+$ monocytes [215] and appear to be an outlier tissue macrophage subset. To date there are three proposed models describing the origin of tissue macrophages: yolk sac-derived macrophages, fetal liver monocytes, and bone marrow monocytes.

1.2.29 Lung macrophage origins

The origins of lung macrophages and their replenishment had been previously attributed to a serial progression of circulating blood monocyte differentiating into interstitial macrophages and finally to alveolar macrophages [186, 216]. However, these experiments utilized diphtheria toxin-mediated macrophage depletion in CD11c-DTR mice followed by adoptive transfer of monocytes. A recent study has demonstrated that similar to other tissue macrophage subsets, lung macrophage populations are embryonically seeded from fetal liver monocyte pools [145]. Mature alveolar macrophage (defined as $CD11c^+SiglecF^+$ cells) development was GM-CSF dependent and first observed during the first week of life (post-natal day 1-3) [145]. The embryonically seeded lung macrophages could then self-renew and maintain the cellular niche throughout life, importantly, without recruitment from the bone marrow-derived monocytes [145, 208]. Recent studies have also demonstrated that only upon devastating experimental manipulations such as macrophage depletion (influenza- or diphtheria toxin- mediated) [208] or lethal irradiation [145] were circulating blood monocytes needed to repopulate the decimated LM cellular niche; however, any remaining LMs following non-genotoxic ablation also contributed to renewal. In addition, another recent study demonstrated that bone marrow monocytes do not contribute to the lung macrophage pool; instead they were shown to migrate to the dLN to present antigen [217]. These latest fate-mapping studies should facilitate further observations defining the nature and function of lung macrophages.

1.2.30 Implications of embryonic tissue macrophage seeding

Seeding tissue macrophage populations during embryonic development or early in life may be advantageous to ensuring the maintenance of homeostasis throughout life. As recent reports demonstrate, most tissue macrophage populations can be preserved independently of bone marrow monocyte input, thereby allowing for vigor and consistency of tissue macrophage function during immunity, repair, and homeostasis. This paradigm shift may remove some of the constraints associated with operating within the current conceptual framework (MPS) (Figure 1.3). By presuming that bone marrow monocytes were direct precursors for all tissue macrophage subsets, their fates were intimately linked. Revealing alternate tissue macrophage origin pathways may allow the field to functionally separate bone marrow monocytes from tissue macrophages and decisively resolve differences in their functional roles: as monocytes are generally associated with inflammation and pathogen challenge, and tissue macrophages are typically associated with development, tissue homeostasis, and the resolution of inflammation.

1.2.31 Tissue macrophages self-maintain

As cell fate-mapping studies have revealed, most tissue macrophage subsets have the ability to self-maintain throughout life. Tissue macrophages are able to accomplish this feat through the combination of long cellular half-lives and low-level local proliferation. Macrophages promote cell survival by suppressing apoptotic pathways such Akt-mediated inhibition of caspase 9 activation [218, 219]. Actually, it has been generally accepted that LMs are long-lived cells [220, 221], with half-lives reported on the order of several months. However, the idea of local macrophage proliferation has been proposed from time to time over the last few decades [222] and has never gained much traction, as it has been the long-held notion that tissue macrophages were terminally differentiated cells unable to proliferate. During the 1970s, 80s, and 90s there were numerous isolated reports of alveolar macrophage proliferation upon a variety of insults [221, 223-230], but until recently, these reports were not resolved, as they did not agree with the MPS conceptual framework.

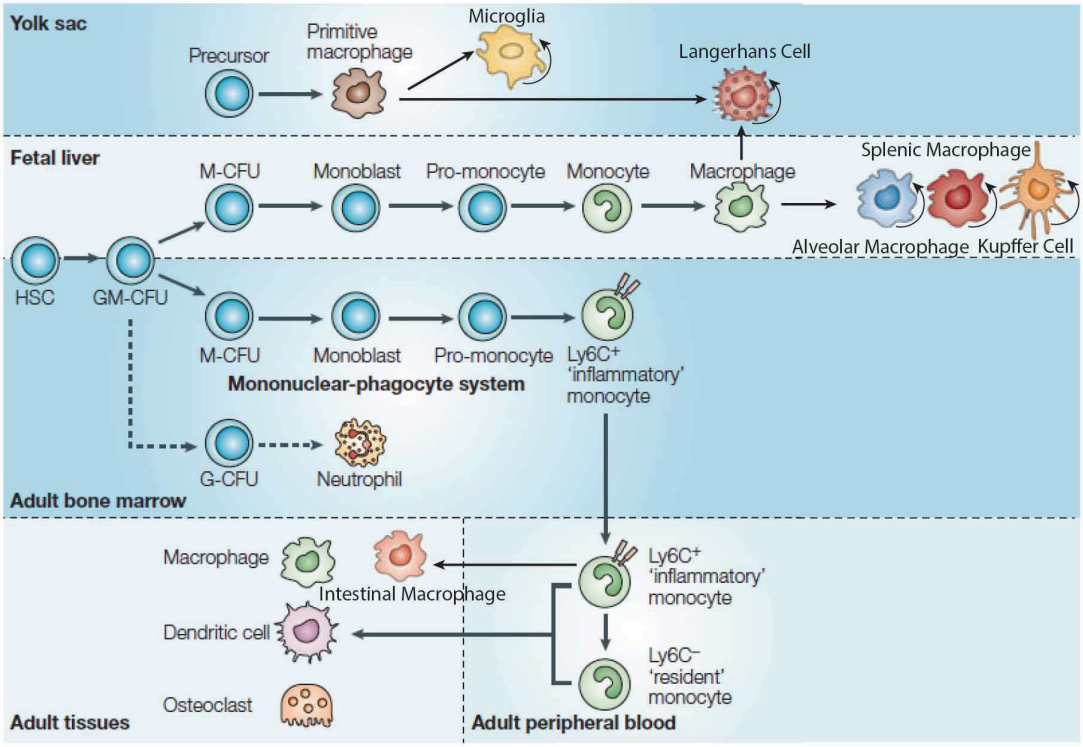

Figure 1.3 Challenge to the MPS: tissue macrophage origins and maintenance.
Cartoon illustrating recent findings of tissue macrophage origins and maintenance challenging the mononuclear phagocytic system (MPS).
Adapted by permission from Macmillan Publishers Ltd: Nature Reviews Immunology. Gordon S, Taylor PR: **Monocyte and macrophage heterogeneity**. Nature Reviews Immunology 2005, 5(12):953-964., copyright 2005.

1.2.32 Macrophage proliferation in general

Recently, there has been another surge in the number of reports that have clearly demonstrated local tissue macrophage proliferation. Macrophages have been shown to proliferate locally upon a variety of insults and tissue environments including parasitic worm infections in the lungs and pleural cavity [46, 231, 232], within atherosclerotic lesions [233], within visceral adipose tissue [234], and following acute self-resolving inflammation (zymosan peritonitis) [235, 236]. While the mechanisms that induce macrophage proliferation are still being elucidated, recently it has been revealed that macrophage subsets can undergo proliferation during T_H2 inflammatory responses. For example, lung macrophages show the propensity to proliferate locally upon infection with the soil-transmitted helminth, *Nippostrongylus brasiliensis* [46]. In addition, it was recently demonstrated that peritoneal macrophages robustly proliferate in an IL-4 dependent fashion upon infection of the pleural cavity with the filarial nematode *Litomosoides sigmodontis* [231]. Evidence of macrophage proliferation during T_H2 inflammation provides a novel condition for macrophage self-renewal outside of tissue development [237] or homeostatic control of tissue macrophage numbers [212]. In thinking about these processes from a resources standpoint, the Allen group proposes that maintenance of a standing circulating macrophage precursor population (blood monocytes) is energetically costly [231]. Therefore in the case of T_H2 immunity, it may be advantageous for tissue resident macrophages to self-replicate in a limited capacity, thereby preventing the undesirable effects of inflammatory cell recruitment and possibility of further tissue injury; this may allow M2-polarized tissue macrophages to carry out wound repair and/or parasite sequestration functions [231].

1.2.33 Lung macrophage proliferation

Lung macrophage proliferation has sporadically been reported over the last forty years. LMs have been shown to proliferate following exposure to inflammatory insults including tobacco smoke [223, 224, 228], marijuana smoke [228], carbon particles [226], irradiation [221], and helminth parasite infection [46]. In addition, lung macrophage proliferation was described during postnatal development [227], steady-state conditions [221, 225], and in patients with idiopathic pulmonary fibrosis, sarcoidosis, or other interstitial lung diseases [224, 230]. Prior to the recent paradigm shift, these reports of local macrophage proliferation were considered outside of the MPS conceptual framework, as they did not support the concept that bone

marrow monocytes maintain tissue macrophage populations. Therefore, these previous reports should be reconsidered through a different lens, as recent findings that fetal liver monocytes seed the lungs during embryonic development and these precursors give rise to long-lived self-maintaining lung macrophage populations have come to light [145, 208]. While the mechanisms directing lung macrophage proliferation have not been fully elucidated, in a recent study, following non-genotoxic depletion, LM proliferation was dependent on macrophage colony stimulating factor (M-CSF or CSF1) and GM-CSF, but IL-4 independent [208]. Certainly further exploration into the signals and mechanisms involved in LM proliferation under a variety of situations is warranted.

1.2.34 Summary

As stated above, the lung is a unique anatomical location from an immunological perspective due to the fact that it contains the confluence of the respiratory and circulatory systems. Just a thin epithelial wall separates the external environment from the host's systemic circulation. Therefore, a dedicated population of innate immune cells is needed to maintain normal function and homeostasis, as the lung undergoes constant bombardment of foreign material introduced via respiration or blood circulation. In order to avoid a perpetual inflammatory state, these innate sentinels must be highly regulated and therefore must possess a high threshold for activation as uncontrolled inflammation within the lung tissue can lead to impaired oxygen exchange and eventually death if not kept in check.

1.3 MALARIA

1.3.1 Public health significance

Malaria is a worldwide public health problem with greater than 200 million yearly infections resulting in over 600,000 deaths per year, mainly in children under the age of five in Sub-Saharan Africa [238]. Approximately 3.4 billion people (forty percent of the world's population) are living in 97 countries where malaria infections are currently transmitted, mostly in tropical and sub-tropical climate zones [238]. It is

estimated that global malaria infections account for 68 million disability-adjusted life years (DALYs) lost and rank as the greatest source of lost DALYs in Southern and Western Sub-Saharan Africa [239].
In addition to malaria's direct impact on public health, the effects of *Plasmodium* infections can also stress economic systems in malaria endemic regions due to a deteriorated workforce and significant health care expenditures [240].

1.3.2 *Plasmodium* life cycle

The protozoan *Plasmodium* parasites, *P. falciparum, P. vivax, P. malariae, P. ovale*, and *P. knowlesi* can infect humans upon transmission of the infective-stage sporozoites from the bite of an infective female *Anopheles* mosquito [241]. Once deposited into the dermis, highly motile sporozoites gain entry to the circulatory system by invading dermal blood vessels and migrate to the liver, where they infect hepatocytes and begin the subclinical exo-erythrocytic (liver stage) of the *Plasmodium* life cycle [242]. Over the following 24-48 hours within a parasitophorous vacuole, a single sporozoite can asexually replicate and differentiate into thousands of erythrocyte-infective merozoite forms [243]. Merozoites erupt from infected hepatocytes and are released into the bloodstream. Upon erythrocyte invasion, the symptomatic phase of malaria begins. Within the parasitophorous vacuole in red blood cells, *Plasmodium* parasites transform from ring stage to late trophozoites and finally to schizonts. As a schizont, the parasite divides until it eventually ruptures the erythrocyte; releasing up to 36 merozoites and continuing the erythrocytic cycle [244]. Synchronous erythrocyte lysis results in systemic pro-inflammatory cytokine responses and the characteristic cyclical fevers, nausea, and headaches experienced by *P. falciparum*-infected individuals [244]. Additionally, parasite-infected erythrocytes can adhere to tissue microvasculature endothelial surfaces leading to other severe clinical manifestations [245]. As the number of *Plasmodium* parasites increases exponentially during the asexual replication stage in red blood cells, a small percentage of gametocytes (male and female gamete precursors) differentiate [246]. Gametocytes ingested during a subsequent *Anopheles* blood meal continue the sexual life cycle within the mosquito host. Once within the midgut, gametocytes develop into gametes, fuse and transform into a zygote and eventually an ookinete [247]. The ookinete traverses the midgut wall to transform into an oocyst, where sporozoites differentiate and eventually rupture the oocyst [248]. Finally, sporozoites migrate through the haemocoele to the

salivary glands where they can infect another mammalian host upon a subsequent *Anopheles* blood meal [249]. For a visual depiction of the *Plasmodium* life cycle in the mosquito and human hosts please refer to Figure 1.4

1.3.3 Severe malaria and pulmonary pathology

While *Plasmodium* infection of erythrocytes commonly results in cyclical fevers and anemia, some of the most serious complications of malaria are at the organ level in the brain, placenta and lungs [250-252]. Of the five *Plasmodium* species that infect humans, *P. falciparum* is responsible for a majority of severe malaria infections [244]. Potentially fatal severe malaria infections are diagnosed clinically by vital organ dysfunction in addition to laboratory evidence. For a complete listing of the WHO's official clinical features of severe *P. falciparum* malaria [238], please refer to Table 1.4

Table 1.4 Official WHO clinical manifestations/features of severe *P. falciparum* malaria infections

Clinical features of severe *P. falciparum* malaria [253, 254]
• impaired consciousness (including unrousable coma)
• prostration (i.e. generalized weakness so that the patient is unable to sit, stand or walk without assistance)
• multiple convulsions: more than two episodes within 24 hours
• deep breathing and respiratory distress (acidotic breathing)
• acute pulmonary edema and acute respiratory distress syndrome
• circulatory collapse or shock (systolic blood pressure < 80mm Hg in adults and < 50mm Hg in children)
• acute kidney injury
• clinical jaundice plus evidence of other vital organ dysfunction
• abnormal bleeding

Pulmonary complications such as edema (fluid build up in the lungs) and acute respiratory distress (ARDS) occur in ~20% of severe malaria patients [241, 254-256] and are officially recognized by the World Health Organization (WHO) as archetypal symptoms of the most severe cases of malaria [238, 257]. It is estimated

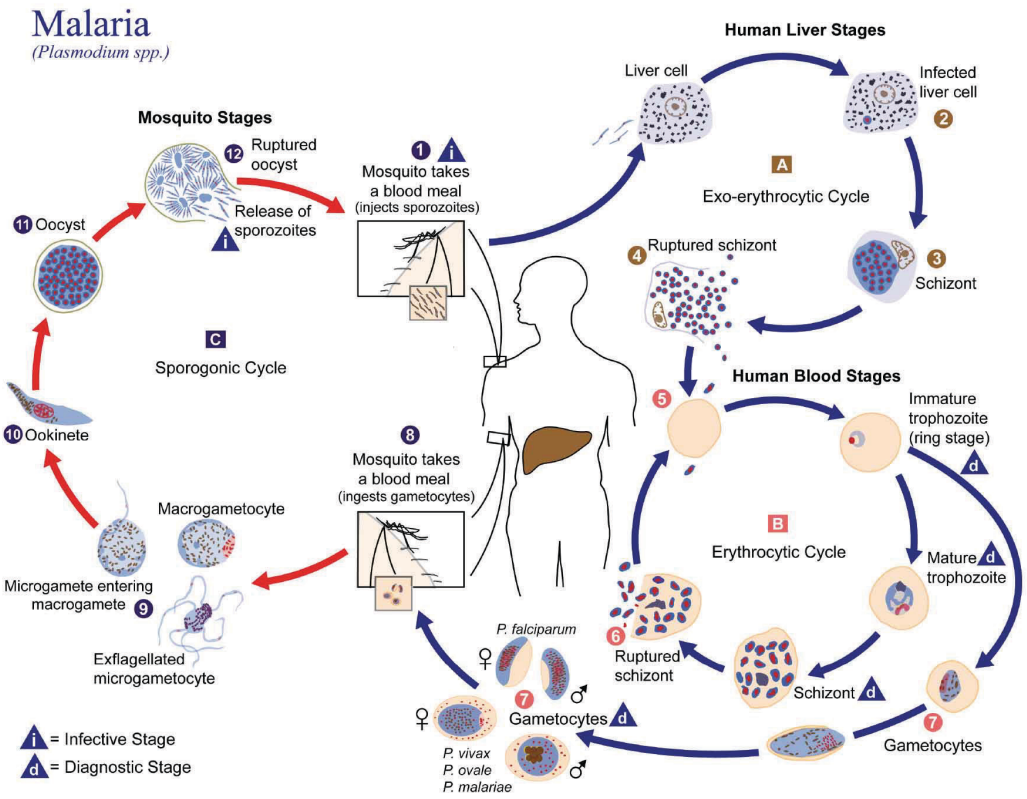

Figure 1.4 *Plasmodium* life cycle
Cartoon depicting the *Plasmodium* life cycle in humans (blue) and *Anopheles* mosquito (red). Mature trophozoites/schizonts of the erthrocytic cycle (B) cytoadhere and sequester to endothelial surfaces within the microvasculature of the placenta, brain, and lungs. Image used with permission: *Centers for Disease Control and Prevention (CDC) - Division of Parasitic Diseases and Malaria (DPDM) Alexander J. da Silva, PhD and Melanie Moser, 2002*

that between 5% and 25% of adults and up to 30% of pregnant women with severe malaria infections develop acute lung injury (ALI) or acute respiratory distress syndrome (ARDS) [241]. Although most prominent in severe *P. falciparum* infections, malaria-induced pulmonary complications have also been associated with severe *P. vivax*, *P. ovale,* and *P. knowlesi* infections [241]. Traditionally, malaria-associated respiratory distress has been attributed to the combined effects of metabolic acidosis, non-cardiogenic pulmonary edema and severe anemia [241, 258]. The respiratory manifestations of malaria infections have also been documented in patients following antimalarial drug treatment, presumably due to host pro-inflammatory responses upon the bolus release of parasite material [254]. However, due to the gravity of cerebral malaria complications, the magnitude of pulmonary manifestations associated with *Plasmodium* infections are commonly overlooked, even though mortality rates among patients presenting with ALI/ARDS exceed 70% [255, 256, 259].

1.3.4 Parasite sequestration

Plasmodium sequestration in small caliber vessels is thought to be the central pathophysiological feature of severe malaria infections [260]. Cytoadherence and sequestration of infected erythrocytes (iRBCs) to the endothelial cell surface within tissue microvasculature impairs circulation and leads to pro-inflammatory immune responses [245, 261-268]. *Plasmodium* sequestration is developmentally advantageous to the parasite because it prevents the recognition and clearance of parasite-containing erythrocytes by monocytes/macrophages in the spleen and affords the parasite time to complete asexual replication within the erythrocyte [263, 267, 269]. The pattern of *P. falciparum* adherence observed in humans is selective in that most sequestration takes place in the lungs, adipose tissue, brain and placenta [270-272]. These adhesion events, largely associated with the malarial trophozoite and schizont life stage, result from interactions between both host and parasite factors [267].

Cytoadherence of infected erythrocytes to endothelial cells has been shown to be dependent on interactions between an array of host- and parasite-derived factors. *P. falciparum* erythrocyte membrane protein 1 (*Pf*EMP1), is the major parasite virulence factor involved in the sequestration of infected erythrocytes and

severe malaria pathology [273-275]. *Pf*EMP1 ligands are a family of highly-variable parasite-produced molecules and a major determinant of malarial antigenic variation encoded by approximately 60 *var* genes [263]. Each *Pf*EMP1 variant is exported to the surface of the infected erythrocyte and endows trophozoite- and schizont-containing red blood cells with the ability to interact with host ligands including chondroitin sulfate A (CSA), the scavenger receptor CD36, intercellular adhesion molecule 1 (ICAM-1; CD54), platelet endothelial cell adhesion molecule 1 (PECAM-1; CD31), and vascular cell adhesion molecule 1 (VCAM-1; CD106) on the luminal surface of vascular endothelium [244, 275-277]. Parasite sequestration in the microvascular compartment is not without consequence, as it results in the impairment of blood flow and local hypoxia as well as endothelial barrier dysfunction leading to edema at sites of heavy parasite burden [278-281]. Cytoadherence of iRBCs to vascular endothelial cells also elicits pro-inflammatory immune responses [281]. In fact, endothelial cell activation by pro-inflammatory cytokines such as TNFα or IL-1β can lead to elevated levels of host adhesion molecules that facilitate *Plasmodium*-binding, thereby further increasing cytoadherence events and parasite burden [282, 283]. While the pathophysiological consequences of parasite sequestration on vascular endothelial cells in the brain and placenta are well documented [250, 260, 280, 284-286], little is known about this process in the lungs.

As described in CHAPTER 1.2.14, CD36 is expressed on early erythrocyte precursors, platelets, monocytes/macrophages, and vascular endothelial cells. CD36 functions in different capacities in a variety of biological systems. In addition to its involvement in the metabolism of low density lipoproteins, CD36 has also been associated with platelet function, innate immunity, the clearance of apoptotic cells, and binding to thrombospondin and a vWF-cleaving protease A Disintegrin And Metalloproteinase with a ThromboSpondin type 1 motif, member 13 (ADAMTS13) [85]. CD36 plays a dual role in the pathogenesis of severe malaria infections [287, 288]. CD36 on the surface of monocytes/macrophages facilitates phagocytosis and clearance of iRBCs through binding to *Pf*EMP1 [289], while CD36 on platelets/endothelial cells facilitates parasite cytoadherence and sequestration to the surface of the vascular endothelium [264, 290]. Even though CD36-mediated parasite sequestration occurs in the brain and the lungs, the underlying mechanisms differ. Interestingly, cerebral vascular endothelial cells do not express CD36 on their surface. CD36-expressing platelets mediate cerebral parasite sequestration by bridging the

gap between activated vascular endothelial cells decorated with von Willebrand factor (vWF) and iRBCs bound via CD36-*Pf*EMP1 interaction [291, 292]. Within the lungs, CD36 is the major host factor associated with parasite sequestration to the vascular endothelium and directly facilitates iRBC sequestration [264, 278, 288, 293, 294]. From the perspective of the host, adherence of parasitized erythrocytes to the pulmonary vasculature is not a benign event, as some injury results from receptor-ligand interactions that trigger changes in barrier integrity [278]. In addition, there is a strong positive correlation between the level of parasite burden in the lungs and the degree of ALI [295, 296]. However, our understanding of the contribution that CD36-mediated sequestration of malaria-infected erythrocytes within the lung microvasculature makes to pulmonary distress is limited.

1.3.5 Innate immune responses to malaria

Malaria induces a robust innate immune response that plays an important role in limiting parasite load through mechanisms that direct phagocytic cells to engulf and kill parasites as well as by initiating the development of an appropriate T cell-mediated effector response [248, 297]. Severe malaria infections are characterized by elevated serum TNFα, IL-1, IL-6, IL-8, IL-4, IL-10, and IFNγ concentrations, which correlate with the severity of infection [241, 298]. In addition, chemokines implicated in the recruitment of myeloid cells and granulocytes such as macrophage inflammatory protein 1α (MIP-1α; CCL3), MCP-1 (CCL2), monokine induced by gamma interferon (MIG; CXCL9) and IL-8 are also detected in severe malaria patients [299]. This systemic pro-inflammatory cytokine and chemokine milieu is indicative of an immune environment supporting mononuclear phagocyte M1 polarization. Not surprisingly, monocytes/macrophages have been shown to be critical innate immune cells responsible for the uptake and clearance of iRBCs [300]. Macrophage/monocyte innate immune responses are important in the control of primary malaria infections as these mechanisms function to limit the maximal level of circulating parasite via clearance mechanisms.

Monocytes and macrophages are able to recognize PAMPs associated with *Plasmodium*-infected erythrocytes or *Plasmodium*-derived products through their vast array of PRRs (as described in CHAPTER 1.2.11). TLRs localized to the cell surface and within endosomes recognize *Plasmodium*–derived PAMPs.

For example, TLR1/2 recognizes *Plasmodium* GPI ligands [301], TLR4 recognizes *Plasmodium* microparticles [302], while TLR9 recognizes *Plasmodium* CpG DNA [303]. In addition, parasite-associated DAMPs including *Plasmodium* DNA are sensed by the cytosolic NALP3 and AIM2 inflammasomes leading to the release of IL-1β and IL-18 [304-307]. Hemozoin, the insoluble black-brown crystalline digestion product of *Plasmodium* hemoglobin metabolism, is generated to protect the parasite from the toxic effects of free heme [308, 309]. Also referred to as "malaria pigment", hemozoin crystals are highly stable compounds that are able to modulate cytokine production and the function of monocytes and macrophages upon phagocytic ingestion [310, 311]. Monocytes and macrophages are the major cell types associated with opsonic and non-opsonic phagocytosis and clearance of *Plasmodium*-infected erythrocytes, free parasites, and parasite-derived material. Opsonic phagocytosis is largely mediated through via complement receptors (CR1) [312, 313], and by activating (FcγRI and FcγRIIIa) [314] and inhibitory (FcγRIIb) [315] Fc-receptors (although not applicable for innate phase of primary infection). Non-opsonic phagocytosis is mediated through CD36 engagement of *Plasmodium*-derived molecules on the surface of iRBCs such as *Pf*EMP1 [84, 289]. While myeloid cells are certainly important players in the clearance of infected erythrocytes, lymphoid cells also contribute to innate immune responses. NK cells and γδT cells play important roles as they provide early sources of IFNγ needed to polarize mononuclear phagocytes towards M1 activation thereby increasing phagocytic and microbial killing activity [316-318]. Still, the contributions that innate molecular and cellular responses make to the control of lung injury are not clear.

1.3.6 Outstanding questions

Although the lungs are known to be sites of severe malaria-associated complications within the clinical setting [241, 253, 256, 257, 259, 261, 319-323], there are still serious gaps in the understanding of the cellular and molecular mechanisms that mediate malaria-associated lung injury. Therefore, there is a significant need to define the role that pulmonary inflammation plays in the morbidity and mortality associated with *Plasmodium* infections. While some malaria-associated pulmonary damage results when *Plasmodium*-infected erythrocytes cytoadhere to the vascular endothelium [278], the contributions that innate immune responses make to malaria-associated ALI are still not clear. AMs have been implicated in the pathogenesis of non-malarial ALI and ARDS [324], yet their role in malaria associated-ALI/ARDS

remains to be investigated. Inflammatory monocytes are key phagocytic cells during innate immune responses as $CD11b^{high}Ly6C^{+}$ cells are central to the clearance of infected-erythrocytes in the spleen, resulting in a partial control of peripheral blood parasitemia [325]. However, the role that blood monocytes and tissue-resident macrophages play in the regulation of parasite burden in the lungs and malaria-induced pulmonary damage has not been defined.

1.3.7 Hypothesis

The ***hypothesis*** to be tested is that lung-resident and recruited monocytes/macrophages control pulmonary pathology and inflammation by clearing sequestered parasites from the microvasculature endothelial surface, therefore maintaining lung homeostasis and function during *Plasmodium* infections.

1.3.8 Approach

Due to the inherent difficulties of studying *P. falciparum* sequestration in the intact lungs of humans, murine models, most of which employ *P. berghei* infection have been developed [288, 295, 326-330]. While, no single animal model can completely reproduce all the hallmarks of severe malaria infections in humans, we employed the *P. berghei* ANKA infection in C57BL/6J inbred mouse strain as a mouse model for severe human malaria infections (Figure 1.5) [293, 331-334]. When infected with *P. berghei,* C57BL/6 mice succumb due to complications of cerebral malaria (CM) with a median survival of approximately 6.5 days (Figure 1.5C) [335]. As has been previously reported, *P. berghei* infected C57BL/6 mice also exhibit other pathologies common amongst severe *P. falciparum* patients including acute lung injury (ALI), acute respiratory distress disorder (ARDS) and pulmonary edema [293, 331, 336]. During the asexual reproductive erythrocytic stage, changes in morbidity measures such as loss of body mass and temperature are evident (Figure 1.5D, 1.5E), in addition to lethargy, piloerection, huddling, and labored breathing while peripheral blood parasitemia levels increase to approximately 15-20% prior to death (Figure 1.5B) [333]. This mouse model of severe human malaria infection enables us to elucidate the

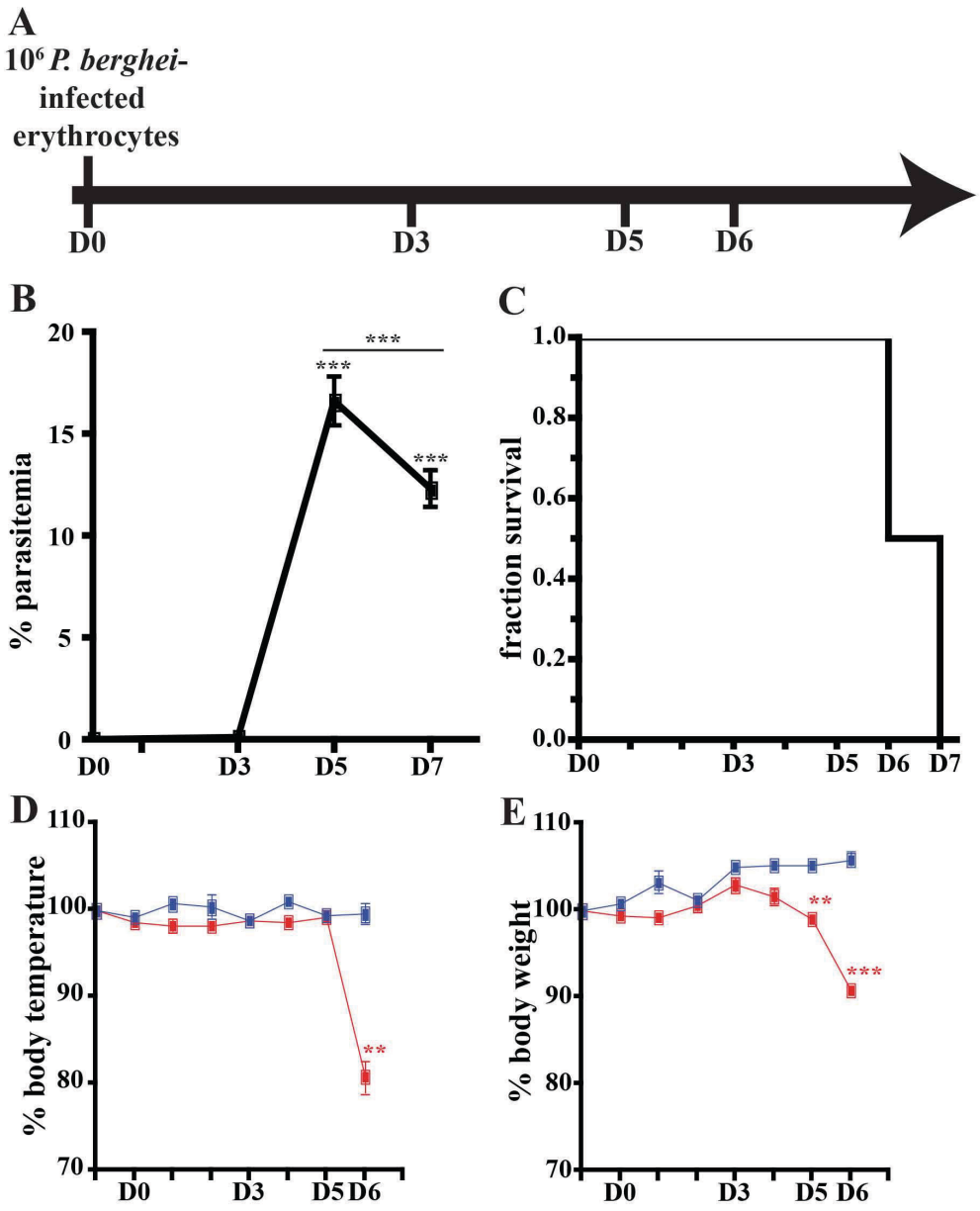

Figure 1.5 Introduction to the *Plasmodium berghei* mouse model of severe malaria. (A) Timeline illustrating the experimental design including parasite infection (D0) of C57BL/6 mice and sample collection times (D3, D5, D6). (B) Peripheral blood parasitemia following *P. berghei* infection (n=3). (C) Fraction survival following *P. berghei* infection (n=12). Normalized body temperature (D) and body weight (E) of un-infected controls (blue line) and following *P. berghei* infection (red line) (n=10). All comparisons versus D0 controls unless noted by line. ** $p < 0.01$, *** $p < 0.001$.

dynamics and function of the cellular players involved in the host's innate immune response to *Plasmodium* parasite sequestration in the lungs (please see Figure 1.5A for experimental design).

Similar to *P. falciparum*, *P. berghei* schizont-containing erythrocytes sequester in the lungs and adipose tissue via interactions with CD36 [266, 288, 295]. Using the *P. berghei* model, it has been demonstrated that sequestration in the lungs, in addition to avoiding clearance in the spleen, has the added benefit of promoting parasite growth [326, 337]. In *P. berghei*, there is no *Pf*EMP1 ortholog, however the parasite-expressed protein SMAC, a conserved rodent malaria protein of unknown function, is transported to the erythrocyte cytoplasm and has been implicated in the sequestration of infected erythrocytes along endothelial surfaces [326]. Not surprisingly, SMAC expression is highest during schizont development [326]. Several studies have demonstrated that CD36 is the major host factor involved in *P. berghei* sequestration to the lungs, spleen and adipose tissue [264, 266, 278, 288, 290]. However, our understanding of the contribution that the intense sequestration of malaria-infected erythrocytes within the lung microvasculature makes to pulmonary distress remains limited.

1.4 EMPHYSEMA

1.4.1 Public health significance

According to the World Health Organization (WHO), chronic obstructive pulmonary disease (COPD) is currently the world's fourth leading cause of death effecting 60 million people worldwide and leading to 3 million deaths per year [338]. The WHO predicts that COPD will increase to the third leading cause of death worldwide by 2030, only behind ischemic heart disease and stroke [338, 339]. COPD was the ninth highest global cause of DALYs lost in 2010 (out of 291 diseases and injuries) [239]. When parsed based on geographic region, COPD ranked as second highest cause of DALYs lost within high income North America, third in East Asia, and fifth in South Asia [239]. According to the Centers for Disease Control and Prevention, COPD ranked as the third leading cause of death in the US in 2011 [340]. An estimated 15 million Americans have been diagnosed as having COPD; however, it is appreciated that this figure is

certainly an underestimate, as 50% of Americans diagnosed as having low pulmonary function were even aware that they have COPD [341, 342].

1.4.2 COPD definitions

COPD is a progressive lung disease comprised of two main conditions, chronic bronchitis and emphysema both characterized by the impairment of airflow in the lower airways, making expelling air difficult, resulting in labored breathing and shortness of breath [343]. Chronic bronchitis is defined as prolonged inflammation of the bronchi and bronchioles leading to swelling, irritation, and increased mucus production [344]. Emphysema is defined as progressive airspace enlargement due to alveolar tissue destruction [345] (Figure 1.6A). Progressive loss of alveolar epithelial cells (AEC) greatly impacts the lung architecture and function, resulting in fewer larger airspaces, a loss of surface area, and impaired gas exchange [344]. Although associated with chronic bronchitis under the umbrella of obstructive lung disease, the work presented in CHAPTER 3 focuses on macrophage dynamics and function in an elastase-driven emphysema model, therefore this introductory material will concentrate on emphysema and its underlying mechanisms (where appropriate).

1.4.3 Clinical features of COPD

Cardinal features of COPD include severe immune cell infiltration of the muscosa and submucosa, increased mucus production, epithelial cell hyperplasia, and dysregulated tissue repair mechanisms [343]. Increased sputum production and long lasting cough are among the most common symptoms of COPD, however, acute breathlessness or dyspnea is the most debilitating feature of severe COPD [345]. Individuals suffering from emphysema present with an impairment of lung emptying upon expiration, with no impact on inspiration [346]. Due to alveolar wall and matrix destruction the lung loses elasticity and recoil ability, resulting in elevated lung compliance (a measure of lung elasticity; change in lung volume for a given change in pressure) [347]. Upon deficits in lung elasticity, more air becomes trapped within the lungs (hyperinflation) and greater effort is required to expel air from the lower airways, leading to shortness of breath and tiredness [348].

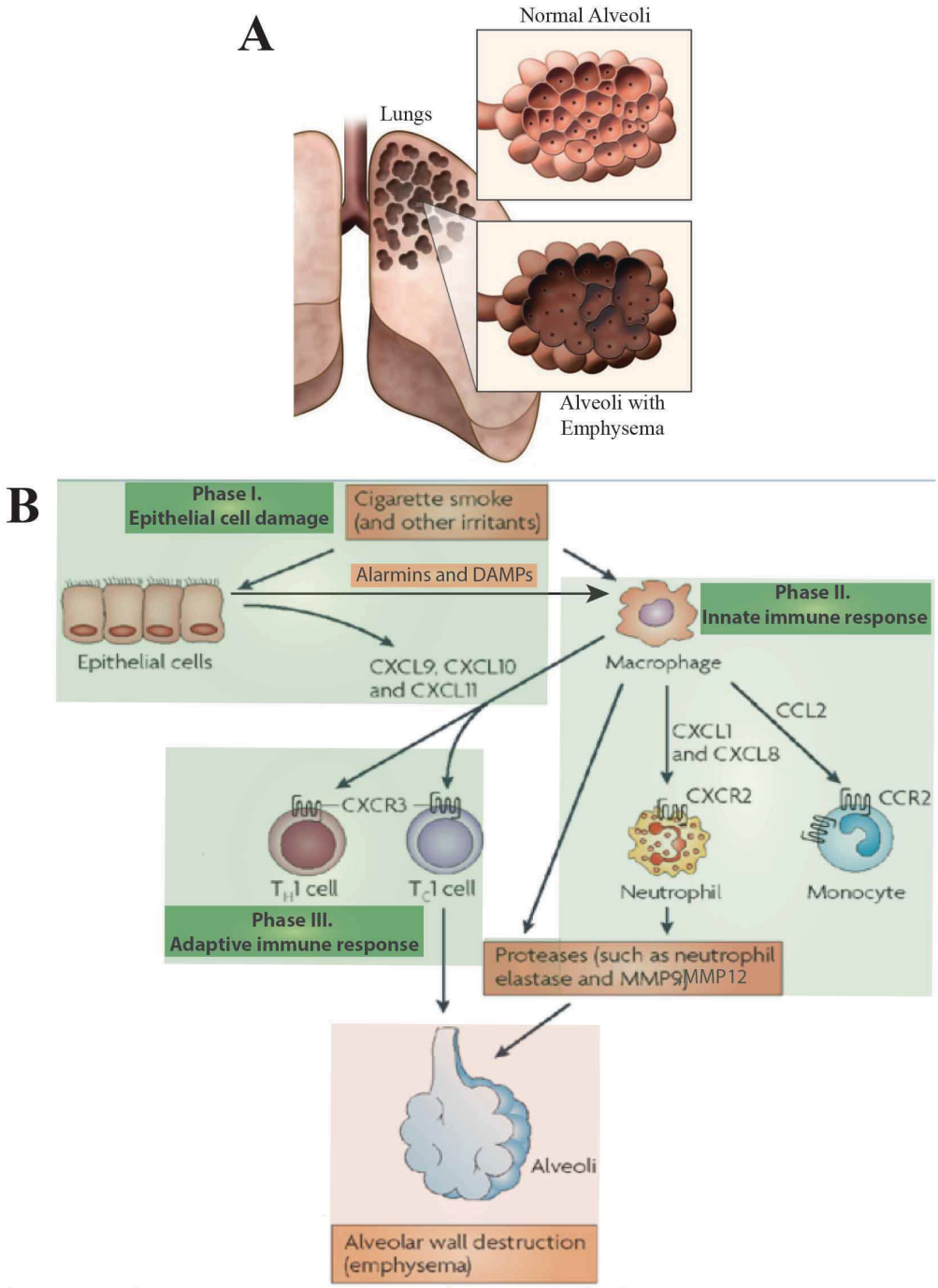

Figure 1.6 Major phases and cellular players in pathogenesis of emphysema
(A) Cartoon illustrating the loss of surface area for gas exchnage foloowing alveolar wall destruction Granted permission from: Taraseviciene-Stewart, L. 2008. Journal of Clinical Investigation 118:394.
(B)Cartoon illustrating the major events and cellular players involved in the initiation and progression of emphysema.
Adapted by permission from Macmillan Publishers Ltd: Nature Reviews Immunology. Barnes PJ: **Immunology of asthma and chronic obstructive pulmonary disease**. Nature Reviews Immunology 2008, 8(3):183-192., copyright 2008.

The degree of lower airway obstruction can be quantified using FEV1% or the Tiffeneau-Pinelli index, a spirometric measurement of lung function defined as the ratio of forced expiratory volume in 1 second (FEV_1) (volume exhaled in first second after full inhalation) to the forced vital capacity (FVC) (total volume exhaled after full inhalation) normalized to a predicted value based on the patient's age, sex, height, and body type [342]. COPD prevalence rates are diagnosed and scored based on the Global Initiative on Obstructive Lung Disease (GOLD) airflow obstruction severity index: with stage 1 (mild): $FEV_1 \geq 80\%$ predicted; stage 2 (moderate): FEV_1 50-80% predicted; stage 3 (severe): FEV_1 30-50% predicted; and stage 4 (very severe): $FEV_1 \leq 30\%$ predicted [346]. According to a meta-analysis, the global prevalence of COPD estimated by spirometric definitions is 9.2% [349]. The most common treatments for COPD are administration of daily inhaled β_2-agonist bronchodilators, anti-cholinergics and corticosteroids in addition to ventilation support through oxygen supplementation and smoking cessation [345, 346]. While these pharmacologic and non-pharmacologic interventions are aimed to relieve the symptoms and reduce the risk of disease progression, exacerbations, or mortality, to date, there is no emphysema-specific clinical course of treatment.

1.4.4 Risk factors

There are a variety of environmental exposures as well as genetic predispositions that are associated with the onset of progressive emphysema. Smoking tobacco is by far the predominant risk factor associated with emphysema; with tobacco smokers accounting for ~80% of all emphysema cases [343, 350]. Other environmental risk factors such as exposure to air pollution (outdoor, indoor, and occupational), second hand smoke, maternal smoking, respiratory infections, other non-respiratory infections (including HIV [345]), childhood asthma, hypersensitivity pneumonitis, and exposure to dust and fumes have also been associated with emphysematous changes to the lungs [343, 350, 351]. While environmental exposures are important, there are also several genetic predispositions associated with the progression of emphysema. For example, α1 antitrypsin deficiency (A1AD) is responsible for ~1-2% of COPD cases [352, 353]. A1AD is a congenital deficiency in α1 antitrypsin (A1AT), the major inhibitor of neutrophil elastase, leading to an imbalance between the activity of proteases and anti-proteases in the lungs and progressive airway enlargement. In addition, a macrophage metalloproteinase 12 (MMP12; macrophage elastase) single

nucleotide polymorphism (SNP) found in the promoter region of the minor allele (-82A->G) is a protective factor for COPD in adult smokers [354]. As more SNP and genome-wide association studies are conducted, a more complete picture of the molecular factors involved in the progression of emphysema will be revealed.

1.4.5 Pathogenesis/pathophysiology

The development of progressive lung airway destruction should be considered an immunological disorder [344]. Broadly, the progression of emphysema pathogenesis can be divided into three major phases: epithelial cell damage, innate immune responses, and adaptive immune responses. Forthcoming, a broad stroke overview will identify some of the major events associated with the progression of emphysema. In addition, several of the major immune cellular players contributing to the pathogenesis of emphysema will be highlighted. For an illustrated depiction underscoring these events please refer to Figure 1.6B.

Initially, tobacco smoke or other pulmonary irritants directly injure or stress alveolar epithelial cells [355]. The compounds in cigarette smoke can also directly breakdown the lung's extracellular matrix (ECM) [356]. AEC cellular damage leads to the release of DAMPs and other danger signals [64]. These products can act as TLR ligands and activate TLR2 and TLR4 signaling [64], while cigarette smoke also directly activates endosomal TLR9 [357]. Upon activation by DAMPs and TLR ligands, AECs and lung macrophages stimulate NF-κB, the main pro-inflammatory transcriptional regulator associated with the progression of emphysema. NF-κB activation results in the release of innate/early inflammatory cytokines such as TNFα, IL-1β, and IL-8 [358]. IL-1β release activates alveolar macrophages and induces release of the neutrophil recruiting chemokine, IL-8 [359]. These initial cytokine and chemokine bursts lead to recruitment of inflammatory cells such as neutrophils, monocytes, and DCs to the lungs.

Upon recruitment to the lungs, inflammatory cells release proteases (elastolytic enzymes) and reactive oxygen species (ROS), which can damage the lung tissue further [360, 361]. Typically these inflammatory processes are kept in check with a wide array of regulatory mechanisms, however, when they are not appropriately controlled by the cadre of anti-proteases [362, 363] and anti-oxidants factors (catalases,

superoxide dismutases, peroxidases) [361], the initial pro-inflammatory response ends up leading to further tissue damage and an uncontrolled positive feedback loop. It is posited that upon cellular damage and irritant-induced necrosis, immature lung DCs take up self-antigens (such as elastin fragments) released upon lung damage or AEC cell death [364] and migrate to the draining lymph nodes where they present antigen to naïve T cells and direct $CD4^+$ differentiation towards a T_H1 program via IL-12 signaling. T_H1 antigen-specific $CD4^+$ and T_c1 $CD8^+$ T cell populations, as well as B cells, subsequently enter the lungs to remove the source of antigen, leading to progressive tissue destruction [365].

1.4.6 Innate immune responses: role of neutrophils

Emphysema is characterized by neutrophilic airway inflammation as these innate immune cells can be detected in the sputum of COPD patients and their numbers correlate with the severity of disease [344, 366, 367]. Neutrophils can be recruited through the release of CXCR2-signaling chemokines interleukin-8 (IL-8; CXCL8) and growth related oncogene alpha (GRO-α; CXCL1), as well as leukotriene B_4 (LTB_4) by lung macrophages and epithelial cells [55] [368, 369]. Upon recruitment and activation, neutrophils become highly phagocytic, secrete serine proteases including neutrophil elastase, cathepsin G, proteinase-3, and MMPs (MMP8 and MMP9), and release myeloperoxidase (MPO) and human neutrophil lipocalin containing granules [370]. In addition, neutrophils can also release their nuclear material in the form of neutrophil extracellular traps (NETs) that act as a physical barrier in order to trap pathogens or patch damaged areas [371]. Although highly active, neutrophils have a very short lifespan, estimated to be 11.4 hours [194]. Following secretion of effector molecules, neutrophils undergo apoptosis and are phagocytosed by macrophages [372]. Despite their association with disease severity, the exact role of neutrophils in the pathogenesis of alveolar tissue destruction remains unanswered.

1.4.7 Innate immune responses: role of macrophages/monocytes

Recent findings have directed attention to the major role that lung macrophages play in the orchestration of immune responses that lead to the progression of tissue destruction [55, 373]. Severe COPD patients are characterized by elevated numbers (5 to 10 fold) of LMs in the lung parenchyma, airways, BAL, and

sputum [360]. Similar to neutrophils, the severity of COPD correlates with lung macrophage numbers [374]. LMs can indirectly impact the progression of emphysema by releasing cytokines and chemokines to recruit other immune cells such as neutrophils, monocytes, and $CD8^+$ T cells into the lungs. Macrophages recruit monocytes via the release of monocyte chemotactic protein 1 (MCP-1; CCL2) [55], and $CD8^+$ lymphocytes by interferon-γ inducible protein 10 (IP-10, CXCL10), monokine-induced by interferon-γ (MIG, CXCL9), and interferon-inducible T-cell α-chemoattractant (I-TAC, CXCL11) [55]. As mentioned above, lung macrophages/monocytes clear apoptotic neutrophils through phagocytosis; in addition, they also clear apoptotic AECs in emphysematous lungs [91, 375]. Most importantly to the pathophysiology of emphysema, LMs secrete a wide variety of effector molecules that contribute either directly to tissue destruction or by promoting sustained inflammation [55, 373, 376]. For example, lung macrophages secrete elastolytic proteases such as matrix metalloproteinase 9 (MMP9) and MMP12 (macrophage elastase) that can directly lead to ECM degradation by cleaving collagen or elastin fibers, resulting in a loss of normal alveolar structure [363, 377]. In particular, MMP12-deficiency has been shown to be protective from cigarette smoke induced emphysema in mice [378]. For a more complete description of macrophage-derived effector molecules relevant to the pathophysiology of emphysema, please refer to Table 1.5.

Table 1.5 Macrophage effector molecules involved in the pathophysiology of emphysema

Effector Molecule Class	Example of Effectors	Role in Pathophysiology of Emphysema [55, 360, 373]
Cytokines and Chemokines	TNFα, IL-1β, IL-8, IL-10, MCP-1, GRO-α, I-TAC, IP-10, MIG	Activation of other cell types. Recruit neutrophils, monocytes and T cells to the lungs.
Elastolytic Enzymes	MMP-2, MMP-9, MMP-12, cathepsin K, L, S, neutrophil elastase	Cleavage of ECM components: elastin and collagen.

Growth Factors	TGFβ1	Stimulates fibroblasts to proliferate causing fibrosis of the small airways.
Lipid Mediators	Leukotriene LTB_4; Prostaglandin PGE_2	LTB_4: recruits neutrophils and promotes adhesion of inflammatory cells to the endothelium. PGE_2: bronchodilator and stimulates mucus secretion.
Reactive Oxygen Species	superoxide anion ($O_2\bullet^-$)	Precursor to other ROS (H_2O_2, •OH, HOCl). Anti-microbial killing, mediates cellular damage and stimulates pro-inflammatory TFs (MAPK, NF-κB, and AP-1).
Reactive Nitrogen Species	NO	Precursor to other RNS ($ONOO^-$). Antimicrobial killing and mediates cellular damage.

1.4.8 Adaptive immune responses: role of DCs and T cells

While cigarette smokers have elevated lung DC numbers [379], their impact on progressive alveolar tissue destruction still remains unclear. As DCs promote antigen-specific T cell responses, it is speculated that lung DCs may take up self-antigens following AEC damage [345], however no specific autoimmune responses have been reported. A possible emphysema-driving antigen could be introduced in cigarette smoke; the tobacco-derived α-glycoprotein has been described as being a highly immunogenic [380]. Still, the specific role that dendritic cells play in the pathogenesis of lung tissue destruction and emphysema is largely unknown.

CCL5 (RANTES) is greatly upregulated in the sputum of individuals with COPD, attracting $CD4^+$ and $CD8^+$ T cells to the lungs via CCR5 [381]. In addition, $CD4^+$ T cells are recruited to the lungs via the chemokines (IP-10, MIG, and I-TAC) which all signal through CXCR3 [365, 381, 382]. While the $CD4^+$ T cell population is largely T_H1 cells [365], there are some regulatory $CD4^+CD25^+Foxp3^+$ (T_{regs}) and T_H17 cells that also reside within the lungs. The exact function these T_{regs} and T_H17 cells remains unclear. $CD8^+$ T cells greatly outnumber the $CD4^+$ T cell population in the lungs during the progression of emphysema [383]. $CXCR3^+$ IFNγ-producing type I cytotoxic $CD8^+$ T cells (T_c1) [365] up-regulate expression of FasL,

perforin and granzyme B [384], so have the potential for cytotoxic killing of type I AEC. $CD4^+$ and $CD8^+$ T cell populations are actively recruited to the lungs by lung macrophages releasing chemokines in response to IFNγ [55]. Activated T_H1 cells release more IFNγ inducing further chemokine signaling from activated macrophages and establishing a positive feedback loop. The exact role and mechanisms for the pathogenesis of emphysema that T cells contribute is still uncertain.

1.4.9 Imbalances contributing to emphysema

Emphysema can be characterized as a disease of immunological imbalances. In particular, there are three arenas that have been identified as contributing to the progression of tissue destruction: imbalance in protease/anti-protease activity, imbalance in oxidant/anti-oxidant activity, and imbalance in lung structure maintenance program. Typically a delicate balance is maintained in these three arenas, however upon initial lung damage induced by cigarette smoke or other pulmonary insult, a dysregulation occurs and the balances are tipped. Together these imbalances may contribute to progressive alveolar wall destruction and airway enlargement. Therefore, understanding the underlying mechanisms responsible for these imbalanced states is key to the pathophysiology of emphysema. For an overview of the molecular factors involved in these imbalances, please refer to Table 1.6.

The action of proteases and anti-proteases in the lungs are both necessary to maintain homeostasis, therefore, it is critical to preserve a balance between their activities. A multitude of enzymes such as elastases, MMPs, cathepsins, caspases, and collagenases can all lead to the degradation of the extracellular matrix (ECM) in the lungs [363, 377]. Typically these enzymes are deployed in order to aid in wound repair processes, embryonic development, promoting fibrosis, and angiogenic remodeling [362]. Due to the dire consequences of their elastolytic and proteolytic activities, proteases are tightly regulated with a cadre of anti-proteases that protect the lungs from long term uncontrolled protease activity. However, in the case of α1-antitrypsin deficiency, this protease/anti-protease balance is no longer maintained and individuals with A1AD develop spontaneous emphysema [352, 353]. Upon exposure to tobacco smoke or other lung irritants, the balance between proteolytic activity and the activity of their inhibitors shifts [362]. This imbalance can result from either increased proteolytic activity (neutrophil elastase, cathepsins, MMPs) or

from deficiencies in anti-proteases (α1-antitrypsin, secretory leukoprotease inhibitor (SLPI), tissue inhibitors of metalloproteinases (TIMPs)) [360]. While there are many MMP family members, only MMP2 (gelatinase A), MMP9 (gelatinase B), and MMP12 (macrophage elastase) are able to cleave elastin [363]. In order to maintain tissue homeostasis, these elastolytic proteases are generally controlled by secreted TIMPs, which bind to MMPs in a 1:1 ratio and inhibit their activity [385]. However, the activity of anti-proteases like α1-antitrypsin and SLPI can be negatively impacted by oxidative stress [386-388].

Reactive oxygen species are a hallmark of innate immune responses. Like protease activity, a balance must be reached between oxidants and anti-oxidants in the lungs in order to maintain homeostasis. Activated neutrophils, macrophages, and AECs can generate strong oxidants such as super oxide anion ($O_2\bullet^-$; generated by NADPH oxidase) that can be converted to hydrogen peroxide (H_2O_2; generated by superoxide dismutase (SOD)), hydroxyl radical (•OH; in the presence of free iron), peroxinitrite ($ONOO^-$; in the presence of macrophage-derived nitric oxide), and hypochlorous acid (HOCl; in the presence of neutrophil-derived myeloperoxidase) [360-362]. These powerful oxidants must be defended against as they can induce significant damage to DNA, proteins, and lipids. Enzymatic anti-oxidants such as catalase, SOD, and glutathione (GSH) peroxidase can counteract the effects of oxidants in the lungs [361]. In addition, non-enzymatic scavengers such as reduced glutathione, vitamin C, and mucins can also counteract the activity of ROS/RNS [362]. In addition, the transcription factor nuclear factor-like 2 (Nrf2), is responsible for the regulation of glutathione peroxidase 2, an antioxidant, by binding to the anti-oxidant response element (ARE) [389]. $Nrf2^{-/-}$ mice are more susceptible to the effects of cigarette smoke (CS) exposure and develop exacerbated emphysema due to loss of oxidant/anti-oxidant balance [390, 391]. Imbalances in oxidants/anti-oxidants can directly lead to AEC damage and increases in pro-inflammatory mediators generated by AECs and LMs [362].

An imbalance in tissue repair mechanisms may contribute to the pathophysiology of emphysema. The lung structure maintenance program requires a balance between cell loss and cell regeneration [392, 393]. In order for balance to be maintained efficient clearance and replacement mechanisms must be in place. Stem cells must substitute for apoptotic cells in order for normal cell turnover to occur and to maintain tissue

structural integrity. In the lungs, vascular endothelial growth factor (VEGF), produced by LMs and type II AECs [394], is one factor that promotes the survival of capillary endothelial cells and AECs [395]. However, pulmonary VEGF and VEGF receptor 2 (VEGFR2; Flk-1/KDR) expression levels are diminished in COPD patients [396]. To that end, experimental VEGFR2 blockade [397] and lung-conditional VEGF-deficiency [398] lead to airspace enlargement and emphysema through elevated apoptosis. Growth factors such as VEGF contribute to lung tissue structural and functional homeostasis, while disruption of the maintenance program (via interactions with other imbalances such as exacerbated protease activity or oxidative stress) can lead to progressive tissue destruction. Cell death, which occurs under a variety of scenarios, is the accepted cause for emphysema. It is imperative to gain further understanding how interactions between the stress pathways (protease/oxidant/maintenance) can impact the pathophysiology of emphysema.

Table 1.6. Imbalances contributing to pathogenesis of emphysema

Imbalance	Major Players	
Protease/anti-protease	Proteases: Neutrophil Elastase, Cathepsins, MMPs	Anti-proteases: α1-AT, SLPI, TIMPs
Oxidant/anti-oxidant	Oxidants: $O_2\bullet^-$, H_2O_2, •OH, HOCl, $ONOO^-$	Anti-oxidants: catalase, SOD, peroxidases, Nrf2
Lung structure maintenance	Tissue destruction: apoptosis, matrix proteolysis, oxidative stress	Tissue regeneration: growth factors (VEGF, TGFβ1), anti-protease (α1-AT), anti-oxidant (Nrf2)

1.4.10 Outstanding questions

There are still many questions surrounding the mechanisms underlying the pathophysiology of emphysematous changes to the lungs. For example, while tobacco smoke exposure is highly correlated with the progression of emphysema, not all long-term heavy smokers develop emphysema. Therefore, there must be other underlying factors that either protect or promote alveolar wall destruction upon environmental insult. Furthermore, the distribution of tissue destruction within the lungs of an emphysema

patient is not necessarily uniform; there may be micro-environmental differences that account for this disease heterogeneity. Also, it is essential to understand how emphysema differs from other pulmonary inflammatory conditions that recruit large numbers of inflammatory cells (such as ALI), as these conditions self-resolve and do not lead to alveolar wall destruction. It is clear that there are many cellular and molecular factors involved in this complex biological process leading to progressive alveolar wall destruction, therefore given their longevity and their ability to mediate inflammation long after acute insults in the study presented in CHAPTER 3, we will focus on the role of lung macrophages on the progression and manifestation of emphysematous changes to the lungs.

It has been reported clinically and experimentally that there is significant expansion in the number of macrophages within the emphysematous lung. In human studies, several reports have shown increases in the number of LMs ranging from 5-10 fold up to 25 fold compared to non-emphysematous smokers with a similar exposure to tobacco smoke [399]. In addition, LMs have been shown to specifically localize near areas of alveolar wall destruction [400, 401]. Lastly, studies have shown that the number of LMs correlates with the degree of emphysema progression [374]. To date, the explanations provided for increased numbers of LMs have been centered on the possibility that additional cells are actively recruited from blood monocyte pools [402, 403], or are holdovers from prolonged macrophage survival or impairment of clearance mechanisms [404]. Interestingly, while the idea of local resident lung macrophage proliferation in the context of emphysema has been proposed in the past [224], the idea of terminally differentiated tissue macrophages proliferating is still not commonplace. In light of the recent paradigm shifts in macrophage biology discussed in CHAPTER 1.2.27, we set out to characterize the dynamics and function of the LM population during emphysematous changes in the lungs. The purpose of the research presented in CHAPTER 3 is to more clearly understand the role that lung macrophages play in the progression and manifestation of emphysematous changes to the lungs.

1.4.11 Hypothesis

The ***hypothesis*** to be tested is that lung-resident macrophages become activated and proliferate, without input from blood-derived monocyte populations, during acute elastase challenge and contribute towards the progression of emphysematous changes in the lungs.

1.4.12 Approach

The porcine pancreatic elastase (PPE) murine model of emphysema has been used since the protease-antiprotease theory was first proposed in the 1960s [353]. Direct instillation of PPE and other proteases such as papain and neutrophil elastase have been used to model human emphysema [405, 406]. The PPE mouse model of human emphysema allows researchers to quickly, potently, and reproducibly activate a cascade of events that occurs in human populations, by tipping the balance between protease and anti-protease activity in the lungs. The elastolytic murine models are much more attractive to the investigator as they are faster and more reliable than cigarette smoke (CS) model of emphysema. Porcine pancreatic elastase (PPE) is a serine protease that cleaves elastin fibers of the extracellular matrix (ECM). The ECM is composed of a dense fibrous network of elastin and collagen surrounding the alveoli and lung capillaries and allows the alveoli to stretch upon inspiration. In a healthy undamaged lung, the surrounding elastin fibers will stretch upon inspiration and cause the alveolus to contract upon expiration forcing out the carbon dioxide. However, in the case of emphysema, damage caused by elastolytic enzymes such as PPE, neutrophil elastase and MMPs impairs the elasticity of the alveoli, thereby leading to pulmonary obstruction. For an overview of the experimental design and histological and cellular dynamics typical of the PPE model of emphysema, please refer to Figure 1.7 (data previously incorporated into doctoral dissertation [407])**.** In addition to monitoring the progression of emphysema by lung structure assessments, pulmonary function tests (PFTs) can be employed to quantify and characterize the impacts of alveolar wall destruction at the tissue level. For an overview of the PFTs employed to assess the progression of emphysema in the PPE model, please refer to Table 1.7. Exogenous administration of this highly potent enzyme, PPE, acts as a spark plug or mimic for the protease imbalance elicited upon prolonged exposure to tobacco smoke in the lungs. The PPE model provides a reliable framework in order to probe the nature and dynamics of immune cell populations in the progression of emphysematous changes to the lungs.

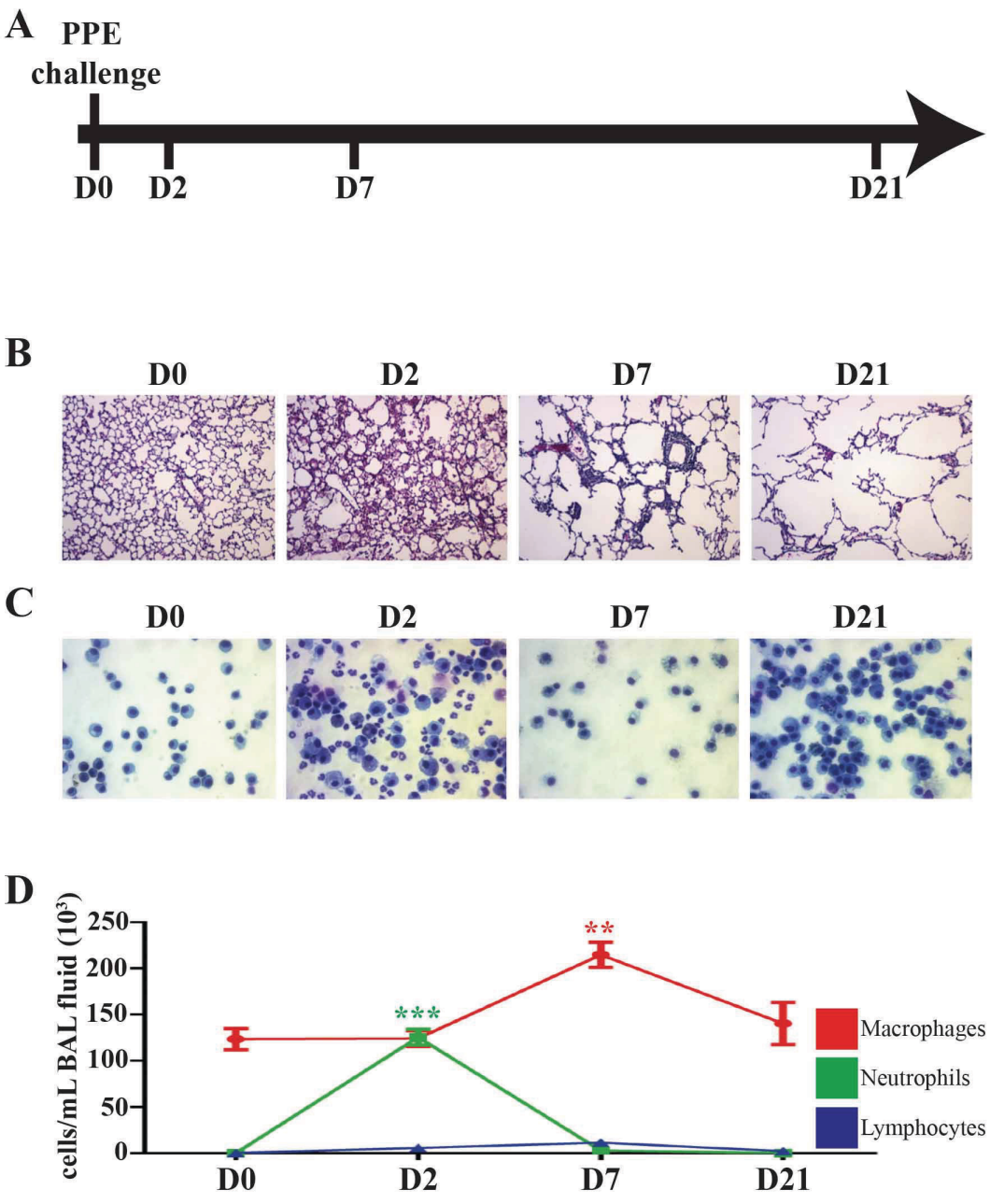

Figure 1.7 Introduction to the porcine pancreatic elastase (PPE) murine model of emphysema. (A) Timeline illustrating the experimental design including elastase challenge (D0) and sample collection times (D2, D7, D21). (B, C) Representative images from C57BL/6 mice at days 2 (D2), 7 (D7) and 21 (D21) post-PPE challenge (6U via intratracheal aspiration) or unchallenged controls (D0). (B) Histological sections of lung tissue . 5μm sections were stained with hematoxylin and eosin (10X objective). (C) Giemsa-stained cytospin preparations of alveolar cells isolated via bronchoalveolar lavage (40X objective).

Table 1.7 Measures Used to Assess Emphysema Progression in PPE Model

Measure	Test	Quantifies	Healthy Value	Emphysema Value	% Change Upon Emphysema	Physiological Significance
Pulmonary Function Test	Total lung capacity (TLC)	Maximal inflation at 35 cmH_20 [mL]	1.378 mL ± 0.04391	1.791 mL ± 0.05326	~30% increase	Hyperinflation "barrel chest"
	Static compliance	Change in volume for any given applied pressure (3-8 cmH_2O) [mL/cmH_2O]	0.08520 mL/cmH_2O ± 0.003820	0.09528 mL/cmH_2O ± 0.002366	~12% increase	Loss of alveolar and elastic tissue, therefore loss of recoil and labored breathing
	Residual volume (RV)	Trapped air volume after airway collapse on deflation [mL]	0.1615 mL ± 0.02626	0.2924 mL ± 0.03347	~81% increase	Respiration ends early and air becomes trapped in lungs
	Diffusing factor of carbon monoxide (DF_{CO})	Transfer of gas from the air to the blood [1-$(CO_9/CO_c)/(Ne_9/Ne_c)$]; 1=	0.7652 ± 0.01096	0.6965 ± 0.01190	~9% decrease	Poor conductance of gas across epithelial layer

		complete uptake of all CO; 0= no uptake of CO				
Lung Structure Assessment	Mean linear intercept length (Lm)	Estimate of volume-to-surface ratio of acinar airspaces [chord length µm][408]	36.19 ± 1.402	54.74 ± 2.951	~51% increase	Airspace enlargement due to destruction of alveolar walls

* All measurements using PPE Model and depicted as mean ± SE

Healthy Value: BALB/c mice administered PBS (i.t.) at day 21

Emphysema Value: BALB/c mice administered 3U PPE (i.t.) at day 21

1.5 THESIS AIMS

In my thesis research I heed Mechnikov's advice by paying particular attention to the phagocyte as I aim to explore the nature and dynamics of lung macrophage responses to distinct inflammatory insults, with the goal of further elucidating their role in immunity and human health. The studies outlined in CHAPTERS 2 & 3 will focus on the role of resident and recruited macrophage subsets within the lungs in response to *Plasmodium* parasite infection (CHAPTER 2) or following protease-induced lung damage (CHAPTER 3). In these two studies, I will explore the nature of pulmonary myeloid cell responses as pertaining to inflammatory monocyte recruitment and local tissue macrophage proliferation. In CHAPTER 2, we investigate the nature of innate immune responses to an antigenic inflammatory insult (*P. berghei*: a pathogenic parasitic infection), which builds as a crescendo within the lung microvasculature. We demonstrate following infection with *P. berghei,* infected erythrocytes sequestered on the vascular endothelial surface result in lung pathology. We reveal that parasitized erythrocytes are cleared via

phagocytosis by inflammatory monocytes, but not by lung resident alveolar macrophages. We also determine that clearance of sequestered parasitized erythrocytes controls malaria-induced lung damage. In CHAPTER 3, we investigate the nature of innate immune responses to an inflammatory point source (elastase protease activity) resulting in sterile inflammation within the lower airways. We demonstrate that lung macrophages alter their surface phenotype in response to damage to the lung epithelium. In addition, we reveal that resident lung macrophages proliferate in response to elastase-mediated lung damage. It is my hope that through these studies, I can add some insight into the nature of lung macrophage function and dynamics in these inflammatory situations.

1.5.1 SPECIFIC AIMS MALARIA:

The overall goal of this project is to define the roles of lung-resident and recruited monocyte/macrophages in the control of malaria-induced inflammation and lung injury.

Specific Aim 1: Define the role of lung-resident AMs in the control of malaria-induced inflammation and lung injury.

Specific Aim 2: Define the role of inflammatory monocytes/macrophages in the control of malaria-induced inflammation and lung injury.

1.5.2 SPECIFIC AIMS EMPHYSEMA:

The overall goal of this project is to define the roles of the lung-resident and recruited monocyte/macrophages in the progression of events leading to elastase-induced emphysematous changes in the lungs.

Specific Aim 1: Define the role of lung-resident AMs in the progression of elastase-induced emphysematous changes in the lungs.

Specific Aim 2: Define the role of inflammatory monocytes/macrophages in the progression of elastase-induced emphysematous changes in the lungs.

CHAPTER 2

RECRUITED MONOCYTES ARE RESPONSIBLE FOR LIMITING MALARIA-INDUCED LUNG INJURY THROUGH CD36-MEDIATED CLEARANCE OF SEQUESTERED INFECTED ERYTHROCYTES

Running title: Monocytes and malaria-induced lung injury

H.A. Daniel Lagassé[1], Ifeanyi U. Anidi[1], John M. Craig[1] and Alan L. Scott[1]

[1]W. Harry Feinstone Department of Molecular Microbiology and Immunology,

Bloomberg School of Public Health, Johns Hopkins University, Baltimore, MD

portions of this work have been submitted for publication and are currently under review

2.1 ABSTRACT

The contributions made by infected erythrocytes sequestered on lung microvasculature and their subsequent clearance by mononuclear cells to pulmonary complications associated with severe malaria have not been defined. Employing the *P. berghei*-C57BL/6 mouse model, we demonstrate that sequestration of infected erythrocytes on lung endothelium results in lung injury and a rapid recruitment of $CCR2^{+}CD11b^{+}Ly6C^{hi}$ monocytes. Recruited monocytes were activated within the pulmonary environment and were instrumental in the phagocytic clearance of adherent cells. In contrast, resident alveolar macrophages were not activated and did not participate in the clearance of malaria-infected cells. Infection of $CCR2^{-/-}$ animals, which exhibited impaired monocyte recruitment, resulted in enhanced levels of parasite sequestration and exacerbated lung injury. Adoptive transfer of $CCR2^{+/+}$ bone marrow-derived monocytes into $CCR2^{-/-}$ animals was sufficient to protect lungs from enhanced injury. Furthermore, results obtained from $CD36^{-/-}$ and CD36 bone marrow chimeric mice show that sequestration in the absence of CD36-mediated phagocytic clearance by monocytes results in exaggerated lung pathology. Hence, the level of malaria-induced lung pathology is proportional to the steady-state levels of infected erythrocytes adhering to the pulmonary vasculature and a major role of recruited monocytes is to reduce parasite burden in a manner that minimizes lung damage.

2.2 INTRODUCTION

Malaria infects over 200 million people each year resulting in over 600,000 deaths, mainly of children living in Sub-Saharan Africa [238]. Of the five species that infect humans, *Plasmodium falciparum, P. vivax, P. malariae, P. ovale*, and *P. knowlesi*, *P. falciparum* is responsible for a majority of the 68 million disability-adjusted life years (DALYs) lost attributed to malaria infection [239]. While malaria is most commonly considered an infection of erythrocytes that results in cyclical fevers and anemia, some of the most serious complications of infection are at the organ level in the brain, placenta and lungs [250-252].

Pulmonary complications occur in up to 25% of adults and 40% of children during the course of severe malaria [241, 254-256]. Furthermore, between 5% and 25% of adults and up to 30% of pregnant women develop acute lung injury (ALI) and acute respiratory distress syndrome (ARDS); some even after administration of antimalarials [241]. Traditionally, this malaria-associated respiratory distress has been attributed to the combined effects of metabolic acidosis, non-cardiogenic pulmonary edema and severe anemia [258]. While the role of parasite sequestration on vascular endothelial cells in the brain and placenta are well documented [409], our understanding of the contribution that the intense sequestration of malaria-infected erythrocytes to lung microvasculature makes to pulmonary distress is limited and still evolving.

Plasmodium sequestration is thought to be developmentally advantageous to the parasite because it prevents the recognition and clearance of the trophozoite- and schizont-containing erythrocytes by macrophages in the spleen [269]. The pattern of *P. falciparum* adherence observed in humans is selective in that most sequestration takes place in the lungs, adipose tissue, brain and placenta [270-272]. While the pathophysiological consequences of parasite sequestration on vascular endothelial cells in the brain and placenta are well documented, little is known about this process in the lungs. The cytoadherence of infected erythrocytes to endothelial cells has been shown to be dependent on interactions between an array of host- and parasite-derived factors *in vitro*. For *P. falciparum*, erythrocyte membrane protein 1 (PfEMP1), a parasite-produced molecule that is exported to the surface of the infected erythrocyte, endows trophozoite-

and schizont-containing red blood cells with the ability to interact with host ligands including chondroitin sulfate A, the scavenger receptor CD36 and the adhesion molecules ICAM-1 and PCAM-1 on the luminal surface of vascular endothelium [244, 275-277].

Because of the inherent difficulties of studying *P. falciparum* sequestration in the intact lungs of humans, murine models, most of which employ *P. berghei* infection, have been developed [288, 295, 326-329]. Similar to *P. falciparum*, *P. berghei* schizont-containing erythrocytes sequester in the lungs and adipose tissue via interactions with CD36 [266, 288, 295]. In *P. berghei*, where there is no clear ortholog of PfEMP1 in the genome, the parasite-expressed molecule designated SMAC has been implicated in the sequestration of schizont-infected erythrocytes on endothelial surfaces [326]. Utilizing the *P. berghei* model, it has been demonstrated that sequestration in the lungs, in addition to avoiding clearance in the spleen, has the added advantage of promoting factors that are beneficial for parasite growth [326, 337]. From the perspective of the host, adherence of parasitized cells to the pulmonary vasculature is not a benign even as there is a strong positive correlation between the level of parasite burden in the lungs and the degree of ALI [295]. While some malaria-associated pulmonary damage results from receptor-ligand interactions that trigger changes in barrier integrity when *Plasmodium*-infected erythrocytes cytoadhere to the vascular endothelium [278], the contributions that innate immune responses make to the pathogenesis of ALI are still not clear.

Malaria induces a robust innate immune response that plays an important role in limiting parasite load through mechanisms that direct phagocytic cells to engulf and kill parasites as well as coordinate the development of an appropriate T cell-mediated effector response [248]. Specifically, mononuclear phagocytes have been shown to critical for the uptake and clearance of malaria-infected erythrocytes [300]. While it has been demonstrated that the $CD11b^{high}Ly6C^{+}$ subset of inflammatory monocytes are central to clearance of infected-erythrocytes in the spleen resulting in a partial control of blood parasitemia [325], the role that blood monocytes and tissue-resident macrophages play in the regulation of parasite burden in the lungs and malaria-induced pulmonary damage have not been defined.

In the work presented here, we employed *P. berghei* infections in mice to define the roles that lung-resident macrophages and recruited monocytes play in the regulation of malaria-induced pulmonary damage. We demonstrate that coincident with the onset of parasite sequestration in the lungs there is a dramatic and rapid recruitment of $CCR2^{+}CD11b^{+}Ly6C^{hi}$ monocytes. These recruited monocytes were shown to be instrumental in controlling the level of damage through clearing infected erythrocytes adherent to lung endothelial cells. Lung pathology was significantly exacerbated in CCR2-deficient animals that were defective in monocyte recruitment and parasite clearance. Adoptive transfer of $CCR2^{+}$ monocytes into the lungs of $CCR2^{-/-}$ animals significantly reduced the level of malaria-induced lung damage. Effective clearance by monocytes was shown to be largely dependent on the expression of CD36 on the surface of mononuclear cells. Importantly, lung-resident macrophages appeared to play only a minor role in clearing parasitized erythrocytes from the lungs, as they showed only minimal activation and did not proliferate in response to malaria challenge.

2.3 MATERIALS AND METHODS

2.3.1 Mice

Age and sex-matched (male 6-12 weeks old) littermates were used for all experiments. C57BL/6J and $CCR2^{-/-}$ (B6.129S4-*Ccr2tm1Ifc*/J)] [410] were obtained from The Jackson Laboratory (Bar Harbor, ME, USA). $CD36^{-/-}$ mice on a C57BL/6 background were obtained from Dr. Maria Febbraio (Cleveland Clinic Foundation, Cleveland, OH, USA) [411]. All mice were maintained within barrier filter-top cages, provided food and water ad libitum, and exposed to a 12-hour light/dark cycle. All animal procedures performed in this study were approved by the Johns Hopkins Animal Care and Use Committee (Baltimore, MD, USA), and were in accordance with the National Research Council's Guide for the Care and Use of Laboratory Animals federal guidelines.

2.3.2 Parasites and infection

P. berghei ANKA (MRA-671) was obtained from the Malaria Research and Reference Reagent Resource Center (MR4) (Manassas, VA, USA). The transgenic parasite *P. berghei* ANKA-tdTomato (tdT*Pb*A), which constitutively expressed the red fluorescent protein (tdTomato) under control of the elongation factor 1 alpha (*eef1a*) promoter region, was obtained from Dr. Volker Heussler at the Bernhard Nocht Institute for Tropical Medicine in Hamburg, Germany [412]. Cryopreserved parasite stocks were passaged through donor mice (C57BL/6J) at least twice prior to infecting experimental mice. Infected donor mice were maintained until the eighth passage, when new parasites were started from cryopreserved stocks. Blood stage infections were initiated by introducing 10^6 parasitized erythrocytes via intra-peritoneal injection. Progression of the infection was measured by tracking changes in body weight and temperature. In addition, peripheral blood parasitemia was monitored via thin blood smear and Giemsa staining.

2.3.3 Antibodies

The following anti-mouse antibodies were purchased from BD Biosciences (San Jose, CA, USA) CD11b-PerCP-Cy5.5 (550993), SiglecF-PE (552126), Ly6C-APC (560595), CD64-PE (558455), and CD86-PE (553692). F4/80-PE (12-4801-80), MHCII-PE (12-5321-81), CD40-PE (12-0401-81), CD45.2-PE (12-0454-81), CD45.1-APC (912-0453-81), CD80-PE (12-0801-81), PD-L1-PE (12-5982-81), PD-L2-PE (12-5986-83), and rat IgG2a κ isotype control-PE (12-4321-80) anti-mouse antibodies were purchased from eBioscience (San Diego, CA, USA). Anti-mouse CD11c-APC (130-091-844) was purchased from Miltenyi Biotec (Auburn, CA, USA).

2.3.4 Flow cytometry

Whole lung homogenates were generated as previously described [46]. Briefly, prior to excision from the chest cavity, lungs were perfused with 10 mL of room temperature sterile Dulbecco's PBS via the right ventricle of the heart. Lungs were carefully removed and placed in 5 mL RPMI 1640 containing 1 mg/mL collagenase type II (1701-015, Life Technologies, Grand Island, NY, USA) and 30 µg/mL DNase I (10104159001, Roche Applied Science, Indianapolis, IN, USA), minced thoroughly, and incubated at 37°C

for 30 minutes. Minced lung suspensions were then ground through a 100-µm nylon cell strainer (352360, BD Biosciences), and the resulting cells were pelleted at 1500g at 4°C. Cells were suspended in ACK lysing buffer (118-156-721, Quality Biological Inc., Gaithersburg, MD, USA) to remove any contaminating erythrocytes, passed through a second cell strainer, and washed in FACS staining buffer [PBS containing 2% heat-inactivated FCS (35-011-CV, Mediatech, Inc., Manassas, VA, USA)]. Cells were then treated with anti-mouse CD16/CD32 Fc Block (553142, BD Biosciences) 10 minutes prior to the addition of cell surface marker specific antibodies. All antibodies were incubated on ice for 20 minutes in the dark. Stained cells were then washed in FACS staining buffer prior to flow cytometric analysis. Cell counts were performed on a hemocytometer using trypan blue stain (15250-061, Life Technologies) to exclude dead cells. All data on whole lung homogenates or peripheral blood cells (collected via tail vein) were collected on a BD FACSCalibur flow cytometer (San Jose, CA, USA) and data analyzed using FlowJo (TreeStar Inc., Ashland, OR, USA). An Amnis ImageStream^X Mark II (Amnis Corporation, Seattle, WA, USA) was used to capture 60X magnification images of phagocytosis of transgenic *P. berghei* expressing tdTomato fluorescent protein by CD11b$^+$ cells in the lungs. Briefly, whole lung homogenates were prepared as described above and stained with anti-mouse CD11b-PerCP-Cy5.5 antibodies (BD Biosciences). Cells were excited with the 560 nm yellow/green laser Channels containing brightfield (Channel 1: 420-480 nm), tdTomato fluorescence (Channel 4: 595-642 nm), or anti-CD11b fluorescence (Channel 5: 642-745 nm) and images were captured as single or two-channel (overlay) mode.

2.3.5 Bronchoalveolar lavage (BAL)

Murine surgeries were performed as previously described [413]. Briefly, mice were anaesthetized with 450 mg/kg 2,2,2-tribromoethanol (Sigma-Aldrich, St. Louis, MO, USA) via intraperitoneal injection. An incision was made through the sternum and BAL fluid was obtained after a tracheostomy and lavaging of the lungs with 800 µl of sterile PBS three separate times at room temperature. BAL fluid from the three collections were pooled and centrifuged at 1,500 rpm for 3 minutes at 4°C. Cells were suspended in PBS and an aliquot was stained with trypan blue (Invitrogen, Grand Island, NY, USA) prior to counting on a hemocytometer using the 10X objective of an Olympus BH-2 microscope (Catharpin, VA, USA). Cells

(10^5) from each mouse were adhered to microscope slides with the aid of cytology funnels (Fisher Scientific, Houston, TX, USA) and a cytocentrifuge (Shandon Cytospin, Thermo Fisher Scientific, Waltham, MA) prior to methanol fixation and subsequent staining with Giemsa for differential cell analyses.

2.3.6 Histology

A 19-gauge gavage tube was inserted into a small hole in the trachea, and the lungs were inflated slowly with zinc-buffered formalin fixative (Z-fix) (174, Anatech Ltd., Battle Creek, MI, USA). The lungs were removed and incubated in Z-fix for 48 hours. Inflated and fixed lungs were embedded in paraffin, and sagittal, 5 μm sections, were cut from four different levels of lung. Lung sections were placed on slides and either left unstained or stained with hematoxylin and eosin. Lung sections (and cytology slides) were examined using a Nikon Eclipse E800 light microscope (Nikon Instruments Inc., Melville, NY, USA), and images were acquired using SPOT RT charge-coupled device imager and software (Diagnostic Instruments, Inc., Sterling Heights, MI, USA).

2.3.7 Evans Blue extravasation

To measure albumin extravasation in the lungs of mice, 100 μL of a 1% (1 mg total) solution of Evan's Blue dye was administered intravenously via tail vein and allowed to circulate for 1 hour. The lungs were then perfused as described above, excised, and weighed. The lungs were homogenized in 1 mL formamide using a Polytron PT 10-35 homogenizer (Kinematica, Inc., Bohemia, NY, USA). Lung homogenates were incubated at 60°C for 24 hours and then centrifuged at 12,000g at 4°C for 30 minutes. The supernatant was removed and the absorbance (OD) was measured at 620 nm and 740 nm using a Molecular Devices SpectraMax M2 microplate reader (Sunnyvale, CA, USA) and compared to a standard curve. Corrected absorbance values were calculated using the following equation: corrected absorbance (620)= absorbance (620)- (1.426 * absorbance (740) + 0.03) [414]. The Evans blue concentration was then converted to μg Evans Blue/g of wet lung.

2.3.8 Hemozoin quantification

Hemozoin was purified as previously described [415]. Briefly, frozen lung samples were homogenized in distilled deionized water using a Polytron PT 10-35 homogenizer (Kinematica, Inc., Bohemia, NY, USA) and centrifuged at 14,000g for 15 minutes. The supernatant fraction was removed and the pellets suspended in 1 mL 2% SDS, 100 mM sodium bicarbonate. These fractions were spun down as above and the pellets washed in 2% SDS and centrifuged. Washed pellets were suspended in a buffered solution of 1 mg/mL proteinase K (Roche, Mannheim, Germany) and incubated overnight at 60°C. Following incubation, samples were washed in distilled deionized water. Purified hemozoin pellets were then decrystallized in 1 ml 2% SDS 20 mM NaOH for 1 hour and spectrophotometrically quantitated by measuring OD 400 nm. Initial hemozoin concentrations were determined using a hemin standard curve in a Perkin Elmer HTS 7000 96 well plate reader (Waltham, MA, USA).

Photographs of representative fields (60X objective lens) from three different levels of the lung were counted for hemozoin crystal/pigment containing cells (parasitized erythrocytes or mononuclear cells containing dense brown crystals). For each mouse, 30 fields (60X) were counted for hemozoin$^+$ cells and cellular area (pixel) was determined by pixel masks (Adobe Photoshop, San Jose, CA). The number of hemozoin$^+$ cells was normalized to the peripheral blood parasitemia and cellular area of each field.

2.3.9 Adoptive transfer of monocytes

Bone marrow derived monocytes (BMMs) were generated as previously described [416]. Briefly, bone marrow cells were flushed from the femurs and tibias of donor (C57BL/6J) mice using complete RPMI media including 10% FCS. The isolated bone marrow cells were filtered through a 70-µm cell strainer (352350, BD Falcon) and pelleted. Erythrocytes were removed by osmotic lysis using ACK buffer. Mononuclear bone marrow cells were enumerated and plated at a density of $1x10^6$/mL in complete RPMI media containing 10% FCS and 20 ng/mL recombinant mouse M-CSF (130-094-129, Miltenyi Biotec) in 6-well ultra low adhesion plates (3471, Corning Incorporated, Tewksbury, MA, USA). Bone marrow cells were differentiated at 37°C with 5% CO_2 for five days. BMMs were collected from the cell culture

supernatant (non-adherent cells), washed in Dulbecco's PBS, and enumerated using a hemocytometer. Prior to adoptive transfer, BMMs were characterized morphologically by cytospin and phenotypically by flow cytometry. For adoptive transfer, $1x10^6$ BMMs/100 μL Dulbecco's PBS were administered via intratracheal aspiration.

2.3.10 Pulmonary Edema

Pulmonary edema was assessed by gravimetric analysis. Lungs from naïve or *Plasmodium*-infected mice were extracted following exsanguination via incision of the left inferior vena cava and the abdominal aorta. Lobes of the lungs were separated, weighed wet, dried completely in a 65°C oven (>72 hours), and then weighed dry to determine the wet:dry ratio.

2.3.11 Nucleic acid isolation and gene expression analysis

Lungs were harvested and flash frozen in liquid nitrogen prior to homogenization in Trizol Reagent (15596018, Life Technologies) using a Polytron PT 10-35 homogenizer (Kinematica, Inc., Bohemia, NY, USA). RNA and genomic DNA were isolated from lung homogenates following the manufacturer's instructions. Lung RNA and genomic DNA quantity and purity were assessed by A260/280 absorbance using a Nanodrop ND-1000 (Nanodrop Products, Wilmington, DE, USA). Lung RNA (1 μg) was then reverse-transcribed using the SuperScript II first-strand synthesis system for RT-PCR (100004925, Life Technologies) using oligo (dT) (12-18) primers (58862, Life Technologies). Quantitative real-time RT-PCR was performed using the Applied Biosystems 7500 realtime PCR system, TaqMan Gene Expression Assays-On-Demand, and Taq-Man Universal Master Mix (Life Technologies). The following assays (Applied Biosystems) were used: *Ccl2* (Mm00441242_m1), *Ccl3* (Mm00441259_g1), *Ccl4* (Mm00443111_m1), *Ccl7* (Mm00443113_m1), *Ccl8* (Mm01297183_m1), *Cx3cl1* (Mm00436454_m1), *Gapdh* (Mm99999915_g1), *Ifng* (Mm00801778_m1), *Nos2* (Mm00440502_m1), and *Tnf* (Mm00443260_g1). TaqMan reactions were performed using 1 μL cDNA product or 100 ng genomic DNA in a 25 μL reaction volume and the following thermal cycler profile: 10 minutes denaturation at 95°C, 50 cycles of 15 seconds denaturation at 95°C, followed by 1 minute extension at 60°C. Analysis was

performed using the Applied Biosystems 7500 system SDS software package (Life Technologies). Relative expression units were generated by comparing individual expression levels to a standard curves generated using pooled cDNAs as a template. All genes were normalized to a housekeeping gene control (*Gapdh*). To calculate parasite genome equivalents, known *P. berghei* genomic DNA standards for comparison with samples from whole lung homogenates [417].

2.3.12 Statistical analysis

Statistical significance was evaluated by using the 2-tailed t test (Tukey) and the one-way analysis of variance (ANOVA) test using GraphPad Prism software (La Jolla, CA, USA).

2.4 RESULTS

2.4.1 *Plasmodium berghei* infection results in acute lung injury (ALI)

As early as day three post-*P. berghei* infection, when parasitemia (Figure 2.1A) and parasite burden in the lungs (Figure 2.1B, 2.1C) was detectible, but limited, mice presented evidence of organ-level pathology with lungs that remained engorged with blood following perfusion (Figure 2.2A). As infection progressed and the number of parasites associated with the lungs increased, the outward appearance of perfused lungs transitioned to a dark, reddish-brown color by day 6 (Figure 2.2A). Employing PCR-based detection of the *P. berghei* 18S rRNA gene, it was estimated that ~1.25 x 10^8 *P. berghei* genomes were present in perfused lungs at day 5 post-infection (Figure 2.1B). Although parasitemia continued to rise in the peripheral blood (Figure 2.1A), the total parasite burden detected in perfused lungs at days 6-7 as measured by 18S (Figure 2.1B) or by hemozoin accumulation (Figure 2.1C) plateaued or decreased.

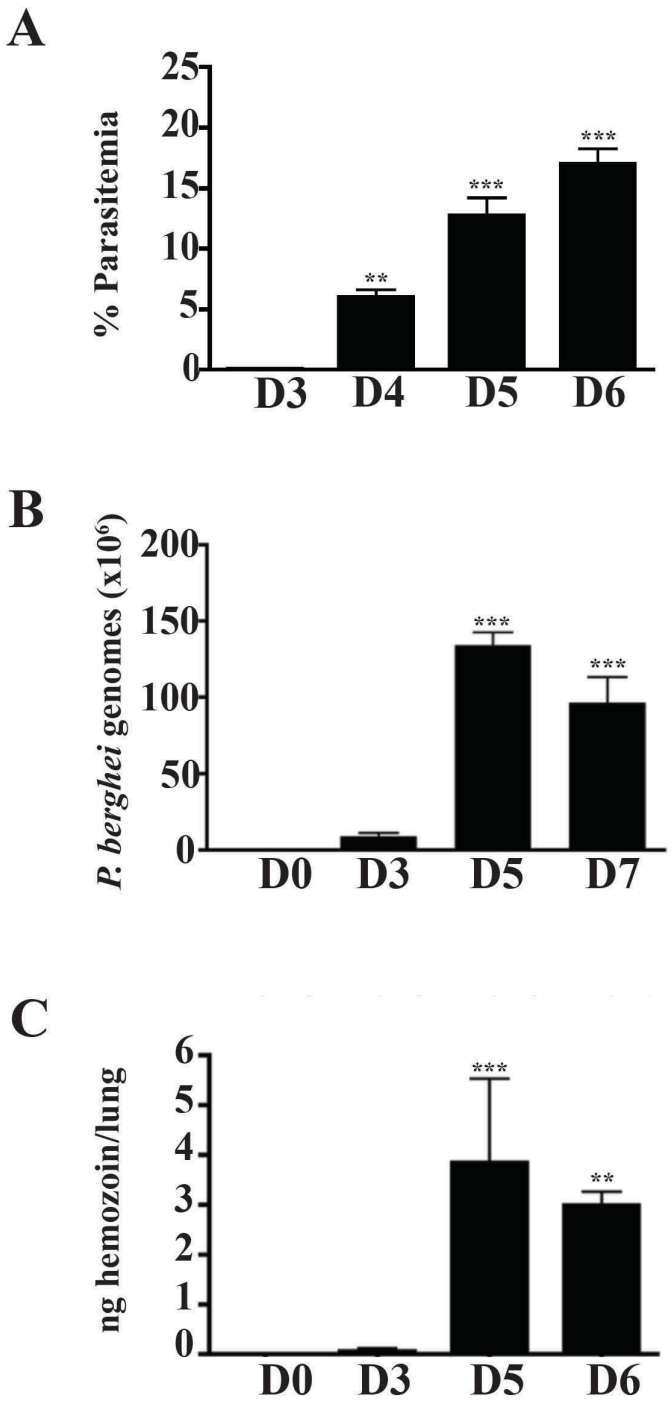

Figure 2.1 Parasite burden in the lungs of *Plasmodium berghei*-infected mice.
(A) Peripheral blood parasitemia of *P. berghei* ANKA-infected C57BL/6 mice at days 3, 4, 5 and 6 of infection. (B-C) Dynamics of parasite burden in perfused lungs of infected mice at various times post-infection using (B) PCR-based detection of 18S rRNA or (C) spectrophotometric quantification of lung-associated hemozoin. Bar graphs depict mean ± SEM. *$p<0.05$; **$p<0.01$, ***$p<0.001$. All comparisons are versus uninfected controls (n=5).

In accordance with the gross appearance of the lungs of infected mice, histological analysis revealed hallmarks of acute lung injury including pulmonary edema, alveolar septal wall thickening and mononuclear cell infiltration (Figure 2.2B), as well as evidence of parasite material contained within mononuclear cells (Figure 2.2C). Parasite accumulation in the lungs was accompanied by a loss of in the integrity of vascular endothelial barrier function denoted by a 30-fold increase in the amount of extravasated Evan's Blue in perfused lungs from infected compared to uninfected animals (Figure 2.2D).

2.4.2 Dynamics of lung-resident macrophages and recruited inflammatory monocytes

The pulmonary damage caused by malaria infection was accompanied by a significant increase in the number of immune cells found in the BAL at day 6 post-infection, which were dominated by mononuclear cells with <1% granulocytes (neutrophils, eosinophils, basophils) and lymphocytes (Figure 2.3A). A majority of the cells in the BAL at day 6 of infection had an activated appearance with highly vacuolated cytoplasm and a small percentage of the cells showed evidence that they had engulfed parasitized cells (Figure 2.3B). The recruitment of inflammatory monocytes into the lungs paralleled changes in transcription of the genes encoding CCL2 (MCP-1), CCL3 (MIP-1α), CCL4 (MIP-1β), CCL7 (MCP-3), and CCL8 (MCP-2) – chemokines reported to promote recruitment of mononuclear cells [418] (Figure 2.4). *Ccl2*, *Ccl4*, *Ccl7*, and *Ccl8* expression levels peaked at day 5 post-infection and waned by day 6. In contrast, expression of fractalkine (*Cx3cl1*), a chemokine involved in recruitment of monocytes and T cells to the lung [419] did not increase in response to *P. berghei* infection (Figure 2.4).

To determine if the observed increase in mononuclear cells in the BAL could be extended to the whole lung, flow cytometry of single-cell suspensions from perfused lungs was employed to determine the population dynamics of macrophages and monocytes at days 3, 5 and 6 post-*P. berghei* infection. Interestingly, while the number of lung-resident alveolar macrophages (AM; $CD11c^{+}$ $SiglecF^{+}$ $CD11b^{-}$ $Ly6C^{lo}$) remained stable over the first six days, there was a substantial increase in the number of cells with the surface signature of inflammatory monocytes ($CD11c^{-}$ $SiglecF^{-}$ $CD11b^{+}$ $Ly6C^{+}$) as early as day 3 post-infection (Figures 2.5A, 2.5B). Since these $CD11c^{-}$ $SiglecF^{-}$ $CD11b^{+}$ $Ly6C^{+}$ cells were no longer in the

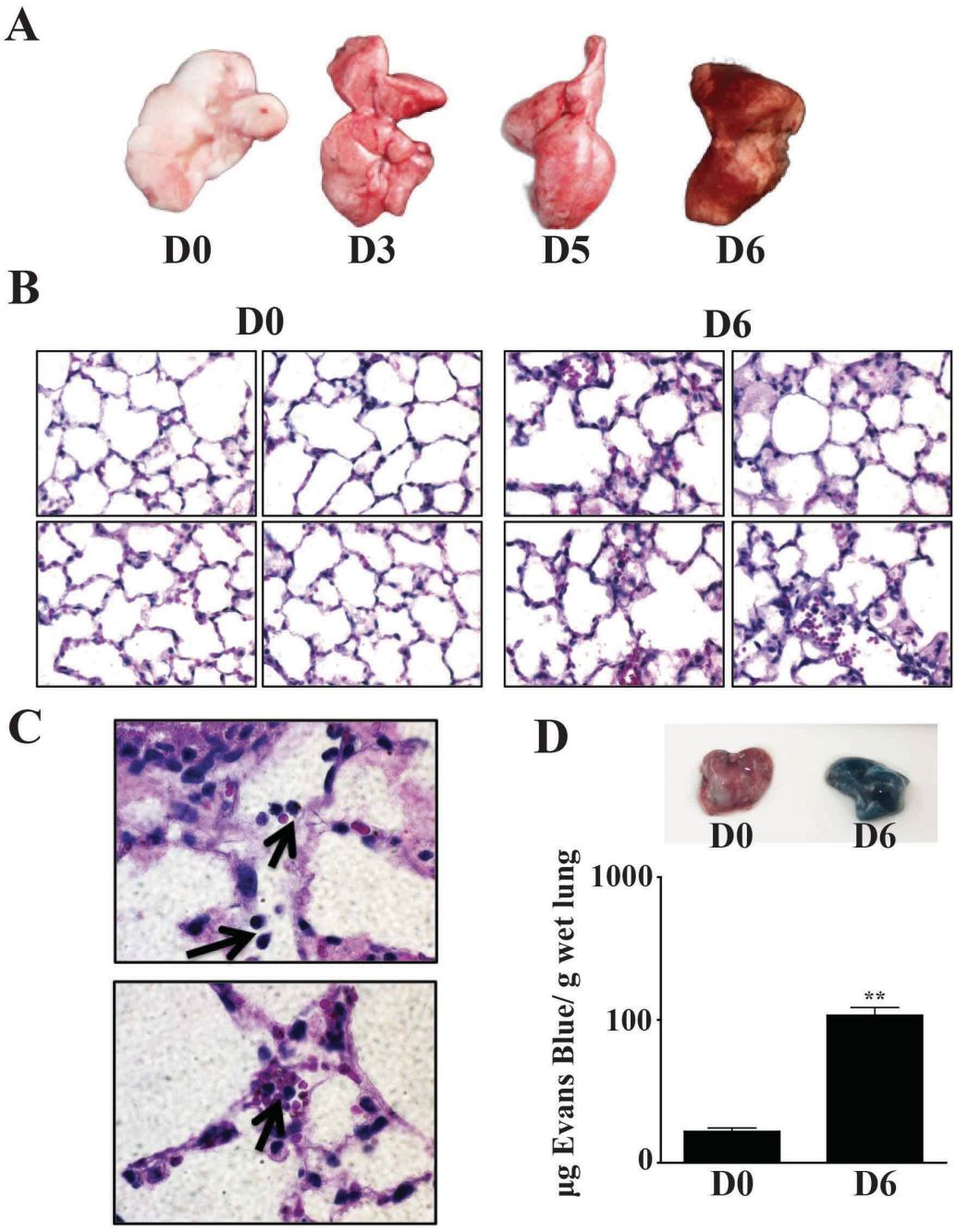

Figure 2.2 ***Plasmodium berghei*** **infection leads to acute lung injury.**
(A) Gross apperance of perfused lungs from C57BL/6 mice at days 0, 3, 5 and 6 following *P. berghei* infection. (B-C) Representative histological sections of lungs from non-infected (D0) or day 6 (D6) post-infection. 5µm sections were stained with hematoxylin and eosin [(B) 60X magnification; (C) 100X magnification, D6 only] Arrowheads highlight parasite^{+} mononuclear cells. (D) Gross appearance (top panels) and spectrophotometric quantitation of Evans Blue extravasation in perfused lungs from non-infected (D0) or day 6 (D6) post-infection mice. Bar graphs depict mean ± SEM. *$p<0.05$; **$p<0.01$, ***$p<0.001$. All comparisons are versus uninfected controls (n=3).

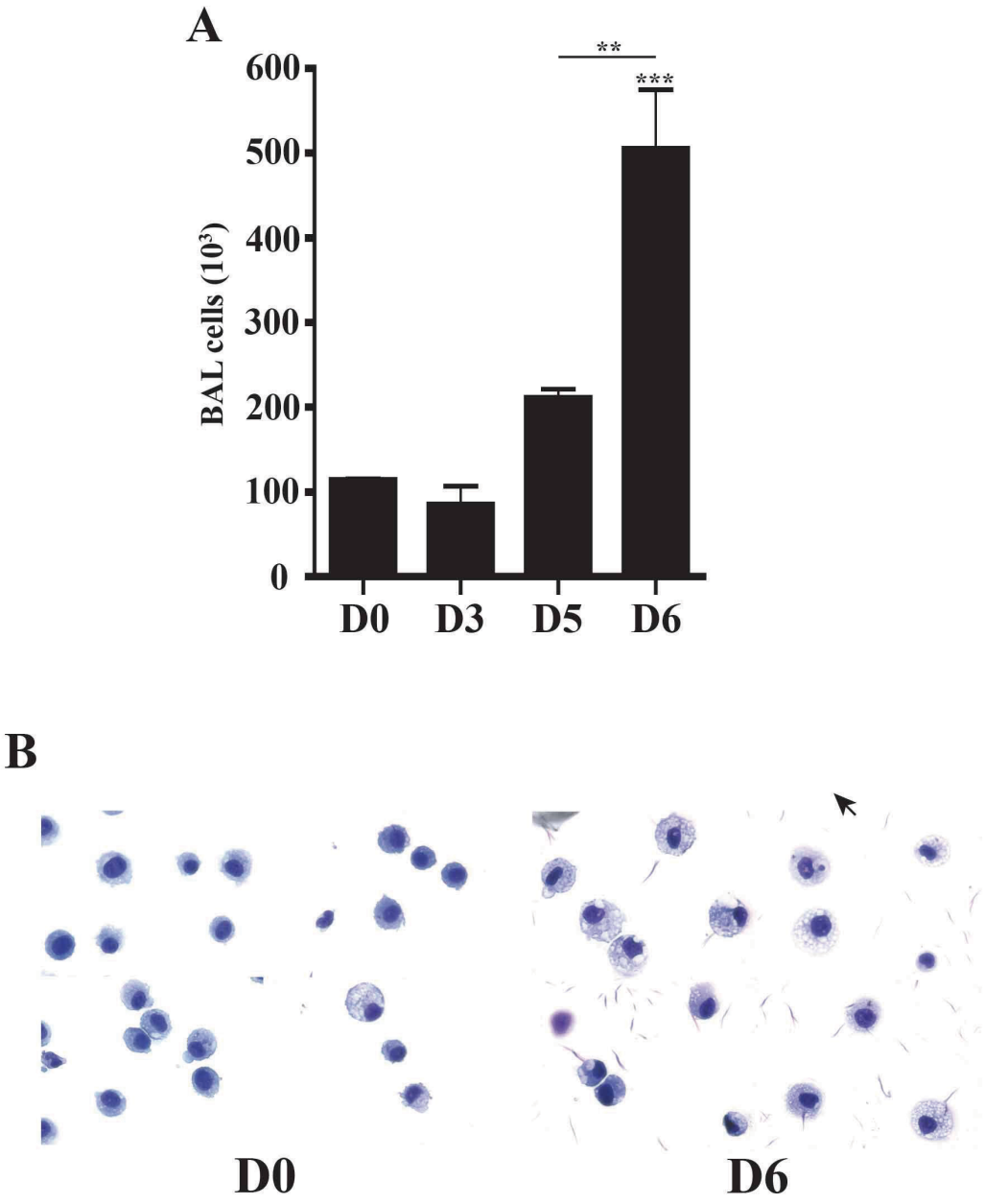

Figure 2.3 Cellular dynamics in the airways during *P. berghei* infection. (A) Number of cells contained in the bronchoalveolar lavage fluid at D0, D3, D5 and D6 of infection. (B) Representative images of hematoxylin and eosin-stained cytospin preparations of mononuclear cells obtained from the BAL at D0 and D6 of infection (60X magnification). Arrowhead denotes engulfed parasite material. All data are mean ± SEM. $^{**}p < 0.01$, $^{***}p < 0.001$. Comparisons are versus non-infected controls unless indicated by line. N=3

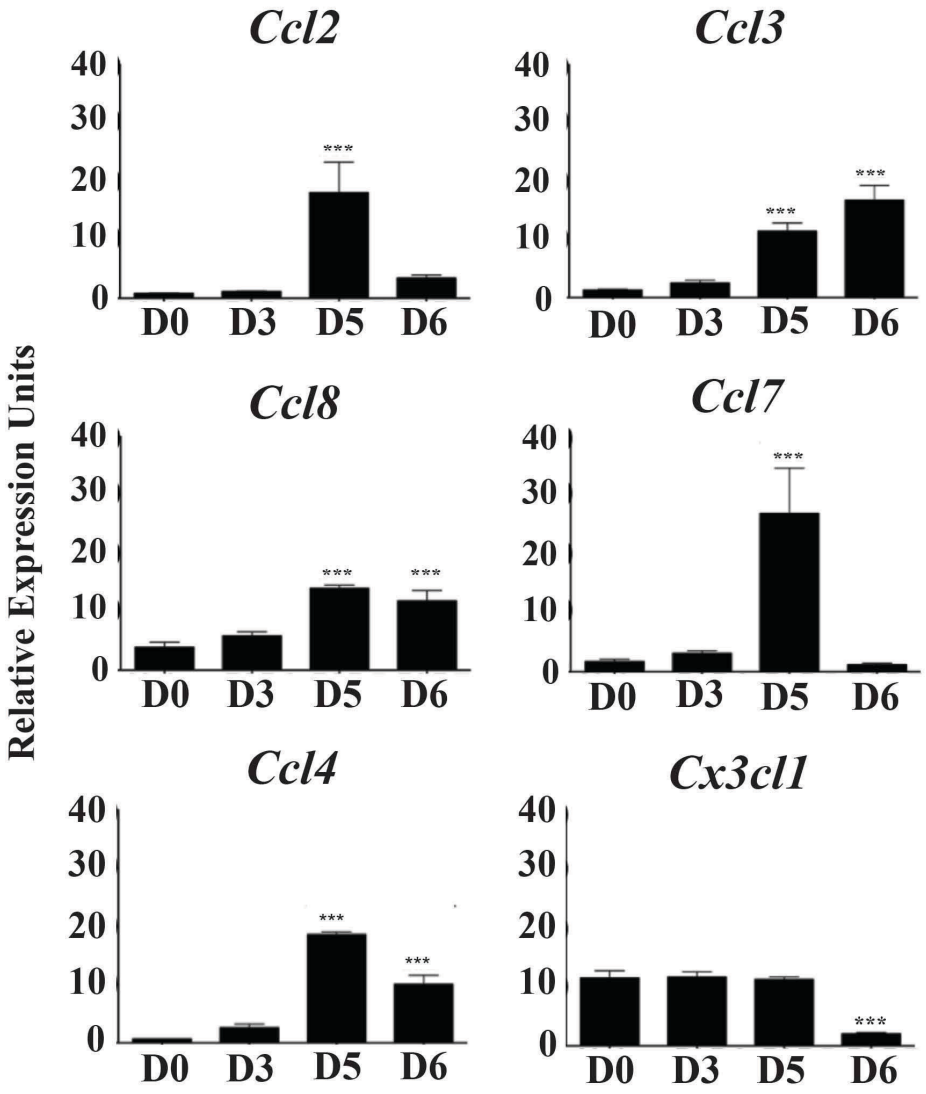

Figure 2.4 Dynamics of cytokine expression in the lungs of C57BL/6 mice during the course of *P. berghei* infection. RNA isolated from perfused lungs at D0, D3, D5 and D6 were processed for real time RT PCR expression analysis of *Ccl2*, *Ccl3*, *Ccl4*, *Ccl7*, *Ccl8* and *Cx3cl1*. The PCR results were normalized to the levels of *Gapdh* and expressed as relative expression units. Bar graphs depict mean ± SEM. *p<0.05; **p<0.01, ***p<0.001. All comparisons are versus uninfected controls. N=5

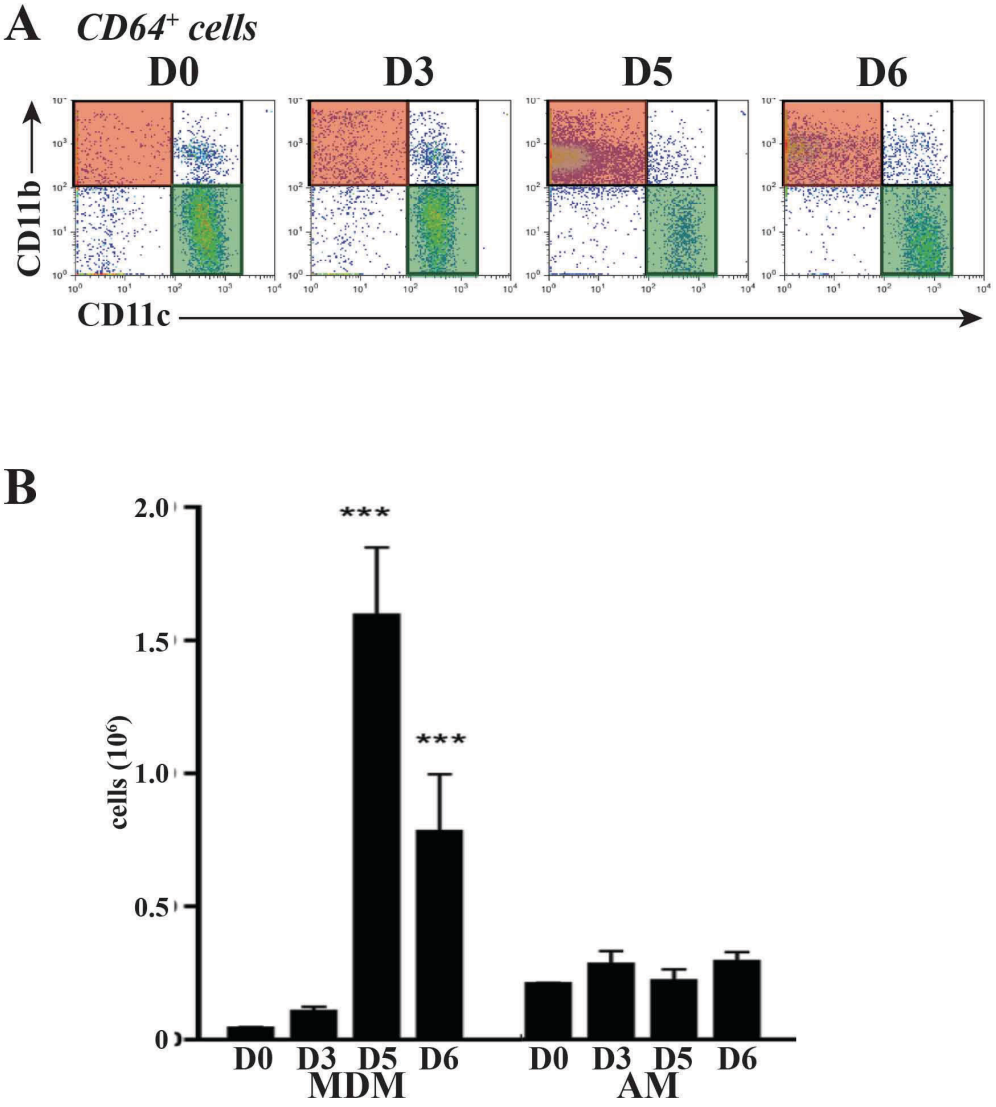

Figure 2.5 Dynamics of mononuclear cells in the lungs during *P. berghei* infection. (A) Flow cytometric analysis of whole perfused lungs obtained at days 3, 5 and 6 post-*P. berghei* ANKA infection gated on $CD64^+$ cells. $CD64^+CD11b^+CD11c^-$ monocyte-derived macrophages (MDM) highlighted in red. $CD64^+CD11b^-CD11c^+$ alveolar macrophages (AM) highlighted in green. (B) Change in the numbers of MDM and AM. The numbers were derived from flow cytometric analysis of whole perfused lungs obtained at days 3, 5 and 6 post-*P. berghei* ANKA infection. Comparisons are versus non-infected controls. All data are mean ± SEM. ***$p < 0.001$. N=3

vascular compartment, they were designated monocyte-derived lung macrophages (MDM). This increase in MDM numbers in perfused lungs was maintained through day 6 of infection (Figure 2.5B).

2.4.3 Recruited monocytes are responsible for parasite clearance in the lungs

The significant influx of MDM and the lack of change in the number of AM in the face of increasing parasite load suggested that these two mononuclear cell populations may have distinct roles in managing parasite load in the lungs. To look at this issue in more detail, we employed a transgenic *P. berghei* ANKA line that constitutively expresses the red fluorescent protein, tdTomato (tdT*Pb*A) [412] to assess the dynamics of parasite clearance by phagocytosis. Increases in blood parasitemia, as measured through detection of the tdTomato signal (Figure 2.6A) and by counting infected red blood cells in smears (data not shown), were comparable to non-transgenic parasites (Figure 2.1A). The fluorescent signal from tdT*Pb*A was employed to determine which macrophage subset is responsible for the phagocytic clearance of schizont-infected erythrocytes. Lungs were perfused and harvested at days 3, 5 and 6 post-infection and the number and surface phenotype of the cells that had taken up the fluorescent parasites were evaluated. There was an increase in the number of parasite-positive cells from days 3 to 6 of infection (Figure 2.6B). Evaluation of the surface phenotype of the tdTomato$^+$ cells revealed that only a small percentage of the fluorescence was associated with AM (8.2%, 3.6%, 3.6% on days 3, 5 and 6, respectively), whereas a vast majority of the tdT*Pb*A fluorescent signal was associated with the MDM population (61%, 88%, 88% at days 3, 5 and 6, respectively) (Figures 2.6C, 2.6D). Employing flow cytometry-assisted fluorescent microscopy it was determined that the nature of the interactions between the MDM and the tdT*Pb*A-infected erythrocytes included surface attachment, engulfment of intact infected erythrocytes and various stages of intracellular degradation of the parasite (Figure 2.7).

2.4.4 Activation status of AM and MDM following *P. berghei* infection

To determine if the distinctions in the dynamics and phagocytic function between resident and recruited lung myeloid cells observed at day 6 post-infection were reflected in their activation status, the expression levels of F4/80, MHCII, SiglecF, CD40, CD80, CD86, PDL1, PDL2, and CD64 on these cells were

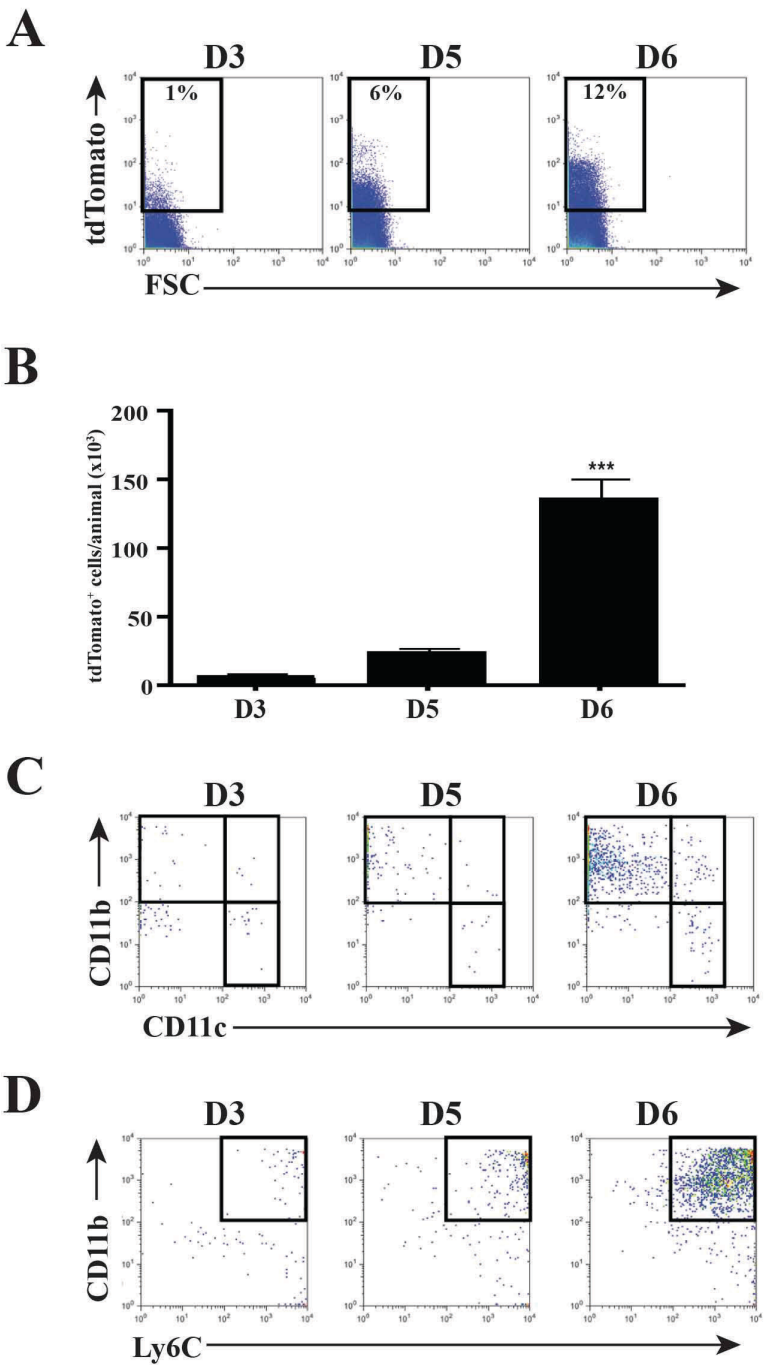

Figure 2.6 Dynamics of parasite phagocytosis in the lungs during *P. berghei* infection.
(A) Representative data depicting flow cytometric analysis of peripheral blood parasitemia at days 3, 5 and 6 after infection with tdTomato-expressing *P. berghei* (tdT*Pb*A). (B, C) Representative data depicting the dynamics of up-take of tdT*Pb*A-infected erythrocytes by $CD11b^{+}CD11c^{-}Ly6C^{hi}$ MDM and $CD11b^{-}CD11c^{+}Ly6C^{lo}$ AM from perfused lungs at days 3, 5 and 6 post-infection. (D) Bar graph depicting the total $tdTomato^{+}$ cells in perfused lungs at days 3, 5 and 6 post-tdT*Pb*A infection (N=3). Mean ± SEM. ***$p < 0.001$

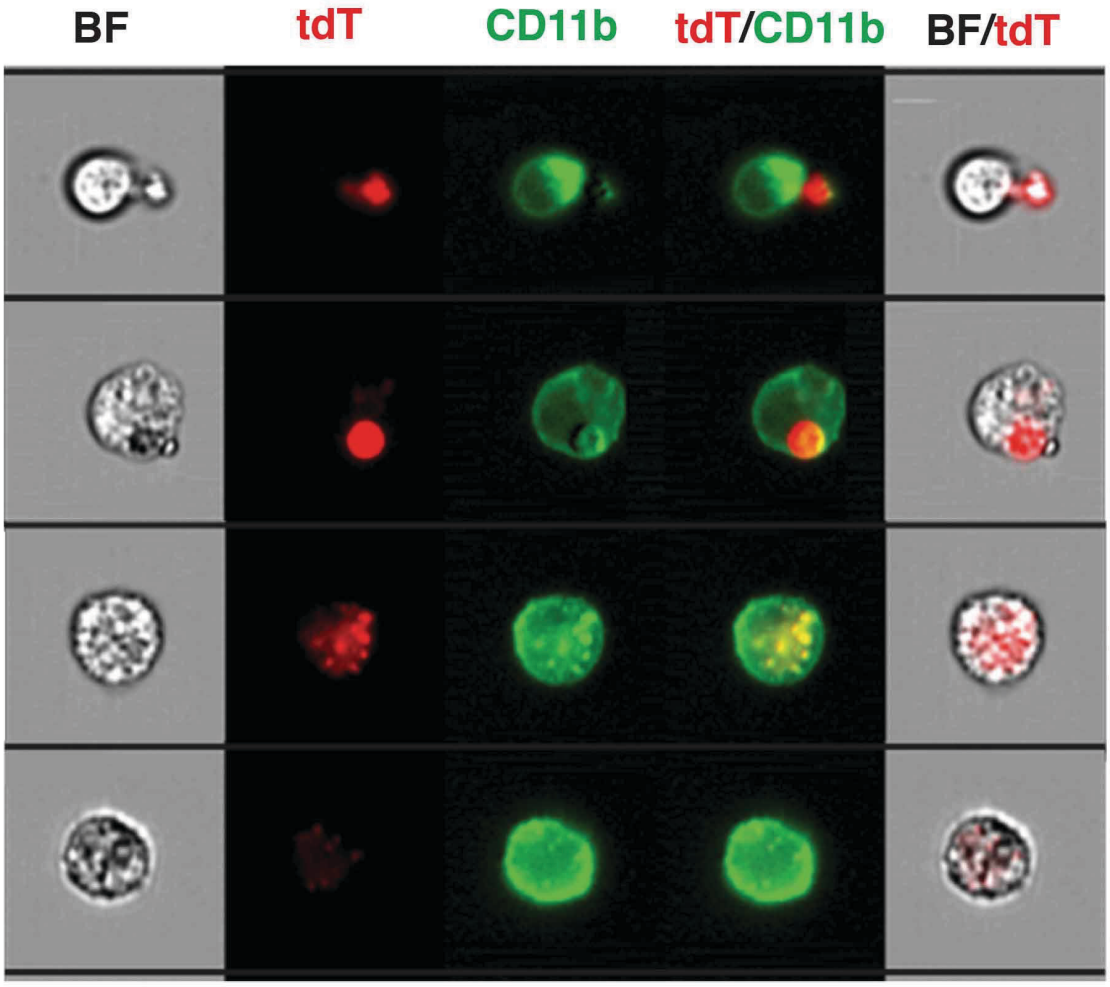

Figure 2.7 Visualization of *P. berghei* phagocytosis.
Representative brightfield, fluorescent and merged images of the interactions between tdT*Pb*A-infected erythrocytes and MDM at day 6 of infection. Images of live cells were acquired on an Amnis ImageStream^X Mark II.

compared. The CD11b$^-$ CD11c$^+$ AM from naïve animals were characteristically F4/80^{low}, MHCII^{low}, SiglecF$^+$, and CD64$^+$ (Figure 2.8A) [11, 57, 58]. The resident cells were also PDL1$^+$ and expressed low levels of CD80 at baseline. With the exception of an increase in the expression of MHCII, the AM isolated from day 6 had a nearly identical surface phenotype as cells from naïve animals (Figure 2.8A) suggesting that AM were only minimally activated by the presence of infected erythrocytes.

Since there was no demonstrable extra-vascular population of monocytes in the lungs of naïve animals, we used cells isolated from the peripheral blood of naïve animals to estimate the pre-infection surface phenotype of blood monocytes. These CD11b$^+$ CD11c$^-$ Ly6C$^+$ peripheral blood monocytes had low levels of F4/80, CD80, and CD86 and minimal detectable levels of MHCII, SiglecF, CD40, PDL1, PDL2, and CD64 (Figure 2.8B). At day 6 of infection, the peripheral blood monocytes showed evidence of partial activation by up-regulated surface expression of F4/80, CD80, PDL1 and CD64. In contrast, the CD11b$^+$ CD11c$^-$ Ly6C$^+$ MDM isolated from perfused whole lungs displayed notably higher surface levels of F4/80, MHCII, CD40, CD80, CD86, PDL1 and CD64 (Figure 2.8C). The recruited MDM remained negative for SiglecF and PDL2. Thus, while there is evidence for limited activation of monocytes in the peripheral blood during malaria infection, these cells take on a more robust activation phenotype after they are recruited to the lungs in the context of malaria infection.

For many of the activation markers on MDM there was a bimodal distribution of staining, suggesting the presence of a population of MDM that robustly increased expression and a second population that did not (Figure 2.8C). It was hypothesized that the population which up-regulated activation markers such as MHCII, CD80 and PDL1 were the MDM in the process of clearing schizont-infected erythrocytes from the pulmonary environment. After establishing that CD80, MHC II and PDL1 were all up-regulated and co-expressed on a common population of MDM (data not shown), the two MDM populations were discriminated based on high or low levels of the activation markers to determine the level of parasite uptake (tdT*Pb*A$^+$ signal) associated with each population (Figure 2.9). A vast majority of the parasite-positive cells were found within the MDM group that had elevated surface levels of MHCII, CD80 and PDL1. These

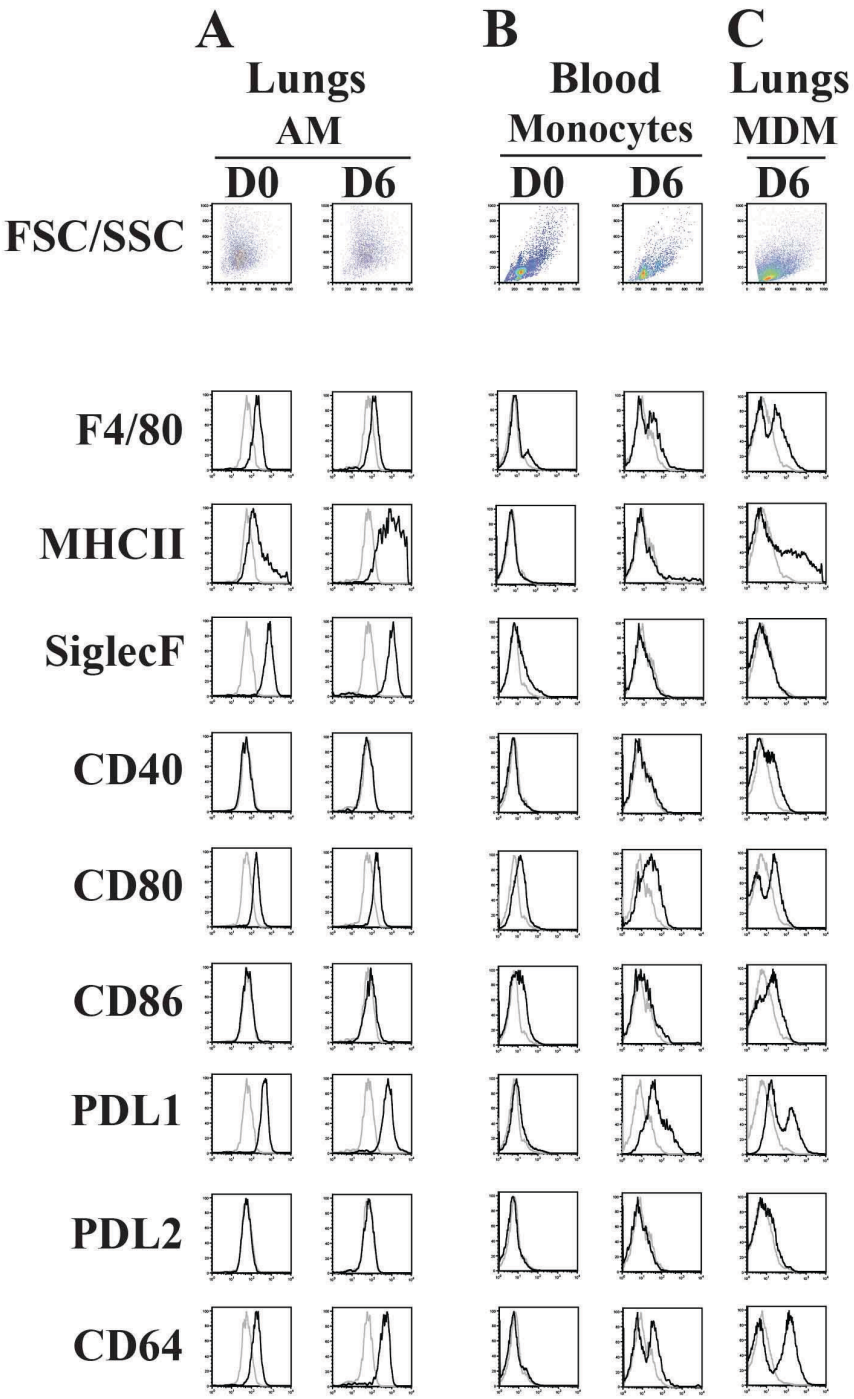

Figure 2.8 Activation of alveolar macrophages (AM) and monocyte-derived macrophage (MDM) populations following malaria infection.
Representative data (N=3) of flow cytometric analyses of gated cell populations from perfused lung homogenates (AM: $CD11b^{-}CD11c^{+}$; MDM: $CD11b^{+}CD11c^{-}$) or peripheral blood mononuclear cells (monocytes: $CD11b^{+}Ly6C^{+}$) of non-infected (D0) or day 6 (D6) post-*Pb*A infection. Histograms depict surface fluorescence signals of F4/80, MHCII, SiglecF, CD40, CD80, CD86, PDL1, PDL2 and CD64 (black line) and their respective isotype controls (grey line).

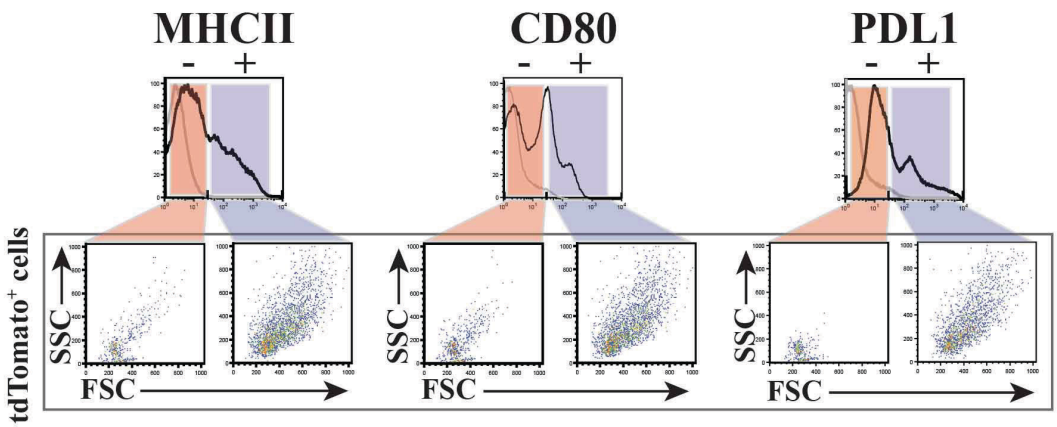

Figure 2.9 Relationship between parasite uptake and activation status following malaria infection. Flow cytometric analysis at day 6 post-tdT*Pb*A infection demonstrating that the activated subset of MDM that expressed elevated MHCII, CD80 and PDL1 were also positive for the tdTomato signal. MDM were first gated for their positive or negative status for MHCII, CD80 and PDL1 and then analyzed for the levels of tdTomato signal. Dot plots below depict the light scatter properties of the tdTomato^{+} cells present in each population.

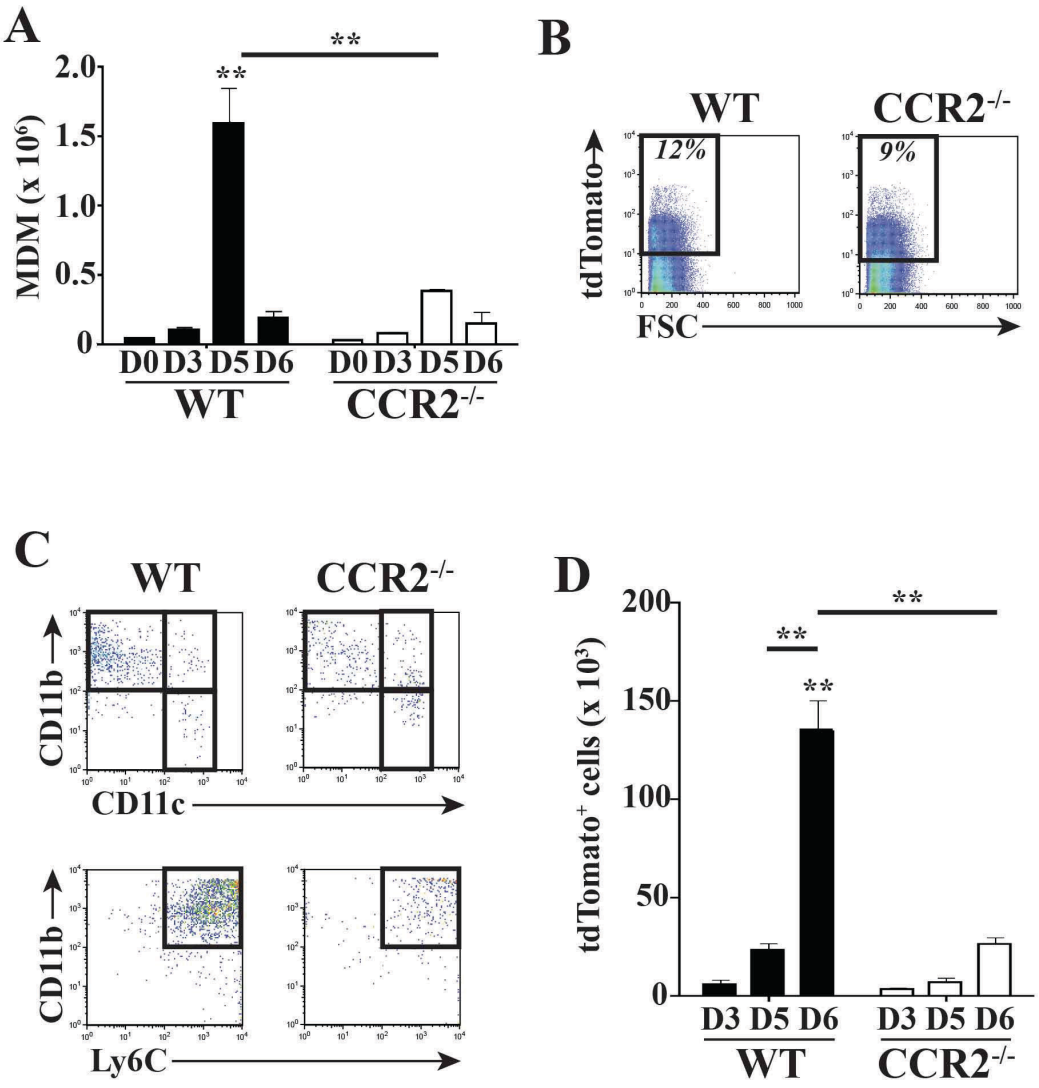

Figure 2.10 CCR2-deficiency results in altered cell trafficking and parasite uptake.
(A) Bar graphs depict total numbers of monocyte-derived macrophages (MDMs: $CD64^{+}CD11b^{+}CD11c^{-}$) in the lungs of WT C57BL/6 (filled) or $CCR2^{-/-}$ (open) mice at days 0, 3, 5 and 6 post-*P. berghei* infection. Data are mean ± SEM, *p < 0.05, **p < 0.01, ***p < 0.001 (N=3). Comparisons are versus non-infected control except were noted with comparison line. (B) Representative data depicting peripheral blood parasitemia measured by tdTomato fluorescence at day 6 post-tdt*Pb*A. (C) Representative data depicting flow cytometric analysis of the distribution of the tdTomato signal at day 6 post-infection associated with cells expressing CD11b, CD11c and Ly6C. (D) Total number of mononuclear cells that are positive for tdTomato signal at days 3, 5, and 6 post-tdT*Pb*A infection for WT (filled) or $CCR2^{-/-}$ (open) mice (N=3). Data are mean ± SEM, **p < 0.01. Comparisons are versus *Pb*D3 except were noted with comparison line.

results indicate that direct contact with the infected erythrocytes may be required for full activation of the monocytes recruited to the lungs during infection.

2.4.5 CCR2-deficiency impairs monocyte recruitment and parasite clearance from the lungs

Based on the result that the MDM appear to be responsible for the bulk of parasite uptake and clearance, we tested the hypothesis that impeding entry of these cells into the lungs results in a higher baseline level of parasite sequestration and exacerbated pulmonary injury. This hypothesis was tested employing CCR2-deficient mice, which do not respond to the major monocyte chemotactic chemokine CCL2 [410], a chemokine that is highly expressed in the lungs during malaria infection (Figure 2.4). Infection of $CCR2^{-/-}$ mice with tdT*Pb*A resulted in parasite levels in the blood (Figure 2.10B) and numbers and activation status of AM (Figure 2.11A) that were not significantly different from WT animals. As expected, the peak in the number of recruited inflammatory monocytes and consequently the number of MDM was greatly diminished in the lungs from $CCR2^{-/-}$ mice (Figure 2.10A). Consistent with previously published observations [195], a majority of the monocytes in CCR2-deficient animals were unable to exit from the bone marrow (data not shown). The monocytes found in the lungs of infected $CCR2^{-/-}$ animals at days 5 and 6 were presumably recruited by chemotactic factors other than CCL2 such as CCL3 and CCL7 (Figure 2.4). Moreover, the inflammatory monocytes that were present in the blood and the MDM in the lungs of $CCR2^{-/-}$ animals at day 6 of infection had a significantly diminished activation status compared to that observed in WT animals. In contrast to the response in WT animals, the levels of $F4/80^{+}$, $MHCII^{+}$, $CD40^{+}$, $CD80^{+}$, $CD86^{+}$, $PDL1^{+}$ and $CD64^{+}$ were not up-regulated on the surface of the MDM isolated from the perfused lungs of $CCR2^{-/-}$ mice (Figure 2.11C). Consistent with their lower numbers, significantly fewer MDM containing tdT*Pb*A-infected RBCs were identified from the lungs of $CCR2^{-/-}$ animals compared to WT at day 6 of infection (Figures 2.10C, 2.10D).

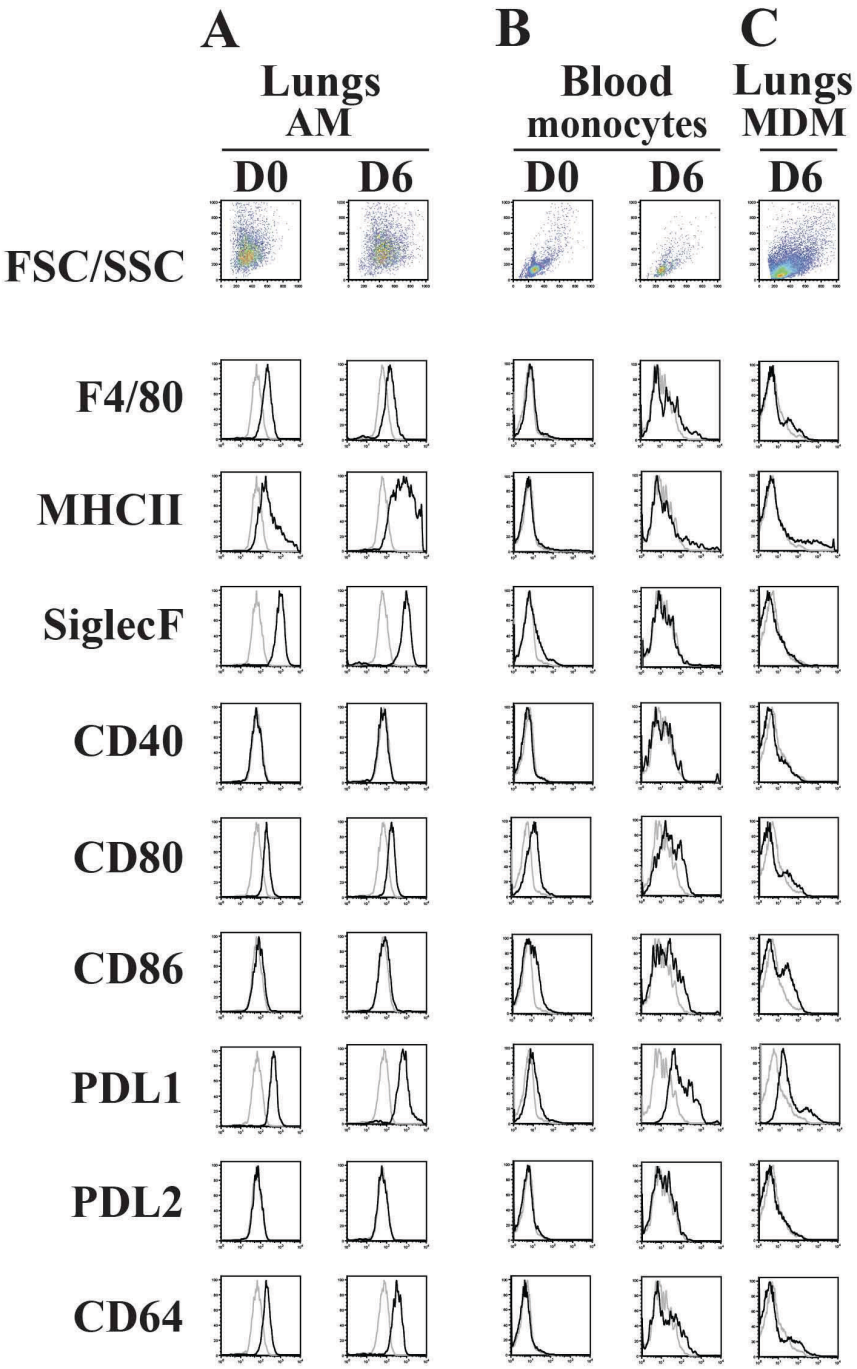

Figure 2.11 Activation of CCR2-deficient alveolar macrophages (AM) and monocyte-derived macrophage (MDM) populations following malaria infection.
Representative data (N=3) of flow cytometric analyses of gated cell populations from CCR2$^{-/-}$ perfused lung homogenates (AM: CD11b^{-}CD11c^{+}; MDM: CD11b^{+}CD11c^{-}) or peripheral blood mononuclear cells (monocytes: CD11b^{+}Ly6C^{+}) of non-infected (D0) or day 6 (D6) post-*Pb*A infection. Histograms depict surface fluorescence signals of F4/80, MHCII, SiglecF, CD40, CD80, CD86, PDL1, PDL2 and CD64 (black line) and their respective isotype controls (grey line).

2.4.6 CCR2-deficiency results in increased parasite burden, elevated pro-inflammatory cytokine expression and exacerbated lung damage.

The observed deficits in monocyte recruitment and parasite uptake in the lungs of CCR2$^{-/-}$ animals suggested that these animals may carry a higher parasite burden and thus suffer elevated levels of parasite-mediated lung damage [278]. Indeed, despite equivalent peripheral blood parasitemia at day 6 post-infection (Figure 2.12A), the lungs from CCR2$^{-/-}$ mice had significantly higher parasite burden, as measured by lung hemozoin content, than WT mice (Figure 2.12B). In order to assess the impact increased parasite burden had on the inflammatory milieu of the lungs, the expression levels of *Ccl2*, *Nos2*, *Tnf*, and *Ifnγ* were measured in the lungs of naïve and *P. berghei*-infected WT and CCR2$^{-/-}$ mice. We observed significantly elevated expression of *Ccl2*, *Tnf*, and *Ifnγ* in both WT and CCR2-deficient mice in response to malaria infection (Figure 2.13). Notably, the transcription levels of *Ccl2*, *Tnf*, and *Ifnγ* in CCR2$^{-/-}$ lungs at day 6 were significantly elevated compared to WT suggesting a heightened inflammatory state. Interestingly, despite the increases in *IFNγ* transcription in WT and CCR2$^{-/-}$ lungs, malaria infection resulted in a similar level of suppression of *Nos2* expression both strains (Figure 2.13). Elevated pulmonary parasite load and pro-inflammatory cytokine expression were associated with significantly higher lung wet:dry ratios in CCR2$^{-/-}$ mice compared to WT controls (Figure 2.14A) indicative of a severe disruption to the lung endothelial barrier. The exacerbated loss of endothelial barrier integrity and edema observed in CCR2$^{-/-}$ mice was also evident when sections of the lungs were examined by light microscopy (Figure 2.14B).

2.4.7 Adoptive transfer of monocytes into CCR2$^{-/-}$ lungs is protective.

The results obtained from CCR2$^{-/-}$ animals suggested that recruited monocytes/MDM play a role in restricting the extent of lung pathology and predicted that adoptive transfer of monocytes into CCR2$^{-/-}$ mice would lead to protection from the exacerbated lung injury phenotype. WT bone marrow-derived monocytes (BMM; 10^6) were administered IT to CCR2$^{-/-}$ animals at day 4 post-*P. berghei* infection and lungs were harvested at day 6 to assess the levels of edema by wet:dry ratios and lung damage by histology. The BMM adoptive transfer resulted in a significant decrease in lung wet:dry ratio (Figure 2.15A) and a notable

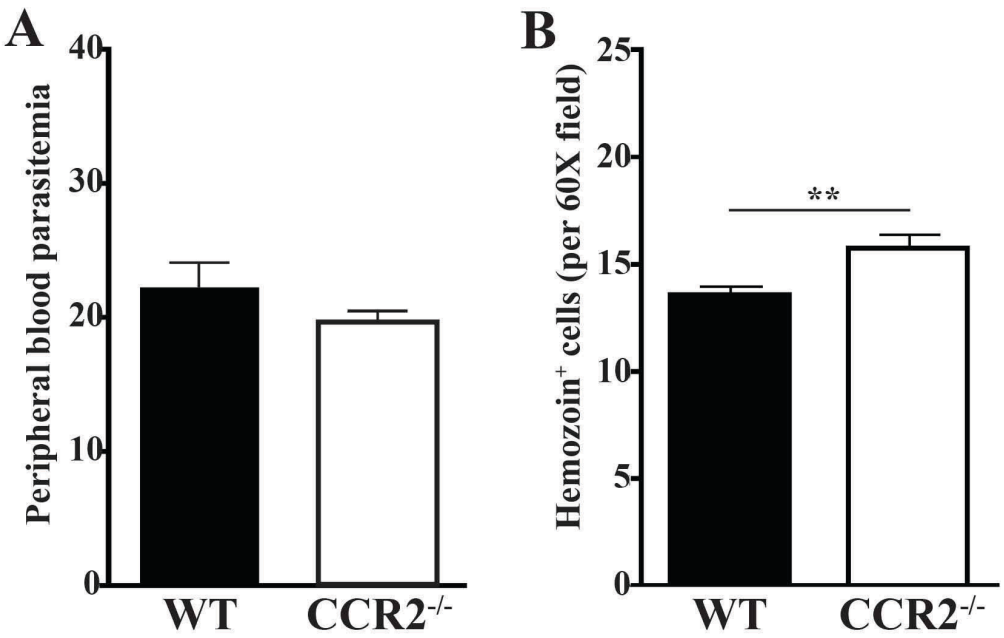

Figure 2.12 CCR2-deficiency results in increased parasite burden.
(A) Peripheral blood parasitemia of WT or CCR2$^{-/-}$ mice (N=15+) at day 6 post-infection assessed by counting parasites on Giemsa-stained thin blood smears. (B) Hemozoin burden in the lungs of WT or CCR2$^{-/-}$ mice at day 6 quantified by number of hemozoin-containing cells per 60X histological field (N=3 mice x 10 fields each). Data are mean ± SEM. **$p < 0.01$. Comparisons are versus wildtype control.

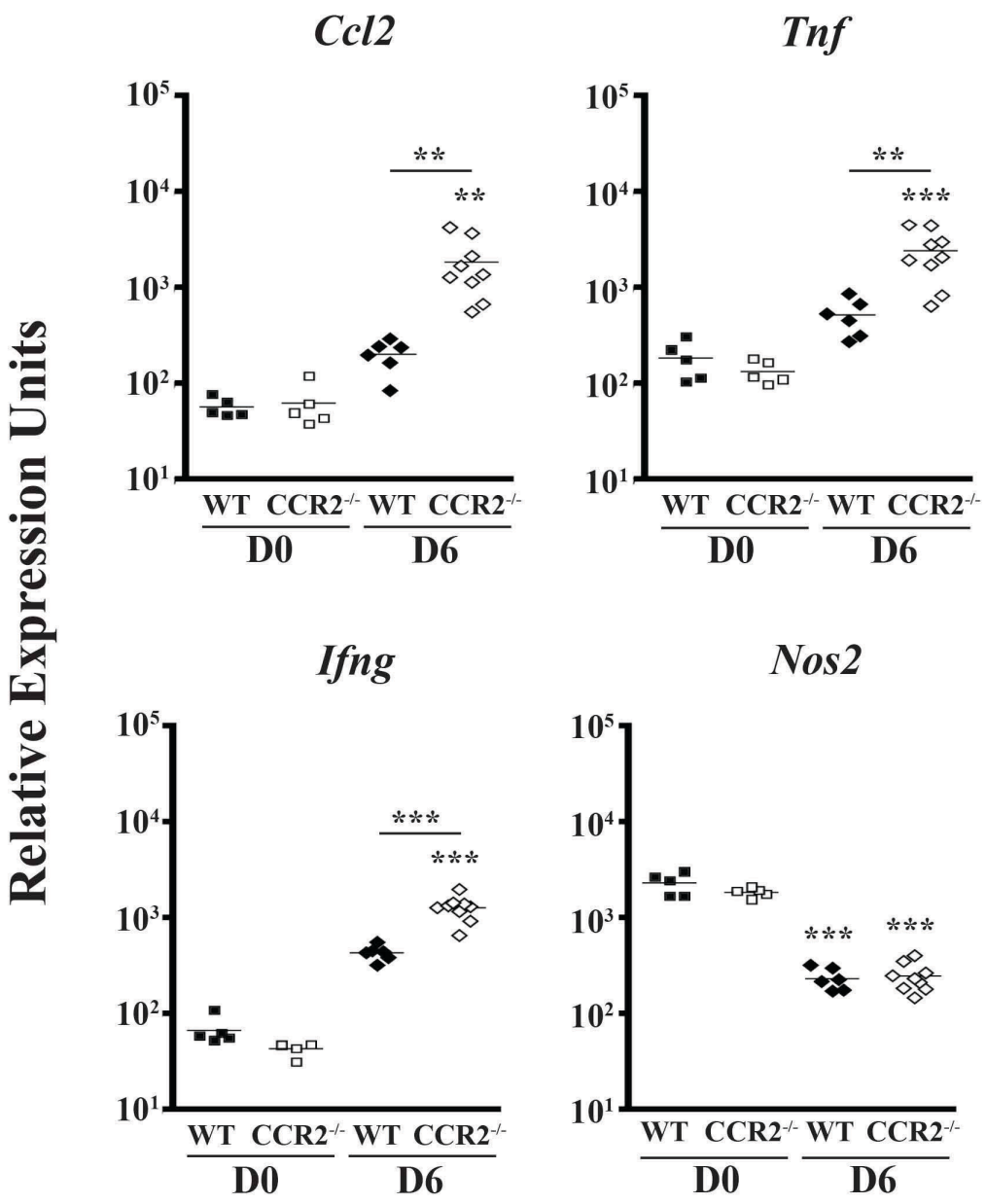

Figure 2.13 CCR2-deficiency results in elevated pro-inflammatory cytokine expression.
RNA was isolated from perfused whole lungs from WT and CCR2$^{-/-}$ mice prior to (D0) and after (D6) malaria infection and processed for real time RT PCR analysis of expression of *Ccl2*, *Tnf*, *Ifng* and *Nos2*. The data was normalized to the expression of *Gapdh* and expressed as relative expression units. Horizontal line represents the mean. **$p < 0.01$, ***$p < 0.001$, (N=5). Comparisons are versus naïve control, unless indicated by line.

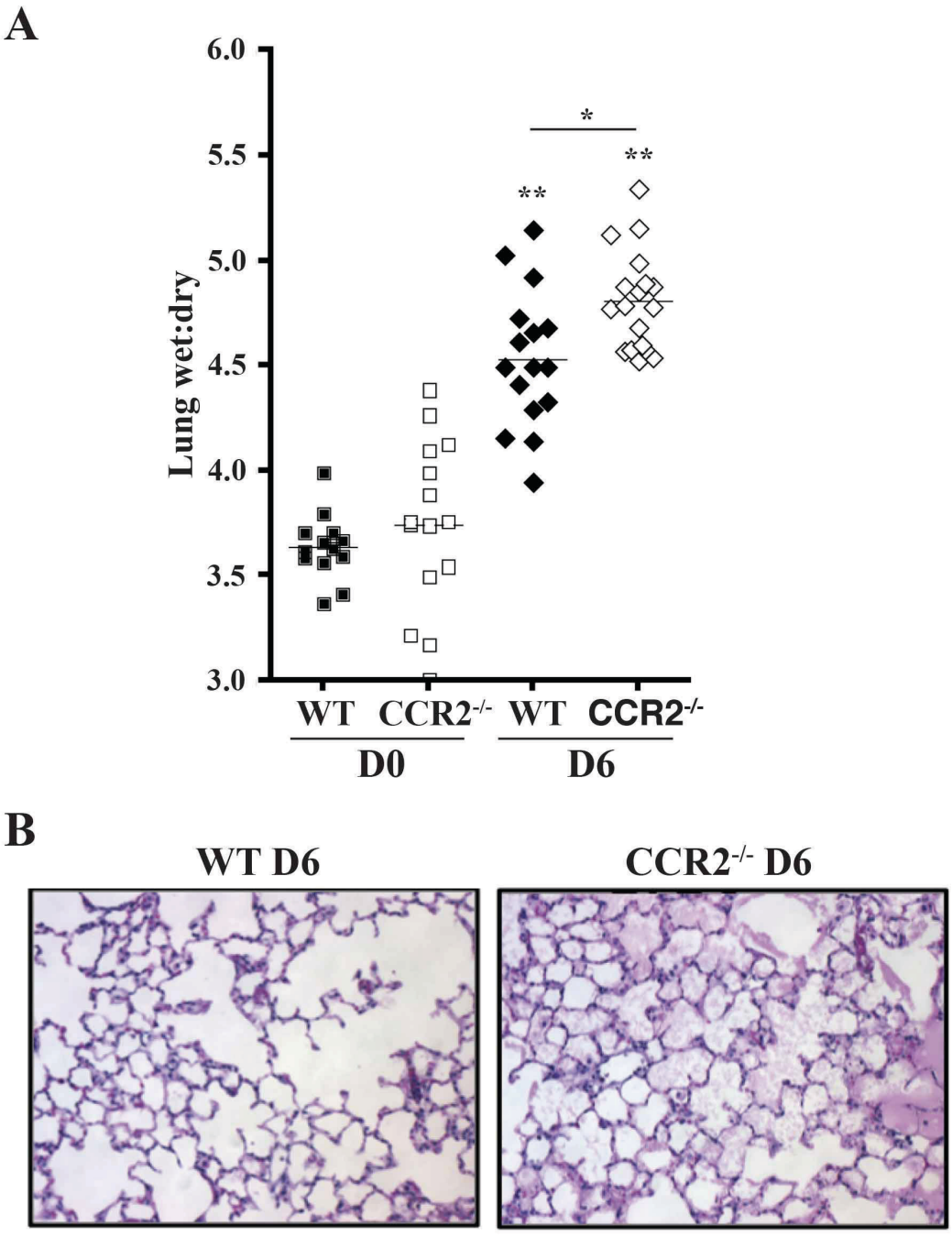

Figure 2.14 CCR2-deficiency results in exacerbation of lung injury.
(A) Lung injury measured as wet:dry ratios for non-infected (D0) and day 6 post-infection (D6) WT or CCR2$^{-/-}$ mice. Horizontal line represents the mean. Data are mean ± SEM, (N=12+) *$p < 0.05$, **$p < 0.01$. Comparisons are versus non-infected control except were noted with comparison line. (B) Representative histological sections (10X magnification) of lung tissue from WT or CCR2$^{-/-}$ mice at day 6 of infection with *P. berghei* ANKA.

decrease in histological evidence of pulmonary edema compared to the PBS controls (Figure 2.15B). These data suggest that a functional MDM population in the lungs is critical for the clearance of parasitized erythrocytes and ameliorating pulmonary lung injury.

2.4.8 CD36 is necessary for efficient clearance of sequestered infected erythrocytes by recruited monocytes

Previous studies have demonstrated that the scavenger receptor CD36 plays important roles in the dynamics of malaria in the lung [295]. CD36 is expressed on lung vascular endothelial cells where it interacts with malaria-derived molecules on the surface of infected erythrocytes and mediates sequestration [326, 420, 421]. In addition, CD36 is expressed on the surface of macrophages and monocytes where it serves as a key receptor for phagocytosis of infected erythrocytes containing late blood-stage parasites [289, 422, 423]. To determine the contribution of CD36 monocyte/macrophage-mediated parasite clearance and the development of lung pathology, we infected CD36-deficient mice with tdT*Pb*A and assessed the lungs for temporal changes in AM and MDM at days 3, 5 and 6 post-infection. As observed for WT mice, infection resulted in a significant increase in $CD11c^{-}$ $SiglecF^{-}$ $CD11b^{+}$ $Ly6C^{+}$ MDM and no change in the number of $CD11c^{+}$ $SiglecF^{+}$ $CD11b^{-}$ $Ly6C^{lo}$ AM in malaria-infected $CD36^{-/-}$ animals (Figure 2.16A). While there was a trend for fewer MDM at each day tested, the numbers in $CD36^{-/-}$ animals were not significantly different from those observed in WT lungs. As expected, due to absence of CD36-mediated sequestration and phagocytosis, CD36-deficient animals had significantly fewer MDM that engulfed parasite material (Figures 2.16B, 2.16C) and on a per cell basis the MDM contained a lower mean fluorescence intensity compared to cells isolated from WT lungs (Figure 2.16D).

The AM from $CD36^{-/-}$ animals at day 0 and 6 of infection had nearly identical surface phenotypes to the AM from WT mice (Figure 2.17A). It is interesting to note that, although lacking a CD36-mediated mechanism to engulf parasitized erythrocytes, the $CD36^{-/-}$ MDM that did take up parasites had an activation profile that closely paralleled what was observed for the phagocytically active WT MDM (Figures 2.17C, 2.17D).

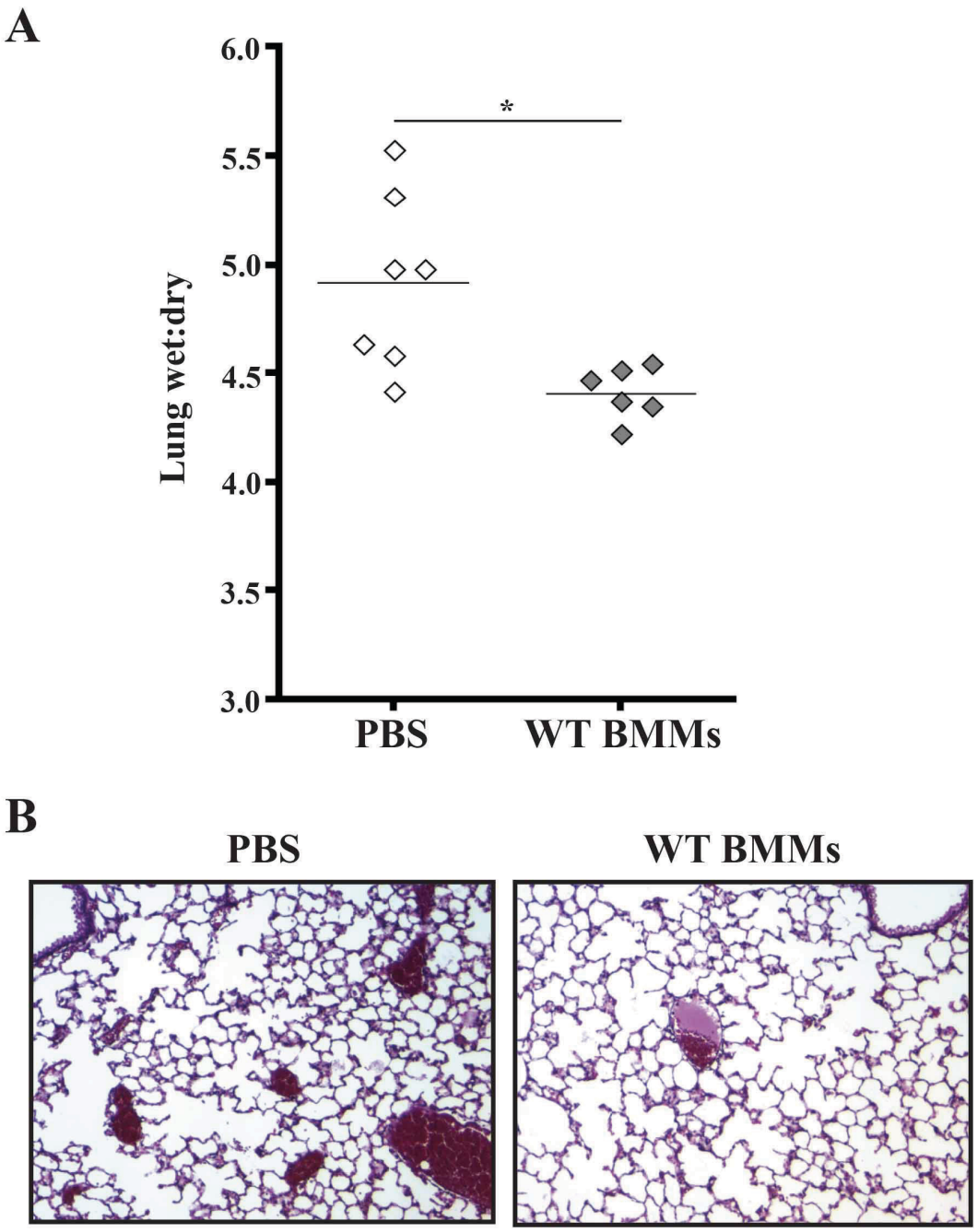

Figure 2.15 Adoptive transfer of CCR2+ monocytes reduces lung injury in infected CCR2-deficient mice.

P. berghei-infected CCR2$^{-/-}$ were administered either PBS or 10^6 wild-type bone marrow-derived monocytes via oropharyngeal aspiration at day 4 post-infection. Lungs were harvested at day 6 post-infection and assessed for lung injury. (A) Lung injury measured as wet:dry ratios for control (PBS) or adoptively transferred (WT BMM) mice. Data are mean ± SEM. *$p < 0.05$. (B) Representative H&E stained histological sections (10X magnification) of lung tissue from control (PBS) or adoptively transferred (WT BMMs) mice.

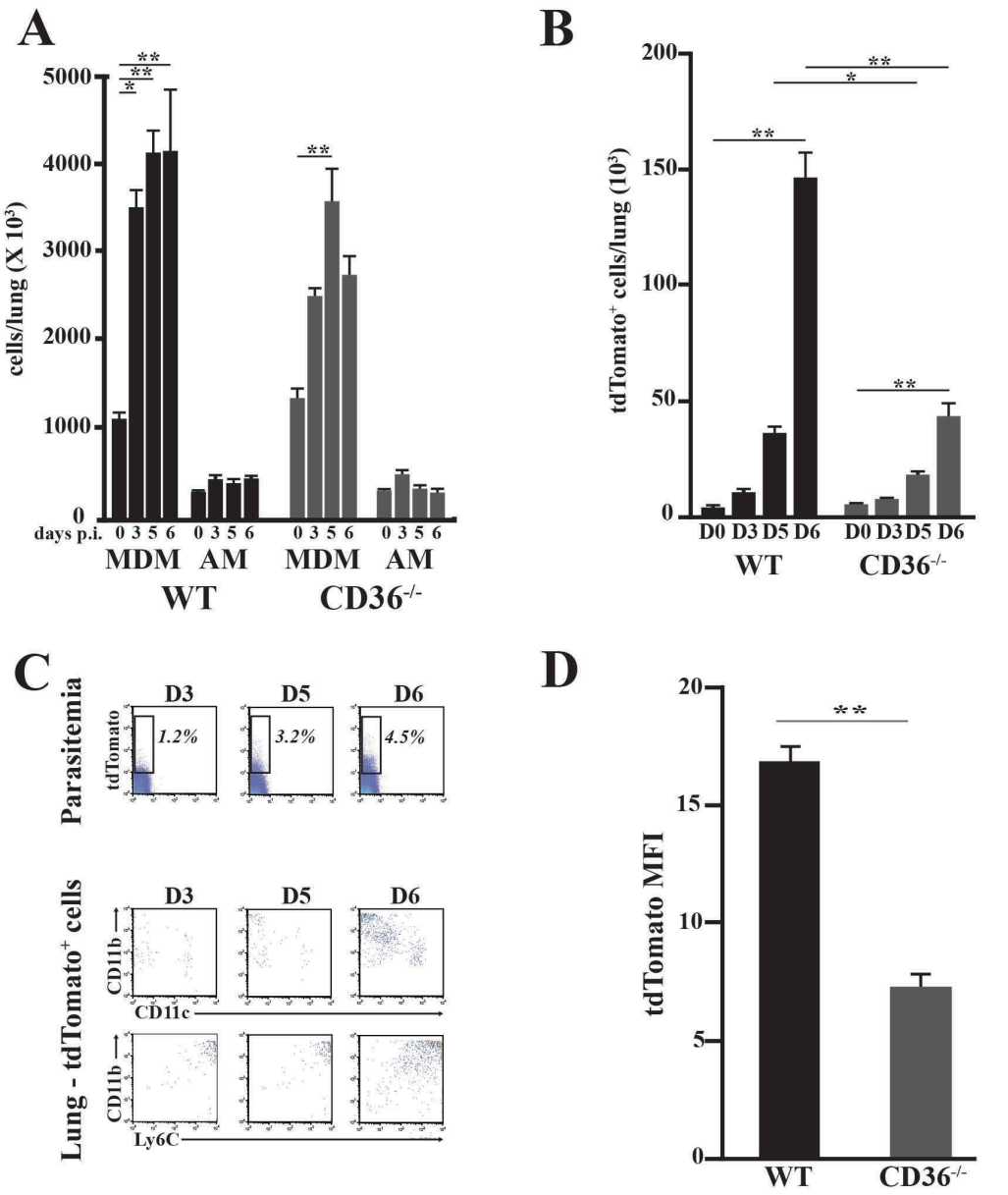

Figure 2.16 Dynamics of mononuclear cells and parasite clearance in the lungs from CD36$^{-/-}$ mice. (A) Change in the numbers CD64^{+}CD11b^{+}CD11c^{-} monocyte-derived macrophages (MDM) and CD64^{+}CD11b^{-}CD11c^{+} alveolar macrophages (AM) in WT and CD36$^{-/-}$ lungs during tdT*Pb*A infection. The numbers were derived from flow cytometric analysis of whole perfused lungs obtained at days 3, 5 and 6 post-infection (N=3). (B, top panel) Representative data depicting flow cytometric analysis of peripheral blood parasitemia in CD36$^{-/-}$ mice at days 3, 5 and 6 after infection with tdT*Pb*A. (B, bottom panel) Representative data depicting the dynamics of up-take of tdT*Pb*A-infected erythrocytes by CD11b^{+}CD11c^{-}Ly6C^{hi} MDM and CD11b^{-}CD11c^{+}Ly6C^{lo} AM from perfused lungs of CD36$^{-/-}$ mice at days 3, 5 and 6 post-infection. (C) The number of tdTomato-positive cells from the perfused lungs of WT and CD36$^{-/-}$ mice at days 0, 3, 5 and 6 post-infection (N=3). (D) The mean fluorescence intensity (MFI) for tdTomato^{+} cells detected in perfused lungs from WT and CD36$^{-/-}$ animals at day 6 post-infection. All data are mean ± SEM. *p < 0.05, **p < 0.01, **p < 0.001.

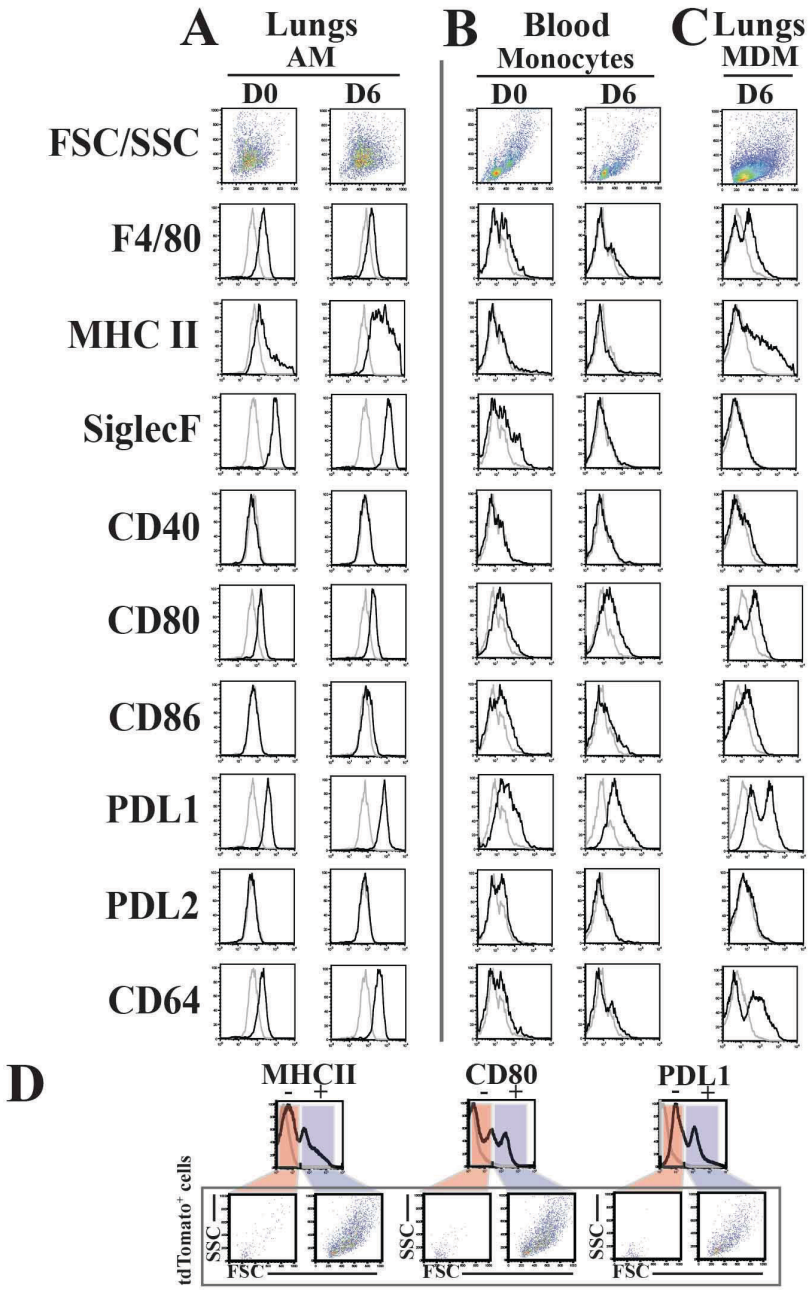

Figure 2.17 Activation of CD36-deficient alveolar macrophages (AM) and monocyte-derived macrophage (MDM) populations following malaria infection.
(A) Representative data (N=3) of flow cytometric analyses of gated cell populations from perfused lung homogenates (AM: $CD11b^{-}CD11c^{+}$; MDM: $CD11b^{+}CD11c^{-}$) or peripheral blood mononuclear cells (monocytes: $CD11b^{+}Ly6C^{+}$) of non-infected (D0) or day 6 (D6) post-*Pb*A infection. Histograms depict surface fluorescence signals of F4/80, MHCII, SiglecF, CD40, CD80, CD86, PDL1, PDL2 and CD64 (black line) and their respective isotype controls (grey line). (B) Flow cytometric analysis at day 6 post-tdT-*Pb*A infection demonstrating that the activated subset of MDM that expressed elevated MHCII, CD80 and PDL1 were also positive for the tdTomato signal. MDM were first gated for their positive or negative status for MHCII, CD80 and PDL1 and then analyzed for the levels of tdTomato signal. Dot plots below depict the light scatter properties of the $tdTomato^{+}$ cells present in each population.

NOTE: Supporting unpublished experiments were carried out in $CD36^{-/-}$ chimeric mice by Dr. Ifeanyi Anidi (data previously incorporated into doctoral dissertation [424]). Please refer to APPENDIX I for all methods, results, and figures. Dr. Anidi's experiments described in APPENDIX I will be referenced in the discussion section to follow (CHAPTER 2.5).

2.5 DISCUSSION

Employing the *P. berghei*-C57BL/6 system to model the dynamics of malaria-induced pathology in the lungs, we demonstrated that coincident with the onset of cytoadherence of infected-erythrocytes to the pulmonary microvasculature there was a rapid and robust recruitment of $CCR2^{+}CD11b^{+}Ly6C^{hi}$ inflammatory monocytes to the lungs. Furthermore, recruited monocyte-derived macrophages (MDM) were instrumental in controlling the extent of lung damage, in part through clearing adherent infected erythrocytes from the vascular endothelium, thus limiting the steady-state parasite burden in the lung.

The significance of $CCR2^{+}CD11b^{+}Ly6C^{hi}$ monocytes as innate effector cells during malaria has been studied previously in the context of the spleen during *P. chabaudi* infection in mice [325]. This prior study demonstrated that a population of $CD11b^{high}Ly6C^{+}$ cells migrated to the spleen during infection and that these monocytes effectively limited acute-stage parasitemia. Similar to the results presented here for the monocytes recruited to the lungs, $CD11b^{high}Ly6C^{+}$ splenic monocytes readily engulfed malaria-infected erythrocytes and up-regulated surface markers associated with cell activation and antigen presentation. Interestingly, although they expressed molecules that suggested the potential for antigen presentation, the recruited $CD11b^{high}Ly6C^{+}$ splenic monocytes were significantly less efficient than DCs in antigen presentation [325]. It is possible that $CCR2^{+}CD11b^{+}Ly6C^{hi}$ monocytes activated in the presence of malarial antigens become committed to rapid and extensive degradation of malaria antigens, thus reducing the monocyte's ability to present antigen to T cells despite high levels of MHCII and co-stimulatory molecules. In future work, it will be of interest to determine if the recruited $CCR2^{+}CD11b^{+}Ly6C^{hi}$ MDM, which also

actively engulfed parasitized cells and showed a robust activation phenotype (Figures 2.6, 2.7, 2.8C), have the ability to efficiently present malaria antigens to T cells.

While the surface markers used here allowed us to track changes in the AM and recruited monocytes/MDM populations [57, 58, 425], these markers precluded evaluation of the response of lung-resident interstitial macrophages to malaria infection. Interstitial macrophages have a distinct surface phenotype [425] which presumably reflects different functional properties compared with alveolar macrophages. Additional work will be required to define the contribution, if any, that interstitial macrophages provide to the overall response to malaria in the lungs.

The activation phenotype of the MDM was distinct from the partial activation status observed for the $CD11b^{+}$ $Ly6C^{hi}$ monocytes sampled from the peripheral blood at the same time (Figures 2.6B, 2.6C). The $CD11b^{+}$ $Ly6C^{hi}$ monocytes in the blood showed little evidence that they were active in taking up parasitized cells prior to entering the lung (data not shown). The data suggest that MDM are activated within the environment of the infected lung, perhaps upon encounter with the local cytokine milieu or as a consequence of engulfing parasitized erythrocytes (Figure 2.7).

Despite increasing numbers of parasitized cells in the blood and, presumably, an increasing number of cells sequestering in the lung, the number of MDM peaked at day 5 of infection suggesting a mechanism that limits the number inflammatory cells entering the lungs. However, it is also possible that monocytes continue to be recruited to the lung, but apoptosis, a substantial change in surface phenotype and/or exit from the lungs could combine to result in the appearance of a limit on recruitment. It is interesting to note that, although the total number appears to plateau, the proportion of the MDM that had taken up parasite-containing cells (as measured by fluorescent signal from tdT*Pb*A) increased significantly from day 5 to day 6 (Figure 2.10D). The use of the fluorescent signal from tdT*Pb*A parasites as a measure of phagocytosis of sequestered cells is likely to identify only recent phagocytic events and to be a significant underestimate of

the extent of parasite up-take. The presumption is that as the infected erythrocyte is degraded in the acidic phagolysosomal compartment of the MDM, the fluorescent signal will be rapidly extinguished.

Lung-resident macrophages (LRM), like the Kupffer cells in the liver, glial cells in the central nervous system and osteoclasts in bone, have distinct functional characteristics that are shaped by their local environment [9]. Recent studies have revealed that tissue-resident macrophages are seeded into tissues prior to birth from progenitors originating from the yolk sac [145, 196, 203, 205] and that these cells have a capacity for *in situ* self-renewal to maintain steady state levels [196, 208], for replacement after depletion [426], or in response to infections [231, 427]. In disease settings, this ability of tissue-resident macrophages to proliferate has prompted a reevaluation of how we interpret the functional dynamics of the mononuclear phagocytes at sites of inflammation and the functional roles assigned to resident macrophages and the monocyte-derived cells that are recruited to inflamed tissues. In the absence of disease, LRM, especially alveolar macrophages, are vital components of the homeostatic mechanism that prevents pulmonary inflammation to common environmental exposures (reviewed in [425]). In the context of the acute malaria infection in the lungs, the AM, which showed no evidence of proliferation and little evidence of activation (Figures 2.5B, 2.8A), appear to have only a minor role in responding in a pro-inflammatory fashion to parasite sequestration in the pulmonary vasculature. The AM retained their apparent non-activated status even under conditions of CCR2-deficiency, where blunted monocyte recruitment resulted in an elevated parasite burden and exacerbated lung reactivity (Figures 2.12, 2.13, 2.14). It appears that a feature of the limited activation status of the AM during malaria is a restricted capacity to engulf and clear schizont-infected erythrocytes from the lungs. As the chief role of AM is to respond to challenges within the alveolar spaces, it is possible that as long as the malaria-infected cells remain in the vascular compartment (or within the phagosomes of MDM), AM do not receive the appropriate activation signals.

This lack of responsiveness during malaria infection is in contrast to the AM proliferation observed in response to helminth and virus challenge [208, 427]. The lack of AM proliferation could reflect an absence of proper signals during the acute phase of infection. Both the larval helminth parasites and influenza virus

result in considerable lung epithelial cell damage resulting in the release of DAMPS, alarmins or other signaling molecules that could serve as a cue for AM proliferation. IL-4, one of the factors shown to induce peritoneal macrophages to proliferate [231, 232], was not detected during the early phase of *P. berghei* infection in C57BL/6 mice (personal communication, J.M. Craig). Although it is clear that AM have the capacity to rapidly expand in response to a pathogen challenge [427], it could be that AM proliferation is delayed during malaria until the chronic phase of the infection.

Instead of playing an active role in controlling parasite burden, it is possible that the role of AM during acute malaria is to regulate the level of activity of the recruited monocytes and set the stage for the appropriate anti-malaria adaptive response that will ensue. The surface phenotype (up-regulation of MHCII, no expression of CD40, CD86 or CD80 and constitutive expression of PDL1 (Figure 2.8A) and their demonstrated capacity to traffic antigen to draining lymph nodes [428] suggests that AM have the potential to regulate T cell-mediated immunity. However, the lack of direct uptake of infected erythrocytes by the AM speaks against a direct role in modulating the adaptive mucosal immune response against malaria. Additional work is required to assign a functional role for the AM during the innate stages of malaria infection.

The diminished monocyte influx and increased parasite burden in the lungs of malaria-infected $CCR2^{-/-}$ mice was associated with a notable increase in pathology (Figure 2.14). While it is likely that the heightened parasite load that resulted from reduced phagocytic clearance played a central role in the enhanced level of edema, we cannot exclude a contribution from the altered cytokine environment in $CCR2^{-/-}$ lungs. In addition to its role as a powerful chemokine for monocytes, CCL2 signaling influences the function of activated mononuclear cells. Defective CCR2 signaling results in cells that produce higher levels of TNF and lower IL-10 [429-432]. CCR2-deficient lungs had significantly elevated expression of *tnf* and *ifnγ* (Figure 2.13) that could contribute indirectly to the severity of the response to malaria.

In an alternate approach to study the relationships between sequestration, macrophage/monocyte function

and lung pathology we utilized CD36-deficient mice. In *P. berghei* infections CD36 plays several important roles. It is expressed on lung vascular endothelial cells where it serves as a binding partner with SMAC on the surface of parasite-infected erythrocytes allowing adhesion and sequestration [326]. CD36 is also expressed on the surface of macrophages and monocytes where it serves as a receptor that mediates recognition and phagocytosis of *Plasmodium*-infected erythrocytes [289, 422, 423]. The results reported here are consistent with the observations that CD36-deficient lungs have a significantly reduced parasite burden and attenuated pathology [295, 328]. Interestingly, despite a reduced parasite burden in the lungs and a notable reduction in phagocytosis, the number of monocytes recruited into the lungs (Figure 2.16A) and the level of activation of the MDM (Figure 2.17C) in $CD36^{-/-}$ animals were similar to WT mice.

A majority of the reports that used $CD36^{-/-}$ animals to study malaria in the lungs observed a significant reduction in parasite burden and ALI [295, 328], but could not differentiate the contributions of endothelial cell-expressed and monocyte/macrophage-expressed CD36 to the phenotype. The single report that employed a bone marrow chimera approach similar to the one used here, concluded, based only on survival data, that CD36 on non-hematopoietic cells was harmful [288]. We used a CD36 bone marrow chimera approach to study the relative contributions of CD36 expression on hematopoietic and non-hematopoietic cells at the cellular and tissue levels (APPENDIX I). The work presented here, provides a cellular mechanism for this observation. Our results are consistent with a model in which the degree of malaria-induced lung pathology is proportional to the steady-state levels of infected erythrocytes adhering to the pulmonary vasculature (Figure AI.1E, AI.2A, AI.2B). Furthermore, parasite burden in the lungs is influenced by the relative level and efficiency of CD36-mediated clearance of sequestered parasites by recruited MDM (Figure AI.1C). This model suggests that targeted inhibition of sequestration in the lungs of humans at risk for developing malaria-associated ALI or ARDS could be a valuable adjunct therapy to limit morbidity and mortality during severe malaria.

2.6 ACKNOWLEDGMENTS

The authors would like to thank Dr. Maria Febbraio for providing the $CD36^{-/-}$ animals, MR4 for providing the *P. berghei* ANKA parasites, Dr. Volker Heussler for providing tdTomato-transgenic *P. berghei* ANKA, Dr. Robert Thacker for his assistance with the Amnis ImageStream^{X} Mark II, and Xin Guo for her assistance with tissue processing for histology. This work was supported in part by a pilot grant (ALS) and pre-doctoral fellowships from the Johns Hopkins Malaria Research Institute (HADL, IUA, JMC) and the Johns Hopkins MD/PhD training program (T32 GM007309) (IUA).

CHAPTER 3

DYNAMIC CHANGES TO CELLULAR MORPHOLOGY, SURFACE PHENOTYPE AND ACTIVATION STATE ACCOMPANY ALVEOLAR MACROPHAGE PROLIFERATION FOLLOWING ELASTASE-INDUCED LUNG DAMAGE.

3.1 ABSTRACT

There is significant need to reveal the contributions made by lung macrophages to the progression of alveolar wall destruction resulting in emphysema. Employing the porcine pancreatic elastase (PPE) mouse model of emphysema, we demonstrate that lung-resident alveolar macrophages became activated following elastase-induced lung injury. Alveolar macrophages (AM) dynamically changed their cell morphology, surface phenotype and activation state. PKH26-PCL, a red fluorescent dye, was used for *in vivo* labeling of lung-resident phagocytic cells prior to PPE administration. Flow cytometric analysis of BAL-derived cells and lung homogenates demonstrated that the total number of AM roughly doubled between days 2 and 7 post-PPE administration before returning to untreated control levels by day 14. Similar AM dynamics were observed in $CCR2^{-/-}$ mice, suggesting that the elevated AM numbers were independent of $CD11b^{+}Ly6C^{+}CCR2^{+}$ inflammatory monocyte recruitment. Further analysis revealed that lung-resident AM enter cell cycle and proliferate following elastase-induced lung injury. Gene expression analysis demonstrated that lung macrophages took on a mixed M1/M2 activation phenotype that changed over a 21 day period. Given their documented longevity and ability to mediate inflammation long after acute insults, this AM subpopulation may contribute to the progression of emphysematous lung injury.

3.2 INTRODUCTION

Chronic obstructive pulmonary disease (COPD) is currently the world's fourth leading cause of death effecting 60 million people and leading to 3 million deaths per year (~ 5% of all deaths) [338]. The WHO predicts that COPD will increase to the third leading cause of death by 2030, only behind ischemic heart disease and stroke [338, 339]. Chronic obstructive pulmonary disease (COPD) is defined as progressive lung destruction encompassing two conditions, chronic bronchitis (inflammation of the bronchi) and emphysema (destruction of the alveolar walls), resulting in reduced gas exchange and impaired airflow in the lower airways [343]. Cardinal features of COPD include severe immune cell infiltration of the muscosa and submucosa, increased mucus production, epithelial cell hyperplasia, and dysregulated tissue repair mechanisms [343]. Increased sputum production and long lasting cough are among the most common symptoms of COPD, however, acute breathlessness or dyspnea is the most debilitating feature of severe COPD [345].

There are a variety of environmental exposures as well as genetic predispositions that are associated with the onset of progressive emphysema. Smoking tobacco, the predominant risk factor accounting for ~80% of cases [343, 350], as well as exposure to air pollution (outdoor, indoor, and occupational), second hand smoke, maternal smoking, respiratory infections, other non-respiratory infections, childhood asthma, hypersensitivity pneumonitis, dust, and fumes have also been linked to the onset of emphysema [343, 350, 351]. Additionally, α1 antitrypsin deficiency (A1AD), a congenital deficiency in α1 antitrypsin (A1AT), the major inhibitor of neutrophil elastase, leads to an imbalance in protease and anti-protease activity in the lungs, progressive airway enlargement and is responsible for ~1-2% of COPD cases [352, 353].

The development of progressive lung airway destruction should be considered an immunological disorder broadly categorized as initial epithelial cell damage followed by innate and adaptive immune responses [344]. Initially, tobacco smoke or other pulmonary irritants directly injure or stress alveolar epithelial cells (AEC) as well as degrade the lung's extracellular matrix (ECM) [355, 356] leading to the release of DAMPs and other danger signals [64] which activate innate immune signaling pathways [64, 357]. Upon

NF-κB stimulation, innate/early inflammatory cytokines and chemokines are released, leading to recruitment of inflammatory cells such as neutrophils, monocytes, and DCs to the lungs [359]. Neutrophils and mononuclear phagocytes release proteases (elastolytic enzymes) and reactive oxygen species (ROS), which can damage the lung tissue further [360, 361]. When these damage-inducing effector molecules are not appropriately controlled by a cadre of anti-proteases [362, 363] and anti-oxidants [361], the initial pro-inflammatory response ends up leading to further tissue damage and an uncontrolled positive feedback loop.

A multitude of enzymes including elastases, matrix metalloproteinases (MMP), cathepsins, caspases, and collagenases can cleave ECM components in the lungs [363, 377]. Typically these enzymes are deployed in order to aid in wound repair processes, embryonic development, promoting fibrosis, and angiogenic remodeling [362]. However, upon exposure to tobacco smoke or other lung irritants, a shift occurs in the balance between proteolytic activity and inhibitor activity [362], the effects of which are evident in the case of A1AD [352, 353]. The porcine pancreatic elastase (PPE) model of emphysema employs an elastolytic serine protease to cleave elastin fibers of the ECM, thereby endowing researchers with a quick, potent, and reproducible approach to activate a cascade of events similar to that which occurs in human populations, by tipping the balance between protease and anti-protease activity in the lungs.

Recent findings have directed attention to the major role that alveolar macrophages (AM) play in the orchestration of immune responses leading to the progression of alveolar tissue destruction [55, 373]. Most importantly to the pathophysiology of emphysema, alveolar macrophages secrete a wide variety of effector molecules that contribute either directly to tissue destruction or by promoting sustained inflammation [55, 373, 376]. For example, AM secrete elastolytic proteases such as MMP9 and MMP12 (macrophage elastase) that degrade collagen or elastin fibers, resulting in a loss of normal alveolar structure [363, 377]. The effects of alveolar wall destruction and loss of lung volume are permanent and currently incurable. Therefore, there is significant need to reveal the underlying cellular mechanisms that are responsible for the initiation and progression of alveolar wall destruction. Given their longevity and their ability to mediate inflammation long after acute insults, we hypothesize that during acute elastase challenge lung-resident

alveolar macrophages become activated and contribute towards the progression and manifestation of emphysematous changes in the lungs.

In the work presented here, we employed the PPE model of emphysema to define the dynamics and roles that lung-resident macrophages and recruited monocytes play in the progression of emphysema. We demonstrate that following acute elastase challenge, the size of the AM cellular niche transiently increases. The approximate doubling in AM numbers was accompanied by dynamic changes to the surface phenotype, changes in cellular morphology, and activation status. Using an *in vivo* phagocytic cell labeling approach, our findings suggested that a lung-resident AM subpopulation proliferated following PPE challenge. Furthermore, experiments carried out in CCR2-null mice suggested that following PPE challenge AM dynamics were $CCR2^{+}$ monocyte-independent. Importantly, lung-resident AM respond acutely to PPE-mediated damage and may contribute to the progression of emphysematous lung injury.

3.3 MATERIAL AND METHODS

3.3.1 Mice

Age and sex-matched (male 6-12 weeks old) littermates were used for all experiments. C57BL/6J, BALB/cJ, and $CCR2^{-/-}$ (B6.129S4-*Ccr2tm1Ifc*/J)] [410] were obtained from The Jackson Laboratory (Bar Harbor, ME, USA). All mice were maintained within barrier filter-top cages, provided food and water ad libitum, and exposed to a 12-hour light/dark cycle. All animal procedures performed in this study were approved by the Johns Hopkins Animal Care and Use Committee (Baltimore, MD, USA), and were in accordance with the National Research Council's Guide for the Care and Use of Laboratory Animals federal guidelines.

3.3.2 Elastase challenge

Porcine pancreatic elastase (EC-134; Elastin Products Co., Inc., Owensville, MO, USA) was administered directly into the airways via intra-tracheal aspiration. Following brief anesthesia under 35% Isoflurane (10019-360-60; Baxter Healthcare Corp., Deerfield, IL, USA), C57BL/6 or BALB/c mice were administered 6U (50 μg) or 3U (25 μg) PPE respectively.

3.3.3 Antibodies

The following anti-mouse antibodies were purchased from BD Biosciences (San Jose, CA, USA) CD11b-PerCP-Cy5.5 (550993), SiglecF-PE (552126), Ly6C-APC (560595). Mouse anti-rat IgG2b k-biotin (553898) was purchased from BD Biosciences. CD11b-APC (17-0112-81), MHCII-PE (12-5321-81), Ki-67-eFluor660 (50-5698-80), rat IgG2aκ-eFluor660 (50-4321-80), and CD200R-APC (17-5201-80) anti-mouse antibodies were purchased from eBioscience (San Diego, CA, USA). Streptavidin-PE (12-4317-87) was purchased from eBioscience. Intracellular nuclear staining was performed using eBioscience Foxp3 Staining Buffer Set (00-5523-00). Anti-mouse CD11c-APC (130-091-844) and CD11c-FITC (120-002-107) were purchased from Miltenyi Biotec (Auburn, CA, USA). Anti-mouse ST2-APC (FAB10041A) antibody was purchased from R&D Systems (Minneapolis, MN, USA). MC-21, rat anti-mouse CCR2 IgG2b κ was generously provided by Dr. Matthias Mack (Universitätsklinikum Regensburg, Regensburg, Germany).

3.3.4 Flow cytometry

Whole lung homogenates were generated as previously described [46]. Briefly, prior to excision from the chest cavity, lungs were perfused with 10 mL of room temperature sterile Dulbecco's PBS via the right ventricle of the heart. Lungs were carefully removed and placed in 5 mL RPMI 1640 containing 1 mg/mL collagenase type II (1701-015, Life Technologies, Grand Island, NY, USA) and 30 μg/mL DNase I (10104159001, Roche Applied Science, Indianapolis, IN, USA), minced thoroughly, and incubated at 37°C for 30 minutes. Minced lung suspensions were then ground through a 100-μm nylon cell strainer (352360, BD Biosciences), and the resulting cells were pelleted at 1500g at 4°C. Cells were suspended in ACK

lysing buffer (118-156-721, Quality Biological Inc., Gaithersburg, MD, USA) to remove any contaminating erythrocytes, passed through a second cell strainer, and washed in FACS staining buffer [PBS containing 2% heat-inactivated FCS (35-011-CV, Mediatech, Inc., Manassas, VA, USA)]. Cells were then treated with anti-mouse CD16/CD32 Fc Block (553142, BD Biosciences) 10 minutes prior to the addition of cell surface marker specific antibodies. All antibodies were incubated on ice for 20 minutes in the dark. Stained cells were then washed in FACS staining buffer prior to flow cytometric analysis. Cell counts were performed on a hemocytometer using trypan blue stain (15250-061, Life Technologies) to exclude dead cells. All data on whole lung homogenates or peripheral blood cells (collected via tail vein) were collected on a BD FACSCalibur flow cytometer (San Jose, CA, USA) and data analyzed using FlowJo (TreeStar Inc., Ashland, OR, USA).

3.3.5 Bronchoalveolar lavage (BAL)

Murine surgeries were performed as previously described [413]. Briefly, mice were anaesthetized with 450 mg/kg 2,2,2-tribromoethanol (Sigma-Aldrich, St. Louis, MO, USA) via intraperitoneal injection. An incision was made through the sternum and BAL fluid was obtained after a tracheostomy and lavaging of the lungs with 800 µl of sterile PBS three separate times at room temperature. BAL fluid from the three collections were pooled and centrifuged at 1,500 rpm for 6 minutes at 4°C. Cells were suspended in PBS and an aliquot was stained with trypan blue (Invitrogen, Grand Island, NY, USA) prior to counting on a hemocytometer using the 10X objective of an Olympus BH-2 microscope (Catharpin, VA, USA). Cells (10^5) from each mouse were adhered to microscope slides with the aid of cytology funnels (Fisher Scientific, Houston, TX, USA) and a cytocentrifuge (Shandon Cytospin, Thermo Fisher Scientific, Waltham, MA) prior to methanol fixation and subsequent staining with Giemsa for differential cell analyses.

3.3.6 *In vivo* labeling of resident lung macrophages

Following brief anesthesia under Isoflurane, mice were administered PKH26-PCL, a red fluorescent dye, (PKH26PCL-1KT, Sigma-Aldrich, St. Louis, MO, USA) (1.25-10µM) in 50µL phosphate-buffered saline

via intra-tracheal aspiration. Typically, PKH26-PCL was used to label lung-resident phagocytic cells one day prior to PPE challenge. Under certain experimental conditions, all groups were *in vivo* labeled on the same day and the PPE challenges were staggered so that the time interval between PKH26-PCL labeling and lung harvest were equalized.

3.3.7 Lung macrophage depletion

Clodronate- or PBS- loaded liposomes suspended in sterile PBS (100 µL liposome suspension per animal) purchased from Dr. Nico von Rooijen (Amsterdam, The Netherlands), were administered via intra-tracheal aspiration following temporary anesthesia under 35% Isoflurane.

3.3.8 Neutrophil depletion

Rat anti-mouse Ly6G monoclonal antibody clone 1A8 (BE0075-1, Bio X Cell, West Lebanon, NH) was used to specifically deplete neutrophils from the circulation [433]. Briefly, mice were administered 500µg antibody formulated in 200 µL sterile Dulbecco's phosphate buffered saline via intra-peritoneal injection one day prior to PPE challenge.

3.3.9 Bead selection of lung macrophages

Single cell suspensions were generated from lung tissue as described above. Following Fc receptor blockade, lung cells were stained with anti-mouse CD11c-APC (130-091-844, Miltenyi Biotec) for 20 minutes on ice in the dark. Following a wash with FACS buffer, stained cells were centrifuged and suspended in 50 µL of anti-APC magnetic bead particle slurry (557932, BD Biosciences) and incubated for 30 minutes on ice in the dark. Following bead incubation, 1mL MACS buffer (phosphate buffered saline + 0.5% BSA + 2 mM EDTA) was added to each sample. Samples were then placed in BD IMagnet cell separator (552311) for 8 minutes. The non bead-bound cell fraction ($CD11c^-$ cells) was removed. The bead-bound fraction ($CD11c^+$ cells) was again suspended in 1 mL MACS buffer and placed on the BD magnetic

cell separator for an additional eight minutes. The cell fraction procedure was repeated as above. Both the positive and negative cell fractions were counted using a hemocytometer prior to pelleting and freezing.

3.3.10 Nucleic acid isolation and gene expression analysis

RNA was isolated from the bead-selected cell samples using the Qiagen RNeasy Plus Mini kit (74134, Qiagen, Valencia, CA). RNA quantity and purity were assessed by A260/280 absorbance using a Nanodrop ND-1000 (Nanodrop Products, Wilmington, DE, USA). RNA (500 ng) was then reverse-transcribed using the SuperScript II first-strand synthesis system for RT-PCR (100004925, Life Technologies) using oligo (dT) (12-18) primers (58862, Life Technologies). Quantitative real-time RT-PCR was performed using the Applied Biosystems 7500 realtime PCR system, TaqMan Gene Expression Assays-On-Demand, and Taq-Man Universal Master Mix (Life Technologies). The following assays (Applied Biosystems) were used: *Arg1* (Mm00475988_m1), *Chil3* (Mm00657889_mH), *Gapdh* (Mm99999915_g1), *Il1b* (Mm00434228_m1), *Il6* (Mm00446190_m1), *Il10* (Mm00439614_m1), *Il12a* (Mm00434165_m1), *Il18* (Mm00434225_m1), *Il33* (Mm00505403_m1), *Ilr1l1* (Mm00516117_m1), *Mmp9* (Mm00442991_m1), *Mmp12* (Mm00500554_m1), *Nos2* (Mm00440502_m1), *Retnla* (Mm00445109_m1), *Tnf* (Mm00443258_m1), *Tgfb1* (Mm01178820_m1). TaqMan reactions were performed using 1 μL cDNA in a 20 μL reaction volume and the following thermal cycler profile: 10 minutes denaturation at 95°C, 50 cycles of 15 seconds denaturation at 95°C, followed by 1 minute extension at 60°C. Analysis was performed using the Applied Biosystems 7500 system SDS software package (Life Technologies). Relative expression units were generated by comparing individual expression levels to a standard curves generated using pooled cDNAs as a template. All genes were normalized to a housekeeping gene control (Gapdh).

3.3.11 Histology

A 19-gauge gavage tube was inserted into a small hole in the trachea, and the lungs were inflated slowly with zinc-buffered formalin fixative (Z-fix) (174, Anatech Ltd., Battle Creek, MI, USA). The lungs were removed and incubated in Z-fix for 48 hours. Inflated and fixed lungs were embedded in paraffin, and sagittal, 5 μm sections, were cut from four different levels of lung. Lung sections were placed on slides and

either left unstained or stained with hematoxylin and eosin. Lung sections (and cytology slides) were examined using a Nikon Eclipse E800 light microscope (Nikon Instruments Inc., Melville, NY, USA), and images were acquired using SPOT RT charge-coupled device imager and software (Diagnostic Instruments, Inc., Sterling Heights, MI, USA).

3.3.12 Immunofluorescence microscopy

Methanol fixed cytospin preparations were stained with biotinylated *Griffonia* (*Bandeiraea*) *simplicifolia* lectin 1 isolectin B_4 (GSL1)-biotin (1:100) (#B-1205; Vector Laboratories, Inc., Burlingame, CA, USA) for 20 minutes. Following 2 x 3 minute washes with DPBS, fluorescein-avidin (1:100) (#A-2001; Vector Laboratories) was added for 15 minutes. The slides were washed prior to the addition of Vectashield Hardset mounting medium with DAPI (#H-1500; Vector Laboratories). Stained slides and coverslips were allowed to set in the dark overnight at 4°C prior to imaging. A Nikon Eclipse Ni-E upright microscope equipped with an Andor Zyla sCMOS camera (Andor Technology, Ltd., Belfast, UK) and NIS-Elements Microscope Imaging Software (Nikon) were used to capture fluorescent images of cytospin preparations using a 20X objective lens (Nikon Instruments Inc., Melville, NY, USA). Images were collected for each fluorescent channel through each Z-stack. Deconvolution (30 iterations) of Z-stacks was performed using NIS-Elements Microscope Imaging Software.

3.3.13 Statistical analysis

Statistical significance was evaluated by using the 2-tailed t test (Tukey) and the one-way analysis of variance (ANOVA) test using GraphPad Prism software version 4 for Mac (La Jolla, CA, USA).

3.4 RESULTS

3.4.1 Preliminary data in the PPE model

Previous studies conducted in the laboratory [407] have demonstrated that significant hemorrhage and alveolar tissue destruction was evident in histopathological lung tissue sections from mice that received porcine pancreatic elastase (PPE) via intra-tracheal aspiration as early as two days post-challenge. Despite administration of a single dose of PPE, with enzymatic activity only lasting approximately 24 hours, the lung tissue damage continued and loss of pulmonary epithelial surfaces progressed over the next three weeks to fully manifested emphysema at day 21 post-elastase (Figure 1.7B). Not surprisingly, at day 21 post-elastase challenge, the lung function as measured by diffusing factor of carbon monoxide (DF_{CO}), total lung capacity (TLC), residual volume (RV), and static compliance was severely compromised (Table 1.7). These studies demonstrated that the composition of cellular populations harvested from the lungs by bronchoalveolar lavage (BAL) varied over time. At baseline (no elastase challenge) the cells residing within the airways were almost exclusively alveolar macrophages (Figure 1.7C, 1.7D). Upon elastase challenge, there was a significant influx of neutrophils, detectable within one hour and peaking at 48 hours (data not shown), as well as a mononuclear cell infiltration (including monocytes and lymphocytes) were observed at day 7 post-elastase challenge (Figure 1.7C, 1.7D).

3.4.2 Dynamics of myeloid cells in the lungs following PPE challenge

Given that the composition of cellular populations isolated via BAL following elastase challenge varied over time, we wanted to assess the dynamics of myeloid cell populations within the lung tissue with special emphasis on monocytes and macrophages. We employed flow cytometric analysis and focused on myeloid cell populations by staining lung homogenates with antibodies specific for binding to monocyte/macrophage cell surface markers including CD11b and CD11c (both members of the integrin family and components of the CR3 and CR4 complement receptors, respectively), SiglecF (a sialic acid binding lectin selectively expressed on eosinophils and lung macrophages [58, 61]), MHCII (major histocompatibility complex class II), and Ly6C (glycophosphatidylinositol-anchored surface protein expressed on monocytes, neutrophils and T cells). To ensure that the cell dynamics profile encompassed both the initiation and progression phases of emphysematous changes in the lungs, we assayed the mononuclear content of perfused lungs at days 0, 2, 7, 14, and 21 post-elastase challenge.

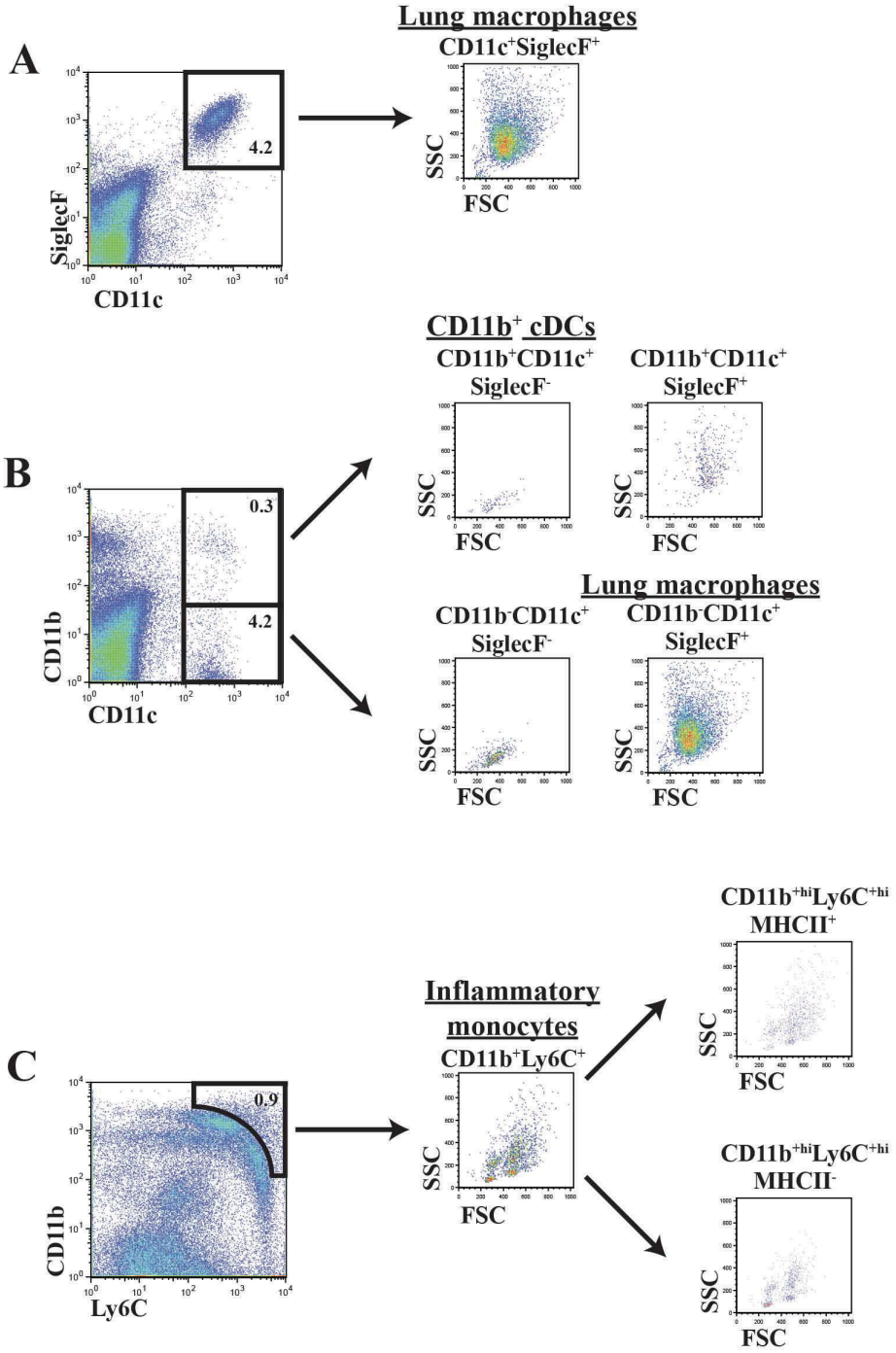

Figure 3.1 Identification of myeloid cell populations in the lungs.
Flow cytometric analysis of perfused lungs isolated from unchallenged C57BL/6 mice. Representative pseudocolor dotplots depict lung cells surface stained with (A) CD11c-APC (x-axis) and SiglecF-PE (y-axis); (B) CD11c-APC (x-axis) and CD11b-PerCP-Cy5.5 (y-axis); (C) Ly6C-APC (x-axis) and CD11b-PerCP-Cy5.5 (y-axis). (A-C) Gating strategies and light scatter properties of lung macrophage ($CD11c^{+}SiglecF^{+}$; $CD11b^{-}CD11c^{+}$), $CD11b^{+}$ cDC ($CD11b^{+}CD11c^{+}SiglecF^{-}$) and inflammatory monocyte ($CD11b^{+hi}Ly6C^{+hi}$) populations. Mean percentage of total lung cells displayed within each gate (n=5).

Based on current literature [14, 57, 58] and confirmatory experimental evidence (data not shown), alveolar macrophages were designated as $CD11c^{+}SiglecF^{+}$ cells. AM typically account for 3-5% of the total cells isolated from perfused lungs (Figure 3.1A) and can also be identified as the $CD11c^{+}CD11b^{-}$ cell population in unchallenged mice (Figure 3.1B). From unchallenged lungs, $CD11b^{+}$ conventional dendritic cells (cDCs) can be identified as the $CD11c^{+}CD11b^{+}$ cell population [57, 434]; however, unlike AM lung DCs do not express SiglecF (Figure 3.1B). We did not include identification of other lung DC populations such as $CD103^{+}$ lung DC or plasmacytoid DC (pDC) in this analysis. Nevertheless, we monitored the dynamics of inflammatory or "classical" monocytes [9], defined here as $CD11b^{+hi}Ly6C^{+hi}$ cells (Figure 3.1C). While circulating inflammatory monocytes are typically characterized as $MHCII^{lo}$ cells, upon migration to inflamed sites these monocytes can increase MHCII surface expression [187]; therefore, we monitored the dynamics of $CD11b^{+hi}Ly6C^{+hi}MHCII^{-}$ and $CD11b^{+hi}Ly6C^{+hi}MHCII^{+}$ monocyte populations in order to distinguish between circulating or recently emigrated monocytes ($MHCII^{-}$) from differentiating monocytes ($MHCII^{+}$) at the site of inflammation. Similar to previously published studies, we have identified and described multiple myeloid cell populations within the lungs based on flow cytometric analysis of cell surface phenotype [57, 58, 435]. While we appreciate that there are a variety of other surface markers and functional characteristics that can be used to refine these cell populations and further define subpopulations, we are confident in the accuracy of the parameters used in this study to discriminate between major myeloid cell populations isolated from whole lung tissue. The surface marker phenotypes and defining characteristics used in this study are summarized below in Table 3.1.

Table 3.1 Myeloid cells subsets in the murine lung

Myeloid cell population	*Defining characteristics (used in this analysis)*	*Other characteristics (not used in this analysis)*
Alveolar macrophages (AM)	$CD11c^{+}$ $CD11b^{-}$ $SiglecF^{+}$	$F4/80^{low}$; $MHCII^{low}$; $CD64^{+}$; PD-$L1^{+}$; high autofluorescence
$CD11b^{+}$ lung DCs	$CD11c^{+}$ $CD11b^{+}$ $SiglecF^{-}$	$MHCII^{low}$; $CD205^{+}$; low autofluorescence

Classical/inflammatory monocytes	$CD11b^{+high}$ $Ly6C^{+high}$ $MHCII^{low/high}$	$F4/80^{+}$; $CD11c^{-}$; $SiglecF^{-}$; $CD64^{+}$; $CD115^{+}$; $CCR2^{+}$

Since expression of the flow cytometry results as a percentage of a selected cell population has the potential to introduce bias into the analysis, the data for each myeloid cell population was expressed in terms of cell number calculated based on the total number of lung cells. Combining flow cytometric percentage output with total lung cell numbers, we were able to track changes in the myeloid cell populations over a 21 day period following elastase challenge (Figure 3.2). The number of $CD11c^{+}SiglecF^{+}$ AM from unchallenged animals was estimated to be near 0.5×10^{6} (Figure 3.2A). By day 7 post-elastase the number of AM had nearly doubled (Figure 3.2A, 3.3A). This significant increase in lung macrophage numbers was transient, as by day 14 and 21 post-PPE, the number of AM was similar to unchallenged mice (Figure 3.2A, 3.3A). While the total number of lung DCs is relatively small in comparison to other myeloid cell populations, there was a significant increase in this population at day 7 post-elastase compared to unchallenged control mice (Figure 3.2B, 3.3B). Surprisingly, the number of inflammatory monocytes ($CD11b^{+}Ly6C^{+}$) in the lungs did not increase compared to controls over the 21 day period (Figure 3.2C, 3.3C, 3.3D), actually there was a significant decrease in the number of $CD11b^{+}Ly6C^{+}MHCII^{+}$ cells at days 14 and 21 (Figure 3.3D). Given the robust neutrophil influx in the airways peaking at day 2 following elastase-challenge, it was expected that monocytes would be recruited to the lungs to clear neutrophil apoptotic bodies. However, under these conditions we did not observe a significant monocyte influx, perhaps, we may have overlooked monocyte recruitment to the lungs occurring between days 2 and 7 post-elastase challenge or focused on an inappropriate monocyte subset for this type of inflammatory insult.

When we focused specifically on $CD11c^{+}SiglecF^{+}$ AM in the lungs, it became clear that as early as two days following elastase challenge, that a subpopulation had emerged. Typically in unchallenged lungs, cells with a $CD11c^{+}SiglecF^{+}CD11b^{+}$ surface phenotype are not present in abundance (Figure 3.1B). However, at days 2 and 7 post-elastase challenge, the number of $CD11c^{+}SiglecF^{+}$ cells staining positive for CD11b surface expression was elevated (Figure 3.4A, 3.4B). The emergence of this $CD11c^{+}SiglecF^{+}CD11b^{+}$ cell

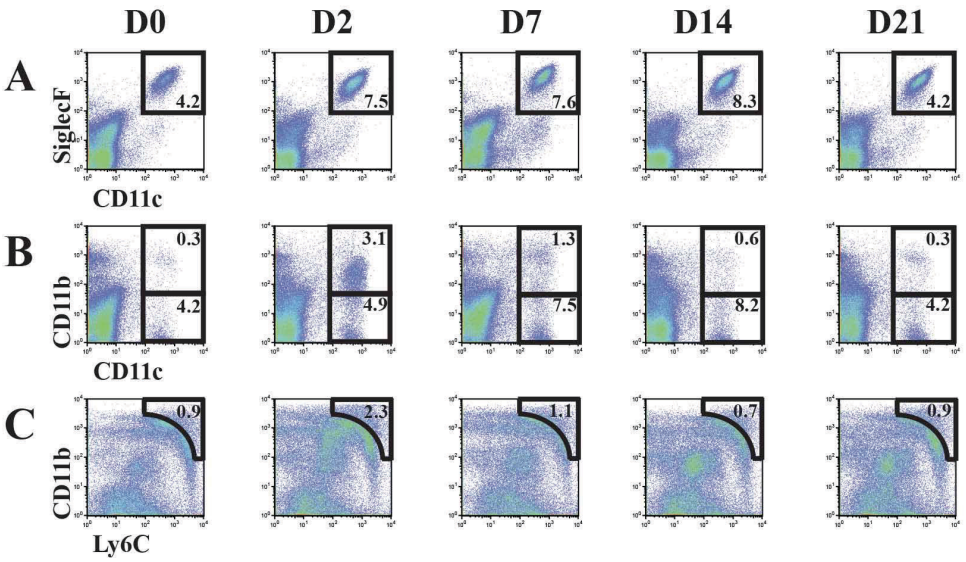

Figure 3.2 Dynamics of myeloid cells in the lungs following PPE challenge.
Flow cytometric analysis of perfused lungs isolated from C57BL/6 mice challenged with 6U PPE via intra-tracheal aspiration at days 0, 2, 7, 14, and 21 post-challenge. Representative pseudocolor dotplots depict lung cells surface stained with (A) CD11c-APC (x-axis) and SiglecF-PE (y-axis); (B) CD11c-APC (x-axis) and CD11b-PerCP-Cy5.5 (y-axis); (C) Ly6C-APC (x-axis) and CD11b-PerCP-Cy5.5 (y-axis). (n=5 per day). Boxes highlight gated (A) $CD11c^{+}SiglecF^{+}$; (B) $CD11b^{+}CD11c^{+}SiglecF^{-}$ and $CD11b^{-}CD11c^{+}SiglecF^{+}$; and (C) $CD11b^{+hi}Ly6C^{+hi}$ cell populations. Mean percentage of total lung cells displayed within each gate (n=5).

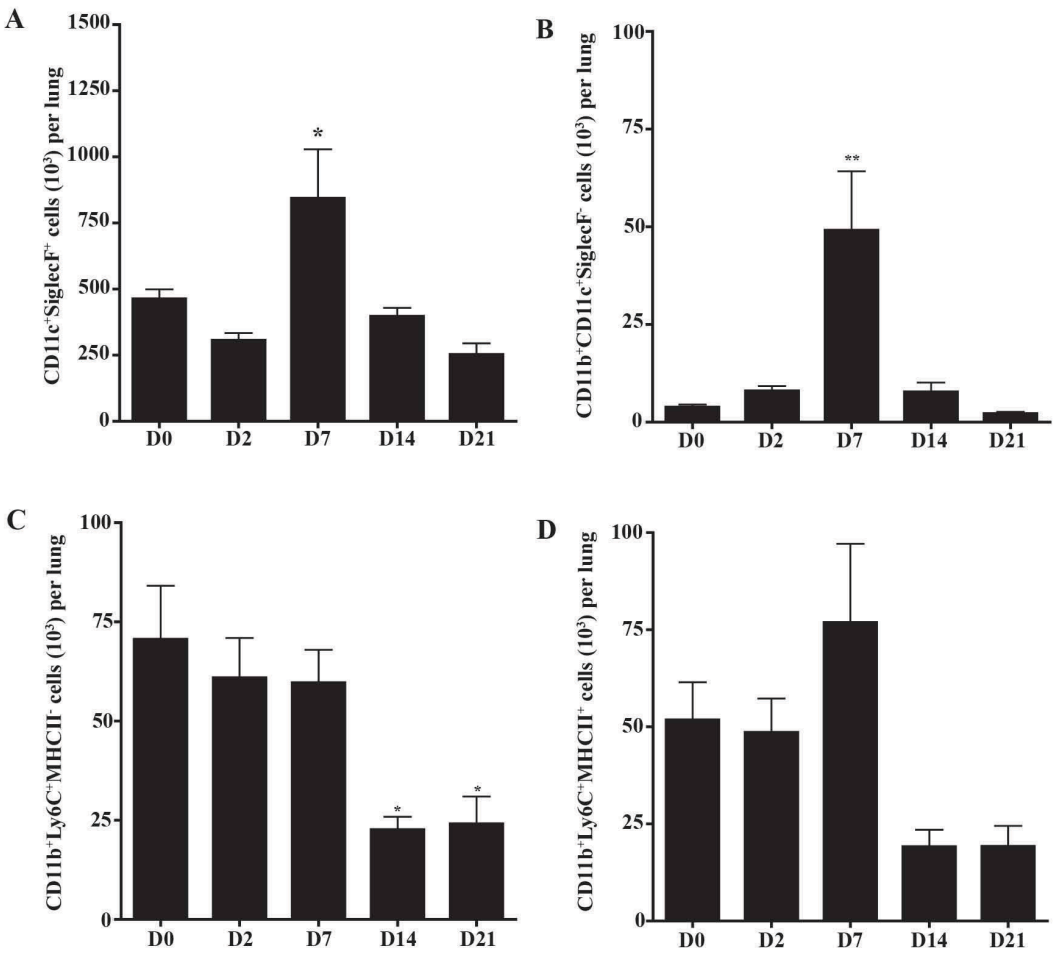

Figure 3.3 Dynamics of myeloid cell populations in the lungs following PPE challenge.
Total number of (A) macrophages ($CD11c^{+}SiglecF^{+}$), (B) dendritic cells ($CD11b^{+}CD11c^{+}SiglecF^{-}$), and inflammatory monocytes (C) $CD11b^{+}Ly6C^{+}MHCII^{+}$ (D) $CD11b^{+}Ly6C^{+}MHCII^{-}$ present in perfused lungs isolated from C57BL/6 mice challenged with 6U PPE via intra-tracheal aspiration at days 0, 2, 7, 14, and 21 post-challenge. (n=5 per day). Bar graph depicts mean ± SEM. * $p<0.05$; ** $p<0.01$. All comparisons are versus unchallenged controls.

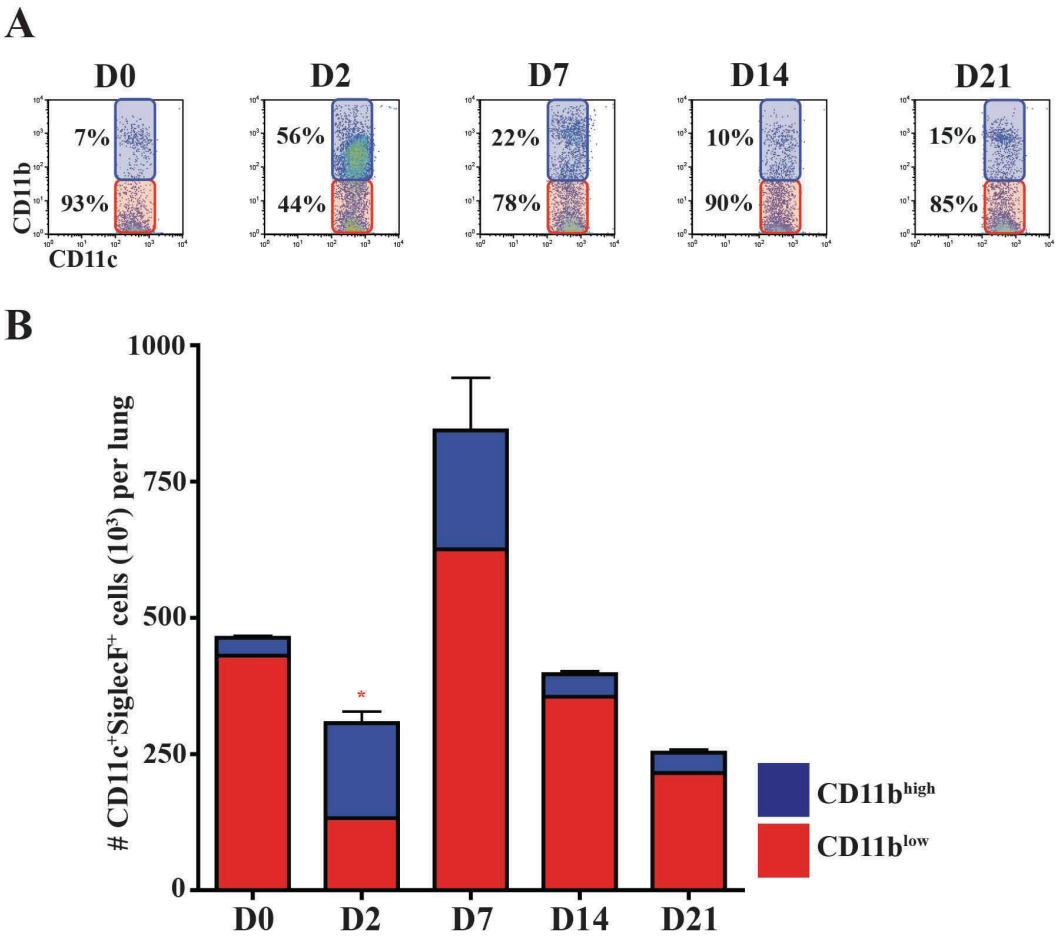

Figure 3.4 Dynamics of lung CD11c^{+}SiglecF^{+} population's surface phenotype following PPE challenge.

(A) Representative data depicting flow cytometric analysis of perfused lungs isolated from C57BL/6 mice following 6U PPE administration via intra-tracheal aspiration at days 0, 2, 7, 14, and 21 post-challenge. Cells were surface stained with anti-mouse antibodies specific for CD11b, CD11c, and SiglecF. Plots show CD11b fluorescence intensity (y-axis) of gated CD11c^{+}SiglecF^{+} cell population. Subpopulations are highlighted with colored boxes: CD11b^{low} (red) and CD11b^{high} (blue). Subpopulation percentage of total gated CD11c^{+}SiglecF^{+} cells is displayed. (B) Total number of CD11c^{+}SiglecF^{+} cells per perfused lung (n=5 per day). Subpopulations are highlighted with colored bars: CD11b^{low} (red) and CD11b^{high} (blue). Bar graph depicts mean ± SEM. * $p<0.05$; ** $p<0.01$. All comparisons are versus unchallenged controls.

subpopulation (highlighted in blue) was transient in nature as the size of this cellular niche resembled unchallenged controls at days 14 and 21 post-elastase (Figure 3.4).

3.4.3 Examining the role of inflammatory monocytes on the progression of elastase-induced emphysema

In an attempt to understand the origin and significance of this elastase-induced myeloid cell subpopulation, we hypothesized that the $CD11c^{+}SiglecF^{+}CD11b^{+}$ subpopulation trafficked into the lungs from the periphery in response to the damage created by the intra-tracheal elastase challenge. Although under these conditions we had measured minimal inflammatory monocyte ($CD11b^{+}Ly6C^{+}$) influx into the lungs following elastase challenge (Figure 3.3C, 3.3D), it was still formally possible that the $CD11c^{+}SiglecF^{+}CD11b^{+}$ subpopulation may have been recruited to the lungs via chemokine gradients similar to those used to recruit monocytes. CCL2/CCR2 acts as the major chemokine axis for the recruitment of inflammatory monocytes to sites of injury from the bone marrow via the blood [9, 187]. To this end, we verified that inflammatory monocytes in the lungs deploy CCR2 on their surface (Figure 3.5).

We employed CCR2-deficient mice to aid in testing the hypothesis that the origin of the elastase-induced $CD11c^{+}SiglecF^{+}CD11b^{+}$ subpopulation was due to monocyte trafficking to the lungs. When we compared the myeloid cell populations in $CCR2^{-/-}$ and wildtype (C57BL/6) mice, it was evident that there were fewer $CD11b^{+}Ly6C^{+}$ monocytes recruited to the lungs at days 0, 2, and 7 post-elastase challenge in $CCR2^{-/-}$ animals compared to WT controls (Figure 3.6A). Not surprisingly, there was no measurable difference in number of $CD11c^{+}SiglecF^{+}$ alveolar macrophages between the wildtype and $CCR2^{-/-}$ animals at days 0, 2, and 7 (Figure 3.6B). Importantly, CCR2-deficiency had no impact on the temporal dynamics or increase in the elastase-induced $CD11c^{+}SiglecF^{+}CD11b^{+}$ subpopulation at days 2 and 7 post-challenge (Figure 3.7). To further assess the possible impact that recruited myeloid cell populations may have on the progression of elastase-induced emphysema, we compared the extent of emphysematous changes in the lungs between $CCR2^{-/-}$ mice and wildtype controls. As the total numbers of inflammatory monocytes present in the lungs following elastase challenge (Figure 3.3C, 3.3D) may have suggested, recruited inflammatory monocytes may not be directly implicated in the pathogenesis of elastase-induced emphysema under these conditions,

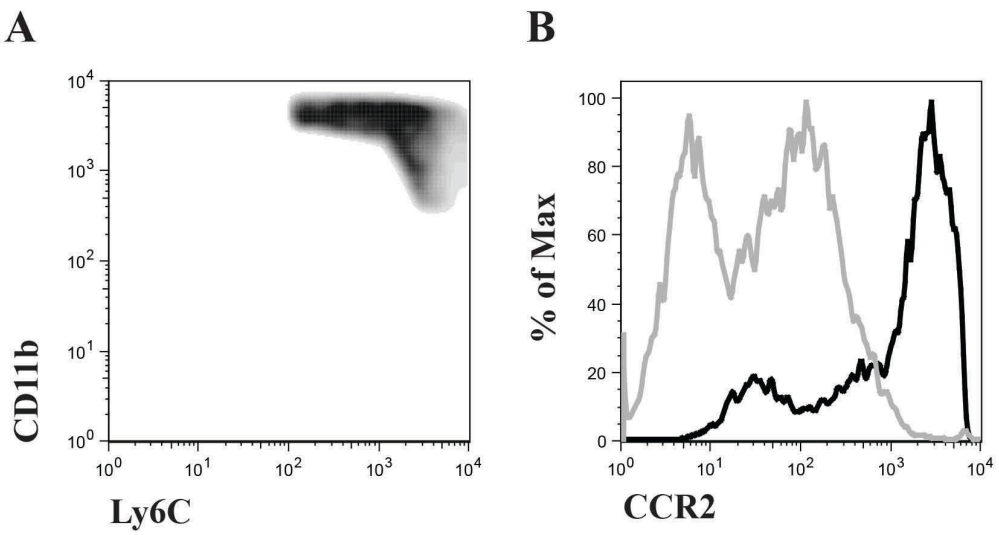

Figure 3.5 CCR2 surface expression on CD11b$^+$Ly6C$^+$ cells in the lungs following PPE challenge. Cells from perfused lungs isolated from C57BL/6 mice challenged with 6U PPE 7 days prior were surface stained with anti-mouse antibodies specific for CD11b, Ly6C, and CCR2. (A) Representative density plot depicting lung cells surface stained with Ly6C-APC (x-axis) and CD11b-PerCP-Cy5.5 (y-axis) gated on CD11b$^+$Ly6C$^+$ cell population. (B) Histogram depicting CCR2 expression (black) on the surface of gated CD11b$^+$Ly6C$^+$ population compared to secondary-alone control (grey).

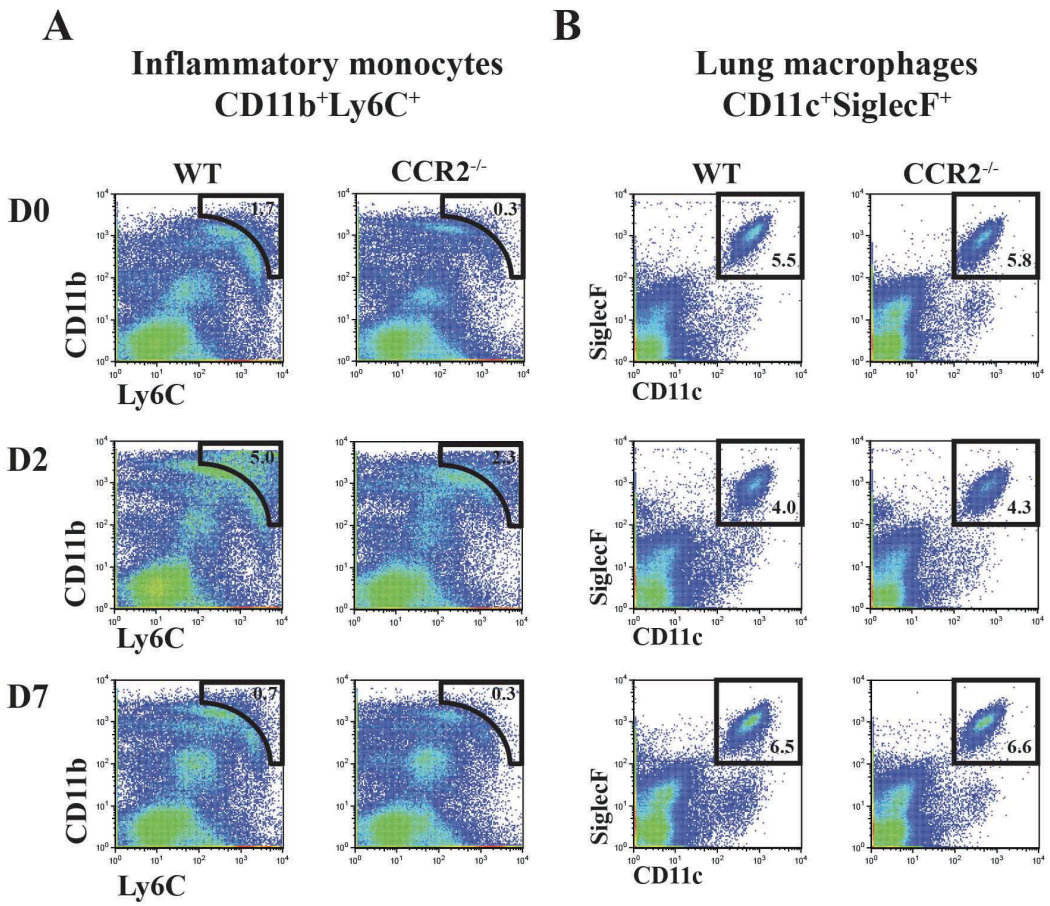

Figure 3.6 Effect of CCR2-deficiency on monocyte and lung macrophage dynamics following PPE challenge.

Representative data depicting flow cytometric analysis of perfused lungs isolated from C57BL/6 or CCR2$^{-/-}$ mice at days 0, 2 and 7 post-6U PPE administration. Cells were surface stained with anti-mouse antibodies specific for CD11b, CD11c, Ly6C, and SiglecF. Pseudocolor dotplots show light scatter properties of gated (A) CD11b^{+}Ly6C^{+} or (B) CD11c^{+}SiglecF^{+} populations.

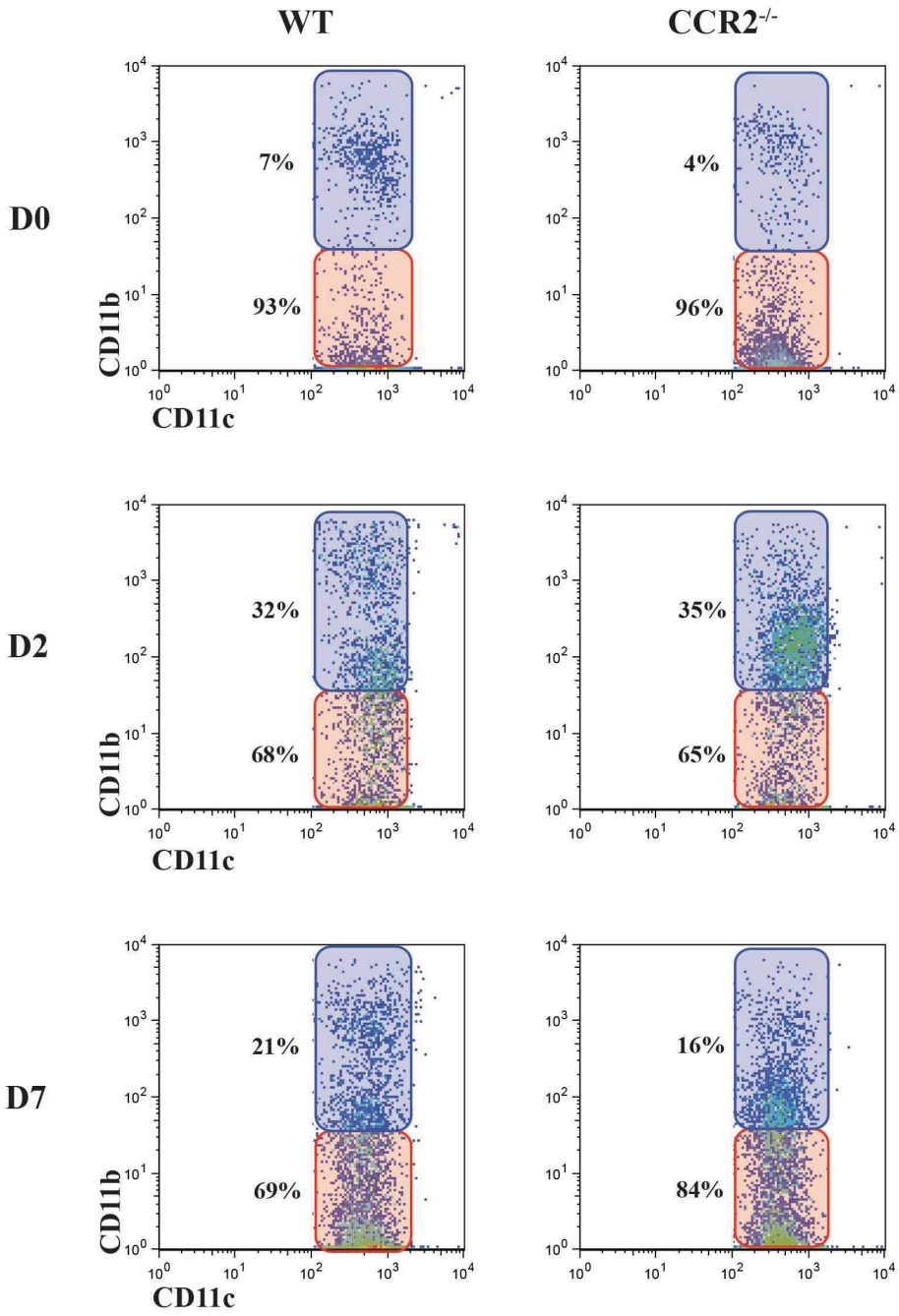

Figure 3.7 Effect of CCR2-deficiency on CD11c^{+}SiglecF^{+} phenotypic changes following PPE challenge.

Representative data depicting flow cytometric analysis of perfused lungs isolated from C57BL/6 or CCR2$^{-/-}$ mice at days 0, 2 and 7 post-6U PPE administration. Cells were surface stained with anti-mouse antibodies specific for CD11b, CD11c, and SiglecF. Pseudocolor dotplots show CD11b fluorescence intensity (y-axis) of gated CD11c^{+}SiglecF^{+} cell population. and percentages of CD11b^{low} (red) and CD11b^{high} (blue) lung macropahge populations. Subpopulations are highlighted with colored boxes: CD11b^{low} (red) and CD11b^{high} (blue). Subpopulation percentage of total gated CD11c^{+}SiglecF^{+} cells is displayed.

as the dynamics of the progression and the extent of the emphysematous changes in the lungs were comparable between $CCR2^{-/-}$ and wildtype mice (Figure 3.8).

3.4.4 *In vivo* lung-resident macrophage staining and cell fate tracking following elastase challenge

Given that blockade of monocyte recruitment from the bone marrow and peripheral blood (via CCR2-deficiency) had no impact on the presence of the $CD11c^{+}SiglecF^{+}CD11b^{+}$ subpopulation in the lungs, we then hypothesized that the elastase-induced myeloid cell population originated locally within the lung tissue. In order to test this hypothesis, we employed an *in vivo* cell labeling strategy in order to track the fates of lung resident phagocytic cells. By *in vivo* labeling cells prior to elastase challenge, we could track the fate of the AM population over time. PKH26, a stable red fluorescent lipophilic dye, when formulated in a specific way forms micro-aggregates that are selectively taken up by phagocytic cells. In addition, the dye remains within endocytic vesicles for greater than thirty days [49]. Due to its long *in vivo* half-life, PKH26-PCL is a valuable tool for tracking lung macrophages when administered intravenously or directly into the lungs [49, 436-439].

To this end, following intra-tracheal PKH26-PCL administration into the lungs of naive mice, we were able to specifically label $CD11c^{+}$ cells residing in the alveolar space (isolated via BAL) (Figure 3.9A) as well as the lung interstitium (from single cell suspensions of lung tissue) (Figure 3.9B). In addition, we were able to titrate an appropriate concentration of dye needed to label lung resident phagocytic cells and monitor them over time using flow cytometry (Figure 3.9C). In fact, intra-tracheal administration of PKH26-PCL resulted in robustly labeled lung-derived macrophages that were stable over two weeks (data not shown). The $PKH26\text{-}PCL^{+}$ cells isolated from perfused lungs were largely $CD11c^{+}CD11b^{-}$ (Figure 3.9D), consistent with our previously described definition of AM (Table 3.1). Throughout the descriptions of the *in vivo* labeling experiments, the lung-resident alveolar macrophage population (LRM) is defined using the short-hand designation of $PKH26\text{-}PCL^{+}CD11c^{+}$ cells. We considered LRM to be lung-resident phagocytic $CD11c^{+}$ cells residing in the airways or lung tissue prior to inflammatory insult. While we appreciate that there were potentially other non-macrophage $CD11c^{+}$ phagocytic cells residing within the lungs prior to elastase challenge (such as $CD11b^{+}$ cDCs), macrophages account for 90-95% of all $CD11c^{+}$ cells in a naïve lung (Figure 3.1, [435]).

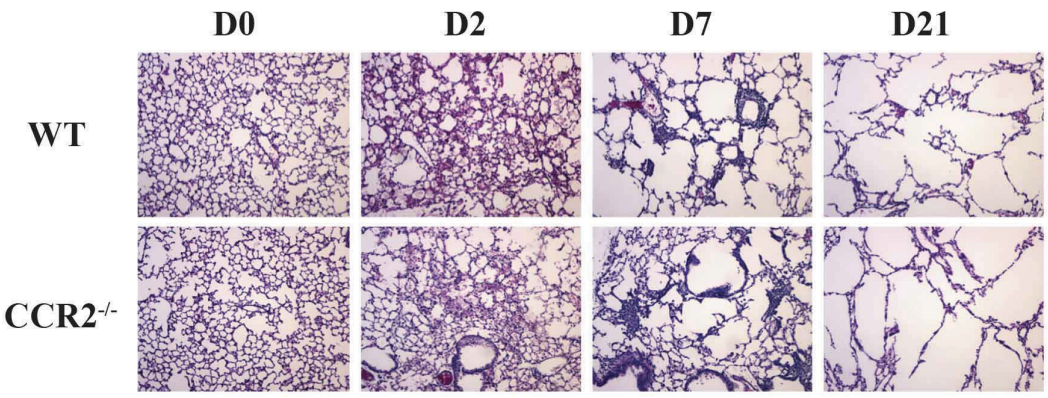

Figure 3.8 Effect of CCR2-deficiency on the progression of emphysema following PPE challenge. Representative histological sections of lungs from C57BL/6 or CCR2$^{-/-}$ mice at days 2 (D2), 7 (D7) and 21 (D21) post-PPE challenge (6U via intratracheal aspiration) or unchallenged controls (D0). 5μm sections were stained with hematoxylin and eosin (10X objective).

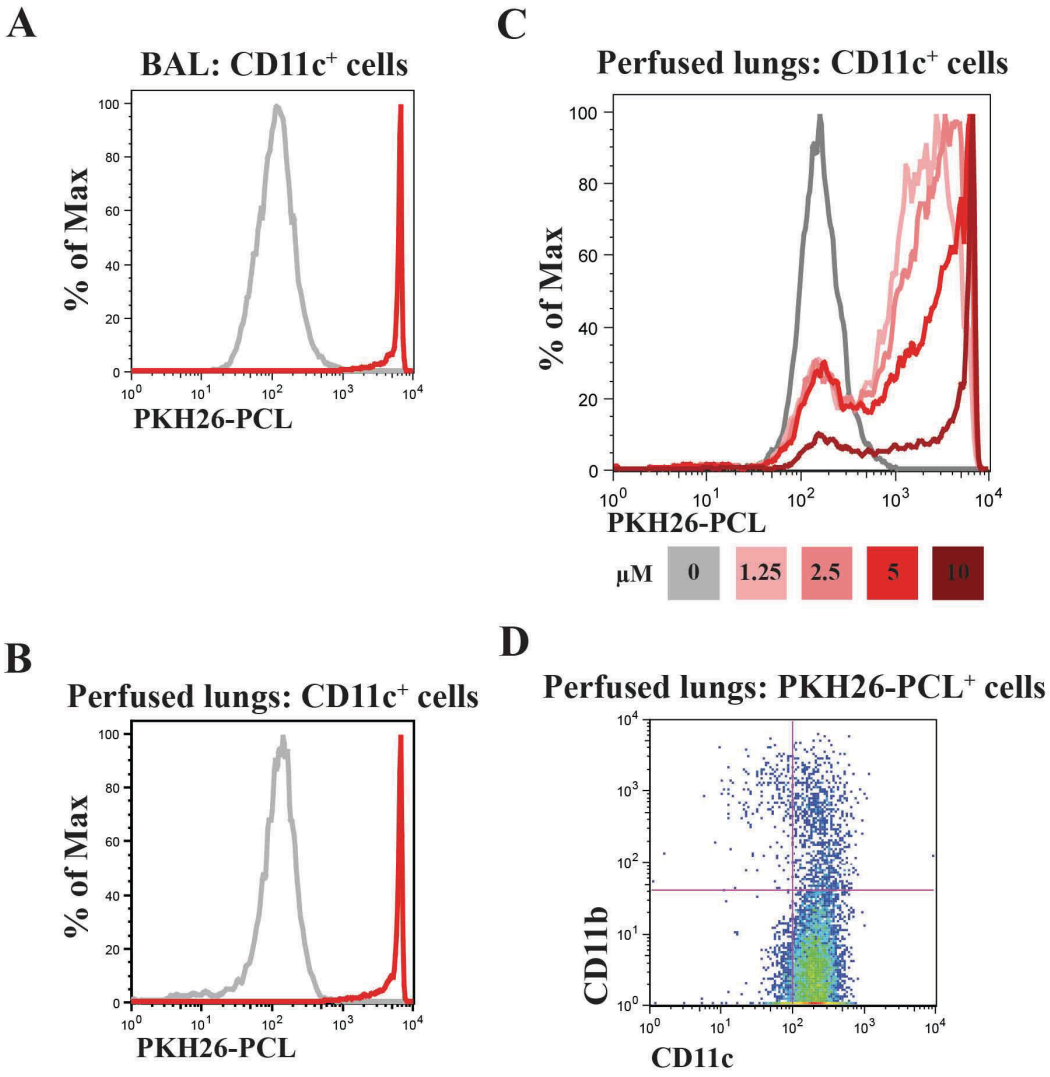

Figure 3.9 ***In vivo*** **labeling of lung-resident phagocytic cells with PKH26-PCL.**
Histograms depict PKH26-PCL fluorescence (red line) in gated CD11c$^+$ cell populations from (A) BAL or (B) perfused lungs isolated from BALB/c mice compared to unstained controls (grey line) following intra-tracheal dye administration one day prior to cell collection. (C) Histogram depicts PKH26-PCL fluorescence (colored lines) in gated CD11c$^+$ cells from perfused lungs administered escalating doses of PKH26-PCL via intra-tracheal aspiration compared to unstained controls (grey line).

We also verified the specificity of PKH26-PCL staining by immunofluorescence microscopy. We employed the plant lectin GSL1 that has been described to specifically bind to α-galactose residues on the surface of lung macrophages [13, 440] as a surrogate marker to identify AM isolated from the lungs of mice via BAL on cytospin preparations. For PKH26-PCL labeled cells isolated in the BAL 4 days following administration of the dye, the red fluorescent signal was associated exclusively with $GSL1^+$ cells (Figure 3.10). Upon examination of deconvolved Z-stacked images, it was evident that the PKH26-PCL dye aggregates were neither associated with the nucleus (DAPI) or cell surface (GSL1), but were cytosolic and punctate in nature; consistent with dye micro-aggregates located within endocytic vesicles (data not shown). Therefore, we were confident that analysis of PKH26-PCL labeled cells upon elastase challenge would allow us to understand the nature and dynamics of LRM over time.

Flow cytometric analyses on LRM ($PKH26\text{-}PCL^+CD11c^+$ cells) isolated from BAL or whole lung homogenates revealed that these cells altered their morphology and surface marker phenotype in response to elastase challenge (Figure 3.11). Multiple characteristics of the $PKH26\text{-}PCL^+CD11c^+$ LRM including their size (forward scatter), granularity (side scatter) and CD11b surface levels increased from days 2 to 6 post-elastase challenge compared to unchallenged controls (Figure 3.11). Since the $PKH26\text{-}PCL^+CD11c^+$ LRM population up-regulated CD11b surface levels early in response to elastase challenge, we recognized that we had determined the origin of the $CD11c^+SiglecF^+CD11b^+$ alveolar macrophage subpopulation. The data suggest that under these conditions, the elastase-induced $CD11b^+$ lung macrophage subpopulation (Figure 3.4) originated within the alveolar spaces and/or lung tissue and was independent of CCR2/CCL2 recruitment from the periphery.

We visually verified these findings using immunofluorescence microscopy to analyze the same cell samples, again utilizing GSL1 as a surrogate marker to identify lung macrophages. The dynamics of the $GSL1^+PKH26\text{-}PCL^+$ cells cell morphologies were consistent with flow cytometric analyses. At days 2 and 4 post-elastase challenge, the $GSL1^+PKH26\text{-}PCL^+$ cells became larger, more granular and ruffled compared to cells isolated from unchallenged mice (Figure 3.12).

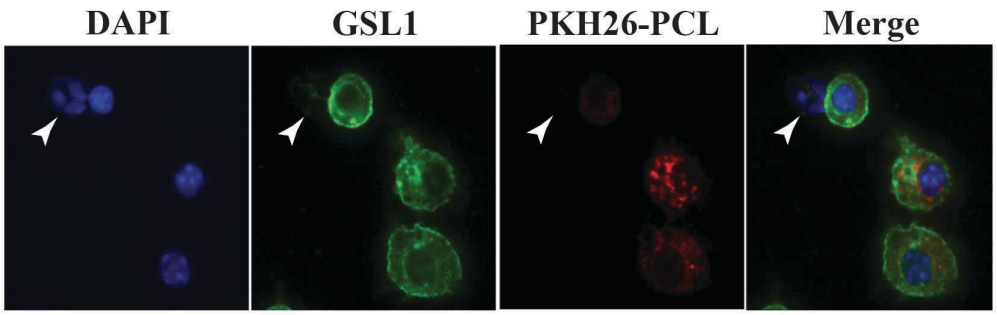

Figure 3.10 Visualization of *in vivo* lung-resident phagocytic cell PKH26-PCL staining specificity. Representative image of cytospin preparation of lung cells isolated via BAL from PKH26-PCL labeled (96 hours post-labeling) BALB/c mice. Cells were fixed and stained with GSL1 lectin and DAPI prior to immunofluorescence microscopy. Each fluorescent channel is displayed separately and in 3-color merged format. Images were captured at 20X objective and cropped to include cells of interest. Arrowhead identifies $GSL1^{-}PKH26\text{-}PCL^{-}$ PMN.

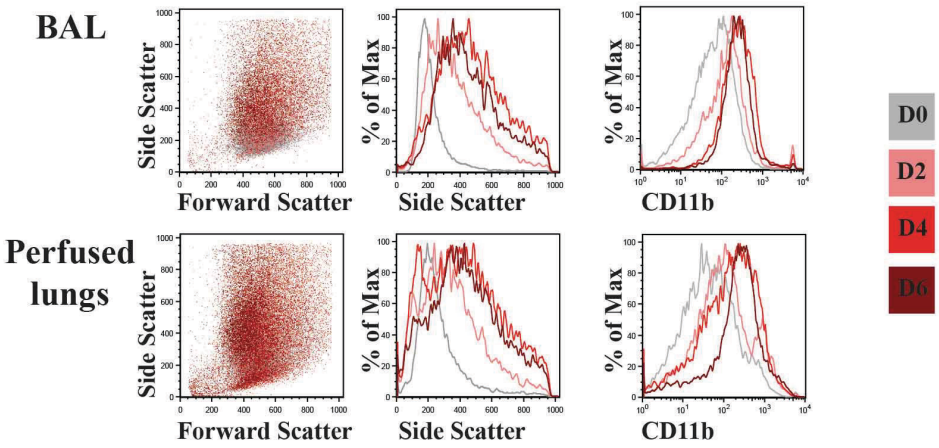

Figure 3.11 Dynamics of lung-resident PKH26-PCL$^+$CD11c$^+$ cells granularity and surface phenotype following PPE challenge.

Representative data depicting flow cytometric analysis of PKH26-PCL$^+$CD11c$^+$ cells from BAL or perfused lungs isolated from BALB/c mice following 3U PPE administration via intra-tracheal aspiration at days 0 (grey), 2 (pink), 4 (red), and 6 (crimson) post-challenge. Cells were surface stained with anti-mouse antibodies specific for CD11b, and CD11c. (Left) Dotplots and histograms show properties of gated PKH26-PCL$^+$CD11c$^+$ cell population: (left) light scatter properties; (middle) granularity; (right) surface CD11b expression level.

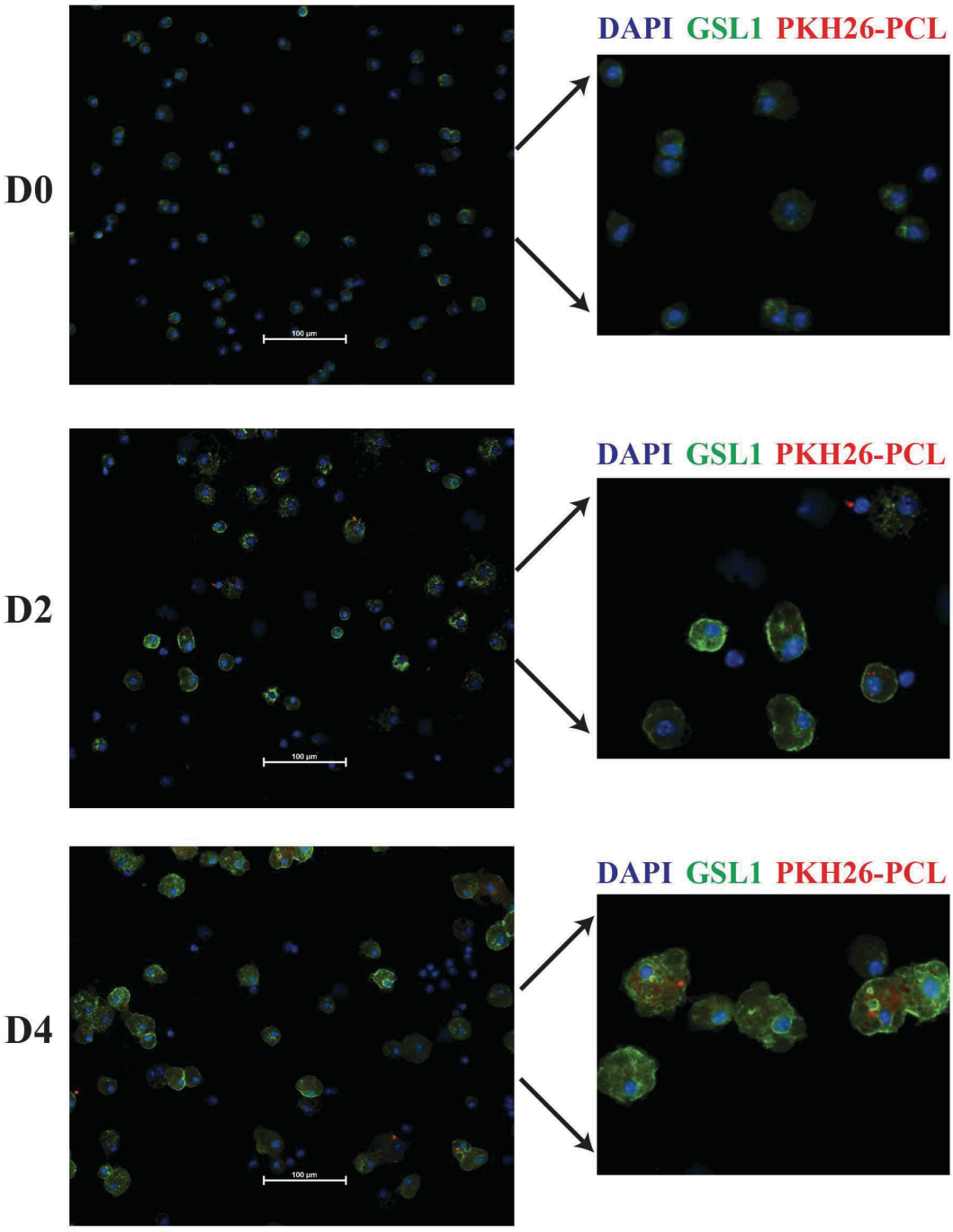

Figure 3.12 Visual evidence for lung-resident macrophage morphological changes following elastase challenge.
Representative image of cytospin preparation of lung cells isolated via BAL from PKH26-PCL labeled BALB/c mice at days 0, 2 and 4 post-PPE challenge. Cells were fixed and stained with GSL1 lectin and DAPI prior to immunofluorescence microscpy. Images are displayed as 3-color merged format. Images were captured using a 20X objective. White bar represents 100 µm. Cropped images were enlarged to the same degree to highlight morphological differences over time.

3.4.5 Dynamics of elastase-induced lung-resident macrophage phenotypic changes

Flow cytometric analysis was used in conjunction with the PKH26-PCL *in vivo* staining to quantify the extent to which the resident AM population was undergoing phenotypic changes in response to elastase challenge. We monitored the change in the surface expression of CD11b on PKH26-PCL^{+}CD11c^{+} cells from perfused lung homogenates at days 2, 4, and 6 post-elastase (Figure 3.13A). At baseline only about 20% of resident AM expressed CD11b on their surface, but following elastase challenge, the LRM significantly up-regulated CD11b surface levels (Figure 3.13B, 3.13D). Over the first six days following elastase challenge, the LRM transformed from a population that was dominated by CD11c^{+}CD11b^{-} cells to a population where more than half the PKH26-PCL^{+} cells were CD11c^{+}CD11b^{+} (Figure 3.13B, 3.13D). By day 6 a distinct subpopulation emerged that expressed high CD11b levels (CD11b^{+high} subpopulation highlighted with gold box) (Figure 3.13B, 3.13C). As noted previously, this AM surface phenotype was not sustained (Figure 3.4), as the CD11c^{+}CD11b^{+} population resembled that of unchallenged mice by day 14 post-elastase challenge (Figure 3.4).

The elastase-induced changes in CD11b expression on the surface of LRM were accompanied by changes in CD200R expression. CD200R (also known as OX-2), upon engagement with its ligand CD200, acts as a negative regulator of macrophage function and activation through Dok2-mediated inhibition of the Erk, Jnk and p38 MAPK pathways [161, 164, 166]. Following elastase challenge, the PKH26-PCL^{+}CD11c^{+} LRM population, known to be CD200R^{+} [47, 163], up-regulated CD200R expression to even greater levels (Figure 3.14B, 3.14C, 3.14D). By days 4 and 6 post-challenge, approximately 30% of the PKH26-PCL^{+} LRM population exhibited CD200R surface levels that exceeded the already high CD200R levels present on LRM from unchallenged mice (Figure 3.14).

In addition, we assessed levels of membrane-associated ST2, a component of the receptor for IL-33, on AM following elastase challenge. IL-33 is an epithelial-derived alarmin released upon cellular stress. Our laboratory has previously demonstrated that IL-33 protein levels in the lung were elevated within two days of elastase-challenge (data not shown). In unchallenged mice, ~8% of the alveolar macrophage population had measurable levels of ST2 expression, however, at day 2 post-elastase, the percentage of ST2^{+}

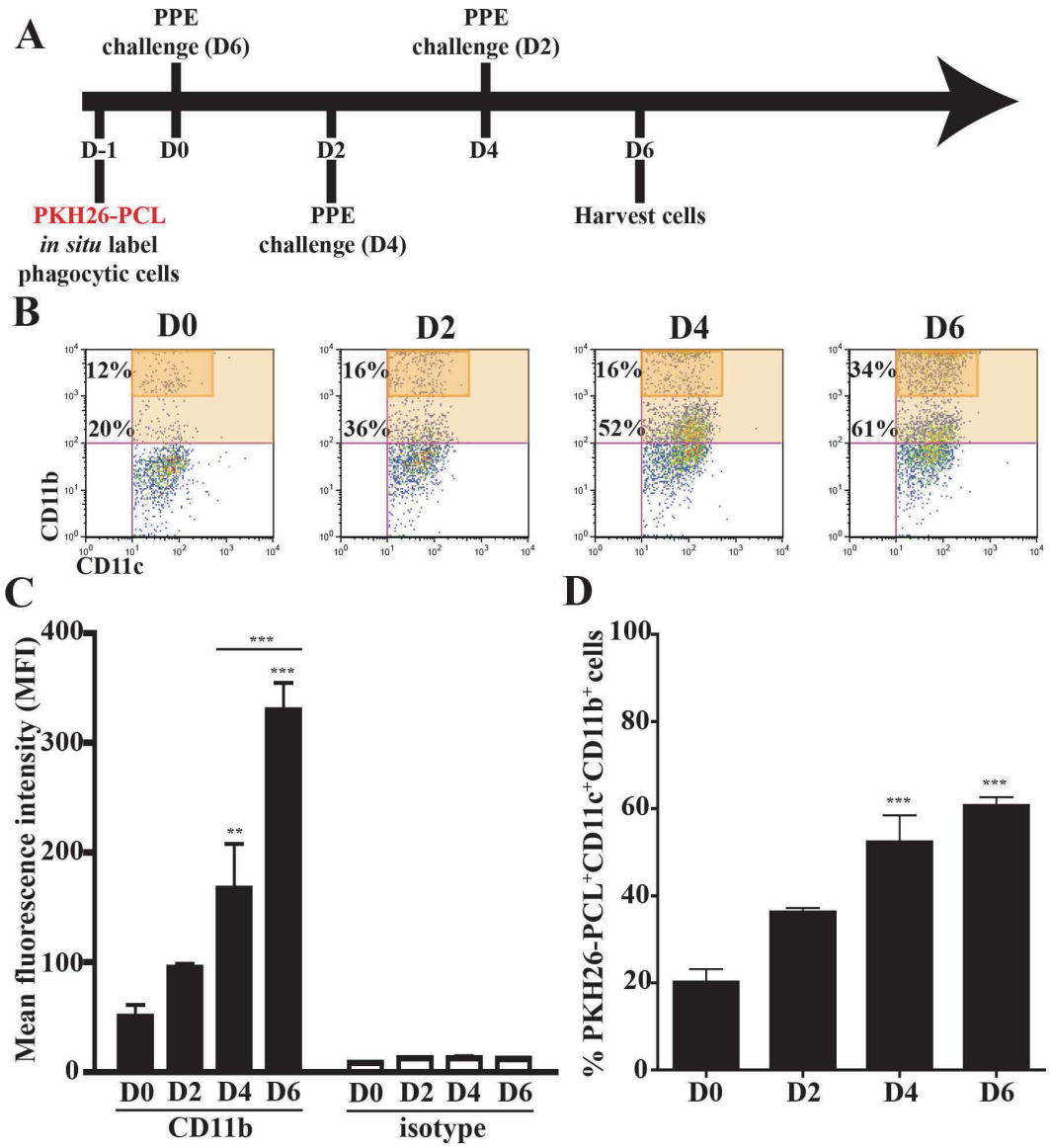

Figure 3.13 Dynamics of PKH26-PCL$^+$CD11c$^+$ population's surface CD11b levels following PPE challenge.

(A) Representative data depicting flow cytometric analysis of perfused lungs isolated from BALB/c mice following 3U PPE administration via intra-tracheal aspiration at days 0, 2, 4, and 6 post-challenge. Cells were surface stained with anti-mouse antibodies specific for CD11b and CD11c. Psuedocolor dotplots show CD11b fluorescence intensity (y-axis) of gated PKH26-PCL$^+$CD11c$^+$ cell population. CD11b^{high} subpopulation percentage of total gated PKH26-PCL$^+$CD11c$^+$ cells is displayed. (B) Percentage of gated PKH26-PCL$^+$CD11c$^+$ populaton that is CD11b positive. (n=3 per day). Bar graph depicts mean ± SEM. *** $p<0.001$. All comparisons are versus unchallenged controls.

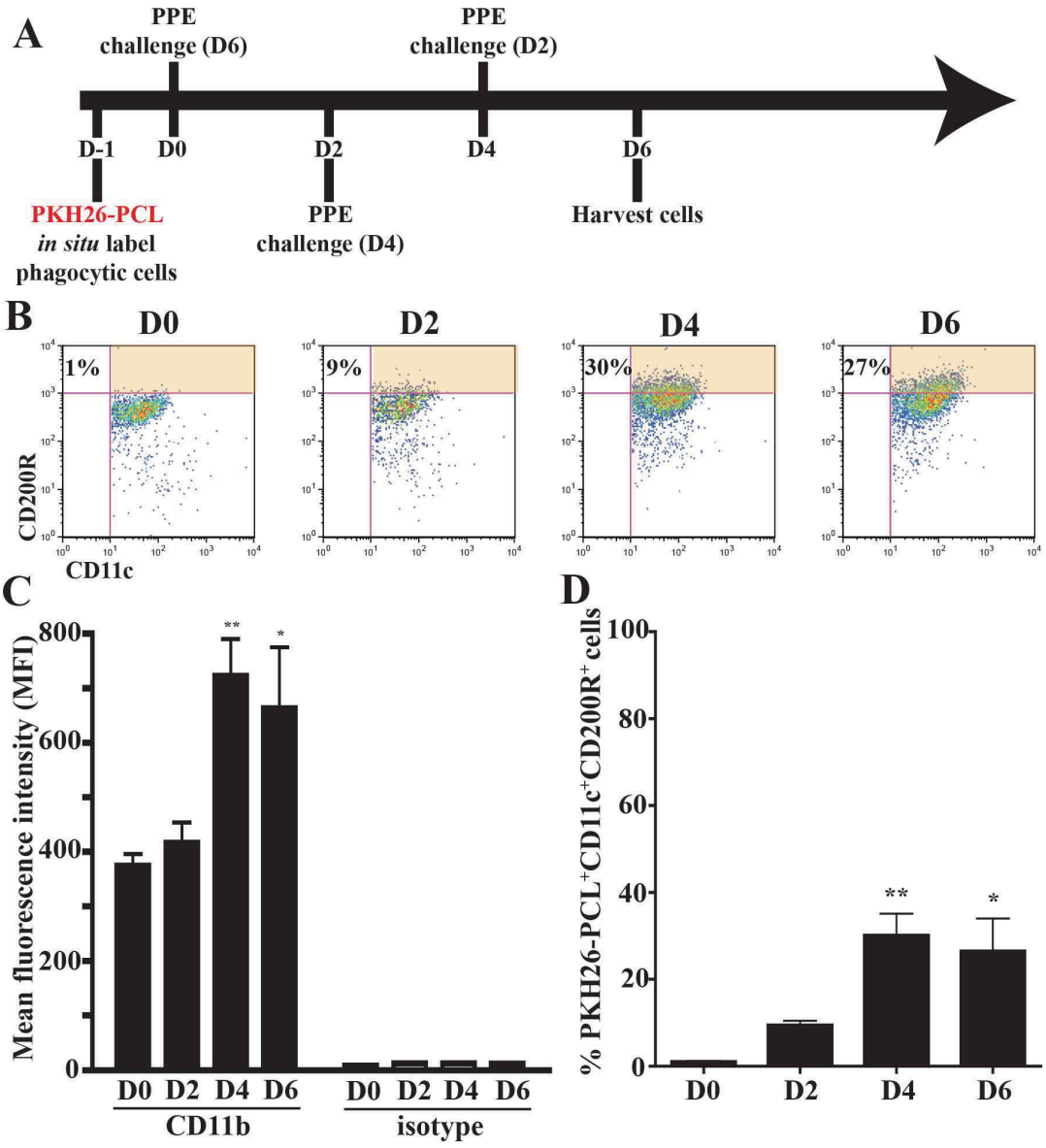

Figure 3.14 Dynamics of PKH26-PCL$^+$CD11c$^+$ population's surface CD200R levels following PPE challenge.

(A) Representative data depicting flow cytometric analysis of perfused lungs isolated from BALB/c mice following 3U PPE administration via intra-tracheal aspiration at days 0, 2, 4, and 6 post-challenge. Cells were surface stained with anti-mouse antibodies specific for CD200R and CD11c. Psuedocolor dotplots show CD11b fluorescence intensity (y-axis) of gated PKH26-PCL$^+$CD11c$^+$ cell population. CD200R^{high} subpopulation percentage of total gated PKH26-PCL$^+$CD11c$^+$ cells is displayed. (B) Percentage of gated PKH26-PCL$^+$CD11c$^+$ populaton that is CD200R^{high} (n=3 per day). Bar graph depicts mean ± SEM. * $p<0.05$; ** $p<0.01$. All comparisons are versus unchallenged controls.

$CD11c^+SiglecF^+$ cells increased significantly to ~33% (Figure 3.15). Similar to the dynamics of surface CD11b, this change in ST2 levels appeared to be transient, as the lung macrophage population resembled that of unchallenged mice by day 14 and 21 post-elastase challenge (Figure 3.15). Further studies are required to more clearly evaluate the dynamics of surface ST2 levels between days 2 and 7 post-elastase challenge.

3.4.6 Lung-resident macrophage dynamics following elastase-challenge to the lung

As noted earlier, we observed a near doubling in the number of $CD11c^+SiglecF^+$ cells in the lungs at seven days post-elastase challenge (Figure 3.3A). A similar kinetic profile was evident when accessing the number of macrophages present in BAL fluid (Figure 1.7D). Under these conditions, our data suggested that the increase in macrophage cell number was not attributable to an influx of $CCR2^+$ cells from the periphery. Therefore, we hypothesized that the observed increase may be due to proliferation of a lung-resident macrophage population. Employing the PKH26-PCL *in vivo* lung macrophage labeling strategy, we were able to follow the size of the LRM population following intra-tracheal elastase challenge (Figure 3.16). Following *in vivo* labeling, we enumerated the $PKH26\text{-}PCL^+CD11c^+$ cell population present in the lungs of animals at days 0, 2, 4, and 6 post-elastase challenge. Consistent with our hypothesis that lung macrophages proliferated following elastase challenge, the number of LRM ($PKH26\text{-}PCL^+CD11c^+$) approximately doubled by day 4 and remained elevated at day 6 compared to unchallenged controls (Figure 3.17). These results were consistent with our previous findings of macrophage population dynamics in the airways (Figure 1.7D) and lung tissue (Figure 3.3A) between days 2 and 7 post-elastase challenge. However, we appreciated that an increased number of $PKH26\text{-}PCL^+CD11c^+$ cells in the lungs following elastase challenge (Figure 3.17) could have arisen from a variety of other sources, therefore these data were not sufficient evidence to characterize the significant increase as proliferation of the LRM pool.

To validate the proliferation phenotype of these cells, we assayed for the presence of Ki67, a nuclear protein only expressed by cells that have entered cell cycle [441]. By flow cytometric intracellular staining, $PKH26\text{-}PCL^+CD11c^+$ cells from unchallenged lungs were ~20% positive for Ki67 (Figure 3.18A). Following elastase challenge, the percentage of $Ki67^+$ lung macrophages significantly increased to levels

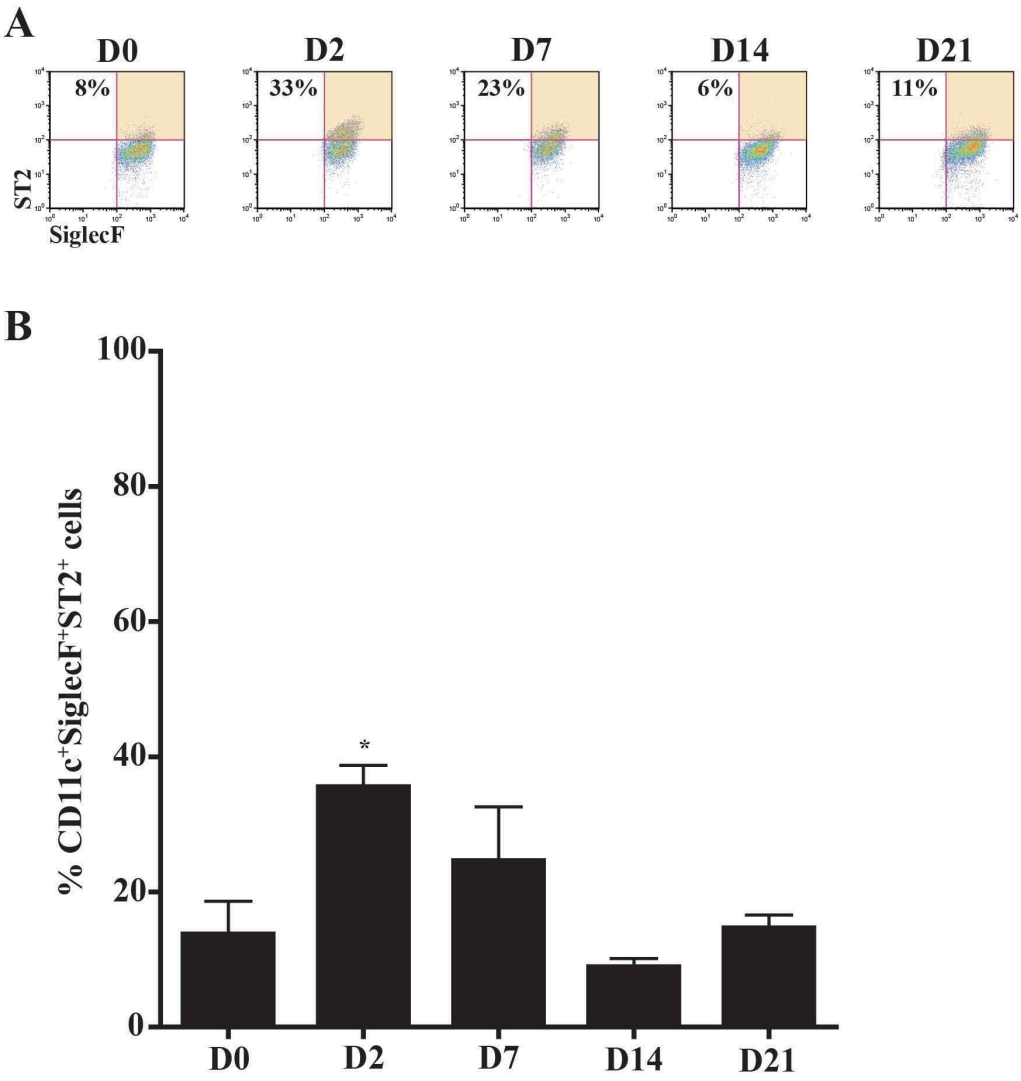

Figure 3.15 Dynamics of CD11c$^+$SiglecF$^+$ population's surface ST2 levels following PPE challenge. (A) Representative data depicting flow cytometric analysis of perfused lungs isolated from BALB/c mice following 3U PPE administration via intra-tracheal aspiration at days 0, 2, 7, 14, and 21 post-challenge. Cells were surface stained with anti-mouse antibodies specific for CD11c, SiglecF, and ST2. Psuedocolor dotplots show ST2 fluorescence intensity (y-axis) of gated CD11c$^+$SiglecF$^+$ cell population. ST2$^+$ subpopulation percentage of total gated CD11c$^+$SiglecF$^+$ cells is displayed. (B) Percentage of gated CD11c$^+$SiglecF$^+$ populaton that is ST2$^+$ (n=3 per day). Bar graph depicts mean ± SEM. * $p<0.05$ All comparisons are versus unchallenged controls.

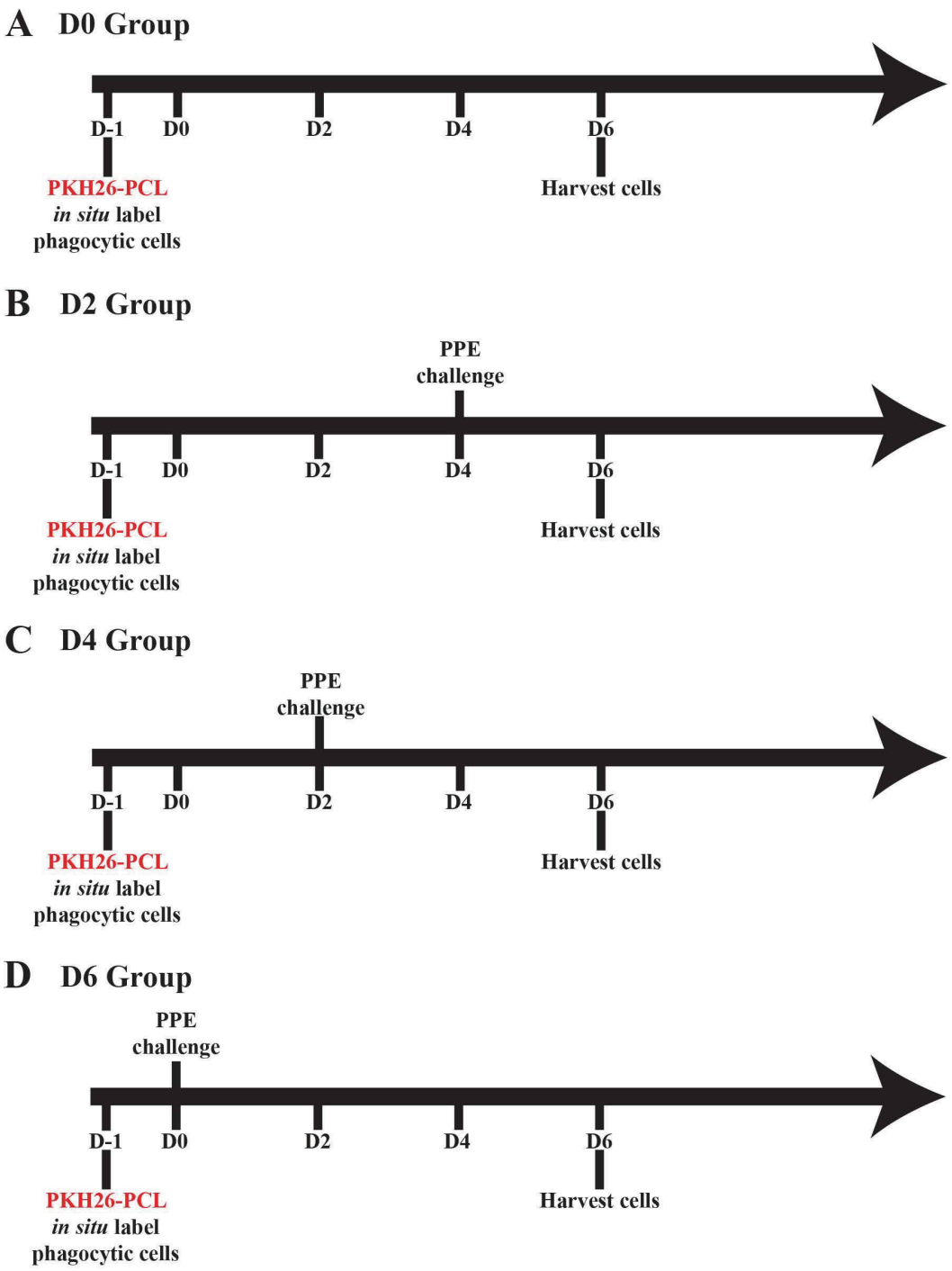

Figure 3.16 Experimental design for monitoring PKH26-PCL^{+}CD11c^{+} LRM population following PPE challenge.
Timeline illustrating the experimental design including PKH26-PCL labeling (D-1), elastase challenge (D4; D2; D0) and sample collection time (D6). This experimental design was used to collect the data shown in Figures 3.17, 3.18, and 3.19.

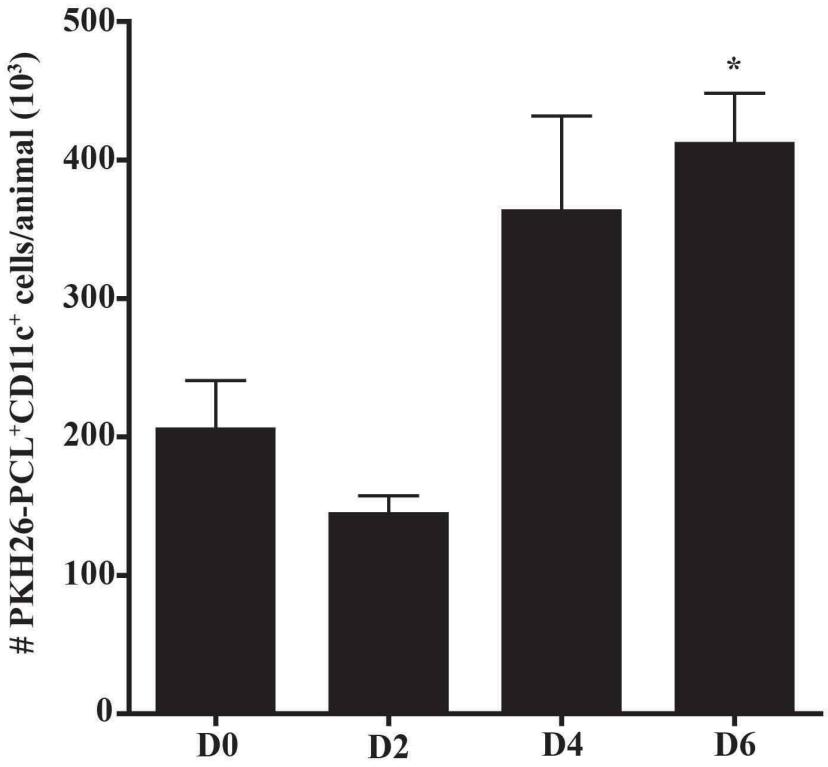

Figure 3.17 Dynamics of lung-resident PKH26-PCL$^+$CD11c$^+$ population numbers following PPE challenge.
Total numbers of gated PKH26-PCL$^+$CD11c$^+$ populaton by flow cytometric analysis of perfused lungs isolated from BALB/c mice following 3U PPE administration via intra-tracheal aspiration at days 0, 2, 4, and 6 post-challenge. (n=3 per day). Bar graph depicts mean ± SEM. * $p<0.05$. All comparisons are versus unchallenged controls.

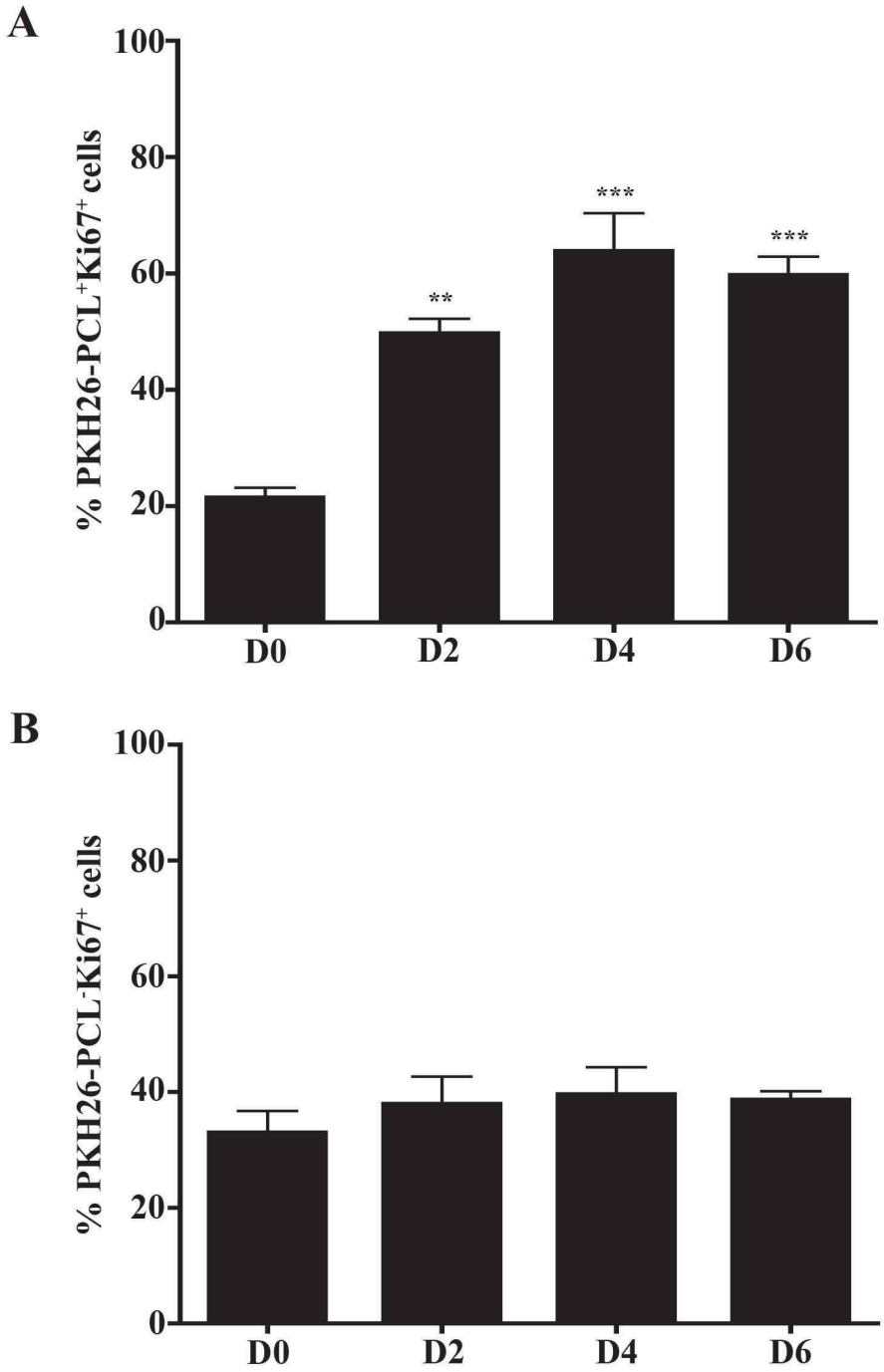

Figure 3.18 Dynamics of Ki-67 positivity in PKH26-PCL$^+$ and PKH26-PCL$^-$ populations following PPE challenge.

Percentage of Ki67 positivity in gated (A) PKH26-PCL$^+$ or (B) PKH26-PCL$^-$ populatons by flow cytometric analysis of perfused lungs isolated from BALB/c mice following 3U PPE administration via intra-tracheal aspiration at days 0, 2, 4, and 6 post-challenge. (n=3 per day). Bar graph depicts mean ± SEM. *** $p<0.001$. All comparisons are versus unchallenged controls.

exceeding 50% at days 2, 4, and 6 post-elastase challenge (Figure 3.18A). This effect was specific to the PKH26-PCL^{+} LRM population, as the percentage of Ki67^{+} cells present in PKH26-PCL^{-} non-phagocytic lung cell populations (including lymphocytes and granulocytes) did not change over the six day period (Figure 3.18B). Under these conditions, the data suggested that half of the LRM population may have entered cell cycle within 2 days of elastase challenge, preceding the increased LRM numbers detected at days four and six post-challenge (Figure 3.17).

Importantly, we also assayed for changes in the amount of PKH26-PCL red fluorescence within the LRM cell population over time. If indeed this cell population was proliferating locally in response to elastase-induced damage, then we hypothesized that the PKH26-PCL dye would be diluted between daughter cells. However, we did not expect even 1:1 dilution of PKH26-PCL dye between daughter cells as observed with amine-reactive dyes such as carboxyfluorescein succinimydl ester (CFSE) [442], due to the nature of PKH26-PCL micro-aggregates localized within endocytic vesicles. It has been demonstrated that during mitosis endosomes and lysosomes do not partition evenly between daughter cells [443]. Therefore, experimental design controlling for decay of the fluorescent signal over time through synchronized labeling of LRM in all groups can be used to monitor changes in PKH26-PCL signal following elastase challenge (Figure 3.19A). We monitored the mean fluorescence intensity (MFI) of the PKH26-PCL red fluorescent signal within the LRM population at days 0, 2, 4, and 6 post-elastase challenge. By monitoring the LRM population as a whole, we determined that the mean red fluorescent signal emitted by a given cell decreases significantly between days 2, 4 and 6 post-elastase challenge (Figure 3.19A). This decrease in fluorescent signal cannot be attributed to progressive quenching or deterioration of the PKH26-PCL signal over time; as the dye was administered to all animals on the same day, the only variable between the groups was the amount of time that had elapsed post-elastase challenge. More specifically, when we sample the PKH26^{+}CD11c^{+} cell population based on Ki67 positivity, we see the trend for PKH26-PCL dilution was pronounced in the Ki67^{+} cell population while the PKH26-PCL signal remained consistently high in the Ki67^{-} subpopulation (Figure 3.19C, 3.19D, 3.19E). This evidence further suggested that two distinct lung resident alveolar macrophage subpopulations were present in the lungs following elastase challenge:

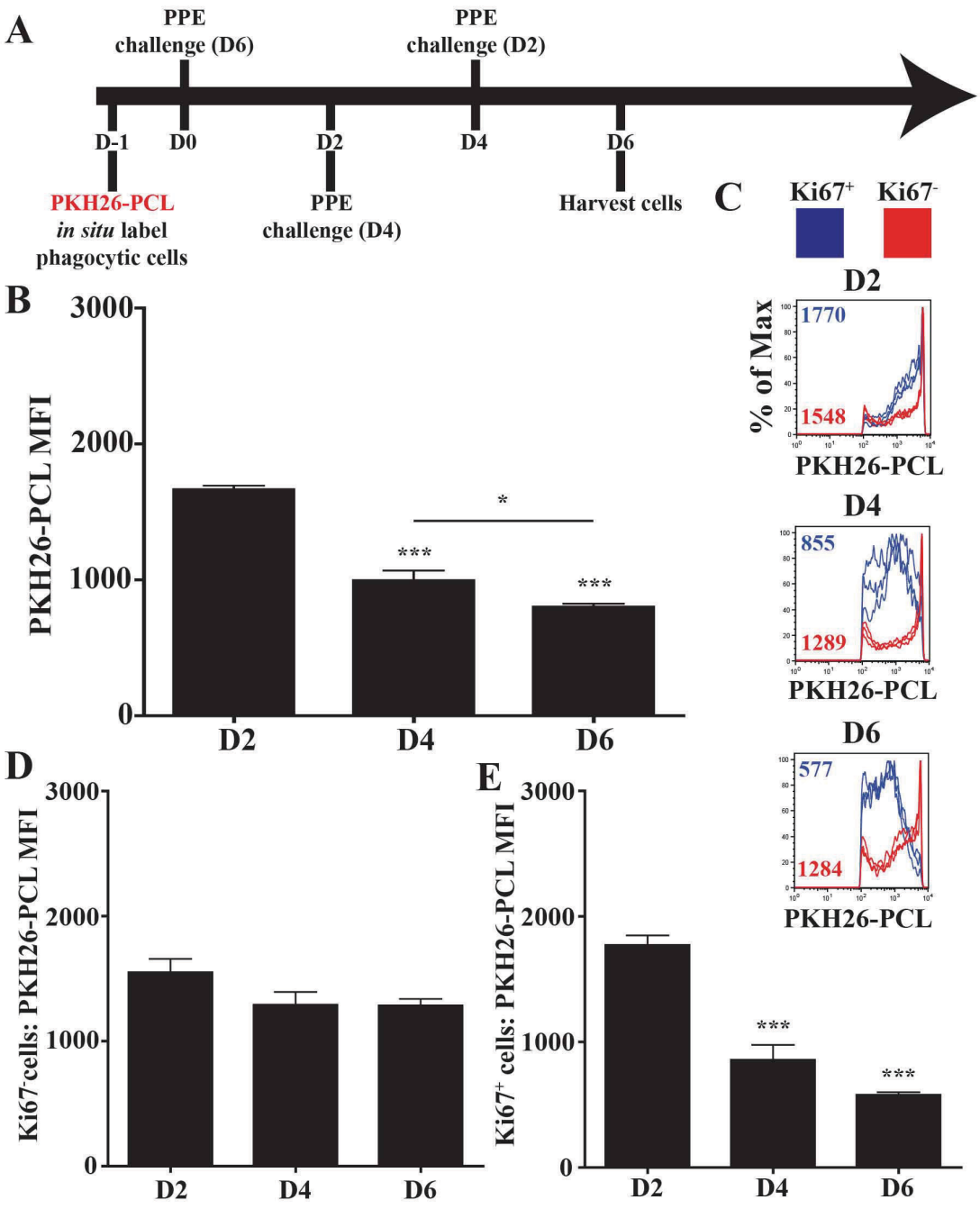

Figure 3.19 Dynamics of PKH26-PCL fluorescence intensity on a per cell basis following PPE challenge.

Flow cytometric analysis of perfused lungs isolated from BALB/c mice following 3U PPE administration via intra-tracheal aspiration at days 2, 4, and 6 post-challenge. (n=3 per day). (A) Bar graph depicts mean PKH26-PCL fluorescence intensity (MFI) of gated PKH26-PCL^{+} cells. Mean ± SEM. * $p<0.05$; ** $p<0.01$; *** $p<0.001$. All comparisons are versus unchallenged controls. (B) Histograms depict PKH26-PCL fluorescence in PKH26-PCL^{+}Ki67^{+} (blue) or PKH26^{-}PCL^{+}Ki67^{-} (red) gated populations. Subpopulation PKH26-PCL MFI is displayed in color code.

that enters cell cycle, proliferates, and dilutes the PKH26-PCL dye between its daughter cells in response to elastase-induced lung damage and another that does not.

Since we focused on understanding the dynamics of lung macrophage population expansion, we did not follow the LRM population beyond day 6 post-challenge. However, our previous findings suggest that following an early proliferative or expansion phase (between days 2 and 7 post-elastase) the alveolar macrophage population may enter a contraction phase (between days 7 and 14 post-elastase), returning the size of the AM population to steady-state levels. However, it is also possible that a subset of the AM population may alter its surface phenotype resulting in an apparent contraction. Further studies are required to understand the nature and dynamics of the possible AM contraction phase.

3.4.7 Gene expression dynamics in CD11c$^+$ cells following elastase-challenge to the lung.

The dynamic changes in cell morphology, surface phenotype and proliferative status of the AM suggested that these cells may become activated following elastase challenge in the lungs. We hypothesized that elevated IL-33 levels in the lungs within two days following elastase challenge would polarize the AM population towards an M2 or alternatively activated macrophage (AAM) phenotype. In order to test this hypothesis, we assessed gene expression of isolated CD11c$^+$ cells from the lungs of control or elastase-challenged mice at days 2, 7, 14, and 21. We measured the relative gene expression of a number of macrophage activation-related genes including: *Arg1, Chi3l3, Il1b, Il6, Il10, Il12a, Il18, Il33, Ilr1l1, Mmp9, Mmp12, Nos2, Retnla, Tnf, and Tgfb1*. All genes were normalized to *Gapdh* expression levels. Interestingly, *Nos2* and *Arg1* expression were both elevated at day 2 post-challenge. Three genes encoding canonical *in vitro* M2 activation markers were elevated following elastase challenge, however each had a different temporal expression profile: *Arg1* peaked at day 2, *Retnla* was elevated at days 2 and 7, and *Chi3l3* was elevated at days 7, 14, and 21 post-challenge (Figure 3.22). While *Nos2* was elevated at days 2 and 7, other M1-associated genes such as *Tnf* and *Il12* did not change significantly from baseline levels (Figure 3.20, 3.21). However, matrix metalloproteinase encoding genes such as *Mmp9* and *Mmp12* were elevated at day 21 and days 7 and 14, respectively (Figure 3.21). Genes encoding inflammasome-associated cytokines, IL-

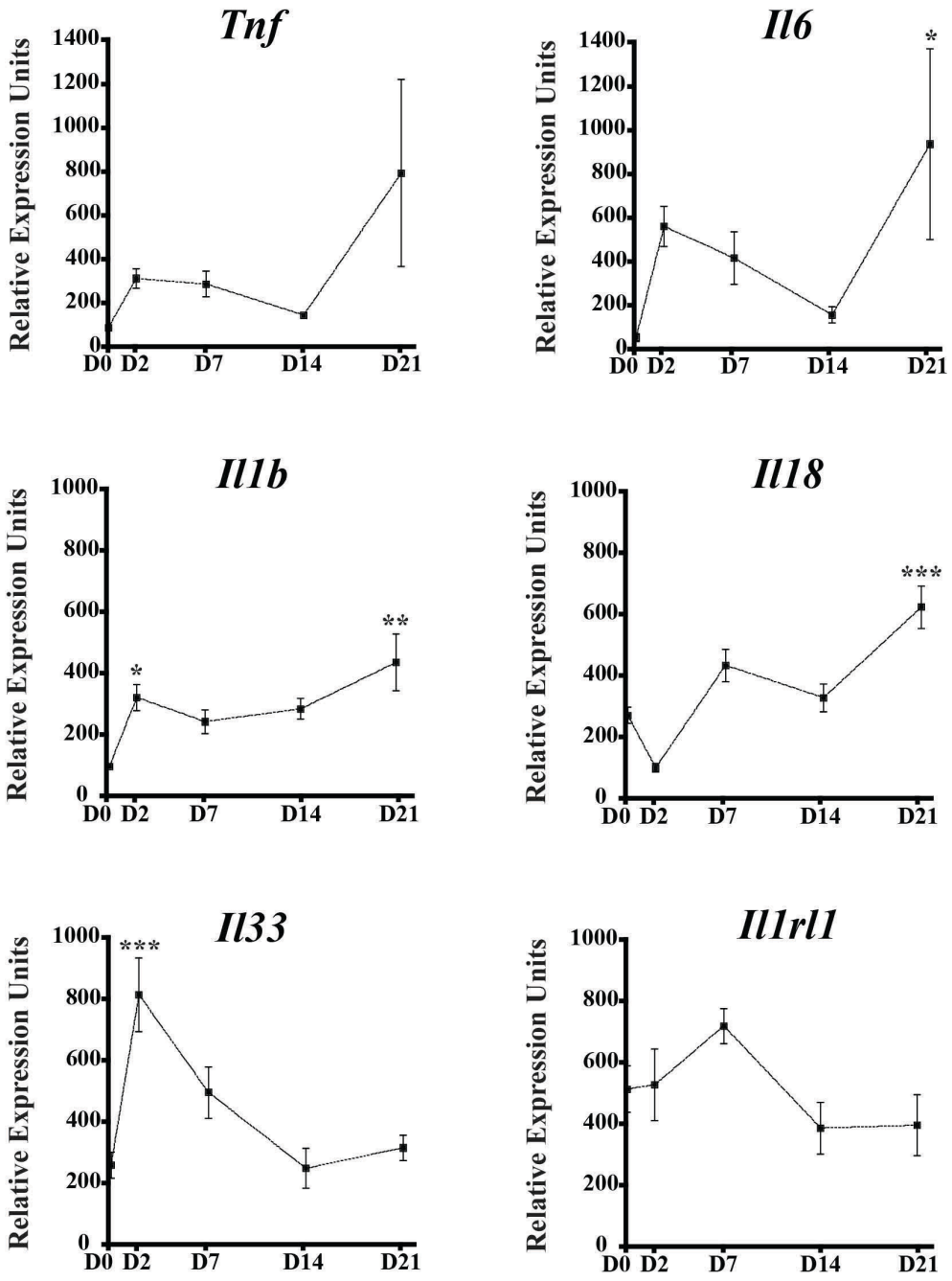

Figure 3.20 Dynamics of macrophage activation (innate/M1) gene expression in CD11c^{+} cells following PPE challenge.

RNA isolated from lung CD11c^{+} cells at D0, D2, D7, D14, and D21 were processed for real time RT PCR expression analysis of *Tnf*, *Il1b*, *Il6*, *Il18*, *Il33*, and *Il1rl1*. The PCR results were normalized to the levels of *Gapdh* and expressed as relative expression units. Line graphs depict mean ± SEM. * $p<0.05$, *** $p<0.001$. All comparsions are versus D0 controls. N=5

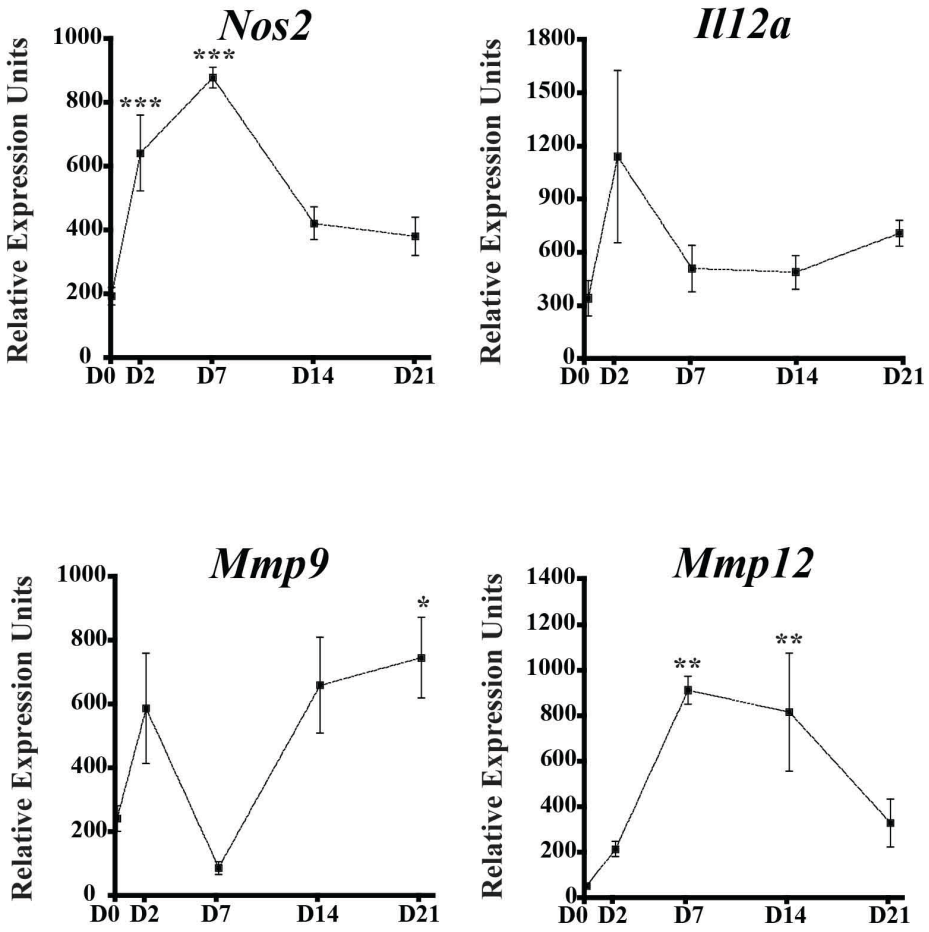

Figure 3.21 Dynamics of macrophage activation (M1/MMP) gene expression in CD11c$^+$ cells following PPE challenge.

RNA isolated from lung CD11c$^+$ cells at D0, D2, D7, D14, and D21 were processed for real time RT PCR expression analysis of *Nos2*, *Il12a*, *Mmp9*, and *Mmp12*. The PCR results were normalized to the levels of *Gapdh* and expressed as relative expression units. Line graphs depict mean ± SEM. * $p<0.05$, ** $p<0.01$, *** $p<0.001$. All comparsions are versus D0 controls. N=5

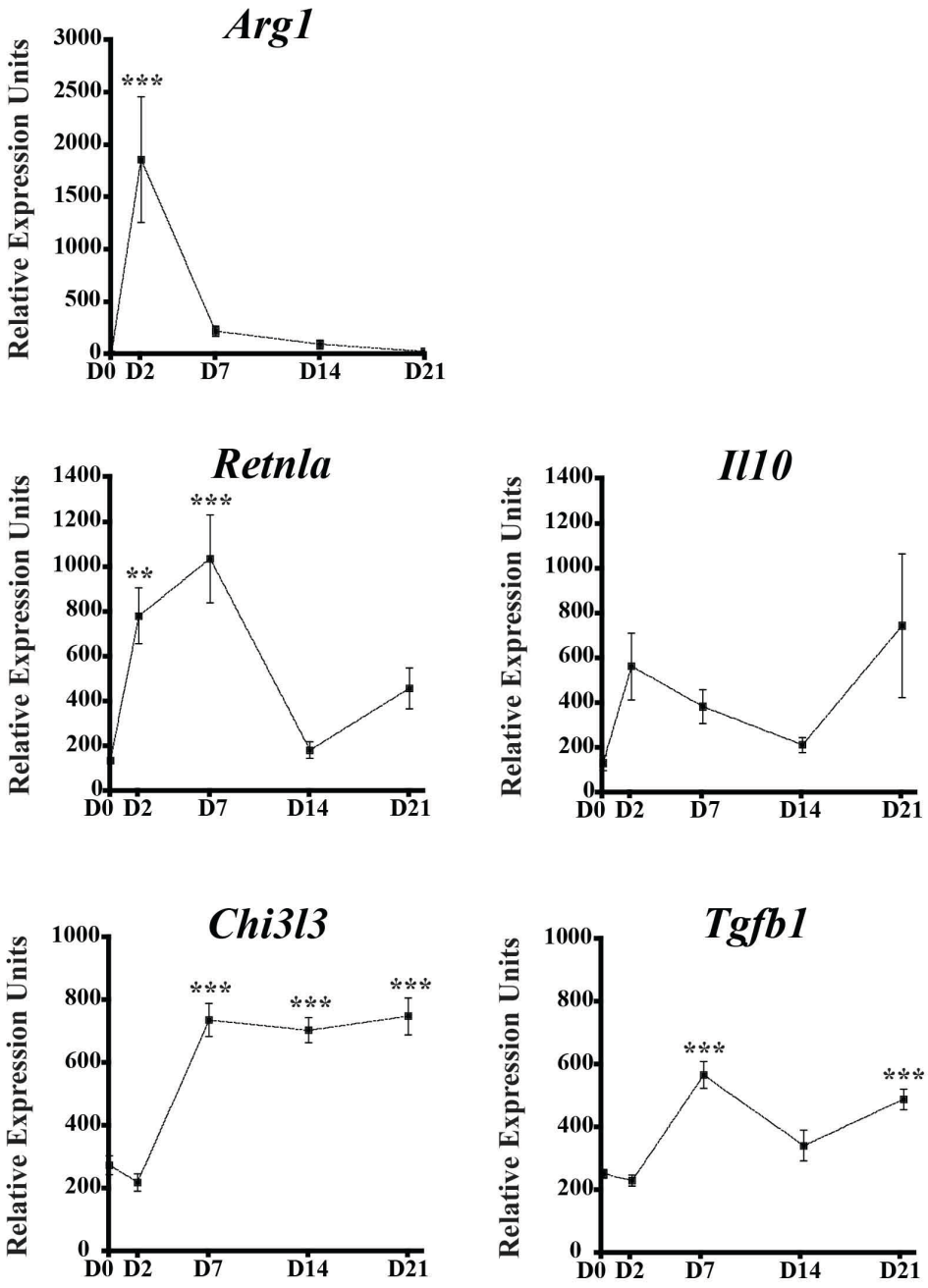

Figure 3.22 Dynamics of macrophage activation (M2a/M2c) gene expression in CD11c^{+} cells following PPE challenge.

RNA isolated from lung CD11c^{+} cells at D0, D2, D7, D14, and D21 were processed for real time RT PCR expression analysis of *Arg1*, *Retnla*, *Chi3l3*, *Il10*, and *Tgfb1*. The PCR results were normalized to the levels of *Gapdh* and expressed as relative expression units. Line graphs depict mean ± SEM. ** $p<0.01$, *** $p<0.001$. All comparsions are versus D0 controls. N=5

1β and IL-18 were both up-regulated at day 21 post-elastase (Figure 3.20). Alarmin encoding gene *Il33* was elevated at day 2 post-elastase, however the gene encoding the ST2 receptor (*Il1rl1*) did not change significantly (Figure 3.20). Inflammasome-associated *Il18* expression was elevated at day 21 post-PPE. The gene encoding the regulatory cytokine IL-10 did not significantly change, however the gene encoding TGFβ1 was elevated at days 7 and 21 post-elastase challenge (Figure 3.22). The effects of elastase challenge had long-lasting effects on AM gene expression as the genes encoding IL-18, MMP9, TGFβ1, and Ym1 were all significantly up-regulated at day 21 post-elastase challenge (Figure 3.20, 3.21, 3.22). The AM exhibited a mixed polarization phenotype, as M1-, M2a, and M2c-associated genes were up-regulated following elastase challenge (Figure 3.20, 3.21, 3.22).

3.4.8 Effect of lung macrophage depletion on the progression of elastase-induced emphysema

Given the anatomical location and longevity of alveolar macrophages and their well-documented production of effector molecules associated with the progression of emphysematous changes in the lungs, we hypothesized that lung macrophages contribute to the initiation and progression of emphysematous changes following elastase challenge. We tested this hypothesis by administering clodronate-loaded liposomes (CLLs) as a strategy to selectively deplete this cellular niche by inducing apoptosis in the lung macrophage population [180]. We hypothesized that depletion of the lung macrophage population would be protective against the progressive emphysematous changes to the lungs following elastase challenge. In preliminary control experiments using naïve mice, we determined that CLL-mediated alveolar macrophage depletion was approximately 90% efficacious and effective for 5-8 days (data not shown). Therefore, to test this hypothesis, we administered CLLs prior to (day -1) and at differing times post-elastase challenge (days 2, 7, and 14) to assess if the lung macrophage population was more important during the initiation or progression phases of elastase-induced emphysema (Figure 3.23A). When we examined the histopathological appearance of lung tissue sections at 21 days post-liposome administration there was no evidence of saline- (PLL; no depletion control) or clodronate- (CLL) loaded liposomes contributing to the progression of emphysema (Figure 3.23B). In the elastase-challenged groups that received CLLs, there were no differences in the extent of emphysema measured at day 21 post-PPE compared to elastase-alone

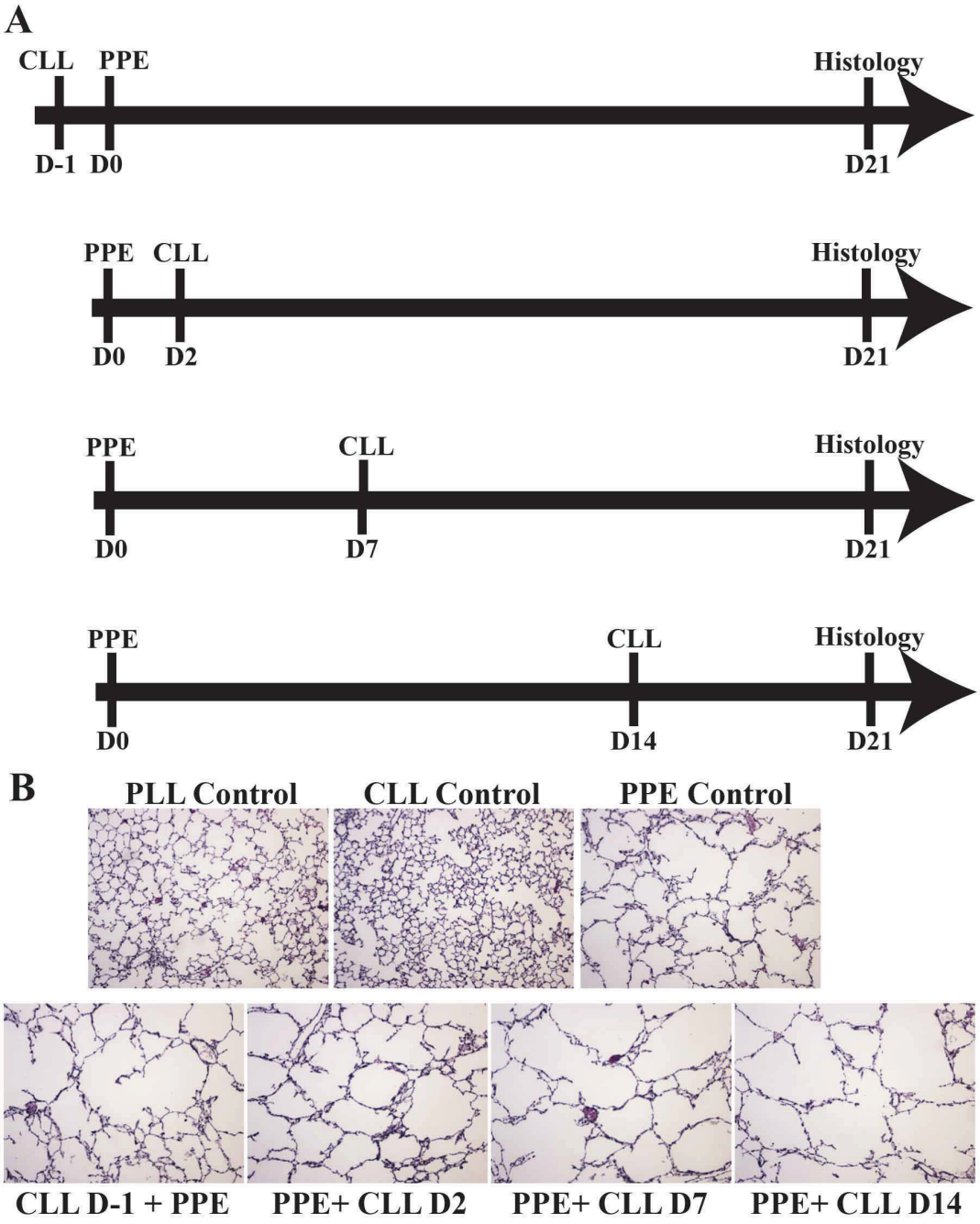

Figure 3.23 Effect of lung macrophage depletion on the progression of emphysema following PPE challenge.

Representative histological sections of lungs from C57BL/6 at day 21 post-PPE challenge (6U via intratracheal aspiration). Lung phagocytic cells were depleted via administration of clodronate-loaded liposomes (CLL) via intra-tracheal aspiration one day pre- (D-1), 2 days post- (D2), 7 days post- (D7), or 14 days post- (D14) PPE challenge. 5μm sections were stained with hematoxylin and eosin (10X objective).

controls (Figure 3.23B). Under these conditions, all groups exhibited similar levels of emphysema, regardless of the depletion time point (Figure 3.23B).

The interpretation of the results of this experiment was complicated by issues associated with the efficiency of lung macrophage depletion in the context of the elastase model. For these studies, in addition to the day 21 post-elastase histological endpoint measure, we also monitored the efficacy of alveolar macrophage depletion by flow cytometry (Figure 3.24A). We compared the number of AM present in the lungs of elastase-challenged animals that were administered saline-loaded liposomes (PLLs) or CLLs at days -1, 2, 7 or 14 at one day following liposome treatment (days 0, 3, 8, 15 post-elastase challenge) (Figure 3.24B). The overall efficacy of AM depletion was highest (83%) when liposomes were administered one day prior to elastase challenge. Unexpectedly, the efficacy of AM depletion dropped to 45%, 68%, and 42% at days 2, 7, and 14 post-elastase, respectively (Figure 3.24B). We also measured differences in the efficacy of $CD11b^-$ and $CD11b^+$ lung macrophage depletion. CLL depletion was more efficacious in depleting the $CD11b^-$ (46-87%) compared to $CD11b^+$ (16-62%) AM when administered at days -1, 2, or 14 post-elastase (Figure 3.24B). However, when liposomes were administered at day 7 post-elastase, the depletion efficacy of $CD11b^+$ AM (80% depletion) exceeded the $CD11b^-$ AM subpopulation (63% depletion). Interestingly, day 7 post-elastase was when we observed an expansion of the AM population (Figure 3.3A); perhaps these cells were more susceptible to clodronate liposome-mediated cell death. Regardless, the variable lung macrophage depletion efficacies measured following elastase challenge suggest that this particular depletion strategy is not appropriate for testing the hypothesis that lung macrophages contribute to the progression of emphysema.

3.4.9 Effect of neutrophil depletion on dynamics of lung-resident macrophage population

Given the early neutrophil influx into the lungs of mice following elastase challenge (data not shown), the well-documented interactions between macrophage and neutrophil populations, and the dynamics of AM phenotypic changes following elastase challenge, we hypothesized that AM may respond to inflammatory mediators released by neutrophils in the lungs. Therefore, in order to test this hypothesis, we employed a

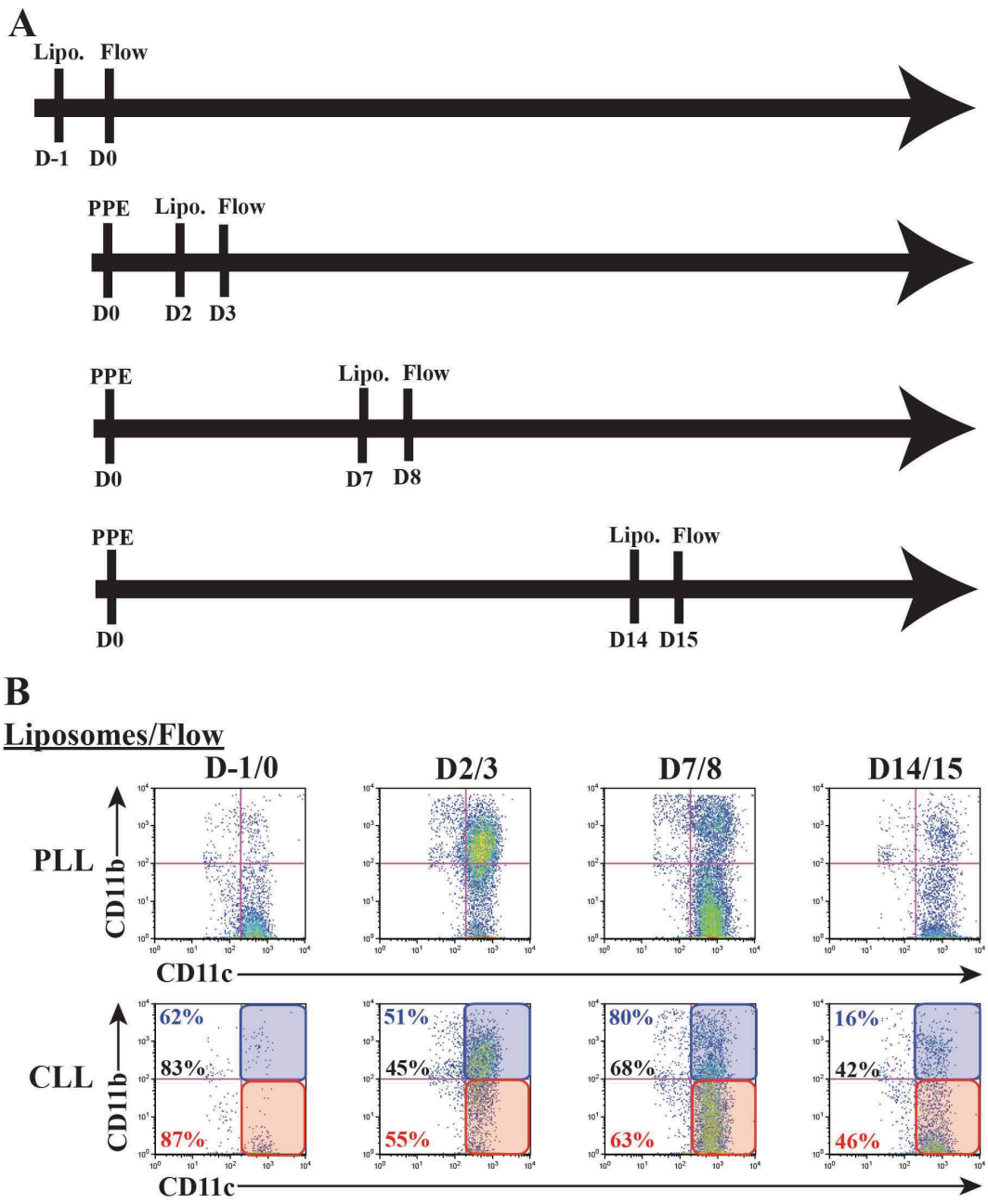

Figure 3.24 Efficacy of lung macrophage depletion following PPE challenge.
Representative data depicting flow cytometric analysis of perfused lungs isolated from C57BL/6 mice following 6U PPE administration via intra-tracheal aspiration at days 0, 3, 8, and 15 post-challenge. Lung phagocytic cells were depleted via administration of clodronate-loaded liposomes (CLL) via intra-tracheal aspiration one day pre- (D-1), 2 days post- (D2), 7 days post- (D7), or 14 days post- (D14) PPE challenge. Cells were surface stained with anti-mouse antibodies specific for CD11b, CD11c, and SiglecF. Plots show fluorescence intensity of CD11c (x-axis) and CD11b (y-axis) for gated $CD11c^{+}SiglecF^{+}$ cell population. Subpopulations are highlighted with colored boxes: $CD11b^{low}$ (red) and $CD11b^{high}$ (blue). Overall (black) and subpopulation (color code) depletion efficancy percentage is displayed. All depletion efficiencies were calculated compared to non-depleted controls (PBS-loaded liposomes [PLL]).

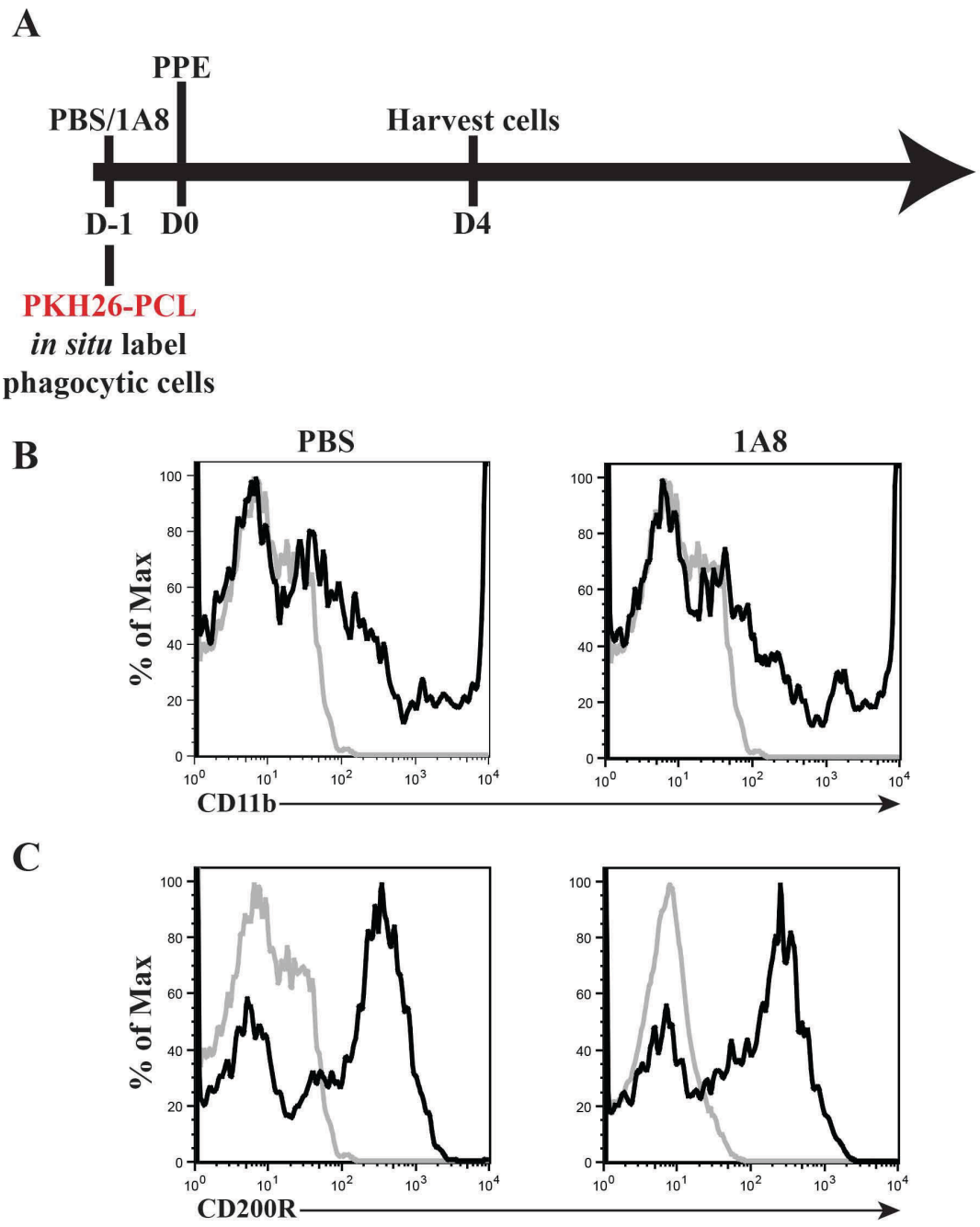

Figure 3.25 Effect of lung neutrophil depletion on lung-resident PKH26-PCL+ population's surface phenotype following PPE challenge.
Representative data depicting flow cytometric analysis of perfused lungs isolated from BALB/c- mice at day 4 post-3U PPE administration. Cells were surface stained with anti-mouse antibodies specific for CD11b or CD200R. Neutrophils were depleted via intra-peritoneal administration of anti-mouse Ly6G (1A8) monoclonal antibody one day pre-PPE challenge; non-depleted controls (PBS). Histograms show (A) CD11b or (B) CD200R (black) fluorescence intensity of gated PKH26-PCL^{+} cell population compared to isotype (grey) controls.

neutrophil depletion strategy to prevent the influx of these cells into the lungs following elastase challenge [433]. Our laboratory has demonstrated that neutrophil depletion via intraperitoneal administration of the anti-mouse Ly6G monoclonal antibody clone 1A8 is specific and long lived. Neutrophil levels in the blood and lungs are well below non-depleted controls at least five days post-depletion (data not shown). Given the neutrophil depletion window and the dynamics lung macrophage phenotypic changes, we assessed the impact of neutrophil depletion (at day -1) on LRM at four days post-elastase challenge (Figure 3.25A). We influx. Flow cytometric analysis on lungs following elastase challenge revealed that surface levels of CD11b and CD200R on PKH26-PCL^{+}CD11c^{+} resident lung macrophages were comparable between neutrophil depleted mice and non-depleted controls (Figure 3.25B, 3.25C). While neutrophil depletion had no impact on the LRM surface marker phenotype under these conditions, we only monitored surface CD11b and CD200R levels and appreciate that this was not an exhaustive LRM phenotyping as many other parameters could be assessed to more completely test the hypothesis. Interestingly, the size of the LRM population approximately doubled in the neutrophil depleted group (1A8) compared to non-depleted controls (PBS) at 4 days post-elastase challenge (Figure 3.26). While under these conditions, this data suggests that the presence of neutrophils impacts the degree of local alveolar macrophage expansion following elastase-induced lung damage, a more complete time course and monitoring is needed to fully understand the nature of neutrophil depletion and its possible impact on macrophage population dynamics.

In this study, the data suggest that the lung-resident alveolar macrophage population responds to a changing lung environment following elastase challenge. Upon monitoring the myeloid cell populations in the lungs over time, we observed a transient elevation in the size of the alveolar macrophage population. An approximate doubling in the size of the lung-resident macrophage population occurred between days 2 and 4 post-elastase challenge and was coincident with a significant increase in the percentage of LRM that were positive for a cell cycle marker, Ki67. Furthermore, the data suggest that the Ki67^{+} LRM population diluted the PKH26-PCL red fluorescent dye while the Ki67^{-} LRM population did not, pointing to the possibility of local macrophage proliferation. In addition, the LRM population exhibited increased cell size and granularity and concomitant increases in cell surface CD11b and CD200R levels following elastase challenge. These morphological and surface phenotypic changes accompanied evidence of macrophage

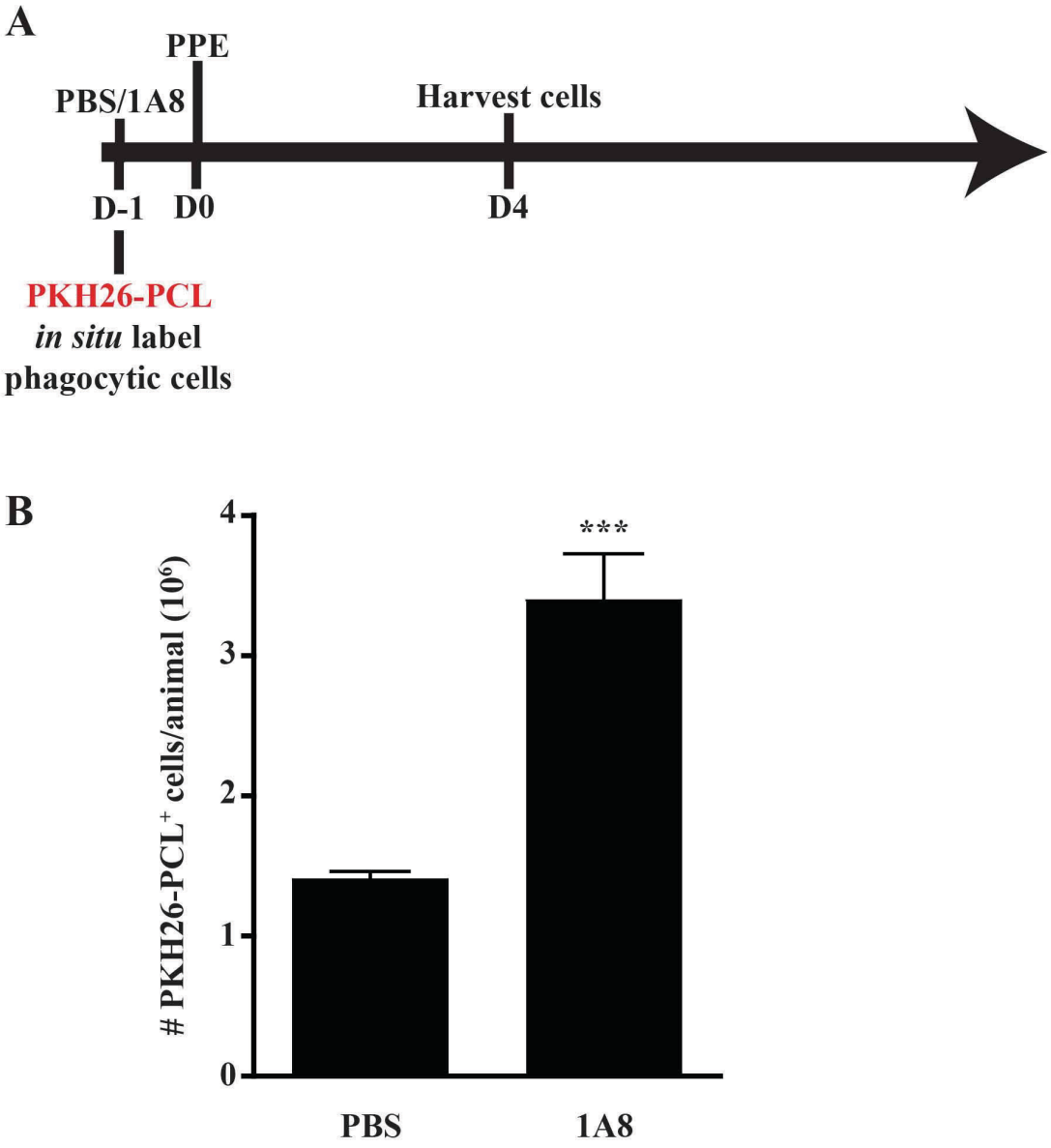

Figure 3.26 Effect of neutrophil depletion on lung-resident PKH26-PCL$^+$ population numbers following PPE challenge.
Total numbers of gated PKH26-PCL$^+$ populaton by flow cytometric analysis of perfused lungs isolated from BALB/c mice 4 days following 3U PPE administration via intra-tracheal aspiration (n=3). Neutrophils were depleted via intra-peritoneal administration of anti-mouse Ly6G (1A8) monoclonal antibody one day pre-PPE challenge. Bar graph depicts mean ± SEM. *** $p<0.001$. All comparisons are versus non-depleted controls (PBS).

activation based on gene expression profiling. Under these conditions, the data suggest that following elastase challenge and damage to the lung's ECM matrix, the lung resident alveolar macrophage population responds in a number of capacities to the elastase-induced damage, indicated by a mixed M1/M2 activation phenotype. We speculate that these observed changes may be influenced by the loss of several key regulatory mechanisms by which alveolar epithelial cells function to keep the alveolar macrophage population in a quiescent state in the normal healthy lung.

3.5 DISCUSSION

Our studies focused on the dynamics of myeloid cell populations in the lungs of mice following exogenous administration of porcine pancreatic elastase (PPE), an enzyme that causes damage to the extracellular matrix (ECM) leading to alveolar epithelial cell (AEC) death, the release of danger signals triggering inflammatory immune responses, progressive alveolar tissue destruction and the manifestation of emphysema. In this murine model of emphysema, under the conditions described above, we observed a transient increase in the size of the AM cellular niche. In addition, we observed morphological and phenotypic alterations to the cell surface following elastase challenge and a mixed M1/M2 activation phenotype. Data collected using an *in vivo* phagocytic cell labeling approach, as well as experiments carried out in CCR2-null mice, suggested that an AM subpopulation, which resided within the lungs prior to PPE challenge, entered cell cycle and proliferated. Because of their documented longevity and ability to mediate inflammation long after acute insults, we speculate that this AM subpopulation may contribute to the progression of emphysematous lung injury.

An elevation in the numbers of AM in emphysema patients compared to non-emphysematous controls has been described numerous times [55, 360, 373]. Estimates of the magnitude of AM increase range from 5-10-fold higher when comparing smokers and patients with COPD to healthy controls [55, 360] to 25-fold when comparing smokers with emphysema to normal smokers [399]. While the increased lung macrophage population in COPD and emphysema patients has been well documented, the mechanisms and dynamics by which this cellular niche expands are still not fully understood.

Several possible etiologies could be responsible for the elevated lung macrophage phenotype associated with emphysema in humans. First, in response to elevated chemokine expression, a robust monocyte infiltration from the periphery could account for the observed increase in lung macrophages. Second, a change in apoptotic mechanisms and/or protracted cell survival could lead to an altered cell turnover and an accumulation of lung macrophages. Third, the elevated number of lung macrophages associated with emphysema could be dependent upon enhanced local cell proliferation. While presented here as autonomous mechanisms, it is unlikely that any one of these mechanisms is fully responsible. It is more likely that these mechanisms work in concert to generate the observed phenotype. Through model systems, researchers can begin to tease apart these mechanisms and elucidate the nature of macrophage dynamics in order to understand how it may impact the progression of emphysema in humans.

Historically, the central dogma within the myeloid cell and macrophage field has accepted that monocytes are the precursors to tissue macrophages [9, 187, 191, 444-452]. Therefore, it is not surprising that most of the COPD and emphysema literature to date supports this idea and operates under the assumption that monocytes play a key role in the pathogenesis of emphysematous changes to the lungs, as they are expected to give rise to the expanded lung macrophage population [453, 454]. Therefore, it was unexpected when we did not detect a clear and robust influx of $CD11b^{+}Ly6C^{+}$ inflammatory monocytes to the lungs following PPE challenge (Figure 3.3C, 3.3D). This phenotype also greatly differs from our findings in a model of malaria-associated acute lung injury (see CHAPTER 2), where we observed significant recruitment of monocytes into the lungs upon inflammatory insult (Figure 2.5B). Under the experimental conditions used here, our data suggest that "classical" inflammatory monocytes ($CD11b^{+high}Ly6C^{+high}CCR2^{+}$) may not play a major role in the pathogenesis of PPE-induced emphysema. However, as discussed in CHAPTER 1.2.26, not all blood monocyte populations express the chemokine receptor CCR2; as other chemoattractant ligand-receptor axes such as CX_3CL1/CX_3CR1 are used for monocyte recruitment. Therefore, it is possible that following elastase-induced damage to the lungs, CCL2/CCR2-independent monocyte populations may contribute to the progression of PPE-induced emphysema. As such, we appreciate that our investigation focused on the $CCR2^{+}$ inflammatory monocyte population (comparable to human $CD14^{+high}CD16^{-}$

monocytes) and there are other circulating monocyte populations such as "resident" fractalkine receptor-positive (CX_3CR1^+) $CCR2^-$ monocytes (comparable to human $CD14^+CD16^+$ monocytes) that may have been recruited to the lungs following elastase-induced damage that fell outside of our analysis [9, 187]. In fact, in the murine cigarette smoke (CS) model of emphysema, "classical" $CCR2^+$ inflammatory monocytes were not found to be recruited to the lungs, instead, a $CX3CR1^+$ monocyte population was shown to expand and associate with the lung interstitium, but not within the alveolar spaces [419, 454]. Our data appears to be consistent these findings in the CS emphysema model and suggest that CCR2-dependent monocyte populations may have minimal impact on the pathogenesis of PPE-induced emphysema; as we observed a similar dynamic pattern for the extent of progressive tissue damage and emphysema in CCR2-deficient mice as wildtype controls (Figure 3.8). Under these experimental conditions, our data do not support the notion that "inflammatory" $CCR2^+$ monocytes serve as the precursors to the expansion of the lung macrophage population we observed in the elastase model of murine emphysema.

Alternatively, the observed increases in the size of the lung macrophage population associated with tissue destruction in emphysema and COPD patients may be due to alterations in the turnover rate of these long-lived tissue-resident cells. Several factors may influence the turnover rate including changes in cell pro-survival signals, apoptotic cell death mechanisms, or cell proliferation. Lung macrophages have a long lifespan, estimated on the order of several months [455] and it is clear that the effects of certain environmental exposures are quite long lived in lung macrophages [122]. For example, in an observational study, a never-smoker with A1AD emphysema received a lung transplant from a donor with a history of heavy cigarette smoking. The transplant recipient was monitored over time for the presence of alveolar macrophages containing inclusion bodies containing tobacco smoke particulate [456]. Surprisingly, greater than 50% of alveolar macrophages isolated by bronchoalveolar lavage (BAL) still contained smoke-associated inclusion bodies at 24 months following transplantation [456]. It is remarkable that environmental exposures such as tobacco smoke are so long-lasting in this cellular niche, as it has been well documented that exposure to tobacco smoke can greatly alter the lung macrophage activation state [376, 457]. This observational study did not address whether these tobacco smoke-containing AM were the original macrophages that encountered the tobacco smoke or their cellular descendants; it is intriguing to

ponder the idea of vertical transmission of an activation state from parent (F_0) to daughter (F_1) generations through epigenetic modifications. Furthermore, there is evidence demonstrating that lung macrophages isolated from tobacco smokers have altered cell survival mechanisms, as these cells have higher expression of Bcl-X_L, an anti-apoptosis factor and therefore increased cell survival [404]. Surely the effects of increased cell survival could result in an enlarged lung macrophage population over time, however, increases in the rate of local lung macrophage proliferation have the potential to enhance the size of the lung macrophage population more quickly. While there is precedent for speculation that there is local lung macrophage proliferation in humans in the context of smoking and COPD [224, 228, 457], direct evidence of resident lung macrophage proliferation during the progression of emphysematous changes in the lungs has not been clearly demonstrated. More broadly, the idea of local lung macrophage proliferation has been sporadically discussed in the field [223, 225], but this notion has never fully taken hold. Only recently, as was outlined in CHAPTER 1.2.27, the myeloid cell and macrophage community is currently undergoing a paradigm shift in regard to the idea that terminally differentiated tissue macrophages have the ability to self renew and maintain themselves via local cell proliferation [208]. Tissue-resident macrophage proliferation has been demonstrated in a variety of situations including parasitic worm infections localized to the lungs [46] and pleural cavity [231], at atherosclerotic lesions [233], and in adipose tissue [234]. Under these conditions, our data suggests that between days 2 and 7 post-elastase challenge, a lung-resident macrophage subpopulation enters cell cycle and proliferates (Figure 3.16, 3.17, 3.18).

We also observed several morphological and phenotypic changes to the surface of the lung resident macrophage population following elastase challenge. These changes were consistent with a lung-resident macrophage population quickly responding to alterations to the local microenvironment upon lung damage. In fact, all tissue macrophages are influenced by factors in their local environment [458]. The local pulmonary environment certainly has a profound impact upon the function of alveolar macrophages, which are constantly exposed to high levels of surfactants [459], granulocyte macrophage colony stimulating factor (GM-CSF) [127], transforming growth factor beta (TGF-β) [154], and other immune-modulatory factors [37, 56, 143, 460]. Generally, changes to the availability of these regulatory factors can lead to

alterations in AM function, but in some cases can lead to a severely dysregulated alveolar macrophage population and chronic pulmonary inflammation.

GM-CSF is a prime example of a soluble regulatory factor that influences the activation state of the alveolar macrophage population. GM-CSF is maintained at high levels in the lung environment and functions to maintain homeostasis, however GM-CSF-deficient ($Csf2^{-/-}$) and GM-CSFR-deficient ($Csf2r^{-/-}$) mice spontaneously develop pulmonary alveolar proteinosis (PAP) [461], a rare condition characterized by the accumulation of high levels of pulmonary surfactants [127, 144]. In addition, $GM\text{-}CSF^{-/-}$ mice have been shown to be devoid of a mature alveolar macrophage population with deficits in phagocytosis, surfactant catabolism, cell adhesion, and innate immune function [37, 145, 461]. GM-CSF produced by AEC controls the maturation as well as the activation of the lung macrophage population through the transcription factor PU.1 [127, 146] and GM-CSF has been shown to directly promote tissue macrophage proliferation [142, 462]. We speculate that it is possible that following elastase challenge, the lung-resident macrophage population may be stimulated to proliferate through the actions of excess GM-CSF in the lungs as elevated GM-CSF levels have measured in the BAL and sputum of COPD patients [463] and in the PPE murine model of emphysema [464].

The expression of integrins on the alveolar macrophage surface can be influenced by several factors present in the lung environment, thereby influencing the cellular function [37]. A key feature and defining characteristic of murine alveolar macrophages is their low expression of the integrin CD11b (integrin α_M) [57, 58]. Using surface marker profiling to identify myeloid cell populations, most tissue macrophages are defined as being $F4/80^{+}CD11b^{+}CD11c^{-}$ cells [9, 11]. However, alveolar macrophages are distinct from other tissue resident macrophage populations, as they are defined as $F4/80^{low}CD11b^{-}CD11c^{+}$ cells; a surface marker phenotype typically used to identify dendritic cell populations [58]. The integrin CD11b (alpha M) performs several functions as it plays a role in phagocytosis, pairs with CD18 (integrin β_2) to form complement receptor 3 (CR3; also known as Mac-1), and in the adhesion of lung macrophages to the ECM and other cell types [234]. An increase in lung macrophage surface CD11b levels has been implicated in the increased phagocytosis of bacteria and apoptotic inflammatory cells [465]. Upon intra-tracheal

elastase-challenge, we observed a transient upregulation of surface CD11b levels on the lung-resident macrophage population (Figures 3.4 and 3.13). Therefore, it would be predicted that a $CD11b^+$ AM population would likely exhibit enhanced phagocytic capacities, possibly to clear increased numbers of apoptotic AEC and neutrophils present in the lungs following elastase-induced damage [466]. Similar alterations to alveolar macrophage CD11b surface levels have been reported upon repeated exposure to organic dust extract (DE) [467]. Such changes to the lung macrophage surface phenotype were associated with increased IL-6 and CXCL1/GROα release and enhanced phagocytic capacity of the lung macrophage pool [467]. Furthermore, a similar phenotype has also been reported in alveolar macrophages following *Streptococcus pneumoniae* infection [63]. At day 3 post-*S. pneumoniae* infection, approximately 65% of the lung macrophage population in the airways and the lung tissue had high levels of CD11b on their surface [63]. This phenotypic alteration in surface CD11b level is roughly equivalent to the degree that we measured following elastase-induced damage to the lungs between days 2 and 7 post-challenge (Figure 3.4, 3.13). In addition, the investigators determined using *in vitro* studies that GM-CSF (and not *S. pneumoniae* lysate, LPS, or IL-10) regulated surface CD11b levels on lung macrophages [63]. The investigators speculated that the transient nature of CD11b up-regulation on the surface of the lung macrophages was associated with an initial increase in local GM-CSF levels and its resolution to steady-state levels. AEC-derived GM-CSF has been implicated as a pathogenic mediator of experimental COPD and potential drug target due to its profound impacts on lung macrophage survival, proliferation, and activation [468, 469].

Recently, multiple studies have illustrated the importance of direct interaction between AM and AEC [47, 154, 167]. In fact, a recent study demonstrated that lung epithelial cells act as a conduit and scaffold for inter-macrophage communications [167]. AM bind to AEC via the gap junction protein connexin 43 and utilize Ca^{2+} fluxes to communicate with distal lung macrophages via AEC [167]. Therefore, appreciating the physical relationship that exists between these cell types becomes especially important when investigating the molecular and cellular mechanisms of emphysema pathogenesis. In the case of PPE-induced emphysema, damage to the ECM and subsequent AEC death may directly impact the activation state of the alveolar macrophage population. When alveolar macrophages adhere to the airway epithelium, the immunomodulatory cytokine TGF-β is maintained in its active form by αvβ6 integrin on airway

epithelial cells [152, 153] and maintains the AM in a quiescent state [154]. Mice deficient in the integrin β6 subunit (Itgb6$^{-/-}$) (functional loss of integrin αvβ6) suffer from elevated MMP12 levels (200-fold increase in the lung macrophage population) in the lungs and the spontaneous development of emphysema [153]. The investigators determined that this activated alveolar macrophage phenotype in Itgb6$^{-/-}$ mice was due to the inability of integrin αvβ6 to bind and activate latent TGFβ, therefore resulting in elevated lung macrophage MMP12 production and the progression of emphysema [153]. These findings suggest a direct link between AEC and AM, thereby controlling macrophage activation via immunomodulatory factors.

CD200-CD200R interaction serves as another immune-modulatory mechanism by which AEC can maintain anti-inflammatory alveolar macrophages [160, 161]. CD200 (also known as OX2) is a surface molecule expressed on the surface of a wide array of cell types including but not limited to AEC, T cells, B cells, and neurons [161, 162]. CD200R is a transmembrane receptor almost exclusively expressed by myeloid cells, but can also be expressed by T cells [162, 164]. Of note, CD200R is expressed at high levels on the surface of lung macrophages [47, 163]. Ligation of the receptor inhibits macrophage activation through recruitment of Dok2 and subsequent RasGAP activation, which mediates inhibition of the Erk, Jnk, and p38 MAPK pathways [164-166]. Engagement of CD200R on the surface of lung macrophages negatively regulates the level of pro-inflammatory activation and maintains lung homeostasis [47], however, failure to engage the inhibitory CD200R can lead to myeloid cell activation. For example, alveolar macrophages from CD200$^{-/-}$ mice have an pronounced activated phenotype, as they do not receive the immune-modulatory signal from the AEC [47]. As a result, CD200$^{-/-}$ mice have elevated numbers (more CD200R^{+} cells in the lungs) and elevated MHC class II and CD80 surface levels on lung macrophages [47]. Owing to an activated lung macrophage population, CD200$^{-/-}$ mice are able to clear influenza infections much more rapidly than wild-type controls, however they also experience higher levels of immunopathology and morbidity associated with influenza infection, due to exacerbated anti-viral responses [47]. Similar to our observations following elastase-challenge (Figure 3.14), influenza infection results in elevated CD200R levels on the surface of the alveolar macrophage population [47]. It would be predicted that elastase-induced AEC death would lead to a loss of TGF-β mediated-regulation as well as CD200-CD200R engagement. We speculate that upon release of these inhibitory signals, the alveolar

macrophage population would elevate surface CD200R levels as a compensatory effect to maintain contact-dependent regulation.

Alarmins, epithelial-derived cytokines such as IL-25, IL-33 and thymic stromal lymphopoietin (TSLP), can be released upon cellular stress and act as another factor involved in the maintenance of the interaction between the AEC and lung macrophages [155, 157, 158]. Stress-induced alarmin release and signaling can lead to the initiation of type 2 immune responses through the promotion of downstream factors such as IL-4, IL-5 and IL-13 [155]. A number of cell populations have recently been shown to respond to IL-25 and IL-33, including type 2 innate lymphoid cells (ILC2s) and macrophages [157]. IL-33, an IL-1 family member, signals through its heterodimeric receptor ST2 (also known as IL1RL1) and IL-1 accessory protein via MyD88 [158]. IL-33 signaling has been demonstrated to drive a wound repair response in the lung [155]. IL-33 also appears to be important in the progression of emphysema, as anti-IL-33 blockade is protective from CS-induced emphysema [470]. Indeed, our laboratory has demonstrated that IL-33 protein levels were elevated within 48 hours after elastase-induced damage in the lungs and that ST2-deficient mice are protected from the progressive stage of emphysema (data not shown). Therefore, we monitored the expression of ST2 surface levels on the alveolar macrophage population following elastase challenge. We observed that the number of $ST2^+$ lung macrophages expanded and peaked at 2 days post-elastase and subsequently returned to baseline levels by day 14 post-PPE challenge (Figure 3.15). Our data suggests that upon AEC damage and cell death the alarmin IL-33 is released and is bound by $ST2^+$ cells in the lungs including lung macrophages, and upon IL-33 stimulation, the AM population increases surface levels of the ST2 receptor.

Interestingly, our data suggest that the AM exhibit a mixed M1/M2 activation phenotype following elastase challenge. Isolated $CD11c^+$ cells concurrently up-regulated *Nos2* and *Arg1* within two days following PPE challenge (Figure 3.20, 3.21). Over the 21 days following elastase-induced lung damage, other M1- and M2-associated genes were also concomitantly up-regulated (Figure 3.19, 3.20, 3.21). Alveolar macrophages up-regulated the expression of elastolytic enzymes associated with the onset of COPD such as MMP12 (days 7 and 14) [153] and MMP9 (day 21) [471]. In addition, AM up-regulated expression of the

alarmin, IL-33, at day 2 post-PPE, suggesting that lung macrophages may have been under stress or endured damage upon elastase challenge. Interestingly, there was no significant change in ST2 expression level; in contrast with our flow cytometric analysis where we observed increased ST2 surface protein levels at day 2 post-elastase (Figure 3.15). Furthermore, the data suggest NLRP3 inflammasome activation occurred several weeks following elastase-induced damage, as both *Il1b* and *Il18* were significantly up-regulated at day 21 (Figure 3.20). IL-1β and IL-18 have both been implicated with the onset of COPD and in mouse models of emphysema [472, 473]. It is possible that reactive oxygen species [474] or extracellular ATP [475] released from dying AEC may trigger NLRP3 inflammasome activation. Overall, the AM activation profile was temporally dynamic as the composition of genes up-regulated at day 2 differed from those at days 7, 14, and 21 post-elastase (Figure 3.19, 3.20, 3.21). In fact, the effects of an acute inflammatory insult such as elastase challenge on macrophage activation can be quite long-lived, as a number of the genes assessed were significantly up-regulated 21 days post-challenge. However, given our results, it is unknown whether individual macrophages exhibit a mixed activation phenotype or whether the population as a whole is composed of a heterogeneous mixture of activated cells.

Macrophages with mixed M1/M2 phenotypes have been previously reported in adipose tissue macrophages [476], peritoneal macrophages [477], as well as lung macrophages from GM-CSF$^{-/-}$ mice [478] or isolated from smoking patients with COPD [479]. The notion of linear macrophage polarization phenotypes (either M1 or M2), as have been characterized *in vitro* through stimulation with LPS and IFNγ or IL-4 and IL-13 respectively, does not translate to *in vivo* systems. Therefore, *in vivo* macrophage polarization should be considered more spectral in nature (reviewed in [112]), as a multitude of macrophage activating factors are present and can differ based on the local tissue environment and inflammatory insult. In fact, many of the soluble and contact-dependent factors discussed above can profoundly influence macrophage activation status. In addition, there is a temporal component to *in vivo* macrophage polarization that must be taken into account as the requirements of macrophage function change from acute inflammatory insult to the resolution phase [477] (reviewed in [480]). The underlying molecular mechanisms that control the mixed macrophage activation phenotype need to be revealed to gain further insight into the function of these cells and their contribution to emphysematous changes to the lungs.

In addition to the interactions with AEC, alveolar macrophages also interact with other cells types, including neutrophils, following elastase-induced lung damage. It is clear that the neutrophil and lung macrophage populations are linked through the release of soluble chemokines, however they are also connected through additional indirect and direct physical interactions. Lung macrophages, like endothelial and epithelial cells, are responsible for the release of IL-8/CXCL8, a neutrophil chemotactic factor, following lung damage [481]. Upon recruitment to the lung, neutrophils phagocytose pathogens or cellular debris, release cytokines, degranulate (release granular contents), and apoptose [482]. Upon neutrophil apoptosis, tissue macrophages and monocyte populations phagocytose the apoptotic bodies, thereby limiting prolonged inflammatory responses [482]. As a consequence of neutrophil activation and degranulation, several serine proteases including neutrophil elastase and cathepsin G are released. Previous studies have demonstrated that neutrophil elastase and cathepsin G are responsible for the cleavage of IL-33 into its bioactive form [159]. It is possible that cleavage of IL-33 into its bioactive form is a prerequisite for up-regulation of surface ST2 levels on AM. Exogenous IL-33 administration has been demonstrated to up-regulate surface ST2 levels on lung macrophages and promotes an alternatively activated macrophage (AAM) phenotype [155]. Data collected previously in our group demonstrated that neutrophils rapidly influx into the lungs following elastase challenge, peak at 48 hours and resolve by 7 days post-PPE challenge (Figure 1.7D). This rapid neutrophil influx paralleled the transient up-regulation of alveolar macrophage ST2 levels observed upon elastase challenge (Figure 13.5). Interestingly, our data suggest that neutrophil depletion may impact the extent of local lung macrophage proliferation following elastase-induced tissue damage (Figure 3.25). Certainly further investigation is warranted to elucidate the relationship between impaired neutrophil influx and the dynamics of the alveolar macrophage niche upon elastase challenge.

In order to test the hypothesis that lung macrophages contribute to the progression of emphysema following elastase-induced damage, we utilized clodronate-loaded liposomes (CLLs) administered via intra-tracheal aspiration as a depletion strategy. However, CLL administration did not impact the dynamics or extent of emphysema progression when administered one day prior to or 2, 7, or 14 days following PPE challenge

(Figure 3.22). When we assessed the efficacy of alveolar macrophage depletion over time, it was clear that following elastase challenge, the efficacy of depletion was decreased compared to unchallenged lungs (Figure 3.23). In an attempt to possibly explain this phenomenon, we devised several hypotheses: first, it is possible that the target cells (alveolar macrophages) are inaccessible due to the extensive damage to the lung architecture following elastase challenge, or second, the AM are indeed being reached by the CLLs however the target cells do not phagocytose the liposomes due to changes in their activation state, possibly due to early efferocytosis of dead AEC and neutrophils. These are certainly testable hypotheses and do warrant further investigation. Alternatively, there are other strategies that could be employed for the depletion of the lung macrophage population that do not require phagocytosis, such as the CD11c-DTR transgenic mice [483-485]. This transgenic depletion strategy only requires the diphtheria toxin to physically engage the toxin receptor on the cell surface and would work around the requirement for phagocytic uptake of the apoptosis-inducing drug. Additionally, we know that CD11c levels on the surface of alveolar macrophages remains constant over the 21 day period following elastase challenge (Figure 3.2), so their DTR surface levels should remain stable. It is appreciated that there are other $CD11c^{+}$ cells in the lungs over this time period including dendritic cells, but DCs can also be unintended target cells during CLL-mediated depletions strategies, so there would be minimal increase in the off-target effects when using the CD11c-DTR depletion strategy compared to CLL-mediated depletions. By employing specific and effective depletion strategies, we may be able to further elucidate the role of the lung resident macrophage population during the initiation and progression of emphysematous changes to the lungs in response to PPE challenge. Previous lung macrophage depletion studies, using an in-house generated rabbit anti-rat monocyte/macrophage polyclonal sera (antiMoMac), have demonstrated that the specific ablation of macrophage-derived elastolytic activity protects from the progression of emphysema following CS exposure in rats [486].

Interestingly, the expansion of the AM population observed following PPE challenge was transient in nature. Following a brief proliferative phase, the AM population returned to homeostatic levels by day 14 post-elastase challenge (Figure 1.7D, Figure 3.3A). While the mechanisms behind this apparent contraction phase remain unknown, it may be due to changes in AM surface phenotype, apoptosis, or migration from

the lungs. In Figure 1.7D, alveolar macrophages were collected by BAL and identified based on morphological assessment, therefore our quantification of AM population size by this method was independent of surface marker profile, so it is unlikely that changes to the macrophage surface phenotype underlie the apparent contraction. Certainly, further investigations into potential apoptosis or macrophage trafficking during this period are warranted.

We have just begun our investigations into the dynamics of the myeloid cell populations in the lungs following elastase-induced damage. The data presented here suggest that under these conditions, the AM population undergoes early transient phenotypic changes, display a mixed M1/M2 activation phenotype, as well as proliferate locally following elastase challenge. We speculate that these morphological, phenotypic, and activation changes to the AM population may be influenced, in part, by the release of several immune-modulatory control mechanisms. Understanding how these interactions with AEC and the lung environment at large control lung macrophage activation status and function is paramount to the understanding of their role in the progression of emphysematous changes in the lungs. We further speculate that an acute insult such as elastase-mediated alveolar ECM destruction and AEC death may lead to alteration of the AM population's activation rheostat. Such a transformation could account for the progressive nature of emphysematous changes to the lungs, as alveolar macrophages are long-lived cells with the ability to directly secrete effector molecules responsible for progressive emphysema or indirectly mediate inflammation long after acute insults. Given the nature of the mediators of emphysema, such a response could be considered a poorly-regulated or imbalanced wound healing response. If so, further elucidation of the molecular and cellular mechanisms responsible for the maintenance of an altered lung macrophage rheostat are necessary, as it may be possible to intervene clinically with the goal of resetting the AM activation setpoint. Such interventions would have significant utility to public health as halting the progression of emphysema could greatly impact the extent of COPD-associated morbidity and mortality.

3.6 ACKNOWLEDGMENTS

We would like to thank Dr. John Matthew Craig for his assistance in the collection of bead-isolated $CD11c^{+}$ cells as well as sample preparation and microscopic analysis of $CCR2^{-/-}$ and liposome-depleted lungs. Nathachit James Limjunyawong performed PFTs presented in Table 1.7. In addition, we would like to thank Dr. Matthias Mack (Regensburg, Germany) for the rat anti-mouse CCR2 monoclonal antibody, Xin Guo for her assistance with tissue processing for histology, and Dr. Jeffry Reidler for his help with the Nikon Eclipse Ni-E upright microscope and NIS-Elements Microscope Imaging Software. This work was supported by National Heart, Lung, Blood Grant #HL10342.

CHAPTER 4

GENERAL DISCUSSION

4.1 Macrophage biology: looking ahead

Recently, there have been substantial advances in our understanding of macrophage and monocyte biology. The current paradigm shifts have left the field somewhat in flux, but have afforded investigators a new perspective and opportunities to assess and reassess the mechanistic roles of tissue-resident and infiltrating mononuclear cells. There are several key areas of investigation in relation to the advancement of our understanding of lung macrophage function that warrant mention. Currently, one of the most intensely studied aspects of macrophage biology is the classification of particular activation states such as M1 (CAM), M2a (AAM), M2b (type II), and M2c (deactivated) under a spectrum of inflammatory conditions [112, 480]. Macrophage activation is not linear in nature as the M1-M2 paradigm initially suggested, as this framework ignores the source and context of activation stimuli. Unlike the single-activator *in vitro* systems, *in vivo* macrophage-activating stimuli are multifactorial, temporally complex and non-mutually exclusive. Recent studies have demonstrated that instead of distinct phenotypes macrophage polarization should be considered spectral in nature [107, 112]. Macrophage polarization is plastic and flexible, as tissue macrophages do not form stable subsets, but instead conform and respond to the local tissue environment [487]. Plasticity of gene expression is particularly important given most tissue macrophages are embryonically seeded cells with the ability to maintain homeostatic levels throughout life. Owing to this dynamic nature, macrophages can be categorized as having mixed phenotypes at the population level or even at the single-cell level [476, 477, 488, 489]. The exact macrophage activation phenotype depends on the milieu of environmental signals that each cell is exposed to within the tissue. Therefore, in response to these dynamic processes, investigators must account for space and time when evaluating the contextual functionality of lung monocytes and macrophages. As such, more comprehensive analyses of lung macrophage activation phenotypes under a variety of conditions are needed.

Researchers continue to strive towards a clearer understanding of the interconnections and functional differences between monocytes, tissue-resident macrophages and DCs. In light of the current paradigm shift, the origins of these cell populations may be more disparate than previously appreciated. Still, questions remain as to why some tissue macrophage populations are constantly replenished by monocytes, whereas other tissue macrophage populations are able to self-maintain independent of monocyte

contributions [196, 208, 210, 215]. The survival signals and underlying mechanisms that control these different situations remain unclear and certainly warrant further investigation. In order to more carefully delineate the function of these cell types, their core homeostatic features must be elucidated through transcriptional, epigenetic, proteomic, and metabolic profiling studies. The field is first working towards defining baseline expression profiles for different mononuclear phagocyte populations within a variety of tissue environments in order to identify key transcriptional networks [11, 490]. In fact, several large collaborative multi-site projects such as the Immunological Genome Project (ImmGen) [491], Human Immunology Project Consortium (HIPC) [492] and InnateDB [493] take advantage of expertise garnered within individual member laboratories and are working towards more clearly defining baseline transcriptional networks controlling immune cell populations both in humans and mice.

4.2 Macrophages in malaria

Human malaria infections result in a complex disease state that differs based on geography, age, prior exposure to *Plasmodium*, prior exposure to other pathogens, immune status, environment, and genetics. While no animal model of malaria is fully able to recapitulate the human disease, certain aspects of malaria pathogenesis in mouse models apply to human malaria infections. With that in mind, we have compiled the findings presented in CHAPTER 2 to create a working model of an understudied aspect of malaria infection – malaria in the lungs. This proposed model is presented in Figure 4.1. Briefly, as peripheral blood parasitemia rises, circulating *Plasmodium*-infected erythrocytes cytoadhere to the luminal surface of pulmonary post-capillary vascular endothelial cells. In our model, these host-pathogen interactions are largely mediated through direct contact between CD36 on the endothelial cell surface and a parasite-derived protein schizont membrane-associated cytoadherence protein (SMAC), a surrogate for the seemingly more complex interactions between parasite-derived *Pf*EMP1 and an array of host proteins in *P. falciparum* malaria in humans (Figure 4.1A). The intimate, receptor-mediated contacts between *Plasmodium*-infected erythrocytes and endothelial cells result in endothelial barrier disruption and pro-inflammatory cytokine and chemokine release, possibly an endothelial cell response to parasite-derived

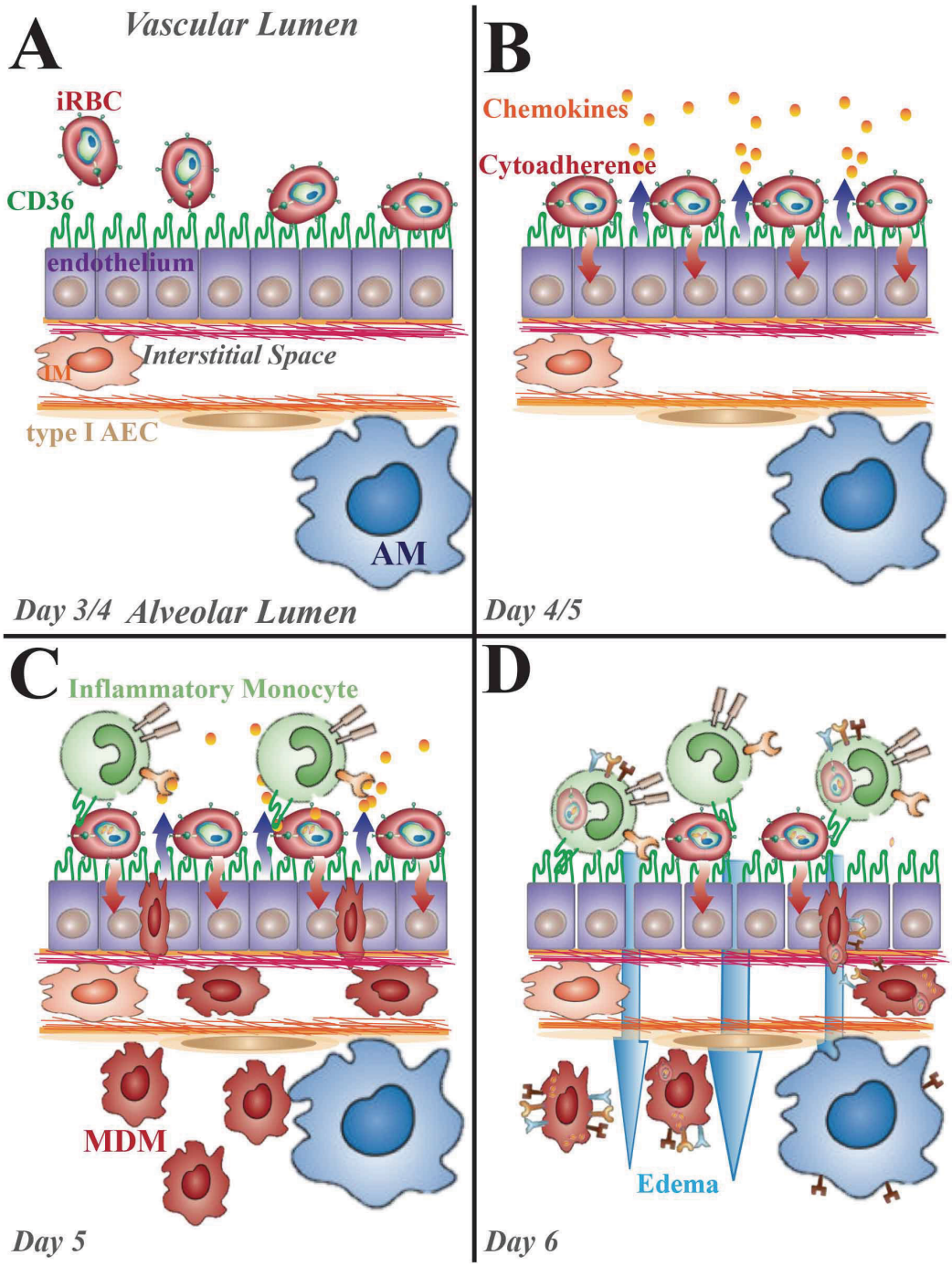

Figure 4.1 Current working model: malaria
Each panel depicts highlighted aspects of the *P. berghei* ANKA model of severe malaria in C57BL/6 mice, as presented in CHAPTER 2. The panels depict selected cells and molecules located within the alveolar space, epithelial cell wall, interstitial space, endothelial surface, and vascular lumen at (A) Day 3/4, (B) Day 4/5, (C) Day 5, or (D) Day 6 post-infection.

reactive oxygen species produced as a consequence of hemoglobin metabolism (Figure 4.1B). In an effort to clear sequestered parasites from the vasculature, a robust chemokine gradient is established; with several mononuclear phagocyte-recruiting chemokines expressed at high levels in the lungs. These chemokines gradients (largely the CCL2-CCR2 axis) recruit $CCR2^{+}$ inflammatory monocytes from the peripheral blood and bone marrow. The recruited inflammatory monocytes may tightly adhere to the luminal endothelial surface or localize in extra-vascular space, as they are retained in the lung tissue following perfusion (because the cells are no longer in the circulation and are lung-associated, we have termed these cells, monocyte-derived macrophages (MDM)). Upon recruitment to the lungs, the MDM population is the major driver of parasite clearance during primary acute infection. CD36-mediated non-opsonic phagocytosis is a key mechanism by which *Plasmodium*-infected erythrocytes are cleared (Figure 4.1C). Associated with parasite uptake, the MDM population up-regulates expression of co-stimulatory and other activation-associated molecules on their surface. Coincident with increasing parasite burden and monocyte recruitment to the endothelial surface, the endothelial barrier is compromised leading to non-cardiogenic pulmonary edema, which impacts gas exchange and lung function, as proteinaceous fluid enters the airways (Figure 4.1D).

Despite lung injury, the data indicates that the resident alveolar macrophage population (AM) does not play a major role in the clearance of sequestered parasites. In fact, with the exception of elevated surface MHCII levels, alveolar macrophages remain in an inactivated state even in the face of the elevated lung injury in CCR2-deficient mice that result from a block in the ability of monocytes to traffic to the lungs (Figure 2.11, 4.2). We hypothesize that alveolar macrophages play an anti-inflammatory/pro-homeostatic role in the resolution of malaria-induced lung injury. Our data suggest a basic model in which the dynamic interplay between the damage generated by CD36-mediated parasite sequestration and the protective action of CD36-mediated monocyte-driven parasite clearance largely determines the extent of malaria-induced lung injury during the acute phase of malaria infection (Figure 4.1, 4.2, 4.3). In future studies, we will use this current working model (Figure 4.1) as a springboard to form new testable hypotheses to mature our understanding of the complex pathophysiological mechanisms involved in malaria-induced lung injury.

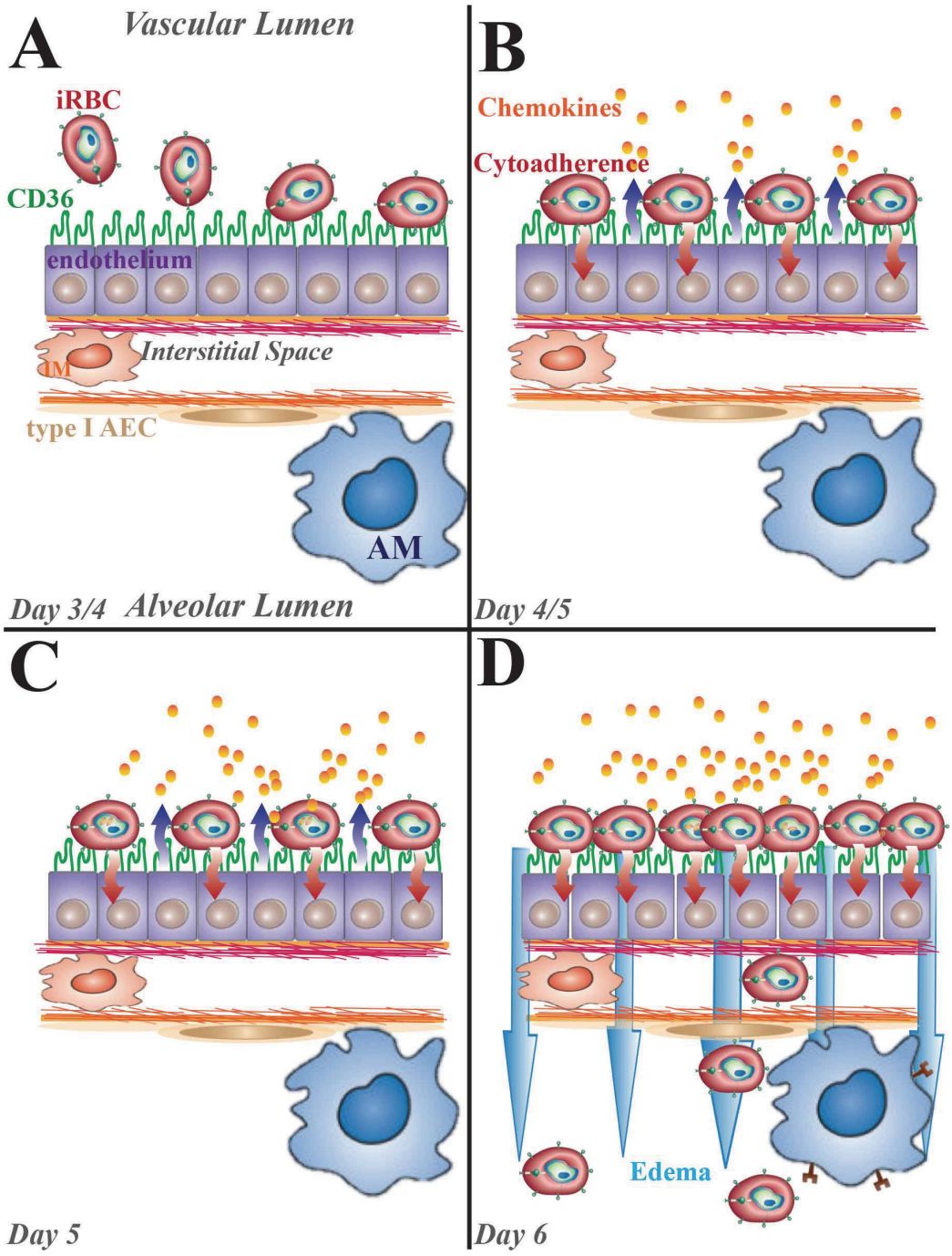

Figure 4.2 Current working model: malaria
Each panel depicts highlighted aspects of the *P. berghei* ANKA model of severe malaria in CCR2$^{-/-}$ mice, as presented in CHAPTER 2. The panels depict selected cells and molecules located within the alveolar space, epithelial cell wall, interstitial space, endothelial surface, and vascular lumen at (A) Day 3/4, (B) Day 4/5, (C) Day 5, or (D) Day 6 post-infection.

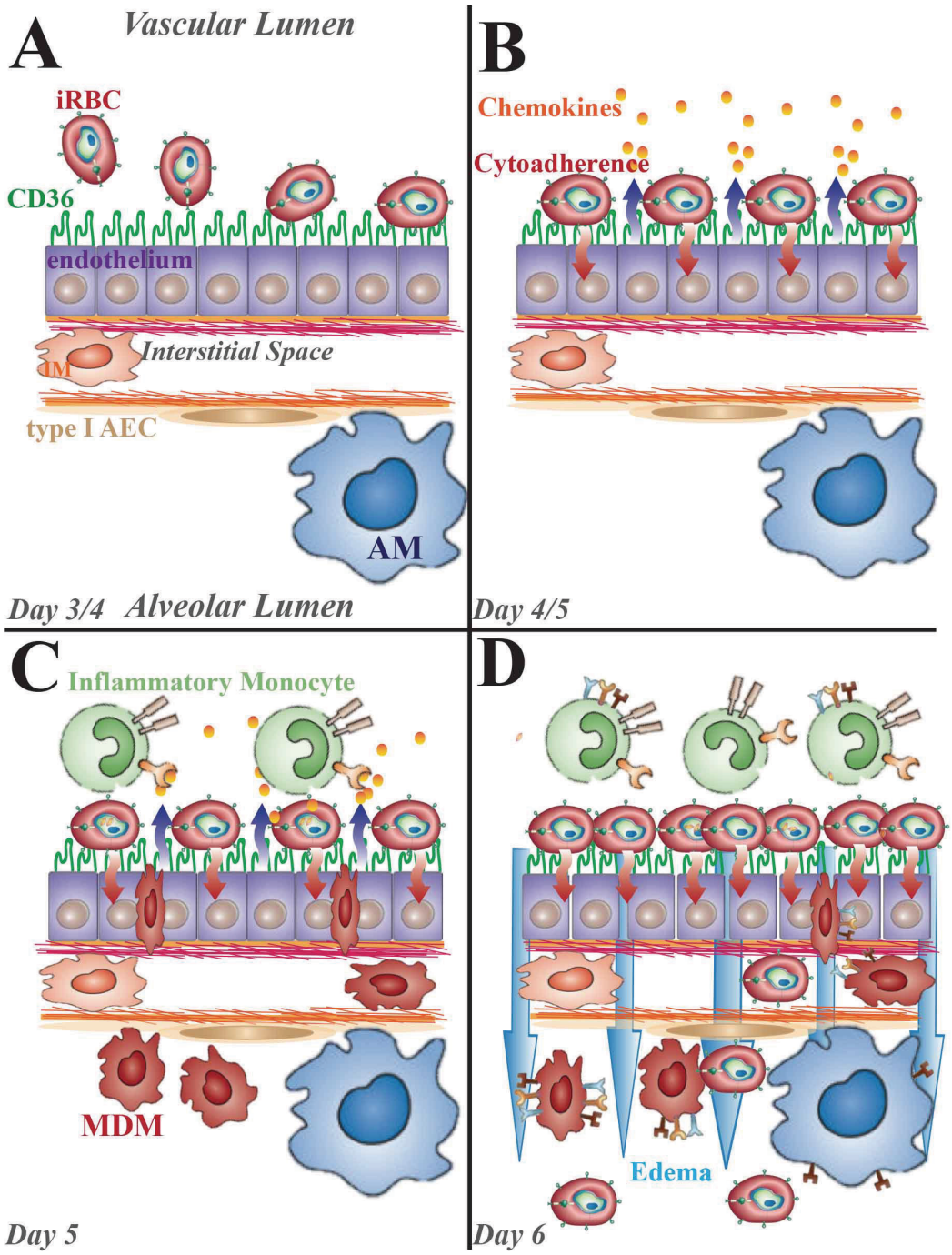

Figure 4.3 Current working model: malaria
Each panel depicts highlighted aspects of the *P. berghei* ANKA model of severe malaria in CD36$^{-/-}$ > WT chimera mice, as presented in CHAPTER 2. The panels depict selected cells and molecules located within the alveolar space, epithelial cell wall, interstitial space, endothelial surface, and vascular lumen at (A) Day 3/4, (B) Day 4/5, (C) Day 5, or (D) Day 6 post-infection.

The use of the available CCR2- and CD36-deficient strains necessitated that experiments be carried out using mice on the C57BL/6 genetic background. Since our C57BL/6 mouse model of severe malaria results in the onset of experimental cerebral malaria (ECM) and death at seven days post-infection, we were only able to study acute, innate immune responses to the presence of parasites in the lungs. It is intriguing to speculate on the fate of the inflammatory monocyte population in mouse strain-*Plasmodium* species combinations that result in more protracted infections. A longer infection window would provide opportunities to investigate the role of adaptive immunity on the parasite-induced lung inflammation and to determine the fate of the MDM that engulf parasite material. It is possible that the inflammatory monocytes are cleared from the lungs via Fas-mediated clearance mechanisms as has been shown in other lung injury models including influenza virus infection and LPS instillation [49]. Furthermore, we would be able to study the dynamics and function of the resident alveolar macrophage population in the context of the adaptive immune response. As the alveolar macrophages are known to play an active role in the maintenance of lung homeostasis, we hypothesize that their role is more pronounced during the adaptive phase. In future studies, it would be beneficial to explore the ability of MDM and alveolar macrophages to traffic to draining lymph nodes and present malaria antigens to T cells. Additionally, it would be advantageous to employ other parasite strains such as *P. chabaudi* or *P. yoelii* to determine if differences exist in the degree of pulmonary parasite sequestration, monocyte clearance and overall malaria-associated lung injury.

The findings presented in CHAPTER 2 contribute towards a clearer understanding of the implications of some of the current proposed approaches to employ pharmacological agents that alter CD36 levels as adjunct therapy for severe malaria patients. Some of these investigations aim to reduce malaria-induced pathology by increasing parasite clearance by employing PPARγ [494, 495] and Nrf2 agonists [496] to pharmacologically up-regulate CD36 levels on the surface of monocytes/macrophages. In addition, other anti-adhesion blocking therapies focus on limiting the level of parasite sequestration through CD36 blockade (reviewed in [497]). For example, the anti-helminthic drug Levamisole limits CD36-mediated sequestration of *Plasmodium*-infected erythrocytes by blocking CD36 dephosphorylation and preventing

the high affinity binding form of CD36 [498, 499]. As our data presented in CHAPTER 2 demonstrates, the relative contributions of both parasite sequestration and monocyte clearance need to be taken into account as both contribute to malaria-induced lung injury (and possibly to injury at other tissue sites). Therefore, careful consideration must be taken when proposing pharmacologic alteration of CD36 levels as a means to increase parasite clearance, as such a strategy may have deleterious consequences on the extent of CD36-mediated parasite sequestration. Conversely, therapeutic blockade of CD36-mediated parasite sequestration may alter the ability of mononuclear phagocytes to effectively clear parasites via non-opsonic phagocytosis. While a complex biological problem, development of adjunct therapies for severe malaria patients may someday prove to be an effective drug regimen.

4.3 Macrophages in emphysema

While exposure to cigarette smoke is the predominant risk factor associated with emphysema, not all smokers develop emphysema and for those that do years of exposure are required to cultivate the disease. It is becoming clear that there are multiple environmental, physiological and genetic factors that contribute to the initial damage that leads to the progressive destruction of alveolar tissue and development of emphysema. While specific initiation events are yet to be identified, lines of evidence suggest that physiological imbalances such as alterations in the relative concentrations of proteases and anti-proteases develop in certain individuals and serve as drivers of emphysema. Given that the exact initiation events are likely to be variable in humans, we employed a mouse model to simulate the protease/anti-protease imbalance associated with the development of emphysema. We have compiled our findings presented in CHAPTER 3 to create a working model. This proposed model is presented in Figure 4.4. In this model, porcine pancreatic elastase (PPE) is used as a surrogate for the complex mixture of proteases released from neutrophils (neutrophil elastase, cathepsin G, proteinase-3) and macrophages (MMP9, MMP12) in response to the toxic substances and epithelial damage caused by cigarette smoke. Upon administration into the lungs, PPE degrades elastin, a component of the lung's extracellular matrix. Matrix degradation leads to epithelial cell stress and death, and release of DAMPS (such as nuclear proteins, DNA, RNA, ATP) and alarmins (such as IL-33, IL-25, TSLP) (Figure 4.4B). Furthermore, due to mechanical stress alveolar epithelial cells die via necrosis as well as apoptosis. Neutrophils are recruited early to the lungs and peak

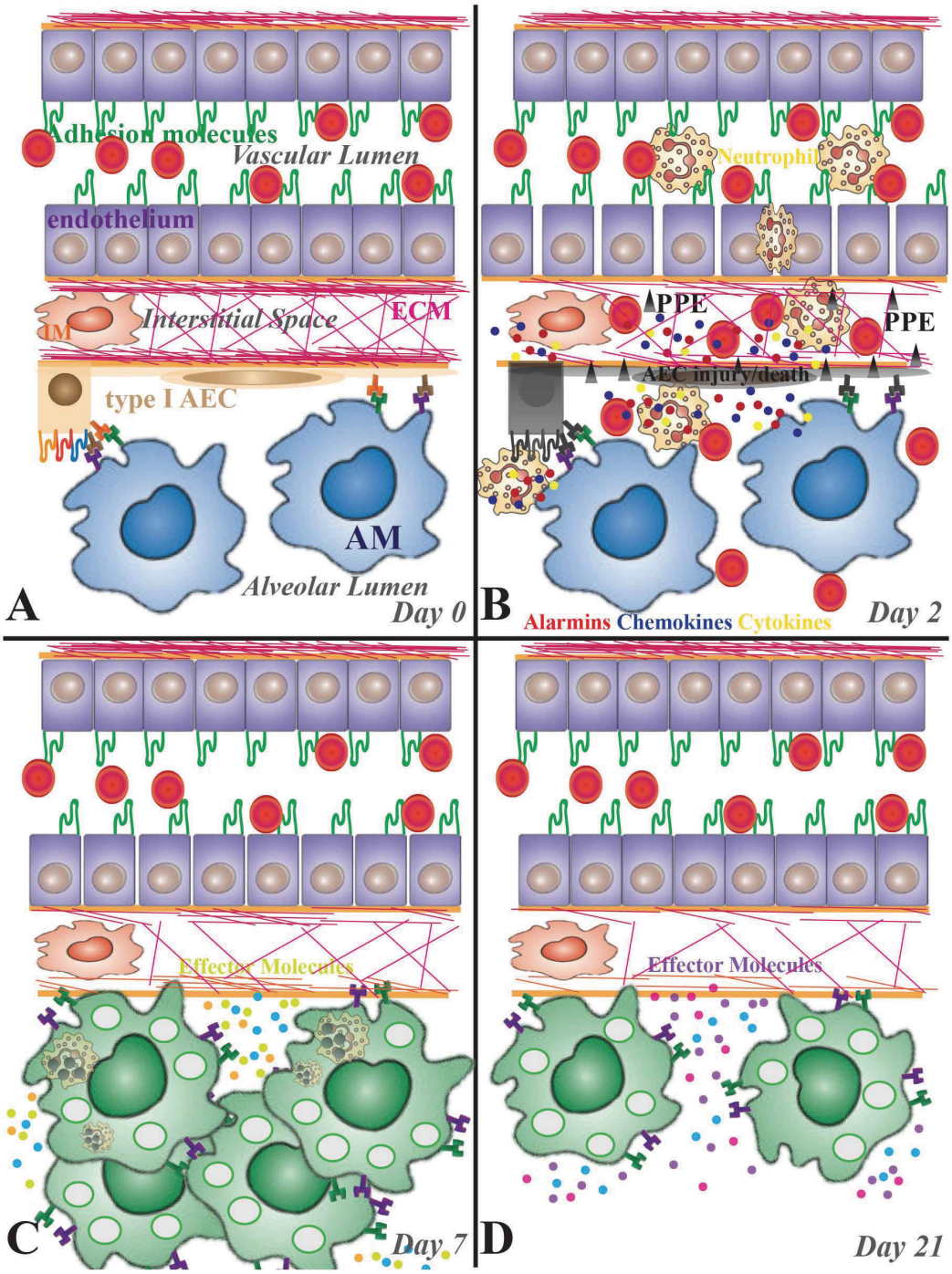

Figure 4.4 Current working model: emphysema
Each panel depicts highlighted aspects of the porcine pancreatic elastase (PPE) mouse model of emphysema, as presented in CHAPTER 3. The panels depict selected cells and molecules located within the alveolar space, epithelial cell wall, interstitial space, endothelial surface, and vascular lumen at (A) Day 0, (B) Day 2, (C) Day 7, or (D) Day 21 post-elastase challenge.

within two days. Unexpectedly, the data suggests that inflammatory monocytes are not recruited to the lungs in large numbers following elastase challenge. Therefore, we presume that alveolar macrophages play a major role in the clearance of apoptotic neutrophils and alveolar epithelial cells (Figure 4.4C). Our data suggest that upon alveolar epithelial cells loss, contact-dependent macrophage regulatory mechanisms (such as CD200-CD200R interactions and active TGFβ engagement by TGFβR) are lost. Relieving macrophage regulatory mechanisms may contribute to alveolar macrophage activation, pro-inflammatory cytokine production and proliferation following elastase-induced lung damage (Figure 4.4C). It is possible that a dysregulation of resident macrophage activation contributes to the progressive destruction of alveolar epithelial cell layer and emphysematous changes in the lungs (Figure 4.4D). Going forward, we will use this working model (Figure 4.4) as a starting point to form new testable hypotheses in order to further our understanding of the role of lung macrophages in the progression of elastase-induced emphysema.

Interestingly, in stark contrast to the vigorous infiltration of inflammatory monocytes observed during the innate phase response to malaria in the lung, PPE challenge did not result in a robust inflammatory monocyte recruitment; instead we observed local macrophage proliferation. In future experiments, it would be valuable to reveal the factors involved in promoting local macrophage proliferation following elastase-induced lung injury. Moreover, it would be advantageous to isolate and assess the activation status of the proliferative and non-proliferative AM subpopulations, as they may acquire distinct activation phenotypes and differ in their contributions to progressive alveolar tissue destruction. While the inflammatory insults studied in CHAPTER 2 and CHAPTER 3 certainly differ, they highlight an issue that has become more pertinent in light of the ongoing paradigm shifts in the macrophage biology. It is still unclear which environmental signals promote local tissue macrophage proliferation. Furthermore, investigators are working to understand the costs and benefits associated with tissue macrophage proliferation versus recruitment of inflammatory monocyte pools from the periphery during inflammatory insults. While inflammatory monocytes exhibit a number of beneficial functions, including facilitating clearance of pathogens, they also require a resolution phase in order to prevent chronic monocyte-driven pathology. Therefore, it has been proposed that under certain settings, it may be beneficial (from an resources

perspective) to contend with inflammatory insults through local proliferation of the tissue macrophage population, as these cells are already in tune with the local tissue environment and function to maintain tissue homeostasis. It is possible that our observation of transient local macrophage proliferation following elastase-induced lung damage may provide insights that contribute to a greater understanding of the underlying factors involved in tissue macrophage proliferation.

The observations presented in CHAPTER 3 have implications for the development of strategies for therapeutic treatment of patients with progressive emphysema. It may be possible and beneficial to reprogram or shift the polarization of lung macrophages in order to treat emphysema. Due to their inherent plasticity, it may be easier to manipulate tissue macrophages than other immune cells (such as T cells) implicated in disease states. Alveolar macrophages in particular are a desirable target for tissue macrophage modification, as they are easily reached through the use of inhalers. There are many potential mechanisms to focus on for reprogramming the alveolar macrophage population. If long-lived activated lung macrophages indeed contribute to the progression of emphysema, it would be beneficial to restore macrophage regulatory mechanisms such as PDL-1 or CD200R that keep the lung macrophage population in check since corticosteroids are ineffective against macrophages of COPD patients [481]. As we observed elevated alveolar macrophage CD200R surface levels following elastase-induced damage, it may be beneficial to use CD200R agonists as a therapeutic. This therapeutic approach would recapitulate the immune-modulatory role that alveolar epithelial cells exert upon the alveolar macrophage [47] and could possibly restore lung homeostasis. Such a therapeutic strategy could potentially benefit other lung diseases in which macrophages have been implicated in the pathogenesis. At present, there is a serious need for any therapy that could halt the progression or even reverse the effects of alveolar tissue destruction leading to emphysema.

4.4 Final thoughts

Upon first glance, the study of the pathogenesis of severe malaria and emphysema may have little in common. However, these seemingly disparate studies have touched upon several key issues currently being tackled within the macrophage biology field. In CHAPTER 2, we studied the differing roles of tissue-

resident macrophages and recruited inflammatory monocytes in an infectious disease setting. We found that monocyte-derived macrophages played a key role in parasite clearance, while alveolar macrophages did not. Conversely, in CHAPTER 3, we studied the dynamics and function of tissue-resident macrophages in a model of sterile inflammation leading to emphysematous changes in the lungs. Unlike our studies using the malaria model, we found that inflammatory monocytes may not contribute in a significant way to the elastase emphysema model, instead, the alveolar macrophage population underwent morphological changes, became activated and proliferated following elastase-mediated lung damage. While both studies involved models of pulmonary inflammation, the dynamics and functions of macrophage and monocyte populations differed quite dramatically. Given that monocytes are no longer thought to be precursors to lung macrophages, our findings presented in CHAPTERS 2 and 3 are but two examples of pulmonary insults in which the roles of tissue macrophages and monocytes differ. Therefore, understanding how the myriad of molecular mechanisms combine to result in a tailored immune response specific to the inflammatory insult at hand and how the local milieu of environmental factors influences the function of these mononuclear phagocytes is of key importance.

Since the initial observations made by Ilya Mechnikov, countless biologists have been captivated by the nature of macrophage biology. While these innate immune cells have been intensely studied for over one hundred years, the field is still dynamic and constantly evolving. Although tissue macrophages reside within varied locales throughout the body, their core functions of phagocytosis, immune surveillance and maintenance of homeostasis connect them. Recent studies have shed new light on the origins of tissue macrophages and the contribution of monocytes to their maintenance.

Basic research investigating the roles of monocytes and tissue macrophages in inflammatory settings has translational potential as these cells have been implicated in many protective as well as pathogenic disease outcomes. In order to develop intervention measures aimed at mitigating their role in damage or harnessing their protective power, a more detailed understanding of phenotypic commitment and activation requirements of tissue-resident macrophages are required. Additionally, understanding the plasticity of these mononuclear phagocytes is key to developing interventions aimed at altering monocyte/macrophage

function during pathogenic situations. Given the recent paradigm shift, this issue has become more important as altering the functional state of tissue macrophages may have profound long-term impacts as most macrophage populations have been identified as embryonically seeded, long lived, self-maintaining tissue-resident phagocytic cells.

APPENDIX I

CHAPTER 2 SUPPLEMENTAL MATERIAL

***** Dr. Ifeanyi Anidi collected all data presented in this Appendix *****

AI.1 MATERIALS AND METHODS

AI.1.1 Mice

Age and sex-matched (male 6-8 weeks old) littermates were used for all experiments. C57BL/6J were obtained from The Jackson Laboratory (Bar Harbor, ME, USA). $CD36^{-/-}$ mice on a C57BL/6 background were obtained from Dr. Maria Febbraio (Cleveland Clinic Foundation, Cleveland, OH, USA) [411]. B6-Ly5.2 congenic mice expressing the Ly5.1 antigen were purchased from the National Cancer Institute (Frederick, MD, USA). All mice were maintained within barrier filter-top cages, provided food and water ad libitum, and exposed to a 12-hour light/dark cycle. All animal procedures performed in this study were approved by the Johns Hopkins Animal Care and Use Committee (Baltimore, MD, USA), and were in accordance with the National Research Council's Guide for the Care and Use of Laboratory Animals federal guidelines.

AI.1.2 Parasites and infection

P. berghei ANKA (MRA-671) was obtained from the Malaria Research and Reference Reagent Resource Center (MR4) (Manassas, VA, USA). Cryopreserved parasite stocks were passaged through donor mice (C57BL/6J) at least twice prior to infecting experimental mice. Infected donor mice were maintained until the eighth passage, when new parasites were started from cryopreserved stocks. Blood stage infections were initiated by introducing 10^6 parasitized erythrocytes via intra-peritoneal injection. Progression of the infection was measured by tracking changes in body weight and temperature. In addition, peripheral blood parasitemia was monitored via thin blood smear and Giemsa staining.

AI.1.3 Bone marrow chimeras

Bone marrow cells were extracted from the femurs and tibias of $CD45.1^+$ C57BL/6 (WT) and $CD45.2^+$ CD36 deficient ($CD36^{-/-}$) mice. After removal of erythrocytes using ACK lysis buffer (Quality Biological, Gaithersburg, MD, USA), bone marrow cells were suspended in PBS. Cohorts of WT and $CD36^{-/-}$ mice

were irradiated with 900 rads using a ^{137}Cs γ-source (MSD Nordion Gammacell 40 Exactor; Laval, Quebec, Canada) and reconstituted 2-4 hours later with 1 x 10^7 heterologous or autologous bone marrow cells introduced via the tail vein in 150 µl of PBS. Mice were subsequently maintained on Sulfatrim (Actavis, Morristown, NJ, USA)-supplemented water for 4 weeks and allowed to recover for nine weeks before infection. At four and eight weeks post-irradiation, the effectiveness of chimerism was evaluated by assessing the levels of CD45.1, CD45.2 and CD36 on CD11b-postive cells. After applying Fc Block™ (BD Pharmingen), cells were incubated with the appropriate fluorochrome-conjugated antibodies in FACS-staining buffer (PBS containing 2% heat-inactivated FCS (35-011-CV, Mediatech, Inc., Manassas, VA, USA)) for 20 minutes on ice in the dark. Data were acquired on a FACSCalibur flow cytometer using CellQuest software (BD Biosciences, Mountain View, CA, USA) and results were analyzed using FlowJo software (Tree Star, Inc., Ashland, OR, USA).

AI.1.4 Antibodies

The following anti-mouse antibodies were purchased from BD Biosciences (San Jose, CA, USA) CD11b-PerCP-Cy5.5 (550993) and anti-CD16/CD32 Fc block (553142). CD45.2-PE (12-0454-81) and CD45.1-APC (912-0453-81) anti-mouse antibodies were purchased from eBioscience (San Diego, CA, USA). Anti-mouse CD11c-APC (130-091-844) was purchased from Miltenyi Biotec (Auburn, CA, USA). Mouse anti-mouse CD36 (ABM-5525) was purchased from Cascade Biosciences (Winchester, MA, USA). Mouse IgG Fc fragments (015-000-007) were purchased from Jackson ImmunoResearch (West Grove, PA, USA).

AI.1.5 Bronchoalveolar lavage (BAL)

Murine surgeries were performed as previously described [413]. Briefly, mice were anaesthetized with 450 mg/kg 2,2,2-tribromoethanol (Sigma-Aldrich, St. Louis, MO, USA) via intraperitoneal injection. An incision was made through the sternum and BAL fluid was obtained after a tracheostomy and lavaging of the lungs with 800 µl of sterile PBS three separate times at room temperature. BAL fluid from the three collections were pooled and centrifuged at 1,500 rpm for 3 minutes at 4°C. Cells were suspended in PBS and an aliquot was stained with trypan blue (Invitrogen, Grand Island, NY, USA) prior to counting on a

hemocytometer using the 10X objective of an Olympus BH-2 microscope (Catharpin, VA, USA). Cells (10^5) from each mouse were adhered to microscope slides with the aid of cytology funnels (Fisher Scientific, Houston, TX, USA) and a cytocentrifuge (Shandon Cytospin, Thermo Fisher Scientific, Waltham, MA) prior to methanol fixation and subsequent staining with Giemsa for differential cell analyses.

AI.1.6 Histology

A 19-gauge gavage tube was inserted into a small hole in the trachea, and the lungs were inflated slowly with zinc-buffered formalin fixative (Z-fix) (174, Anatech Ltd., Battle Creek, MI, USA). The lungs were removed and incubated in Z-fix for 48 hours. Inflated and fixed lungs were embedded in paraffin, and sagittal, 5 μm sections, were cut from four different levels of lung. Lung sections were placed on slides and either left unstained or stained with hematoxylin and eosin. Lung sections (and cytology slides) were examined using a Nikon Eclipse E800 light microscope (Nikon Instruments Inc., Melville, NY, USA), and images were acquired using SPOT RT charge-coupled device imager and software (Diagnostic Instruments, Inc., Sterling Heights, MI, USA).

AI.1.7 Lung injury scores

Hematoxylin and eosin-stained histological sections from test and control groups were evaluated in a blinded fashion by three investigators. A lung injury score was devised using three categories of histological change: intra-alveolar hemorrhaging and infiltrates, alveolar septal thickening and intra-alveolar edema. Each of these categories was scored using a four point system: 0 = no injury; 1 = < 10% of tissue section involved; 2 = 10 – 30% of tissue section involved; 3 = 30 – 50% of tissue section involved; 4 = > 50% of tissue section involved.

AI.1.8 Statistical analysis

Statistical significance was evaluated by using the 2-tailed t test (Tukey) and the one-way analysis of

variance (ANOVA) test using GraphPad Prism software (La Jolla, CA, USA).

AI.2 RESULTS

AI.2.1 CD36 and malaria-induced ALI

To determine the relative contributions of endothelial cell- and mononuclear cell-associated CD36 to malaria-induced lung pathology, we generated CD36 chimera mice where CD36 expression in the lungs was restricted to either vascular endothelial cells or cells of hematopoietic origin (Figure AI.1A). CD36 chimeric and control mice were infected with *P. berghei* ANKA at 9 weeks post-bone marrow transfer. Groups that were deficient for CD36 expression on cells of hematopoietic origin ($CD36^{-/-}$>WT and $CD36^{-/-}$ >$CD36^{-/-}$) had a significantly greater drop in body weight at day 6 post-infection (Figure AI.1B). Compared to WT>WT animals, all of the other transfer groups had a significantly lower percentage drop in body temperature (Figure AI.1B). It was notable that the animals in the $CD36^{-/-}$>$CD36^{-/-}$ group were best able to maintain their body temperature during malaria. Parasitemia was significantly higher at days 5 and 6 post-infection in the group that selectively expressed CD36 on the vascular endothelium ($CD36^{-/-}$>WT) (Figure AI.1B).

The gross appearance of the lungs from mice where CD36 was expressed exclusively on endothelial cells ($CD36^{-/-}$>WT) was markedly red and inflamed compared to the lungs from mice that expressed CD36 on cells of hematopoietic origin but not on vascular endothelial cells (WT>$CD36^{-/-}$) (Figure AI.2A). This observation was in contrast to the lungs derived from the $CD36^{-/-}$>$CD36^{-/-}$ controls, which consistently appeared the least congested and inflamed of the four groups. The outward appearance of the lungs was reflected in the intensity of the cellular responses. $CD36^{-/-}$>WT animals had the most robust cellular infiltrate and the $CD36^{-/-}$>$CD36^{-/-}$ animals had the lowest intensity cellular infiltrate (Figure AI.1D). The recruited cells found in the BAL at day 6 post-infection from all groups were dominated by monocytes with <1% granulocytes (neutrophils, eosinophils, basophils) and lymphocytes (data not shown).

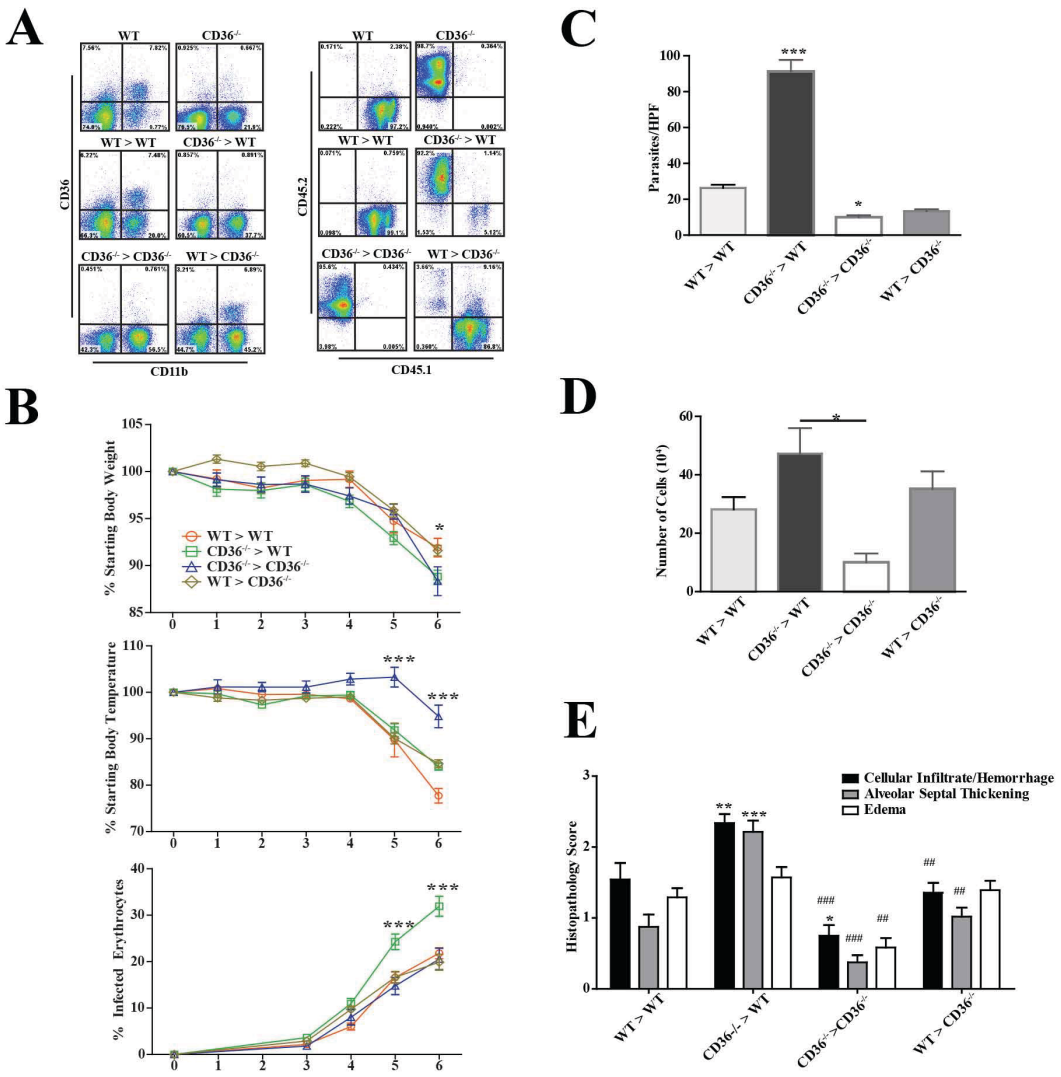

Figure AI.1 Generation of CD36$^{-/-}$ bone marrow chimeras and morbidity and lung pathology following *Plasmodium berghei* infection in chimeric mice.

(A) Representative flow cytometry scatter plots of the peripheral blood cells from WT, CD36$^{-/-}$ and chimeric animals immunostained prior to bone marrow transfer (top row) or 8 weeks after bone marrow transfer (middle and bottom rows). The cells were stained with antibodies for CD36, CD11b, CD45.1 and CD45.2. (B) Changes in body weight (top), temperature (middle) and parasitemia (bottom) of mice after receiving an intraperitoneal injection of 10^6 *Plasmodium berghei* ANKA-infected erythrocytes. Weight and temperature are expressed as the percentage change from the weight or temperature at day 0. Data are presented as the means ± SE (N = 7–21/group). Heterologous transfer experiments were repeated twice while homologous transfers were performed once (C) The number of sequestered infected erythrocytes per high power field (HPF) in the four bone marrow chimera transfer groups. Data are means ± SE. (N = 2 mice per group and 10 HPFs per lung). (D) Number of mononuclear cells isolated in the BAL of *P. berghei*-infected mice at day 6 from each bone marrow chimera transfer group. (E) Histopathological scoring of intra-alveolar inflammatory infiltrates/hemorrhage, alevolar septal thickening, and alveolar edema in the lungs of animals from the four transfer groups at day 6 post-*P. berghei* infection. Data are presented as the means ± SE (N = 24 – 56 slides per group) * $p < 0.05$; ** $p < 0.01$; *** $p < 0.001$.

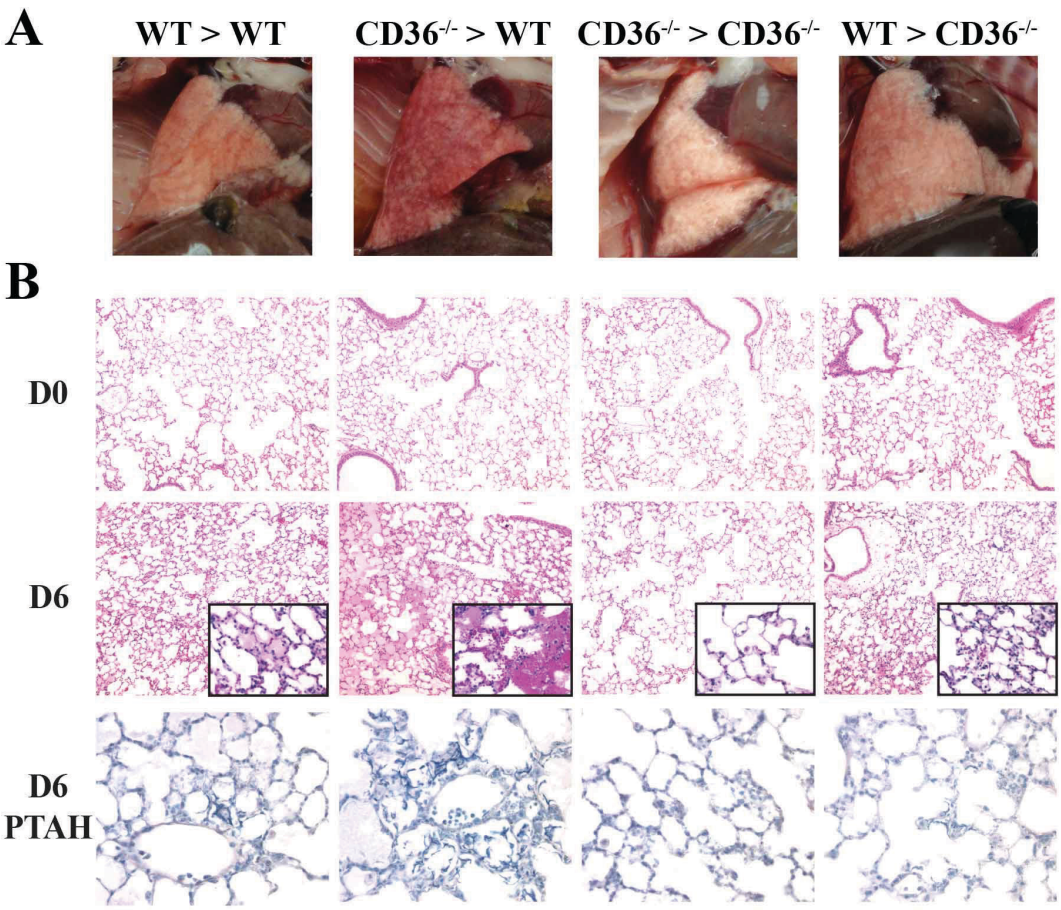

Figure AI.2 Malaria-induced pathology in the lungs of CD36$^{-/-}$ bone marrow chimeras.
(A) Gross appearance of lungs from CD36 bone marrow chimeric mice at day 6 following *P. berghei* ANKA infection. (B) Representative histological sections of lungs from non-infected (D0) or day 6 (D6) post-infection WT>WT, CD36$^{-/-}$>WT, CD36$^{-/-}$>CD36$^{-/-}$ or WT>CD36$^{-/-}$ bone marrow chimeric mice. Sections were stained with hematoxylin and eosin [top and middle rows] (10X magnification) or Mallory's phosphotungstic acid-hematoxylin (PTAH) [bottom row] (60X magnification).

Histological analysis showed that the lungs from the CD36$^{-/-}$>WT animals exhibited markedly more malaria-induced pulmonary pathology than the other three bone marrow transplant groups (Figure AI.2B, center panels). The lungs of CD36$^{-/-}$>WT mice displayed areas of widespread edema, focal regions of erythrocyte and inflammatory cell leakage into the air spaces, and extensive thickening of alveolar walls. The WT>WT and WT>CD36$^{-/-}$ groups showed similar forms of lung injury, but to a lesser extent. In contrast, the lungs from the CD36$^{-/-}$>CD36$^{-/-}$ group exhibited the lowest levels of malaria-induced lung pathology. Additionally, staining for intra-alveolar fibrin, a pathological hallmark of ALI [500], revealed that the highest levels of fibrin production were in lungs from CD36$^{-/-}$>WT mice that expressed CD36 only on the vascular endothelial cells (Figure AI.2B, bottom panels). Focal areas of fibrin deposition were also found in the lungs from the WT>WT and WT>CD36$^{-/-}$ groups, but these areas were absent in the CD36$^{-/-}$>CD36$^{-/-}$ lungs. Employing a blinded scoring system to quantify the histopathological outcomes, the CD36$^{-/-}$>WT lungs scored significantly higher and the CD36$^{-/-}$>CD36$^{-/-}$ lungs scored significantly lower compared to WT>WT for all of the measures of lung damage (Figure AI.1E). Given the importance of CD36 in the ability of macrophages/monocytes to clear malaria-infected RBCs [84, 289, 328], it was hypothesized that the lungs from mice that selectively expressed CD36 only on the vascular endothelial cells (CD36$^{-/-}$>WT) would have the highest levels of lung-associated malaria-infected RBCs. The heightened pathology in the lungs from CD36$^{-/-}$>WT animals was associated with significantly more parasites sequestered in the lungs (Figure AI.1C). Conversely, the lungs from CD36$^{-/-}$>CD36$^{-/-}$ had the lowest number of parasite-positive cells sequestered on the pulmonary vascular endothelium.

REFERENCES

1. Mechnikov I: **On the Present State of the Question of Immunity in Infectious Diseases**. *Nobel Lecture* 1908(December 11 1908).

2. Gordon S: **The macrophage: past, present and future**. *European journal of immunology* 2007, **37 Suppl 1**:S9-17.

3. Hume DA: **The mononuclear phagocyte system**. *Current opinion in immunology* 2006, **18**(1):49-53.

4. van Furth R, Cohn ZA: **The origin and kinetics of mononuclear phagocytes**. *The Journal of experimental medicine* 1968, **128**(3):415-435.

5. Hume DA: **Differentiation and heterogeneity in the mononuclear phagocyte system**. *Mucosal immunology* 2008, **1**(6):432-441.

6. Fogg DK, Sibon C, Miled C, Jung S, Aucouturier P, Littman DR, Cumano A, Geissmann F: **A clonogenic bone marrow progenitor specific for macrophages and dendritic cells**. *Science* 2006, **311**(5757):83-87.

7. McWhorter FY, Wang T, Nguyen P, Chung T, Liu WF: **Modulation of macrophage phenotype by cell shape**. *Proceedings of the National Academy of Sciences of the United States of America* 2013, **110**(43):17253-17258.

8. Davies LC, Jenkins SJ, Allen JE, Taylor PR: **Tissue-resident macrophages**. *Nature immunology* 2013, **14**(10):986-995.

9. Gordon S, Taylor PR: **Monocyte and macrophage heterogeneity**. *Nature reviews Immunology* 2005, **5**(12):953-964.

10. Murray PJ, Wynn TA: **Protective and pathogenic functions of macrophage subsets**. *Nature reviews Immunology* 2011, **11**(11):723-737.

11. Gautier EL, Shay T, Miller J, Greter M, Jakubzick C, Ivanov S, Helft J, Chow A, Elpek KG, Gordonov S *et al*: **Gene-expression profiles and transcriptional regulatory pathways that underlie the identity and diversity of mouse tissue macrophages**. *Nature immunology* 2012, **13**(11):1118-1128.

12. Gonzalez-Juarrero M, Shim TS, Kipnis A, Junqueira-Kipnis AP, Orme IM: **Dynamics of macrophage cell populations during murine pulmonary tuberculosis**. *Journal of immunology* 2003, **171**(6):3128-3135.

13. Reece JJ, Siracusa MC, Scott AL: **Innate immune responses to lung-stage helminth infection induce alternatively activated alveolar macrophages**. *Infection and immunity* 2006, **74**(9):4970-4981.

14. Kirby AC, Coles MC, Kaye PM: **Alveolar macrophages transport pathogens to lung draining lymph nodes**. *Journal of immunology* 2009, **183**(3):1983-1989.

15. Holt PG, Oliver J, Bilyk N, McMenamin C, McMenamin PG, Kraal G, Thepen T: **Downregulation of the antigen presenting cell function(s) of pulmonary dendritic cells in vivo by resident alveolar macrophages**. *The Journal of experimental medicine* 1993, **177**(2):397-407.

16. Fels AO, Cohn ZA: **The alveolar macrophage**. *Journal of applied physiology* 1986, **60**(2):353-369.

17. Ganz T: **Macrophages and systemic iron homeostasis**. *Journal of innate immunity* 2012, **4**(5-6):446-453.

18. Merad M, Ginhoux F, Collin M: **Origin, homeostasis and function of Langerhans cells and other langerin-expressing dendritic cells**. *Nature reviews Immunology* 2008, **8**(12):935-947.

19. Prinz M, Priller J, Sisodia SS, Ransohoff RM: **Heterogeneity of CNS myeloid cells and their roles in neurodegeneration**. *Nature neuroscience* 2011, **14**(10):1227-1235.

20. Chang MK, Raggatt LJ, Alexander KA, Kuliwaba JS, Fazzalari NL, Schroder K, Maylin ER, Ripoll VM, Hume DA, Pettit AR: **Osteal tissue macrophages are intercalated throughout human and mouse bone lining tissues and regulate osteoblast function in vitro and in vivo**. *Journal of immunology* 2008, **181**(2):1232-1244.

21. Pettit AR, Chang MK, Hume DA, Raggatt LJ: **Osteal macrophages: a new twist on coupling during bone dynamics**. *Bone* 2008, **43**(6):976-982.

22. Kohyama M, Ise W, Edelson BT, Wilker PR, Hildner K, Mejia C, Frazier WA, Murphy TL, Murphy KM: **Role for Spi-C in the development of red pulp macrophages and splenic iron homeostasis**. *Nature* 2009, **457**(7227):318-321.

23. McGaha TL, Chen Y, Ravishankar B, van Rooijen N, Karlsson MC: **Marginal zone macrophages suppress innate and adaptive immunity to apoptotic cells in the spleen**. *Blood* 2011, **117**(20):5403-5412.

24. Aichele P, Zinke J, Grode L, Schwendener RA, Kaufmann SH, Seiler P: **Macrophages of the splenic marginal zone are essential for trapping of blood-borne particulate antigen but dispensable for induction of specific T cell responses**. *Journal of immunology* 2003, **171**(3):1148-1155.

25. Junt T, Moseman EA, Iannacone M, Massberg S, Lang PA, Boes M, Fink K, Henrickson SE, Shayakhmetov DM, Di Paolo NC *et al*: **Subcapsular sinus macrophages in lymph nodes clear lymph-borne viruses and present them to antiviral B cells**. *Nature* 2007, **450**(7166):110-114.

26. Pilette C, Ouadrhiri Y, Godding V, Vaerman JP, Sibille Y: **Lung mucosal immunity: immunoglobulin-A revisited**. *The European respiratory journal* 2001, **18**(3):571-588.

27. Macdonald TT, Monteleone G: **Immunity, inflammation, and allergy in the gut**. *Science* 2005, **307**(5717):1920-1925.

28. Murphy K, Travers P, Walport M, Janeway C: **Janeway's immunobiology**, 8th edn. New York: Garland Science; 2012.

29. Holt PG, Strickland DH, Wikstrom ME, Jahnsen FL: **Regulation of immunological homeostasis in the respiratory tract**. *Nature reviews Immunology* 2008, **8**(2):142-152.

30. Florens M, Sapoval B, Filoche M: **An anatomical and functional model of the human tracheobronchial tree**. *Journal of applied physiology* 2011, **110**(3):756-763.

31. Irvin CG, Bates JH: **Measuring the lung function in the mouse: the challenge of size**. *Respiratory research* 2003, **4**:4.

32. Crapo JD, Barry BE, Gehr P, Bachofen M, Weibel ER: **Cell number and cell characteristics of the normal human lung**. *The American review of respiratory disease* 1982, **126**(2):332-337.

33. Fehrenbach H: **Alveolar epithelial type II cell: defender of the alveolus revisited**. *Respiratory research* 2001, **2**(1):33-46.

34. Wright JR: **Immunoregulatory functions of surfactant proteins**. *Nature reviews Immunology* 2005, **5**(1):58-68.

35. Reynolds HY: **Bronchoalveolar lavage**. *The American review of respiratory disease* 1987, **135**(1):250-263.

36. Gordon SB, Read RC: **Macrophage defences against respiratory tract infections**. *Br Med Bull* 2002, **61**:45-61.

37. Guth AM, Janssen WJ, Bosio CM, Crouch EC, Henson PM, Dow SW: **Lung environment determines unique phenotype of alveolar macrophages**. *American journal of physiology Lung cellular and molecular physiology* 2009, **296**(6):L936-946.

38. MacLean JA, Xia W, Pinto CE, Zhao L, Liu HW, Kradin RL: **Sequestration of inhaled particulate antigens by lung phagocytes. A mechanism for the effective inhibition of pulmonary cell-mediated immunity**. *The American journal of pathology* 1996, **148**(2):657-666.

39. Vlahos R, Bozinovski S, Jones JE, Powell J, Gras J, Lilja A, Hansen MJ, Gualano RC, Irving L, Anderson GP: **Differential protease, innate immunity, and NF-kappaB induction profiles during lung inflammation induced by subchronic cigarette smoke exposure in mice**. *American journal of physiology Lung cellular and molecular physiology* 2006, **290**(5):L931-945.

40. Shaykhiev R, Krause A, Salit J, Strulovici-Barel Y, Harvey BG, O'Connor TP, Crystal RG: **Smoking-dependent reprogramming of alveolar macrophage polarization: implication for pathogenesis of chronic obstructive pulmonary disease**. *Journal of immunology* 2009, **183**(4):2867-2883.

41. Schoenberger CI, Hunninghake GW, Kawanami O, Ferrans VJ, Crystal RG: **Role of alveolar macrophages in asbestosis: modulation of neutrophil migration to the lung after acute asbestos exposure**. *Thorax* 1982, **37**(11):803-809.

42. Poole JA, Wyatt TA, Kielian T, Oldenburg P, Gleason AM, Bauer A, Golden G, West WW, Sisson JH, Romberger DJ: **Toll-like receptor 2 regulates organic dust-induced airway inflammation**. *American journal of respiratory cell and molecular biology* 2011, **45**(4):711-719.

43. Kim HM, Lee YW, Lee KJ, Kim HS, Cho SW, van Rooijen N, Guan Y, Seo SH: **Alveolar macrophages are indispensable for controlling influenza viruses in lungs of pigs**. *Journal of virology* 2008, **82**(9):4265-4274.

44. Knapp S, Leemans JC, Florquin S, Branger J, Maris NA, Pater J, van Rooijen N, van der Poll T: **Alveolar macrophages have a protective antiinflammatory role during murine pneumococcal pneumonia**. *American journal of respiratory and critical care medicine* 2003, **167**(2):171-179.

45. Philippe B, Ibrahim-Granet O, Prevost MC, Gougerot-Pocidalo MA, Sanchez Perez M, Van der Meeren A, Latge JP: **Killing of *Aspergillus fumigatus* by alveolar macrophages is mediated by reactive oxidant intermediates**. *Infection and immunity* 2003, **71**(6):3034-3042.

46. Siracusa MC, Reece JJ, Urban JF, Jr., Scott AL: **Dynamics of lung macrophage activation in response to helminth infection**. *Journal of leukocyte biology* 2008, **84**(6):1422-1433.

47. Snelgrove RJ, Goulding J, Didierlaurent AM, Lyonga D, Vekaria S, Edwards L, Gwyer E, Sedgwick JD, Barclay AN, Hussell T: **A critical function for CD200 in lung immune homeostasis and the severity of influenza infection**. *Nature immunology* 2008, **9**(9):1074-1083.

48. Wilson MS, Wynn TA: **Pulmonary fibrosis: pathogenesis, etiology and regulation**. *Mucosal immunology* 2009, **2**(2):103-121.

49. Janssen WJ, Barthel L, Muldrow A, Oberley-Deegan RE, Kearns MT, Jakubzick C, Henson PM: **Fas determines differential fates of resident and recruited macrophages during resolution of acute lung injury**. *American journal of respiratory and critical care medicine* 2011, **184**(5):547-560.

50. Hunninghake GW: **Release of interleukin-1 by alveolar macrophages of patients with active pulmonary sarcoidosis**. *The American review of respiratory disease* 1984, **129**(4):569-572.

51. Wynn TA: **Cellular and molecular mechanisms of fibrosis**. *J Pathol* 2008, **214**(2):199-210.

52. Careau E, Bissonnette EY: **Adoptive transfer of alveolar macrophages abrogates bronchial hyperresponsiveness**. *American journal of respiratory cell and molecular biology* 2004, **31**(1):22-27.

53. Song C, Luo L, Lei Z, Li B, Liang Z, Liu G, Li D, Zhang G, Huang B, Feng ZH: **IL-17-producing alveolar macrophages mediate allergic lung inflammation related to asthma**. *Journal of immunology* 2008, **181**(9):6117-6124.

54. Lauzon-Joset JF, Marsolais D, Langlois A, Bissonnette EY: **Dysregulation of alveolar macrophages unleashes dendritic cell-mediated mechanisms of allergic airway inflammation**. *Mucosal immunology* 2014, **7**(1):155-164.

55. Barnes PJ: **Alveolar macrophages as orchestrators of COPD**. *Copd* 2004, **1**(1):59-70.

56. Hussell T, Bell TJ: **Alveolar macrophages: plasticity in a tissue-specific context**. *Nature reviews Immunology* 2014.

57. Zaynagetdinov R, Sherrill TP, Kendall PL, Segal BH, Weller KP, Tighe RM, Blackwell TS: **Identification of myeloid cell subsets in murine lungs using flow cytometry**. *American journal of respiratory cell and molecular biology* 2013, **49**(2):180-189.

58. Misharin AV, Morales-Nebreda L, Mutlu GM, Budinger GR, Perlman H: **Flow cytometric analysis of macrophages and dendritic cell subsets in the mouse lung**. *American journal of respiratory cell and molecular biology* 2013, **49**(4):503-510.

59. Geissmann F, Gordon S, Hume DA, Mowat AM, Randolph GJ: **Unravelling mononuclear phagocyte heterogeneity**. *Nature reviews Immunology* 2010, **10**(6):453-460.

60. Stevens WW, Kim TS, Pujanauski LM, Hao X, Braciale TJ: **Detection and quantitation of eosinophils in the murine respiratory tract by flow cytometry**. *Journal of immunological methods* 2007, **327**(1-2):63-74.

61. Bochner BS: **Siglec-8 on human eosinophils and mast cells, and Siglec-F on murine eosinophils, are functionally related inhibitory receptors**. *Clinical and experimental allergy : journal of the British Society for Allergy and Clinical Immunology* 2009, **39**(3):317-324.

62. Jakubzick C, Tacke F, Llodra J, van Rooijen N, Randolph GJ: **Modulation of dendritic cell trafficking to and from the airways**. *Journal of immunology* 2006, **176**(6):3578-3584.

63. Kirby AC, Raynes JG, Kaye PM: **CD11b regulates recruitment of alveolar macrophages but not pulmonary dendritic cells after pneumococcal challenge**. *The Journal of infectious diseases* 2006, **193**(2):205-213.

64. Bianchi ME: **DAMPs, PAMPs and alarmins: all we need to know about danger**. *Journal of leukocyte biology* 2007, **81**(1):1-5.

65. Janeway CA, Jr.: **Approaching the asymptote? Evolution and revolution in immunology**. *Cold Spring Harbor symposia on quantitative biology* 1989, **54 Pt 1**:1-13.

66. Matzinger P: **Tolerance, danger, and the extended family**. *Annual review of immunology* 1994, **12**:991-1045.

67. Akira S, Takeda K: **Toll-like receptor signalling**. *Nature reviews Immunology* 2004, **4**(7):499-511.

68. Ichinohe T, Lee HK, Ogura Y, Flavell R, Iwasaki A: **Inflammasome recognition of influenza virus is essential for adaptive immune responses**. *The Journal of experimental medicine* 2009, **206**(1):79-87.

69. Wu J, Yan Z, Schwartz DE, Yu J, Malik AB, Hu G: **Activation of NLRP3 inflammasome in alveolar macrophages contributes to mechanical stretch-induced lung inflammation and injury**. *Journal of immunology* 2013, **190**(7):3590-3599.

70. Kumagai Y, Takeuchi O, Kato H, Kumar H, Matsui K, Morii E, Aozasa K, Kawai T, Akira S: **Alveolar macrophages are the primary interferon-alpha producer in pulmonary infection with RNA viruses**. *Immunity* 2007, **27**(2):240-252.

71. Serezani CH, Kane S, Collins L, Morato-Marques M, Osterholzer JJ, Peters-Golden M: **Macrophage dectin-1 expression is controlled by leukotriene B4 via a GM-CSF/PU.1 axis**. *Journal of immunology* 2012, **189**(2):906-915.

72. Arredouani M, Yang Z, Ning Y, Qin G, Soininen R, Tryggvason K, Kobzik L: **The scavenger receptor MARCO is required for lung defense against pneumococcal pneumonia and inhaled particles**. *The Journal of experimental medicine* 2004, **200**(2):267-272.

73. Kawai T, Akira S: **Toll-like receptors and their crosstalk with other innate receptors in infection and immunity**. *Immunity* 2011, **34**(5):637-650.

74. Rohmann K, Tschernig T, Pabst R, Goldmann T, Dromann D: **Innate immunity in the human lung: pathogen recognition and lung disease**. *Cell and tissue research* 2011, **343**(1):167-174.

75. Rogers DF: **Airway goblet cells: responsive and adaptable front-line defenders**. *The European respiratory journal* 1994, **7**(9):1690-1706.

76. Gordon SB, Read RC: **Macrophage defences against respiratory tract infections**. *Br Med Bull* 2002, **61**:45-61.

77. Underhill DM, Goodridge HS: **Information processing during phagocytosis**. *Nature reviews Immunology* 2012, **12**(7):492-502.

78. van Lookeren Campagne M, Wiesmann C, Brown EJ: **Macrophage complement receptors and pathogen clearance**. *Cellular microbiology* 2007, **9**(9):2095-2102.

79. Nimmerjahn F, Ravetch JV: **Fcgamma receptors as regulators of immune responses**. *Nature reviews Immunology* 2008, **8**(1):34-47.

80. Gauldie J, Richards C, Lamontagne L: **Fc receptors for IgA and other immunoglobulins on resident and activated alveolar macrophages**. *Molecular immunology* 1983, **20**(9):1029-1037.

81. Geijtenbeek TB, Gringhuis SI: **Signalling through C-type lectin receptors: shaping immune responses**. *Nature reviews Immunology* 2009, **9**(7):465-479.

82. Zhang J, Tachado SD, Patel N, Zhu J, Imrich A, Manfruelli P, Cushion M, Kinane TB, Koziel H: **Negative regulatory role of mannose receptors on human alveolar macrophage proinflammatory cytokine release in vitro**. *Journal of leukocyte biology* 2005, **78**(3):665-674.

83. Ghosh S, Gregory D, Smith A, Kobzik L: **MARCO regulates early inflammatory responses against influenza: a useful macrophage function with adverse outcome**. *American journal of respiratory cell and molecular biology* 2011, **45**(5):1036-1044.

84. Erdman LK, Cosio G, Helmers AJ, Gowda DC, Grinstein S, Kain KC: **CD36 and TLR interactions in inflammation and phagocytosis: implications for malaria**. *Journal of immunology* 2009, **183**(10):6452-6459.

85. Silverstein RL, Febbraio M: **CD36, a scavenger receptor involved in immunity, metabolism, angiogenesis, and behavior**. *Science signaling* 2009, **2**(72):re3.

86. Crocker PR, Paulson JC, Varki A: **Siglecs and their roles in the immune system**. *Nature reviews Immunology* 2007, **7**(4):255-266.

87. Angata T, Hingorani R, Varki NM, Varki A: **Cloning and characterization of a novel mouse Siglec, mSiglec-F: differential evolution of the mouse and human (CD33) Siglec-3-related gene clusters**. *The Journal of biological chemistry* 2001, **276**(48):45128-45136.

88. Tateno H, Crocker PR, Paulson JC: **Mouse Siglec-F and human Siglec-8 are functionally convergent paralogs that are selectively expressed on eosinophils and recognize 6'-sulfo-sialyl Lewis X as a preferred glycan ligand**. *Glycobiology* 2005, **15**(11):1125-1135.

89. Guo JP, Brummet ME, Myers AC, Na HJ, Rowland E, Schnaar RL, Zheng T, Zhu Z, Bochner BS: **Characterization of expression of glycan ligands for Siglec-F in normal mouse lungs**. *American journal of respiratory cell and molecular biology* 2011, **44**(2):238-243.

90. Zhang M, Angata T, Cho JY, Miller M, Broide DH, Varki A: **Defining the in vivo function of Siglec-F, a CD33-related Siglec expressed on mouse eosinophils**. *Blood* 2007, **109**(10):4280-4287.

91. Savill J, Dransfield I, Gregory C, Haslett C: **A blast from the past: clearance of apoptotic cells regulates immune responses**. *Nature reviews Immunology* 2002, **2**(12):965-975.

92. Korns D, Frasch SC, Fernandez-Boyanapalli R, Henson PM, Bratton DL: **Modulation of macrophage efferocytosis in inflammation**. *Frontiers in immunology* 2011, **2**:57.

93. Fadok VA, Voelker DR, Campbell PA, Cohen JJ, Bratton DL, Henson PM: **Exposure of phosphatidylserine on the surface of apoptotic lymphocytes triggers specific recognition and removal by macrophages**. *Journal of immunology* 1992, **148**(7):2207-2216.

94. Kazeros A, Harvey BG, Carolan BJ, Vanni H, Krause A, Crystal RG: **Overexpression of apoptotic cell removal receptor MERTK in alveolar macrophages of cigarette smokers**. *American journal of respiratory cell and molecular biology* 2008, **39**(6):747-757.

95. Scott RS, McMahon EJ, Pop SM, Reap EA, Caricchio R, Cohen PL, Earp HS, Matsushima GK: **Phagocytosis and clearance of apoptotic cells is mediated by MER**. *Nature* 2001, **411**(6834):207-211.

96. Lemke G, Rothlin CV: **Immunobiology of the TAM receptors**. *Nature reviews Immunology* 2008, **8**(5):327-336.

97. Cohen PL, Caricchio R, Abraham V, Camenisch TD, Jennette JC, Roubey RA, Earp HS, Matsushima G, Reap EA: **Delayed apoptotic cell clearance and lupus-like autoimmunity in mice lacking the c-mer membrane tyrosine kinase**. *The Journal of experimental medicine* 2002, **196**(1):135-140.

98. Serezani CH, Chung J, Ballinger MN, Moore BB, Aronoff DM, Peters-Golden M: **Prostaglandin E2 suppresses bacterial killing in alveolar macrophages by inhibiting NADPH oxidase**. *American journal of respiratory cell and molecular biology* 2007, **37**(5):562-570.

99. Stafford JL, Neumann NF, Belosevic M: **Macrophage-mediated innate host defense against protozoan parasites**. *Critical reviews in microbiology* 2002, **28**(3):187-248.

100. Lambeth JD: **NOX enzymes and the biology of reactive oxygen**. *Nature reviews Immunology* 2004, **4**(3):181-189.

101. DeLeo FR, Allen LA, Apicella M, Nauseef WM: **NADPH oxidase activation and assembly during phagocytosis**. *Journal of immunology* 1999, **163**(12):6732-6740.

102. Segal AW: **The NADPH oxidase and chronic granulomatous disease**. *Molecular medicine today* 1996, **2**(3):129-135.

103. Honey K, Rudensky AY: **Lysosomal cysteine proteases regulate antigen presentation**. *Nature reviews Immunology* 2003, **3**(6):472-482.

104. Guilliams M, Lambrecht BN, Hammad H: **Division of labor between lung dendritic cells and macrophages in the defense against pulmonary infections**. *Mucosal immunology* 2013, **6**(3):464-473.

105. Chelen CJ, Fang Y, Freeman GJ, Secrist H, Marshall JD, Hwang PT, Frankel LR, DeKruyff RH, Umetsu DT: **Human alveolar macrophages present antigen ineffectively due to defective expression of B7 costimulatory cell surface molecules**. *The Journal of clinical investigation* 1995, **95**(3):1415-1421.

106. Balbo P, Silvestri M, Rossi GA, Crimi E, Burastero SE: **Differential role of CD80 and CD86 on alveolar macrophages in the presentation of allergen to T lymphocytes in asthma**. *Clinical and experimental allergy : journal of the British Society for Allergy and Clinical Immunology* 2001, **31**(4):625-636.

107. Xue J, Schmidt SV, Sander J, Draffehn A, Krebs W, Quester I, De Nardo D, Gohel TD, Emde M, Schmidleithner L *et al*: **Transcriptome-based network analysis reveals a spectrum model of human macrophage activation**. *Immunity* 2014, **40**(2):274-288.

108. Murray PJ, Wynn TA: **Obstacles and opportunities for understanding macrophage polarization**. *Journal of leukocyte biology* 2011, **89**(4):557-563.

109. Mackaness GB: **Cellular resistance to infection**. *The Journal of experimental medicine* 1962, **116**:381-406.

110. Nathan CF, Murray HW, Wiebe ME, Rubin BY: **Identification of interferon-gamma as the lymphokine that activates human macrophage oxidative metabolism and antimicrobial activity**. *The Journal of experimental medicine* 1983, **158**(3):670-689.

111. Stein M, Keshav S, Harris N, Gordon S: **Interleukin 4 potently enhances murine macrophage mannose receptor activity: a marker of alternative immunologic macrophage activation**. *The Journal of experimental medicine* 1992, **176**(1):287-292.

112. Mosser DM, Edwards JP: **Exploring the full spectrum of macrophage activation**. *Nature reviews Immunology* 2008, **8**(12):958-969.

113. Gordon S: **Alternative activation of macrophages**. *Nature reviews Immunology* 2003, **3**(1):23-35.

114. Gerber JS, Mosser DM: **Reversing lipopolysaccharide toxicity by ligating the macrophage Fc gamma receptors**. *Journal of immunology* 2001, **166**(11):6861-6868.

115. Mantovani A, Sica A, Sozzani S, Allavena P, Vecchi A, Locati M: **The chemokine system in diverse forms of macrophage activation and polarization**. *Trends in immunology* 2004, **25**(12):677-686.

116. O'Shea JJ, Paul WE: **Mechanisms underlying lineage commitment and plasticity of helper CD4+ T cells**. *Science* 2010, **327**(5969):1098-1102.

117. Krausgruber T, Blazek K, Smallie T, Alzabin S, Lockstone H, Sahgal N, Hussell T, Feldmann M, Udalova IA: **IRF5 promotes inflammatory macrophage polarization and TH1-TH17 responses**. *Nature immunology* 2011, **12**(3):231-238.

118. Weiss M, Blazek K, Byrne AJ, Perocheau DP, Udalova IA: **IRF5 is a specific marker of inflammatory macrophages in vivo**. *Mediators of inflammation* 2013, **2013**:245804.

119. Lawrence T, Natoli G: **Transcriptional regulation of macrophage polarization: enabling diversity with identity**. *Nature reviews Immunology* 2011, **11**(11):750-761.

120. Porta C, Rimoldi M, Raes G, Brys L, Ghezzi P, Di Liberto D, Dieli F, Ghisletti S, Natoli G, De Baetselier P *et al*: **Tolerance and M2 (alternative) macrophage polarization are related processes orchestrated by p50 nuclear factor kappaB**. *Proceedings of the National Academy of Sciences of the United States of America* 2009, **106**(35):14978-14983.

121. Satoh T, Takeuchi O, Vandenbon A, Yasuda K, Tanaka Y, Kumagai Y, Miyake T, Matsushita K, Okazaki T, Saitoh T *et al*: **The Jmjd3-Irf4 axis regulates M2 macrophage polarization and host responses against helminth infection**. *Nature immunology* 2010, **11**(10):936-944.

122. Reece JJ, Siracusa MC, Southard TL, Brayton CF, Urban JF, Jr., Scott AL: **Hookworm-induced persistent changes to the immunological environment of the lung**. *Infection and immunity* 2008, **76**(8):3511-3524.

123. Gordon S, Martinez FO: **Alternative Activation of Macrophages: Mechanism and Functions**. *Immunity* 2010, **32**(5):593-604.

124. Mantovani A, Biswas SK, Galdiero MR, Sica A, Locati M: **Macrophage plasticity and polarization in tissue repair and remodelling**. *J Pathol* 2013, **229**(2):176-185.

125. Reddy RC: **Immunomodulatory role of PPAR-gamma in alveolar macrophages**. *Journal of investigative medicine : the official publication of the American Federation for Clinical Research* 2008, **56**(2):522-527.

126. Ricote M, Li AC, Willson TM, Kelly CJ, Glass CK: **The peroxisome proliferator-activated receptor-gamma is a negative regulator of macrophage activation**. *Nature* 1998, **391**(6662):79-82.

127. Shibata Y, Berclaz PY, Chroneos ZC, Yoshida M, Whitsett JA, Trapnell BC: **GM-CSF regulates alveolar macrophage differentiation and innate immunity in the lung through PU.1**. *Immunity* 2001, **15**(4):557-567.

128. Berclaz PY, Carey B, Fillipi MD, Wernke-Dollries K, Geraci N, Cush S, Richardson T, Kitzmiller J, O'Connor M, Hermoyian C *et al*: **GM-CSF regulates a PU.1-dependent transcriptional program determining the pulmonary response to LPS**. *American journal of respiratory cell and molecular biology* 2007, **36**(1):114-121.

129. Sato-Nishiwaki M, Aida Y, Abe S, Shibata Y, Kimura T, Yamauchi K, Kishi H, Igarashi A, Inoue S, Sato M *et al*: **Reduced number and morphofunctional change of alveolar macrophages in MafB gene-targeted mice**. *PloS one* 2013, **8**(9):e73963.

130. Modolell M, Corraliza IM, Link F, Soler G, Eichmann K: **Reciprocal regulation of the nitric oxide synthase/arginase balance in mouse bone marrow-derived macrophages by TH1 and TH2 cytokines**. *European journal of immunology* 1995, **25**(4):1101-1104.

131. Hesse M, Modolell M, La Flamme AC, Schito M, Fuentes JM, Cheever AW, Pearce EJ, Wynn TA: **Differential regulation of nitric oxide synthase-2 and arginase-1 by type 1/type 2 cytokines in vivo: granulomatous pathology is shaped by the pattern of L-arginine metabolism**. *Journal of immunology* 2001, **167**(11):6533-6544.

132. Bronte V, Zanovello P: **Regulation of immune responses by L-arginine metabolism**. *Nature reviews Immunology* 2005, **5**(8):641-654.

133. Martinez FO, Gordon S, Locati M, Mantovani A: **Transcriptional profiling of the human monocyte-to-macrophage differentiation and polarization: new molecules and patterns of gene expression**. *Journal of immunology* 2006, **177**(10):7303-7311.

134. Biswas SK, Mantovani A: **Orchestration of metabolism by macrophages**. *Cell metabolism* 2012, **15**(4):432-437.

135. Brown GP, Monick MM, Hunninghake GW: **Human alveolar macrophage arachidonic acid metabolism**. *The American journal of physiology* 1988, **254**(6 Pt 1):C809-815.

136. Betz C, Hall MN: **Where is mTOR and what is it doing there?** *The Journal of cell biology* 2013, **203**(4):563-574.

137. Byles V, Covarrubias AJ, Ben-Sahra I, Lamming DW, Sabatini DM, Manning BD, Horng T: **The TSC-mTOR pathway regulates macrophage polarization**. *Nature communications* 2013, **4**:2834.

138. Robert H, Samuel C, Yee C-L, Jonathan P, Maureen RH: **MTOR Regulates The Differentiation Of Classically And Alternatively Activated Macrophages**. In: *C92 CONTROL OF MACROPHAGE POLARIZATION AND EFFECTOR FUNCTIONS.* American Thoracic Society: A5061-A5061.

139. Reidy MF, Wright JR: **Surfactant protein A enhances apoptotic cell uptake and TGF-beta1 release by inflammatory alveolar macrophages**. *American journal of physiology Lung cellular and molecular physiology* 2003, **285**(4):L854-861.

140. Senft AP, Korfhagen TR, Whitsett JA, LeVine AM: **Surfactant protein D regulates the cell surface expression of alveolar macrophage beta(2)-integrins**. *American journal of physiology Lung cellular and molecular physiology* 2007, **292**(2):L469-475.

141. Wang J, Snider DP, Hewlett BR, Lukacs NW, Gauldie J, Liang H, Xing Z: **Transgenic expression of granulocyte-macrophage colony-stimulating factor induces the differentiation and activation of a novel dendritic cell population in the lung**. *Blood* 2000, **95**(7):2337-2345.

142. Chen BD, Mueller M, Chou TH: **Role of granulocyte/macrophage colony-stimulating factor in the regulation of murine alveolar macrophage proliferation and differentiation**. *Journal of immunology* 1988, **141**(1):139-144.

143. von Garnier C, Filgueira L, Wikstrom M, Smith M, Thomas JA, Strickland DH, Holt PG, Stumbles PA: **Anatomical location determines the distribution and function of dendritic cells and other APCs in the respiratory tract**. *Journal of immunology* 2005, **175**(3):1609-1618.

144. Paine R, 3rd, Morris SB, Jin H, Wilcoxen SE, Phare SM, Moore BB, Coffey MJ, Toews GB: **Impaired functional activity of alveolar macrophages from GM-CSF-deficient mice**.

American journal of physiology Lung cellular and molecular physiology 2001, **281**(5):L1210-1218.

145. Guilliams M, De Kleer I, Henri S, Post S, Vanhoutte L, De Prijck S, Deswarte K, Malissen B, Hammad H, Lambrecht BN: **Alveolar macrophages develop from fetal monocytes that differentiate into long-lived cells in the first week of life via GM-CSF**. *The Journal of experimental medicine* 2013, **210**(10):1977-1992.

146. Huffman JA, Hull WM, Dranoff G, Mulligan RC, Whitsett JA: **Pulmonary epithelial cell expression of GM-CSF corrects the alveolar proteinosis in GM-CSF-deficient mice**. *The Journal of clinical investigation* 1996, **97**(3):649-655.

147. Fernandez S, Jose P, Avdiushko MG, Kaplan AM, Cohen DA: **Inhibition of IL-10 receptor function in alveolar macrophages by Toll-like receptor agonists**. *Journal of immunology* 2004, **172**(4):2613-2620.

148. Oswald IP, Wynn TA, Sher A, James SL: **Interleukin 10 inhibits macrophage microbicidal activity by blocking the endogenous production of tumor necrosis factor alpha required as a costimulatory factor for interferon gamma-induced activation**. *Proceedings of the National Academy of Sciences of the United States of America* 1992, **89**(18):8676-8680.

149. Shull MM, Ormsby I, Kier AB, Pawlowski S, Diebold RJ, Yin M, Allen R, Sidman C, Proetzel G, Calvin D *et al*: **Targeted disruption of the mouse transforming growth factor-beta 1 gene results in multifocal inflammatory disease**. *Nature* 1992, **359**(6397):693-699.

150. Pittet JF, Griffiths MJ, Geiser T, Kaminski N, Dalton SL, Huang X, Brown LA, Gotwals PJ, Koteliansky VE, Matthay MA *et al*: **TGF-beta is a critical mediator of acute lung injury**. *The Journal of clinical investigation* 2001, **107**(12):1537-1544.

151. Bartram U, Speer CP: **The role of transforming growth factor beta in lung development and disease**. *Chest* 2004, **125**(2):754-765.

152. Munger JS, Huang X, Kawakatsu H, Griffiths MJ, Dalton SL, Wu J, Pittet JF, Kaminski N, Garat C, Matthay MA *et al*: **The integrin alpha v beta 6 binds and activates latent TGF beta 1: a mechanism for regulating pulmonary inflammation and fibrosis**. *Cell* 1999, **96**(3):319-328.

153. Morris DG, Huang X, Kaminski N, Wang Y, Shapiro SD, Dolganov G, Glick A, Sheppard D: **Loss of integrin alpha(v)beta6-mediated TGF-beta activation causes Mmp12-dependent emphysema**. *Nature* 2003, **422**(6928):169-173.

154. Takabayshi K, Corr M, Hayashi T, Redecke V, Beck L, Guiney D, Sheppard D, Raz E: **Induction of a homeostatic circuit in lung tissue by microbial compounds**. *Immunity* 2006, **24**(4):475-487.

155. Kurowska-Stolarska M, Stolarski B, Kewin P, Murphy G, Corrigan CJ, Ying S, Pitman N, Mirchandani A, Rana B, van Rooijen N *et al*: **IL-33 amplifies the polarization of alternatively activated macrophages that contribute to airway inflammation**. *Journal of immunology* 2009, **183**(10):6469-6477.

156. Chang YJ, Kim HY, Albacker LA, Baumgarth N, McKenzie AN, Smith DE, Dekruyff RH, Umetsu DT: **Innate lymphoid cells mediate influenza-induced airway hyper-reactivity independently of adaptive immunity**. *Nature immunology* 2011, **12**(7):631-638.

157. Yang Z, Grinchuk V, Urban JF, Jr., Bohl J, Sun R, Notari L, Yan S, Ramalingam T, Keegan AD, Wynn TA *et al*: **Macrophages as IL-25/IL-33-responsive cells play an important role in the induction of type 2 immunity**. *PloS one* 2013, **8**(3):e59441.

158. Liew FY, Pitman NI, McInnes IB: **Disease-associated functions of IL-33: the new kid in the IL-1 family**. *Nature reviews Immunology* 2010, **10**(2):103-110.

159. Lefrancais E, Roga S, Gautier V, Gonzalez-de-Peredo A, Monsarrat B, Girard JP, Cayrol C: **IL-33 is processed into mature bioactive forms by neutrophil elastase and cathepsin G**. *Proceedings of the National Academy of Sciences of the United States of America* 2012, **109**(5):1673-1678.

160. Hatherley D, Barclay AN: **The CD200 and CD200 receptor cell surface proteins interact through their N-terminal immunoglobulin-like domains**. *European journal of immunology* 2004, **34**(6):1688-1694.

161. Hoek RM, Ruuls SR, Murphy CA, Wright GJ, Goddard R, Zurawski SM, Blom B, Homola ME, Streit WJ, Brown MH *et al*: **Down-regulation of the macrophage lineage through interaction with OX2 (CD200)**. *Science* 2000, **290**(5497):1768-1771.

162. Wright GJ, Cherwinski H, Foster-Cuevas M, Brooke G, Puklavec MJ, Bigler M, Song Y, Jenmalm M, Gorman D, McClanahan T *et al*: **Characterization of the CD200 receptor family in mice and humans and their interactions with CD200**. *Journal of immunology* 2003, **171**(6):3034-3046.

163. Holt PG, Strickland DH: **The CD200-CD200R axis in local control of lung inflammation**. *Nature immunology* 2008, **9**(9):1011-1013.

164. Jenmalm MC, Cherwinski H, Bowman EP, Phillips JH, Sedgwick JD: **Regulation of myeloid cell function through the CD200 receptor**. *Journal of immunology* 2006, **176**(1):191-199.

165. Gorczynski RM: **CD200:CD200R-Mediated Regulation of Immunity**. *ISRN Immunology* 2012, **2012**:18.

166. Zhang S, Cherwinski H, Sedgwick JD, Phillips JH: **Molecular mechanisms of CD200 inhibition of mast cell activation**. *Journal of immunology* 2004, **173**(11):6786-6793.

167. Westphalen K, Gusarova GA, Islam MN, Subramanian M, Cohen TS, Prince AS, Bhattacharya J: **Sessile alveolar macrophages communicate with alveolar epithelium to modulate immunity**. *Nature* 2014, **506**(7489):503-506.

168. Bilyk N, Holt PG: **Cytokine modulation of the immunosuppressive phenotype of pulmonary alveolar macrophage populations**. *Immunology* 1995, **86**(2):231-237.

169. Bingisser RM, Tilbrook PA, Holt PG, Kees UR: **Macrophage-derived nitric oxide regulates T cell activation via reversible disruption of the Jak3/STAT5 signaling pathway**. *Journal of immunology* 1998, **160**(12):5729-5734.

170. Medeiros AI, Serezani CH, Lee SP, Peters-Golden M: **Efferocytosis impairs pulmonary macrophage and lung antibacterial function via PGE2/EP2 signaling**. *The Journal of experimental medicine* 2009, **206**(1):61-68.

171. Blumenthal RL, Campbell DE, Hwang P, DeKruyff RH, Frankel LR, Umetsu DT: **Human alveolar macrophages induce functional inactivation in antigen-specific CD4 T cells**. *The Journal of allergy and clinical immunology* 2001, **107**(2):258-264.

172. Fife BT, Pauken KE, Eagar TN, Obu T, Wu J, Tang Q, Azuma M, Krummel MF, Bluestone JA: **Interactions between PD-1 and PD-L1 promote tolerance by blocking the TCR-induced stop signal**. *Nature immunology* 2009, **10**(11):1185-1192.

173. Gollwitzer ES, Saglani S, Trompette A, Yadava K, Sherburn R, McCoy KD, Nicod LP, Lloyd CM, Marsland BJ: **Lung microbiota promotes tolerance to allergens in neonates via PD-L1**. *Nature medicine* 2014.

174. Topalian SL, Drake CG, Pardoll DM: **Targeting the PD-1/B7-H1(PD-L1) pathway to activate anti-tumor immunity**. *Current opinion in immunology* 2012, **24**(2):207-212.

175. Loke P, Allison JP: **PD-L1 and PD-L2 are differentially regulated by Th1 and Th2 cells**. *Proceedings of the National Academy of Sciences of the United States of America* 2003, **100**(9):5336-5341.

176. Huber S, Hoffmann R, Muskens F, Voehringer D: **Alternatively activated macrophages inhibit T-cell proliferation by Stat6-dependent expression of PD-L2**. *Blood* 2010, **116**(17):3311-3320.

177. Noman MZ, Desantis G, Janji B, Hasmim M, Karray S, Dessen P, Bronte V, Chouaib S: **PD-L1 is a novel direct target of HIF-1alpha, and its blockade under hypoxia enhanced MDSC-mediated T cell activation**. *The Journal of experimental medicine* 2014.

178. Nizet V, Johnson RS: **Interdependence of hypoxic and innate immune responses**. *Nature reviews Immunology* 2009, **9**(9):609-617.

179. Stumbles PA, Upham JW, Holt PG: **Airway dendritic cells: co-ordinators of immunological homeostasis and immunity in the respiratory tract**. *APMIS : acta pathologica, microbiologica, et immunologica Scandinavica* 2003, **111**(7-8):741-755.

180. Thepen T, Van Rooijen N, Kraal G: **Alveolar macrophage elimination in vivo is associated with an increase in pulmonary immune response in mice**. *The Journal of experimental medicine* 1989, **170**(2):499-509.

181. Jang S, Uzelac A, Salgame P: **Distinct chemokine and cytokine gene expression pattern of murine dendritic cells and macrophages in response to *Mycobacterium tuberculosis* infection**. *Journal of leukocyte biology* 2008, **84**(5):1264-1270.

182. Winter C, Taut K, Srivastava M, Langer F, Mack M, Briles DE, Paton JC, Maus R, Welte T, Gunn MD *et al*: **Lung-specific overexpression of CC chemokine ligand (CCL) 2 enhances the host defense to *Streptococcus pneumoniae* infection in mice: role of the CCL2-CCR2 axis**. *Journal of immunology* 2007, **178**(9):5828-5838.

183. Hall JD, Kurtz SL, Rigel NW, Gunn BM, Taft-Benz S, Morrison JP, Fong AM, Patel DD, Braunstein M, Kawula TH: **The impact of chemokine receptor CX3CR1 deficiency during respiratory infections with *Mycobacterium tuberculosis* or *Francisella tularensis***. *Clinical and experimental immunology* 2009, **156**(2):278-284.

184. Skold M, Behar SM: **Tuberculosis triggers a tissue-dependent program of differentiation and acquisition of effector functions by circulating monocytes**. *Journal of immunology* 2008, **181**(9):6349-6360.

185. Lin KL, Suzuki Y, Nakano H, Ramsburg E, Gunn MD: **CCR2+ monocyte-derived dendritic cells and exudate macrophages produce influenza-induced pulmonary immune pathology and mortality**. *Journal of immunology* 2008, **180**(4):2562-2572.

186. Landsman L, Varol C, Jung S: **Distinct differentiation potential of blood monocyte subsets in the lung**. *Journal of immunology* 2007, **178**(4):2000-2007.

187. Geissmann F, Jung S, Littman DR: **Blood monocytes consist of two principal subsets with distinct migratory properties**. *Immunity* 2003, **19**(1):71-82.

188. Maus U, von Grote K, Kuziel WA, Mack M, Miller EJ, Cihak J, Stangassinger M, Maus R, Schlondorff D, Seeger W *et al*: **The role of CC chemokine receptor 2 in alveolar monocyte and neutrophil immigration in intact mice**. *American journal of respiratory and critical care medicine* 2002, **166**(3):268-273.

189. Tsou CL, Peters W, Si Y, Slaymaker S, Aslanian AM, Weisberg SP, Mack M, Charo IF: **Critical roles for CCR2 and MCP-3 in monocyte mobilization from bone marrow and recruitment to inflammatory sites**. *The Journal of clinical investigation* 2007, **117**(4):902-909.

190. Gunn MD, Nelken NA, Liao X, Williams LT: **Monocyte chemoattractant protein-1 is sufficient for the chemotaxis of monocytes and lymphocytes in transgenic mice but requires an additional stimulus for inflammatory activation**. *Journal of immunology* 1997, **158**(1):376-383.

191. Shi C, Pamer EG: **Monocyte recruitment during infection and inflammation**. *Nature reviews Immunology* 2011, **11**(11):762-774.

192. Liu K, Waskow C, Liu X, Yao K, Hoh J, Nussenzweig M: **Origin of dendritic cells in peripheral lymphoid organs of mice**. *Nature immunology* 2007, **8**(6):578-583.

193. Varol C, Landsman L, Fogg DK, Greenshtein L, Gildor B, Margalit R, Kalchenko V, Geissmann F, Jung S: **Monocytes give rise to mucosal, but not splenic, conventional dendritic cells**. *The Journal of experimental medicine* 2007, **204**(1):171-180.

194. Basu S, Hodgson G, Katz M, Dunn AR: **Evaluation of role of G-CSF in the production, survival, and release of neutrophils from bone marrow into circulation**. *Blood* 2002, **100**(3):854-861.

195. Serbina NV, Pamer EG: **Monocyte emigration from bone marrow during bacterial infection requires signals mediated by chemokine receptor CCR2**. *Nature immunology* 2006, **7**(3):311-317.

196. Yona S, Kim KW, Wolf Y, Mildner A, Varol D, Breker M, Strauss-Ayali D, Viukov S, Guilliams M, Misharin A *et al*: **Fate mapping reveals origins and dynamics of monocytes and tissue macrophages under homeostasis**. *Immunity* 2013, **38**(1):79-91.

197. Auffray C, Fogg D, Garfa M, Elain G, Join-Lambert O, Kayal S, Sarnacki S, Cumano A, Lauvau G, Geissmann F: **Monitoring of blood vessels and tissues by a population of monocytes with patrolling behavior**. *Science* 2007, **317**(5838):666-670.

198. Landsman L, Bar-On L, Zernecke A, Kim KW, Krauthgamer R, Shagdarsuren E, Lira SA, Weissman IL, Weber C, Jung S: **CX3CR1 is required for monocyte homeostasis and atherogenesis by promoting cell survival**. *Blood* 2009, **113**(4):963-972.

199. Kuziel WA, Morgan SJ, Dawson TC, Griffin S, Smithies O, Ley K, Maeda N: **Severe reduction in leukocyte adhesion and monocyte extravasation in mice deficient in CC chemokine receptor 2**. *Proceedings of the National Academy of Sciences of the United States of America* 1997, **94**(22):12053-12058.

200. Emile JF, Geissmann F, Martin OC, Radford-Weiss I, Lepelletier Y, Heymer B, Espanol T, de Santes KB, Bertrand Y, Brousse N *et al*: **Langerhans cell deficiency in reticular dysgenesis**. *Blood* 2000, **96**(1):58-62.

201. Hambleton S, Salem S, Bustamante J, Bigley V, Boisson-Dupuis S, Azevedo J, Fortin A, Haniffa M, Ceron-Gutierrez L, Bacon CM *et al*: **IRF8 mutations and human dendritic-cell immunodeficiency**. *The New England journal of medicine* 2011, **365**(2):127-138.

202. Takahashi K, Yamamura F, Naito M: **Differentiation, maturation, and proliferation of macrophages in the mouse yolk sac: a light-microscopic, enzyme-cytochemical, immunohistochemical, and ultrastructural study**. *Journal of leukocyte biology* 1989, **45**(2):87-96.

203. Ginhoux F, Greter M, Leboeuf M, Nandi S, See P, Gokhan S, Mehler MF, Conway SJ, Ng LG, Stanley ER *et al*: **Fate mapping analysis reveals that adult microglia derive from primitive macrophages**. *Science* 2010, **330**(6005):841-845.

204. Hoeffel G, Wang Y, Greter M, See P, Teo P, Malleret B, Leboeuf M, Low D, Oller G, Almeida F *et al*: **Adult Langerhans cells derive predominantly from embryonic fetal liver monocytes with a minor contribution of yolk sac-derived macrophages**. *The Journal of experimental medicine* 2012, **209**(6):1167-1181.

205. Schulz C, Gomez Perdiguero E, Chorro L, Szabo-Rogers H, Cagnard N, Kierdorf K, Prinz M, Wu B, Jacobsen SE, Pollard JW *et al*: **A lineage of myeloid cells independent of Myb and hematopoietic stem cells**. *Science* 2012, **336**(6077):86-90.

206. Virolainen M: **Hematopoietic origin of macrophages as studied by chromosome markers in mice**. *The Journal of experimental medicine* 1968, **127**(5):943-952.

207. Parwaresch MR, Wacker HH: **Origin and kinetics of resident tissue macrophages. Parabiosis studies with radiolabelled leucocytes**. *Cell and tissue kinetics* 1984, **17**(1):25-39.

208. Hashimoto D, Chow A, Noizat C, Teo P, Beasley MB, Leboeuf M, Becker CD, See P, Price J, Lucas D *et al*: **Tissue-resident macrophages self-maintain locally throughout adult life with minimal contribution from circulating monocytes**. *Immunity* 2013, **38**(4):792-804.

209. Alliot F, Godin I, Pessac B: **Microglia derive from progenitors, originating from the yolk sac, and which proliferate in the brain**. *Brain research Developmental brain research* 1999, **117**(2):145-152.

210. Ginhoux F, Jung S: **Monocytes and macrophages: developmental pathways and tissue homeostasis**. *Nature reviews Immunology* 2014, **14**(6):392-404.

211. Ajami B, Bennett JL, Krieger C, Tetzlaff W, Rossi FM: **Local self-renewal can sustain CNS microglia maintenance and function throughout adult life**. *Nature neuroscience* 2007, **10**(12):1538-1543.

212. Merad M, Manz MG, Karsunky H, Wagers A, Peters W, Charo I, Weissman IL, Cyster JG, Engleman EG: **Langerhans cells renew in the skin throughout life under steady-state conditions**. *Nature immunology* 2002, **3**(12):1135-1141.

213. Epelman S, Lavine KJ, Beaudin AE, Sojka DK, Carrero JA, Calderon B, Brija T, Gautier EL, Ivanov S, Satpathy AT *et al*: **Embryonic and adult-derived resident cardiac macrophages are maintained through distinct mechanisms at steady state and during inflammation**. *Immunity* 2014, **40**(1):91-104.

214. Orkin SH, Zon LI: **Hematopoiesis: an evolving paradigm for stem cell biology**. *Cell* 2008, **132**(4):631-644.

215. Varol C, Landsman L, Jung S: **Probing in vivo origins of mononuclear phagocytes by conditional ablation and reconstitution**. *Methods in molecular biology* 2009, **531**:71-87.

216. Landsman L, Jung S: **Lung macrophages serve as obligatory intermediate between blood monocytes and alveolar macrophages**. *Journal of immunology* 2007, **179**(6):3488-3494.

217. Jakubzick C, Gautier EL, Gibbings SL, Sojka DK, Schlitzer A, Johnson TE, Ivanov S, Duan Q, Bala S, Condon T *et al*: **Minimal differentiation of classical monocytes as they survey steady-state tissues and transport antigen to lymph nodes**. *Immunity* 2013, **39**(3):599-610.

218. Kelley TW, Graham MM, Doseff AI, Pomerantz RW, Lau SM, Ostrowski MC, Franke TF, Marsh CB: **Macrophage colony-stimulating factor promotes cell survival through Akt/protein kinase B**. *The Journal of biological chemistry* 1999, **274**(37):26393-26398.

219. Parihar A, Eubank TD, Doseff AI: **Monocytes and macrophages regulate immunity through dynamic networks of survival and cell death**. *Journal of innate immunity* 2010, **2**(3):204-215.

220. Murphy J, Summer R, Wilson AA, Kotton DN, Fine A: **The prolonged life-span of alveolar macrophages**. *American journal of respiratory cell and molecular biology* 2008, **38**(4):380-385.

221. Tarling JD, Lin HS, Hsu S: **Self-renewal of pulmonary alveolar macrophages: evidence from radiation chimera studies**. *Journal of leukocyte biology* 1987, **42**(5):443-446.

222. Daems WT, de Bakker JM: **Do resident macrophages proliferate?** *Immunobiology* 1982, **161**(3-4):204-211.

223. Golde DW, Byers LA, Finley TN: **Proliferative capacity of human alveolar macrophage**. *Nature* 1974, **247**(5440):373-375.

224. Bitterman PB, Saltzman LE, Adelberg S, Ferrans VJ, Crystal RG: **Alveolar macrophage replication. One mechanism for the expansion of the mononuclear phagocyte population in the chronically inflamed lung**. *The Journal of clinical investigation* 1984, **74**(2):460-469.

225. Coggle JE, Tarling JD: **The proliferation kinetics of pulmonary alveolar macrophages**. *Journal of leukocyte biology* 1984, **35**(3):317-327.

226. Evans MJ, Shami SG, Martinez LA: **Enhanced proliferation of pulmonary alveolar macrophages after carbon instillation in mice depleted of blood monocytes by strontium-89**. *Laboratory investigation; a journal of technical methods and pathology* 1986, **54**(2):154-159.

227. Evans MJ, Sherman MP, Campbell LA, Shami SG: **Proliferation of pulmonary alveolar macrophages during postnatal development of rabbit lungs**. *The American review of respiratory disease* 1987, **136**(2):384-387.

228. Barbers RG, Evans MJ, Gong H, Jr., Tashkin DP: **Enhanced alveolar monocytic phagocyte (macrophage) proliferation in tobacco and marijuana smokers**. *The American review of respiratory disease* 1991, **143**(5 Pt 1):1092-1095.

229. Wallace WA, Gillooly M, Lamb D: **Intra-alveolar macrophage numbers in current smokers and non-smokers: a morphometric study of tissue sections**. *Thorax* 1992, **47**(6):437-440.

230. Pforte A, Gerth C, Voss A, Beer B, Haussinger K, Jutting U, Burger G, Ziegler-Heitbrock HW: **Proliferating alveolar macrophages in BAL and lung function changes in interstitial lung disease**. *The European respiratory journal* 1993, **6**(7):951-955.

231. Jenkins SJ, Ruckerl D, Cook PC, Jones LH, Finkelman FD, van Rooijen N, MacDonald AS, Allen JE: **Local macrophage proliferation, rather than recruitment from the blood, is a signature of TH2 inflammation**. *Science* 2011, **332**(6035):1284-1288.

232. Jenkins SJ, Ruckerl D, Thomas GD, Hewitson JP, Duncan S, Brombacher F, Maizels RM, Hume DA, Allen JE: **IL-4 directly signals tissue-resident macrophages to proliferate beyond homeostatic levels controlled by CSF-1**. *The Journal of experimental medicine* 2013, **210**(11):2477-2491.

233. Robbins CS, Hilgendorf I, Weber GF, Theurl I, Iwamoto Y, Figueiredo JL, Gorbatov R, Sukhova GK, Gerhardt LM, Smyth D *et al*: **Local proliferation dominates lesional macrophage accumulation in atherosclerosis**. *Nature medicine* 2013, **19**(9):1166-1172.

234. Amano SU, Cohen JL, Vangala P, Tencerova M, Nicoloro SM, Yawe JC, Shen Y, Czech MP, Aouadi M: **Local proliferation of macrophages contributes to obesity-associated adipose tissue inflammation**. *Cell metabolism* 2014, **19**(1):162-171.

235. Davies LC, Rosas M, Jenkins SJ, Liao CT, Scurr MJ, Brombacher F, Fraser DJ, Allen JE, Jones SA, Taylor PR: **Distinct bone marrow-derived and tissue-resident macrophage lineages proliferate at key stages during inflammation**. *Nature communications* 2013, **4**:1886.

236. Davies LC, Rosas M, Smith PJ, Fraser DJ, Jones SA, Taylor PR: **A quantifiable proliferative burst of tissue macrophages restores homeostatic macrophage populations after acute inflammation**. *European journal of immunology* 2011, **41**(8):2155-2164.

237. Chorro L, Sarde A, Li M, Woollard KJ, Chambon P, Malissen B, Kissenpfennig A, Barbaroux JB, Groves R, Geissmann F: **Langerhans cell (LC) proliferation mediates neonatal development, homeostasis, and inflammation-associated expansion of the epidermal LC network**. *The Journal of experimental medicine* 2009, **206**(13):3089-3100.

238. World Health Organization.: **World malaria report**. In. Geneva, Switzerland: World Health Organization; 2013: v.

239. Murray CJ, Vos T, Lozano R, Naghavi M, Flaxman AD, Michaud C, Ezzati M, Shibuya K, Salomon JA, Abdalla S *et al*: **Disability-adjusted life years (DALYs) for 291 diseases and injuries in 21 regions, 1990-2010: a systematic analysis for the Global Burden of Disease Study 2010**. *Lancet* 2012, **380**(9859):2197-2223.

240. Gallup JL, Sachs JD: **The economic burden of malaria**. *The American journal of tropical medicine and hygiene* 2001, **64**(1-2 Suppl):85-96.

241. Taylor WR, Hanson J, Turner GD, White NJ, Dondorp AM: **Respiratory manifestations of malaria**. *Chest* 2012, **142**(2):492-505.

242. Sturm A, Heussler V: **Live and let die: manipulation of host hepatocytes by exoerythrocytic Plasmodium parasites**. *Medical microbiology and immunology* 2007, **196**(3):127-133.

243. Sturm A, Graewe S, Franke-Fayard B, Retzlaff S, Bolte S, Roppenser B, Aepfelbacher M, Janse C, Heussler V: **Alteration of the parasite plasma membrane and the parasitophorous vacuole membrane during exo-erythrocytic development of malaria parasites**. *Protist* 2009, **160**(1):51-63.

244. Miller LH, Baruch DI, Marsh K, Doumbo OK: **The pathogenic basis of malaria**. *Nature* 2002, **415**(6872):673-679.

245. Beeson JG, Brown GV: **Pathogenesis of *Plasmodium falciparum* malaria: the roles of parasite adhesion and antigenic variation**. *Cellular and molecular life sciences : CMLS* 2002, **59**(2):258-271.

246. Khan SM, Franke-Fayard B, Mair GR, Lasonder E, Janse CJ, Mann M, Waters AP: **Proteome analysis of separated male and female gametocytes reveals novel sex-specific *Plasmodium* biology**. *Cell* 2005, **121**(5):675-687.

247. Franke-Fayard B, Trueman H, Ramesar J, Mendoza J, van der Keur M, van der Linden R, Sinden RE, Waters AP, Janse CJ: **A *Plasmodium berghei* reference line that constitutively expresses GFP at a high level throughout the complete life cycle**. *Molecular and biochemical parasitology* 2004, **137**(1):23-33.

248. Good MF, Doolan DL: **Malaria vaccine design: immunological considerations**. *Immunity* 2010, **33**(4):555-566.

249. Ghosh AK, Jacobs-Lorena M: ***Plasmodium* sporozoite invasion of the mosquito salivary gland**. *Current opinion in microbiology* 2009, **12**(4):394-400.

250. Idro R, Marsh K, John CC, Newton CR: **Cerebral malaria: mechanisms of brain injury and strategies for improved neurocognitive outcome**. *Pediatr Res* 2010, **68**(4):267-274.

251. Menendez C, Ordi J, Ismail MR, Ventura PJ, Aponte JJ, Kahigwa E, Font F, Alonso PL: **The impact of placental malaria on gestational age and birth weight**. *The Journal of infectious diseases* 2000, **181**(5):1740-1745.

252. Mohan A, Sharma SK, Bollineni S: **Acute lung injury and acute respiratory distress syndrome in malaria**. *J Vector Borne Dis* 2008, **45**(3):179-193.

253. Taylor WR, White NJ: **Malaria and the lung**. *Clinics in chest medicine* 2002, **23**(2):457-468.

254. World Health Organization.: **Guidelines for the treatment of malaria**, 2nd edn. Geneva: World Health Organization; 2010.

255. Asiedu DK, Sherman CB: **Adult respiratory distress syndrome complicating *Plasmodium falciparum* malaria**. *Heart & lung : the journal of critical care* 2000, **29**(4):294-297.

256. Aursudkij B, Wilairatana P, Vannaphan S, Walsh DS, Gordeux VR, Looareesuwan S: **Pulmonary edema in cerebral malaria patients in Thailand**. *The Southeast Asian journal of tropical medicine and public health* 1998, **29**(3):541-545.

257. Taylor WR, Canon V, White NJ: **Pulmonary manifestations of malaria : recognition and management**. *Treatments in respiratory medicine* 2006, **5**(6):419-428.

258. Taylor WR, Canon V, White NJ: **Pulmonary manifestations of malaria : recognition and management**. *Treatments in respiratory medicine* 2006, **5**(6):419-428.

259. Jindal SK, Aggarwal AN, Gupta D: **Adult respiratory distress syndrome in the tropics**. *Clinics in chest medicine* 2002, **23**(2):445-455.

260. Cunnington AJ, Walther M, Riley EM: **Piecing together the puzzle of severe malaria**. *Science translational medicine* 2013, **5**(211):211ps218.

261. Corbett CE, Duarte MI, Lancellotti CL, Silva MA, Andrade Junior HF: **Cytoadherence in human falciparum malaria as a cause of respiratory distress**. *The Journal of tropical medicine and hygiene* 1989, **92**(2):112-120.

262. Pongponratn E, Riganti M, Punpoowong B, Aikawa M: **Microvascular sequestration of parasitized erythrocytes in human falciparum malaria: a pathological study**. *The American journal of tropical medicine and hygiene* 1991, **44**(2):168-175.

263. Sherman IW, Eda S, Winograd E: **Cytoadherence and sequestration in *Plasmodium falciparum*: defining the ties that bind**. *Microbes Infect* 2003, **5**(10):897-909.

264. Franke-Fayard B, Janse CJ, Cunha-Rodrigues M, Ramesar J, Buscher P, Que I, Lowik C, Voshol PJ, den Boer MA, van Duinen SG *et al*: **Murine malaria parasite sequestration: CD36 is the major receptor, but cerebral pathology is unlinked to sequestration**. *Proceedings of the National Academy of Sciences of the United States of America* 2005, **102**(32):11468-11473.

265. Pettersson F, Vogt AM, Jonsson C, Mok BW, Shamaei-Tousi A, Bergstrom S, Chen Q, Wahlgren M: **Whole-body imaging of sequestration of *Plasmodium falciparum* in the rat**. *Infection and immunity* 2005, **73**(11):7736-7746.

266. Franke-Fayard B, Waters AP, Janse CJ: **Real-time in vivo imaging of transgenic bioluminescent blood stages of rodent malaria parasites in mice**. *Nature protocols* 2006, **1**(1):476-485.

267. Franke-Fayard B, Fonager J, Braks A, Khan SM, Janse CJ: **Sequestration and tissue accumulation of human malaria parasites: can we learn anything from rodent models of malaria?** *PLoS pathogens* 2010, **6**(9):e1001032.

268. El-Assaad F, Wheway J, Mitchell AJ, Lou J, Hunt NH, Combes V, Grau GE: **Cytoadherence of *Plasmodium berghei*-infected red blood cells to murine brain and lung microvascular endothelial cells in vitro**. *Infection and immunity* 2013, **81**(11):3984-3991.

269. Buffet PA, Safeukui I, Deplaine G, Brousse V, Prendki V, Thellier M, Turner GD, Mercereau-Puijalon O: **The pathogenesis of *Plasmodium falciparum* malaria in humans: insights from splenic physiology**. *Blood* 2011, **117**(2):381-392.

270. Gamain B, Smith JD, Viebig NK, Gysin J, Scherf A: **Pregnancy-associated malaria: parasite binding, natural immunity and vaccine development**. *International journal for parasitology* 2007, **37**(3-4):273-283.

271. Haldar K, Murphy SC, Milner DA, Taylor TE: **Malaria: mechanisms of erythrocytic infection and pathological correlates of severe disease**. *Annual review of pathology* 2007, **2**:217-249.

272. Seydel KB, Milner DA, Jr., Kamiza SB, Molyneux ME, Taylor TE: **The distribution and intensity of parasite sequestration in comatose Malawian children**. *J Infect Dis* 2006, **194**(2):208-205.

273. Pouvelle B, Buffet PA, Lepolard C, Scherf A, Gysin J: **Cytoadhesion of *Plasmodium falciparum* ring-stage-infected erythrocytes**. *Nature medicine* 2000, **6**(11):1264-1268.

274. Sanni LA, Allsopp CE, Reubsaet L, Sanni A, Newbold C, Chauhan VS, Langhorne J: **Cellular responses to *Plasmodium falciparum* erythrocyte membrane protein-1: use of relatively conserved synthetic peptide pools to determine CD4 T cell responses in malaria-exposed individuals in Benin, West Africa**. *Malaria journal* 2002, **1**:7.

275. Maier AG, Cooke BM, Cowman AF, Tilley L: **Malaria parasite proteins that remodel the host erythrocyte**. *Nature reviews Microbiology* 2009, **7**(5):341-354.

276. Ochola LB, Siddondo BR, Ocholla H, Nkya S, Kimani EN, Williams TN, Makale JO, Liljander A, Urban BC, Bull PC *et al*: **Specific receptor usage in *Plasmodium falciparum* cytoadherence is associated with disease outcome**. *PloS one* 2011, **6**(3):e14741.

277. Sherman IW, Eda S, Winograd E: **Cytoadherence and sequestration in *Plasmodium falciparum*: defining the ties that bind**. *Microbes Infect* 2003, **5**(10):897-909.

278. Anidi IU, Servinsky LE, Rentsendorj O, Stephens RS, Scott AL, Pearse DB: **CD36 and Fyn kinase mediate malaria-induced lung endothelial barrier dysfunction in mice infected with *Plasmodium berghei***. *PloS one* 2013, **8**(8):e71010.

279. van der Heyde HC, Bauer P, Sun G, Chang WL, Yin L, Fuseler J, Granger DN: **Assessing vascular permeability during experimental cerebral malaria by a radiolabeled monoclonal antibody technique**. *Infection and immunity* 2001, **69**(5):3460-3465.

280. Neill AL, Hunt NH: **Pathology of fatal and resolving *Plasmodium berghei* cerebral malaria in mice**. *Parasitology* 1992, **105 (Pt 2)**:165-175.

281. Clark IA, Budd AC, Alleva LM, Cowden WB: **Human malarial disease: a consequence of inflammatory cytokine release**. *Malaria journal* 2006, **5**:85.

282. Turner GD, Ly VC, Nguyen TH, Tran TH, Nguyen HP, Bethell D, Wyllie S, Louwrier K, Fox SB, Gatter KC *et al*: **Systemic endothelial activation occurs in both mild and severe malaria. Correlating dermal microvascular endothelial cell phenotype and soluble cell adhesion molecules with disease severity**. *The American journal of pathology* 1998, **152**(6):1477-1487.

283. Kim H, Higgins S, Liles WC, Kain KC: **Endothelial activation and dysregulation in malaria: a potential target for novel therapeutics**. *Current opinion in hematology* 2011, **18**(3):177-185.

284. Serghides L, Patel SN, Ayi K, Kain KC: **Placental chondroitin sulfate A-binding malarial isolates evade innate phagocytic clearance**. *The Journal of infectious diseases* 2006, **194**(1):133-139.

285. Rodrigues-Duarte L, de Moraes LV, Barboza R, Marinho CR, Franke-Fayard B, Janse CJ, Penha-Goncalves C: **Distinct placental malaria pathology caused by different *Plasmodium berghei* lines that fail to induce cerebral malaria in the C57BL/6 mouse**. *Malaria journal* 2012, **11**:231.

286. Hunt NH, Grau GE: **Cytokines: accelerators and brakes in the pathogenesis of cerebral malaria**. *Trends in immunology* 2003, **24**(9):491-499.

287. Serghides L, Smith TG, Patel SN, Kain KC: **CD36 and malaria: friends or foes?** *Trends in parasitology* 2003, **19**(10):461-469.

288. Cunha-Rodrigues M, Portugal S, Febbraio M, Mota MM: **Bone marrow chimeric mice reveal a dual role for CD36 in *Plasmodium berghei* ANKA infection**. *Malaria journal* 2007, **6**:32.

289. Patel SN, Serghides L, Smith TG, Febbraio M, Silverstein RL, Kurtz TW, Pravenec M, Kain KC: **CD36 mediates the phagocytosis of *Plasmodium falciparum*-infected erythrocytes by rodent macrophages**. *The Journal of infectious diseases* 2004, **189**(2):204-213.

290. Fonager J, Pasini EM, Braks JA, Klop O, Ramesar J, Remarque EJ, Vroegrijk IO, van Duinen SG, Thomas AW, Khan SM *et al*: **Reduced CD36-dependent tissue sequestration of *Plasmodium*-infected erythrocytes is detrimental to malaria parasite growth in vivo**. *The Journal of experimental medicine* 2012, **209**(1):93-107.

291. Larkin D, de Laat B, Jenkins PV, Bunn J, Craig AG, Terraube V, Preston RJ, Donkor C, Grau GE, van Mourik JA *et al*: **Severe *Plasmodium falciparum* malaria is associated with circulating ultra-large von Willebrand multimers and ADAMTS13 inhibition**. *PLoS pathogens* 2009, **5**(3):e1000349.

292. Bridges DJ, Bunn J, van Mourik JA, Grau G, Preston RJ, Molyneux M, Combes V, O'Donnell JS, de Laat B, Craig A: **Rapid activation of endothelial cells enables *Plasmodium falciparum* adhesion to platelet-decorated von Willebrand factor strings**. *Blood* 2010, **115**(7):1472-1474.

293. Lovegrove FE, Gharib SA, Pena-Castillo L, Patel SN, Ruzinski JT, Hughes TR, Liles WC, Kain KC: **Parasite burden and CD36-mediated sequestration are determinants of acute lung injury in an experimental malaria model**. *PLoS pathogens* 2008, **4**(5):e1000068.

294. Muanza K, Gay F, Behr C, Scherf A: **Primary culture of human lung microvessel endothelial cells: a useful in vitro model for studying *Plasmodium falciparum*-infected erythrocyte cytoadherence**. *Research in immunology* 1996, **147**(3):149-163.

295. Lovegrove FE, Gharib SA, Pena-Castillo L, Patel SN, Ruzinski JT, Hughes TR, Liles WC, Kain KC: **Parasite burden and CD36-mediated sequestration are determinants of acute lung injury in an experimental malaria model**. *PLoS pathogens* 2008, **4**(5):e1000068.

296. Deroost K, Tyberghein A, Lays N, Noppen S, Schwarzer E, Vanstreels E, Komuta M, Prato M, Lin JW, Pamplona A *et al*: **Hemozoin induces lung inflammation and correlates with malaria-associated acute respiratory distress syndrome**. *American journal of respiratory cell and molecular biology* 2013, **48**(5):589-600.

297. Stevenson MM, Riley EM: **Innate immunity to malaria**. *Nature reviews Immunology* 2004, **4**(3):169-180.

298. Jaramillo M, Plante I, Ouellet N, Vandal K, Tessier PA, Olivier M: **Hemozoin-inducible proinflammatory events in vivo: potential role in malaria infection**. *Journal of immunology* 2004, **172**(5):3101-3110.

299. Schofield L, Grau GE: **Immunological processes in malaria pathogenesis**. *Nature reviews Immunology* 2005, **5**(9):722-735.

300. Chua CL, Brown G, Hamilton JA, Rogerson S, Boeuf P: **Monocytes and macrophages in malaria: protection or pathology?** *Trends in parasitology* 2013, **29**(1):26-34.

301. Zhu J, Krishnegowda G, Li G, Gowda DC: **Proinflammatory responses by glycosylphosphatidylinositols (GPIs) of *Plasmodium falciparum* are mainly mediated through the recognition of TLR2/TLR1**. *Experimental parasitology* 2011, **128**(3):205-211.

302. Barrera V, Skorokhod OA, Baci D, Gremo G, Arese P, Schwarzer E: **Host fibrinogen stably bound to hemozoin rapidly activates monocytes via TLR-4 and CD11b/CD18-integrin: a new paradigm of hemozoin action**. *Blood* 2011, **117**(21):5674-5682.

303. Coban C, Igari Y, Yagi M, Reimer T, Koyama S, Aoshi T, Ohata K, Tsukui T, Takeshita F, Sakurai K *et al*: **Immunogenicity of whole-parasite vaccines against *Plasmodium falciparum* involves malarial hemozoin and host TLR9**. *Cell host & microbe* 2010, **7**(1):50-61.

304. Dolinay T, Kim YS, Howrylak J, Hunninghake GM, An CH, Fredenburgh L, Massaro AF, Rogers A, Gazourian L, Nakahira K *et al*: **Inflammasome-regulated cytokines are critical mediators of**

acute lung injury. *American journal of respiratory and critical care medicine* 2012, **185**(11):1225-1234.

305. Dostert C, Guarda G, Romero JF, Menu P, Gross O, Tardivel A, Suva ML, Stehle JC, Kopf M, Stamenkovic I *et al*: **Malarial hemozoin is a Nalp3 inflammasome activating danger signal**. *PloS one* 2009, **4**(8):e6510.

306. Griffith JW, Sun T, McIntosh MT, Bucala R: **Pure Hemozoin is inflammatory in vivo and activates the NALP3 inflammasome via release of uric acid**. *Journal of immunology* 2009, **183**(8):5208-5220.

307. Kalantari P, DeOliveira RB, Chan J, Corbett Y, Rathinam V, Stutz A, Latz E, Gazzinelli RT, Golenbock DT, Fitzgerald KA: **Dual engagement of the NLRP3 and AIM2 inflammasomes by *Plasmodium*-derived hemozoin and DNA during malaria**. *Cell reports* 2014, **6**(1):196-210.

308. Pisciotta JM, Sullivan D: **Hemozoin: oil versus water**. *Parasitology international* 2008, **57**(2):89-96.

309. Goldie P, Roth EF, Jr., Oppenheim J, Vanderberg JP: **Biochemical characterization of *Plasmodium falciparum* hemozoin**. *The American journal of tropical medicine and hygiene* 1990, **43**(6):584-596.

310. Frita R, Carapau D, Mota MM, Hanscheid T: **In Vivo Hemozoin Kinetics after Clearance of *Plasmodium berghei* Infection in Mice**. *Malar Res Treat* 2012, **2012**:373086.

311. Prada J, Malinowski J, Muller S, Bienzle U, Kremsner PG: **Hemozoin differentially modulates the production of interleukin 6 and tumor necrosis factor in murine malaria**. *Eur Cytokine Netw* 1995, **6**(2):109-112.

312. Silver KL, Higgins SJ, McDonald CR, Kain KC: **Complement driven innate immune response to malaria: fuelling severe malarial diseases**. *Cellular microbiology* 2010, **12**(8):1036-1045.

313. Stoute JA: **Complement receptor 1 and malaria**. *Cellular microbiology* 2011, **13**(10):1441-1450.

314. Tebo AE, Kremsner PG, Luty AJ: **Fcgamma receptor-mediated phagocytosis of *Plasmodium falciparum*-infected erythrocytes in vitro**. *Clinical and experimental immunology* 2002, **130**(2):300-306.

315. Hunter S, Indik ZK, Kim MK, Cauley MD, Park JG, Schreiber AD: **Inhibition of Fcgamma receptor-mediated phagocytosis by a nonphagocytic Fcgamma receptor**. *Blood* 1998, **91**(5):1762-1768.

316. De Souza JB, Williamson KH, Otani T, Playfair JH: **Early gamma interferon responses in lethal and nonlethal murine blood-stage malaria**. *Infection and immunity* 1997, **65**(5):1593-1598.

317. Mohan K, Moulin P, Stevenson MM: **Natural killer cell cytokine production, not cytotoxicity, contributes to resistance against blood-stage *Plasmodium chabaudi* AS infection**. *Journal of immunology* 1997, **159**(10):4990-4998.

318. Seixas E, Fonseca L, Langhorne J: **The influence of gammadelta T cells on the CD4+ T cell and antibody response during a primary *Plasmodium chabaudi chabaudi* infection in mice**. *Parasite immunology* 2002, **24**(3):131-140.

319. Charoenpan P, Indraprasit S, Kiatboonsri S, Suvachittanont O, Tanomsup S: **Pulmonary edema in severe falciparum malaria. Hemodynamic study and clinicophysiologic correlation**. *Chest* 1990, **97**(5):1190-1197.

320. Valecha N, Pinto RG, Turner GD, Kumar A, Rodrigues S, Dubhashi NG, Rodrigues E, Banaulikar SS, Singh R, Dash AP *et al*: **Histopathology of fatal respiratory distress caused by *Plasmodium vivax* malaria**. *The American journal of tropical medicine and hygiene* 2009, **81**(5):758-762.

321. Tatke M, Malik GB: **Pulmonary pathology in severe malaria infection in health and protein deprivation**. *The Journal of tropical medicine and hygiene* 1990, **93**(6):377-382.

322. Maguire GP, Handojo T, Pain MC, Kenangalem E, Price RN, Tjitra E, Anstey NM: **Lung injury in uncomplicated and severe falciparum malaria: a longitudinal study in papua, Indonesia**. *The Journal of infectious diseases* 2005, **192**(11):1966-1974.

323. Janka JJ, Koita OA, Traore B, Traore JM, Mzayek F, Sachdev V, Wang X, Sanogo K, Sangare L, Mendelsohn L *et al*: **Increased pulmonary pressures and myocardial wall stress in children with severe malaria**. *The Journal of infectious diseases* 2010, **202**(5):791-800.

324. Matthay MA, Zimmerman GA: **Acute lung injury and the acute respiratory distress syndrome: four decades of inquiry into pathogenesis and rational management**. *American journal of respiratory cell and molecular biology* 2005, **33**(4):319-327.

325. Sponaas AM, Freitas do Rosario AP, Voisine C, Mastelic B, Thompson J, Koernig S, Jarra W, Renia L, Mauduit M, Potocnik AJ *et al*: **Migrating monocytes recruited to the spleen play an important role in control of blood stage malaria**. *Blood* 2009, **114**(27):5522-5531.

326. Fonager J, Pasini EM, Braks JAM, Klop O, Ramesar J, Remarque EJ, Vroegrijk IOCM, van Duinen SG, Thomas AW, Khan SM *et al*: **Reduced CD36-dependent tissue sequestration of *Plasmodium*-infected erythrocytes is detrimental to malaria parasite growth in vivo**. *The Journal of experimental medicine* 2012, **209**(1):93-107.

327. Franke-Fayard B, Fonager J, Braks A, Khan SM, Janse CJ: **Sequestration and tissue accumulation of human malaria parasites: can we learn anything from rodent models of malaria?** *PLoS pathogens* 2010, **6**(9):e1001032.

328. Franke-Fayard B, Janse CJ, Cunha-Rodrigues M, Ramesar J, Buscher P, Que I, Lowik C, Voshol PJ, den Boer MA, van Duinen SG *et al*: **Murine malaria parasite sequestration: CD36 is the major receptor, but cerebral pathology is unlinked to sequestration**. *Proceedings of the National Academy of Sciences of the United States of America* 2005, **102**(32):11468-11473.

329. Van den Steen PE, Geurts N, Deroost K, Van Aelst I, Verhenne S, Heremans H, Van Damme J, Opdenakker G: **Immunopathology and dexamethasone therapy in a new model for malaria-associated acute respiratory distress syndrome**. *American journal of respiratory and critical care medicine* 2010, **181**(9):957-968.

330. Craig AG, Grau GE, Janse C, Kazura JW, Milner D, Barnwell JW, Turner G, Langhorne J, participants of the Hinxton Retreat meeting on Animal Models for Research on Severe M: **The role of animal models for research on severe malaria**. *PLoS pathogens* 2012, **8**(2):e1002401.

331. Van den Steen PE, Geurts N, Deroost K, Van Aelst I, Verhenne S, Heremans H, Van Damme J, Opdenakker G: **Immunopathology and dexamethasone therapy in a new model for malaria-associated acute respiratory distress syndrome**. *American journal of respiratory and critical care medicine* 2010, **181**(9):957-968.

332. Epiphanio S, Campos MG, Pamplona A, Carapau D, Pena AC, Ataide R, Monteiro CA, Felix N, Costa-Silva A, Marinho CR *et al*: **VEGF promotes malaria-associated acute lung injury in mice**. *PLoS pathogens* 2010, **6**(5):e1000916.

333. de Oca MM, Engwerda C, Haque A: ***Plasmodium berghei* ANKA (PbA) infection of C57BL/6J mice: a model of severe malaria**. *Methods in molecular biology* 2013, **1031**:203-213.

334. Weiss ML, Kubat K: ***Plasmodium berghei*: a mouse model for the "sudden death" and "malarial lung" syndromes**. *Experimental parasitology* 1983, **56**(1):143-151.

335. Amante FH, Haque A, Stanley AC, Rivera Fde L, Randall LM, Wilson YA, Yeo G, Pieper C, Crabb BS, de Koning-Ward TF *et al*: **Immune-mediated mechanisms of parasite tissue sequestration during experimental cerebral malaria**. *Journal of immunology* 2010, **185**(6):3632-3642.

336. Souza MC, Silva JD, Padua TA, Capelozzi VL, Rocco PR, Henriques M: **Early and late acute lung injury and their association with distal organ damage in murine malaria**. *Respiratory physiology & neurobiology* 2013, **186**(1):65-72.

337. Gruring C, Heiber A, Kruse F, Ungefehr J, Gilberger TW, Spielmann T: **Development and host cell modifications of *Plasmodium falciparum* blood stages in four dimensions**. *Nature communications* 2011, **2**:165.

338. Organization. WH: **World Health Statistics 2008.** 2008.

339. Mathers CD, Loncar D: **Projections of global mortality and burden of disease from 2002 to 2030**. *PLoS medicine* 2006, **3**(11):e442.

340. Hoyert DL XJ: **Deaths: preliminary data for 2011**. *National vital statistics reports : from the Centers for Disease Control and Prevention, National Center for Health Statistics, National Vital Statistics System* 2012, **61**(6):1-65.

341. Centers for Disease C, Prevention: **Chronic obstructive pulmonary disease among adults--United States, 2011**. *MMWR Morbidity and mortality weekly report* 2012, **61**(46):938-943.

342. Mannino DM, Gagnon RC, Petty TL, Lydick E: **Obstructive lung disease and low lung function in adults in the United States: data from the National Health and Nutrition Examination Survey, 1988-1994**. *Archives of internal medicine* 2000, **160**(11):1683-1689.

343. Decramer M, Janssens W, Miravitlles M: **Chronic obstructive pulmonary disease**. *Lancet* 2012, **379**(9823):1341-1351.

344. Barnes PJ: **Immunology of asthma and chronic obstructive pulmonary disease**. *Nature reviews Immunology* 2008, **8**(3):183-192.

345. Taraseviciene-Stewart L, Voelkel NF: **Molecular pathogenesis of emphysema**. *The Journal of clinical investigation* 2008, **118**(2):394-402.

346. Vestbo J, Hurd SS, Agusti AG, Jones PW, Vogelmeier C, Anzueto A, Barnes PJ, Fabbri LM, Martinez FJ, Nishimura M *et al*: **Global strategy for the diagnosis, management, and prevention of chronic obstructive pulmonary disease: GOLD executive summary**. *American journal of respiratory and critical care medicine* 2013, **187**(4):347-365.

347. Hogg JC: **Pathophysiology of airflow limitation in chronic obstructive pulmonary disease**. *Lancet* 2004, **364**(9435):709-721.

348. O'Donnell DE: **Hyperinflation, dyspnea, and exercise intolerance in chronic obstructive pulmonary disease**. *Proceedings of the American Thoracic Society* 2006, **3**(2):180-184.

349. Halbert RJ, Natoli JL, Gano A, Badamgarav E, Buist AS, Mannino DM: **Global burden of COPD: systematic review and meta-analysis**. *The European respiratory journal* 2006, **28**(3):523-532.

350. Mannino DM, Buist AS: **Global burden of COPD: risk factors, prevalence, and future trends**. *Lancet* 2007, **370**(9589):765-773.

351. Salvi SS, Barnes PJ: **Chronic obstructive pulmonary disease in non-smokers**. *Lancet* 2009, **374**(9691):733-743.

352. American Thoracic S, European Respiratory S: **American Thoracic Society/European Respiratory Society statement: standards for the diagnosis and management of individuals with alpha-1 antitrypsin deficiency**. *American journal of respiratory and critical care medicine* 2003, **168**(7):818-900.

353. Laurell C-B, Eriksson S: **The Electrophoretic α;1-Globulin Pattern of Serum in α;1-Antitrypsin Deficiency**. *Scandinavian Journal of Clinical & Laboratory Investigation* 1963, **15**(2):132-140.

354. Hunninghake GM, Cho MH, Tesfaigzi Y, Soto-Quiros ME, Avila L, Lasky-Su J, Stidley C, Melen E, Soderhall C, Hallberg J *et al*: **MMP12, lung function, and COPD in high-risk populations**. *The New England journal of medicine* 2009, **361**(27):2599-2608.

355. Wickenden JA, Clarke MC, Rossi AG, Rahman I, Faux SP, Donaldson K, MacNee W: **Cigarette smoke prevents apoptosis through inhibition of caspase activation and induces necrosis**. *American journal of respiratory cell and molecular biology* 2003, **29**(5):562-570.

356. Churg A, Zay K, Shay S, Xie C, Shapiro SD, Hendricks R, Wright JL: **Acute cigarette smoke-induced connective tissue breakdown requires both neutrophils and macrophage metalloelastase in mice**. *American journal of respiratory cell and molecular biology* 2002, **27**(3):368-374.

357. Mortaz E, Adcock IM, Ito K, Kraneveld AD, Nijkamp FP, Folkerts G: **Cigarette smoke induces CXCL8 production by human neutrophils via activation of TLR9 receptor**. *The European respiratory journal* 2010, **36**(5):1143-1154.

358. Mills PR, Davies RJ, Devalia JL: **Airway epithelial cells, cytokines, and pollutants**. *American journal of respiratory and critical care medicine* 1999, **160**(5 Pt 2):S38-43.

359. Kaur M, Singh D: **Neutrophil chemotaxis caused by chronic obstructive pulmonary disease alveolar macrophages: the role of CXCL8 and the receptors CXCR1/CXCR2**. *The Journal of pharmacology and experimental therapeutics* 2013, **347**(1):173-180.

360. Barnes PJ: **Mediators of chronic obstructive pulmonary disease**. *Pharmacological reviews* 2004, **56**(4):515-548.

361. MacNee W: **Oxidative stress and lung inflammation in airways disease**. *European journal of pharmacology* 2001, **429**(1-3):195-207.

362. Owen CA: **Proteinases and oxidants as targets in the treatment of chronic obstructive pulmonary disease**. *Proceedings of the American Thoracic Society* 2005, **2**(4):373-385; discussion 394-375.

363. Elkington PT, Friedland JS: **Matrix metalloproteinases in destructive pulmonary pathology**. *Thorax* 2006, **61**(3):259-266.

364. Lee SH, Goswami S, Grudo A, Song LZ, Bandi V, Goodnight-White S, Green L, Hacken-Bitar J, Huh J, Bakaeen F *et al*: **Antielastin autoimmunity in tobacco smoking-induced emphysema**. *Nature medicine* 2007, **13**(5):567-569.

365. Grumelli S, Corry DB, Song LZ, Song L, Green L, Huh J, Hacken J, Espada R, Bag R, Lewis DE *et al*: **An immune basis for lung parenchymal destruction in chronic obstructive pulmonary disease and emphysema**. *PLoS medicine* 2004, **1**(1):e8.

366. Keatings VM, Collins PD, Scott DM, Barnes PJ: **Differences in interleukin-8 and tumor necrosis factor-alpha in induced sputum from patients with chronic obstructive pulmonary disease or asthma**. *American journal of respiratory and critical care medicine* 1996, **153**(2):530-534.

367. Peleman RA, Rytila PH, Kips JC, Joos GF, Pauwels RA: **The cellular composition of induced sputum in chronic obstructive pulmonary disease**. *The European respiratory journal* 1999, **13**(4):839-843.

368. Gernez Y, Tirouvanziam R, Chanez P: **Neutrophils in chronic inflammatory airway diseases: can we target them and how?** *The European respiratory journal* 2010, **35**(3):467-469.

369. Yamamoto C, Yoneda T, Yoshikawa M, Fu A, Tokuyama T, Tsukaguchi K, Narita N: **Airway inflammation in COPD assessed by sputum levels of interleukin-8**. *Chest* 1997, **112**(2):505-510.

370. Keatings VM, Barnes PJ: **Granulocyte activation markers in induced sputum: comparison between chronic obstructive pulmonary disease, asthma, and normal subjects**. *American journal of respiratory and critical care medicine* 1997, **155**(2):449-453.

371. Mocsai A: **Diverse novel functions of neutrophils in immunity, inflammation, and beyond**. *The Journal of experimental medicine* 2013, **210**(7):1283-1299.

372. Meagher LC, Savill JS, Baker A, Fuller RW, Haslett C: **Phagocytosis of apoptotic neutrophils does not induce macrophage release of thromboxane B2**. *Journal of leukocyte biology* 1992, **52**(3):269-273.

373. Shapiro SD: **The macrophage in chronic obstructive pulmonary disease**. *American journal of respiratory and critical care medicine* 1999, **160**(5 Pt 2):S29-32.

374. Di Stefano A, Capelli A, Lusuardi M, Balbo P, Vecchio C, Maestrelli P, Mapp CE, Fabbri LM, Donner CF, Saetta M: **Severity of airflow limitation is associated with severity of airway inflammation in smokers**. *American journal of respiratory and critical care medicine* 1998, **158**(4):1277-1285.

375. Hodge S, Hodge G, Scicchitano R, Reynolds PN, Holmes M: **Alveolar macrophages from subjects with chronic obstructive pulmonary disease are deficient in their ability to phagocytose apoptotic airway epithelial cells**. *Immunology and cell biology* 2003, **81**(4):289-296.

376. Woodruff PG, Koth LL, Yang YH, Rodriguez MW, Favoreto S, Dolganov GM, Paquet AC, Erle DJ: **A distinctive alveolar macrophage activation state induced by cigarette smoking**. *American journal of respiratory and critical care medicine* 2005, **172**(11):1383-1392.

377. Shapiro SD, Senior RM: **Matrix metalloproteinases. Matrix degradation and more**. *American journal of respiratory cell and molecular biology* 1999, **20**(6):1100-1102.

378. Hautamaki RD, Kobayashi DK, Senior RM, Shapiro SD: **Requirement for macrophage elastase for cigarette smoke-induced emphysema in mice**. *Science* 1997, **277**(5334):2002-2004.

379. Soler P, Moreau A, Basset F, Hance AJ: **Cigarette smoking-induced changes in the number and differentiated state of pulmonary dendritic cells/Langerhans cells**. *The American review of respiratory disease* 1989, **139**(5):1112-1117.

380. Francus T, Klein RF, Staiano-Coico L, Becker CG, Siskind GW: **Effects of tobacco glycoprotein (TGP) on the immune system. II. TGP stimulates the proliferation of human T cells and the differentiation of human B cells into Ig secreting cells**. *Journal of immunology* 1988, **140**(6):1823-1829.

381. Costa C, Rufino R, Traves SL, Lapa ESJR, Barnes PJ, Donnelly LE: **CXCR3 and CCR5 chemokines in induced sputum from patients with COPD**. *Chest* 2008, **133**(1):26-33.

382. Saetta M, Mariani M, Panina-Bordignon P, Turato G, Buonsanti C, Baraldo S, Bellettato CM, Papi A, Corbetta L, Zuin R *et al*: **Increased expression of the chemokine receptor CXCR3 and its ligand CXCL10 in peripheral airways of smokers with chronic obstructive pulmonary disease**. *American journal of respiratory and critical care medicine* 2002, **165**(10):1404-1409.

383. Saetta M, Di Stefano A, Turato G, Facchini FM, Corbino L, Mapp CE, Maestrelli P, Ciaccia A, Fabbri LM: **CD8+ T-lymphocytes in peripheral airways of smokers with chronic obstructive pulmonary disease**. *American journal of respiratory and critical care medicine* 1998, **157**(3 Pt 1):822-826.

384. Chrysofakis G, Tzanakis N, Kyriakoy D, Tsoumakidou M, Tsiligianni I, Klimathianaki M, Siafakas NM: **Perforin expression and cytotoxic activity of sputum CD8+ lymphocytes in patients with COPD**. *Chest* 2004, **125**(1):71-76.

385. Brew K, Dinakarpandian D, Nagase H: **Tissue inhibitors of metalloproteinases: evolution, structure and function**. *Biochimica et biophysica acta* 2000, **1477**(1-2):267-283.

386. Carp H, Janoff A: **Possible mechanisms of emphysema in smokers. In vitro suppression of serum elastase-inhibitory capacity by fresh cigarette smoke and its prevention by antioxidants**. *The American review of respiratory disease* 1978, **118**(3):617-621.

387. Taggart CC, Greene CM, McElvaney NG, O'Neill S: **Secretory leucoprotease inhibitor prevents lipopolysaccharide-induced IkappaBalpha degradation without affecting phosphorylation or ubiquitination**. *The Journal of biological chemistry* 2002, **277**(37):33648-33653.

388. Taggart C, Cervantes-Laurean D, Kim G, McElvaney NG, Wehr N, Moss J, Levine RL: **Oxidation of either methionine 351 or methionine 358 in alpha 1-antitrypsin causes loss of anti-neutrophil elastase activity**. *The Journal of biological chemistry* 2000, **275**(35):27258-27265.

389. Singh A, Rangasamy T, Thimmulappa RK, Lee H, Osburn WO, Brigelius-Flohe R, Kensler TW, Yamamoto M, Biswal S: **Glutathione peroxidase 2, the major cigarette smoke-inducible isoform of GPX in lungs, is regulated by Nrf2**. *American journal of respiratory cell and molecular biology* 2006, **35**(6):639-650.

390. Iizuka T, Ishii Y, Itoh K, Kiwamoto T, Kimura T, Matsuno Y, Morishima Y, Hegab AE, Homma S, Nomura A *et al*: **Nrf2-deficient mice are highly susceptible to cigarette smoke-induced emphysema**. *Genes to cells : devoted to molecular & cellular mechanisms* 2005, **10**(12):1113-1125.

391. Rangasamy T, Cho CY, Thimmulappa RK, Zhen L, Srisuma SS, Kensler TW, Yamamoto M, Petrache I, Tuder RM, Biswal S: **Genetic ablation of Nrf2 enhances susceptibility to cigarette smoke-induced emphysema in mice**. *The Journal of clinical investigation* 2004, **114**(9):1248-1259.

392. Tuder RM, Yoshida T, Fijalkowka I, Biswal S, Petrache I: **Role of lung maintenance program in the heterogeneity of lung destruction in emphysema**. *Proceedings of the American Thoracic Society* 2006, **3**(8):673-679.

393. Tuder RM, McGrath S, Neptune E: **The pathobiological mechanisms of emphysema models: what do they have in common?** *Pulmonary pharmacology & therapeutics* 2003, **16**(2):67-78.

394. Acarregui MJ, Penisten ST, Goss KL, Ramirez K, Snyder JM: **Vascular endothelial growth factor gene expression in human fetal lung in vitro**. *American journal of respiratory cell and molecular biology* 1999, **20**(1):14-23.

395. Tuder RM, Flook BE, Voelkel NF: **Increased gene expression for VEGF and the VEGF receptors KDR/Flk and Flt in lungs exposed to acute or to chronic hypoxia. Modulation of gene expression by nitric oxide**. *The Journal of clinical investigation* 1995, **95**(4):1798-1807.

396. Kasahara Y, Tuder RM, Cool CD, Lynch DA, Flores SC, Voelkel NF: **Endothelial cell death and decreased expression of vascular endothelial growth factor and vascular endothelial growth factor receptor 2 in emphysema**. *American journal of respiratory and critical care medicine* 2001, **163**(3 Pt 1):737-744.

397. Kasahara Y, Tuder RM, Taraseviciene-Stewart L, Le Cras TD, Abman S, Hirth PK, Waltenberger J, Voelkel NF: **Inhibition of VEGF receptors causes lung cell apoptosis and emphysema**. *The Journal of clinical investigation* 2000, **106**(11):1311-1319.

398. Tang K, Rossiter HB, Wagner PD, Breen EC: **Lung-targeted VEGF inactivation leads to an emphysema phenotype in mice**. *Journal of applied physiology* 2004, **97**(4):1559-1566; discussion 1549.

399. Retamales I, Elliott WM, Meshi B, Coxson HO, Pare PD, Sciurba FC, Rogers RM, Hayashi S, Hogg JC: **Amplification of inflammation in emphysema and its association with latent adenoviral infection**. *American journal of respiratory and critical care medicine* 2001, **164**(3):469-473.

400. Finkelstein R, Fraser RS, Ghezzo H, Cosio MG: **Alveolar inflammation and its relation to emphysema in smokers**. *American journal of respiratory and critical care medicine* 1995, **152**(5 Pt 1):1666-1672.

401. Meshi B, Vitalis TZ, Ionescu D, Elliott WM, Liu C, Wang XD, Hayashi S, Hogg JC: **Emphysematous lung destruction by cigarette smoke. The effects of latent adenoviral infection on the lung inflammatory response**. *American journal of respiratory cell and molecular biology* 2002, **26**(1):52-57.

402. Traves SL, Culpitt SV, Russell RE, Barnes PJ, Donnelly LE: **Increased levels of the chemokines GROalpha and MCP-1 in sputum samples from patients with COPD**. *Thorax* 2002, **57**(7):590-595.

403. Capelli A, Di Stefano A, Gnemmi I, Balbo P, Cerutti CG, Balbi B, Lusuardi M, Donner CF: **Increased MCP-1 and MIP-1beta in bronchoalveolar lavage fluid of chronic bronchitics**. *The European respiratory journal* 1999, **14**(1):160-165.

404. Tomita K, Caramori G, Lim S, Ito K, Hanazawa T, Oates T, Chiselita I, Jazrawi E, Chung KF, Barnes PJ *et al*: **Increased p21(CIP1/WAF1) and B cell lymphoma leukemia-x(L) expression and reduced apoptosis in alveolar macrophages from smokers**. *American journal of respiratory and critical care medicine* 2002, **166**(5):724-731.

405. Shapiro SD: **Animal models for COPD**. *Chest* 2000, **117**(5 Suppl 1):223S-227S.

406. Kuhn C, Yu SY, Chraplyvy M, Linder HE, Senior RM: **The induction of emphysema with elastase. II. Changes in connective tissue**. *Laboratory investigation; a journal of technical methods and pathology* 1976, **34**(4):372-380.

407. Craig JM: **Immune-mediated regulation of pulmonary inflammation in diverse model systems: Malaria, Hookworm, and emphysema**. *Ph.D.* Ann Arbor: The Johns Hopkins University; 2013.

408. Hsia CC, Hyde DM, Ochs M, Weibel ER, Structure AEJTFoQAoL: **An official research policy statement of the American Thoracic Society/European Respiratory Society: standards for quantitative assessment of lung structure**. *American journal of respiratory and critical care medicine* 2010, **181**(4):394-418.

409. Miller LH, Ackerman HC, Su XZ, Wellems TE: **Malaria biology and disease pathogenesis: insights for new treatments**. *Nat Med* 2013, **19**(2):156-167.

410. Boring L, Gosling J, Chensue SW, Kunkel SL, Farese RV, Jr., Broxmeyer HE, Charo IF: **Impaired monocyte migration and reduced type 1 (Th1) cytokine responses in C-C chemokine receptor 2 knockout mice**. *The Journal of clinical investigation* 1997, **100**(10):2552-2561.

411. Febbraio M, Abumrad NA, Hajjar DP, Sharma K, Cheng W, Pearce SF, Silverstein RL: **A null mutation in murine CD36 reveals an important role in fatty acid and lipoprotein metabolism**. *The Journal of biological chemistry* 1999, **274**(27):19055-19062.

412. Graewe S, Retzlaff S, Struck N, Janse CJ, Heussler VT: **Going live: a comparative analysis of the suitability of the RFP derivatives RedStar, mCherry and tdTomato for intravital and in vitro live imaging of *Plasmodium* parasites**. *Biotechnology journal* 2009, **4**(6):895-902.

413. Reece JJ, Siracusa MC, Scott AL: **Innate immune responses to lung-stage helminth infection induce alternatively activated alveolar macrophages**. *Infect Immun* 2006, **74**(9):4970-4981.

414. Garcia AN, Vogel SM, Komarova YA, Malik AB: **Permeability of endothelial barrier: cell culture and in vivo models**. *Methods in molecular biology* 2011, **763**:333-354.

415. Chen MM, Shi L, Sullivan DJ, Jr.: ***Haemoproteus* and *Schistosoma* synthesize heme polymers similar to *Plasmodium* hemozoin and beta-hematin**. *Molecular and biochemical parasitology* 2001, **113**(1):1-8.

416. Francke A, Herold J, Weinert S, Strasser RH, Braun-Dullaeus RC: **Generation of mature murine monocytes from heterogeneous bone marrow and description of their properties**. *The journal of histochemistry and cytochemistry : official journal of the Histochemistry Society* 2011, **59**(9):813-825.

417. Lee MA, Tan CH, Aw LT, Tang CS, Singh M, Lee SH, Chia HP, Yap EP: **Real-time fluorescence-based PCR for detection of malaria parasites**. *Journal of clinical microbiology* 2002, **40**(11):4343-4345.

418. Shi C, Pamer EG: **Monocyte recruitment during infection and inflammation**. *Nat Rev Immunol* 2011, **11**(11):762-774.

419. McComb JG, Ranganathan M, Liu XH, Pilewski JM, Ray P, Watkins SC, Choi AM, Lee JS: **CX3CL1 up-regulation is associated with recruitment of CX3CR1+ mononuclear phagocytes and T lymphocytes in the lungs during cigarette smoke-induced emphysema**. *The American journal of pathology* 2008, **173**(4):949-961.

420. Amante FH, Haque A, Stanley AC, Rivera Fde L, Randall LM, Wilson YA, Yeo G, Pieper C, Crabb BS, de Koning-Ward TF *et al*: **Immune-mediated mechanisms of parasite tissue sequestration during experimental cerebral malaria**. *Journal of immunology* 2010, **185**(6):3632-3642.

421. Ockenhouse CF, Tegoshi T, Maeno Y, Benjamin C, Ho M, Kan KE, Thway Y, Win K, Aikawa M, Lobb RR: **Human vascular endothelial cell adhesion receptors for *Plasmodium falciparum*-infected erythrocytes: roles for endothelial leukocyte adhesion molecule 1 and vascular cell adhesion molecule 1**. *The Journal of experimental medicine* 1992, **176**(4):1183-1189.

422. McGilvray ID, Serghides L, Kapus A, Rotstein OD, Kain KC: **Nonopsonic monocyte/macrophage phagocytosis of *Plasmodium falciparum*-parasitized erythrocytes: a role for CD36 in malarial clearance**. *Blood* 2000, **96**(9):3231-3240.

423. Serghides L, Kain KC: **Peroxisome proliferator-activated receptor gamma-retinoid X receptor agonists increase CD36-dependent phagocytosis of *Plasmodium falciparum*-parasitized erythrocytes and decrease malaria-induced TNF-alpha secretion by monocytes/macrophages**. *Journal of immunology* 2001, **166**(11):6742-6748.

424. Anidi IU: **Malaria in the lung: The role of the scavenger receptor CD36 in malaria-induced acute lung injury**. *Ph.D.* Ann Arbor: The Johns Hopkins University; 2013.

425. Hussell T, Bell TJ: **Alveolar macrophages: plasticity in a tissue-specific context**. *Nat Rev Immunol* 2014, **14**(2):81-93.

426. Sawyer RT, Strausbauch PH, Volkman A: **Resident macrophage proliferation in mice depleted of blood monocytes by strontium-89**. *Laboratory investigation; a journal of technical methods and pathology* 1982, **46**(2):165-170.

427. Siracusa MC, Reece JJ, Urban JF, Jr., Scott AL: **Dynamics of lung macrophage activation in response to helminth infection**. *Journal of leukocyte biology* 2008, **84**(6):1422-1433.

428. Kirby AC, Coles MC, Kaye PM: **Alveolar macrophages transport pathogens to lung draining lymph nodes**. *Journal of immunology* 2009, **183**(3):1983-1989.

429. Gu L, Tseng S, Horner RM, Tam C, Loda M, Rollins BJ: **Control of TH2 polarization by the chemokine monocyte chemoattractant protein-1**. *Nature* 2000, **404**(6776):407-411.

430. Roca H, Varsos ZS, Sud S, Craig MJ, Ying C, Pienta KJ: **CCL2 and interleukin-6 promote survival of human CD11b+ peripheral blood mononuclear cells and induce M2-type macrophage polarization**. *The Journal of biological chemistry* 2009, **284**(49):34342-34354.

431. Sierra-Filardi E, Nieto C, Dominguez-Soto A, Barroso R, Sanchez-Mateos P, Puig-Kroger A, Lopez-Bravo M, Joven J, Ardavin C, Rodriguez-Fernandez JL *et al*: **CCL2 Shapes Macrophage Polarization by GM-CSF and M-CSF: Identification of CCL2/CCR2-Dependent Gene Expression Profile**. *Journal of immunology* 2014, **192**(8):3858-3867.

432. van Zoelen MA, Verstege MI, Draing C, de Beer R, van't Veer C, Florquin S, Bresser P, van der Zee JS, te Velde AA, von Aulock S *et al*: **Endogenous MCP-1 promotes lung inflammation induced by LPS and LTA**. *Molecular immunology* 2011, **48**(12-13):1468-1476.

433. Daley JM, Thomay AA, Connolly MD, Reichner JS, Albina JE: **Use of Ly6G-specific monoclonal antibody to deplete neutrophils in mice**. *Journal of leukocyte biology* 2008, **83**(1):64-70.

434. GeurtsvanKessel CH, Lambrecht BN: **Division of labor between dendritic cell subsets of the lung**. *Mucosal immunology* 2008, **1**(6):442-450.

435. Vermaelen K, Pauwels R: **Accurate and simple discrimination of mouse pulmonary dendritic cell and macrophage populations by flow cytometry: methodology and new insights**. *Cytometry Part A : the journal of the International Society for Analytical Cytology* 2004, **61**(2):170-177.

436. Jennings JH, Linderman DJ, Hu B, Sonstein J, Curtis JL: **Monocytes recruited to the lungs of mice during immune inflammation ingest apoptotic cells poorly**. *American journal of respiratory cell and molecular biology* 2005, **32**(2):108-117.

437. Wilson AA, Murphy GJ, Hamakawa H, Kwok LW, Srinivasan S, Hovav AH, Mulligan RC, Amar S, Suki B, Kotton DN: **Amelioration of emphysema in mice through lentiviral transduction of long-lived pulmonary alveolar macrophages**. *The Journal of clinical investigation* 2010, **120**(1):379-389.

438. Maus U, Herold S, Muth H, Maus R, Ermert L, Ermert M, Weissmann N, Rosseau S, Seeger W, Grimminger F *et al*: **Monocytes recruited into the alveolar air space of mice show a monocytic phenotype but upregulate CD14**. *American journal of physiology Lung cellular and molecular physiology* 2001, **280**(1):L58-68.

439. Sun K, Metzger DW: **Inhibition of pulmonary antibacterial defense by interferon-gamma during recovery from influenza infection**. *Nature medicine* 2008, **14**(5):558-564.

440. Shinagawa K, Anderson GP: **Rapid isolation of homogeneous murine bronchoalveolar lavage fluid eosinophils by differential lectin affinity interaction and negative selection**. *Journal of immunological methods* 2000, **237**(1-2):65-72.

441. Gerdes J, Schwab U, Lemke H, Stein H: **Production of a mouse monoclonal antibody reactive with a human nuclear antigen associated with cell proliferation**. *International journal of cancer Journal international du cancer* 1983, **31**(1):13-20.

442. Lyons AB: **Analysing cell division in vivo and in vitro using flow cytometric measurement of CFSE dye dilution**. *Journal of immunological methods* 2000, **243**(1-2):147-154.

443. Bergeland T, Widerberg J, Bakke O, Nordeng TW: **Mitotic partitioning of endosomes and lysosomes**. *Current biology : CB* 2001, **11**(9):644-651.

444. Geissmann F, Manz MG, Jung S, Sieweke MH, Merad M, Ley K: **Development of monocytes, macrophages, and dendritic cells**. *Science* 2010, **327**(5966):656-661.

445. Ingersoll MA, Platt AM, Potteaux S, Randolph GJ: **Monocyte trafficking in acute and chronic inflammation**. *Trends in immunology* 2011, **32**(10):470-477.

446. Mildner A, Yona S, Jung S: **A close encounter of the third kind: monocyte-derived cells**. *Advances in immunology* 2013, **120**:69-103.

447. Saha P, Geissmann F: **Toward a functional characterization of blood monocytes**. *Immunology and cell biology* 2011, **89**(1):2-4.

448. Serbina NV, Jia T, Hohl TM, Pamer EG: **Monocyte-mediated defense against microbial pathogens**. *Annual review of immunology* 2008, **26**:421-452.

449. Strauss-Ayali D, Conrad SM, Mosser DM: **Monocyte subpopulations and their differentiation patterns during infection**. *Journal of leukocyte biology* 2007, **82**(2):244-252.

450. Sunderkotter C, Nikolic T, Dillon MJ, Van Rooijen N, Stehling M, Drevets DA, Leenen PJ: **Subpopulations of mouse blood monocytes differ in maturation stage and inflammatory response**. *Journal of immunology* 2004, **172**(7):4410-4417.

451. Tacke F, Randolph GJ: **Migratory fate and differentiation of blood monocyte subsets**. *Immunobiology* 2006, **211**(6-8):609-618.

452. Yona S, Jung S: **Monocytes: subsets, origins, fates and functions**. *Current opinion in hematology* 2010, **17**(1):53-59.

453. Lee JS: **Heterogeneity of lung mononuclear phagocytes in chronic obstructive pulmonary disease**. *Journal of innate immunity* 2012, **4**(5-6):489-497.

454. Xiong Z, Leme AS, Ray P, Shapiro SD, Lee JS: **CX3CR1+ lung mononuclear phagocytes spatially confined to the interstitium produce TNF-alpha and IL-6 and promote cigarette smoke-induced emphysema**. *Journal of immunology* 2011, **186**(5):3206-3214.

455. Blusse van Oud Alblas A, Mattie H, van Furth R: **A quantitative evaluation of pulmonary macrophage kinetics**. *Cell and tissue kinetics* 1983, **16**(3):211-219.

456. Marques LJ, Teschler H, Guzman J, Costabel U: **Smoker's lung transplanted to a nonsmoker. Long-term detection of smoker's macrophages**. *American journal of respiratory and critical care medicine* 1997, **156**(5):1700-1702.

457. Hodge S, Hodge G, Ahern J, Jersmann H, Holmes M, Reynolds PN: **Smoking alters alveolar macrophage recognition and phagocytic ability: implications in chronic obstructive pulmonary disease**. *American journal of respiratory cell and molecular biology* 2007, **37**(6):748-755.

458. Gordon S, Crocker PR, Morris L, Lee SH, Perry VH, Hume DA: **Localization and function of tissue macrophages**. *Ciba Foundation symposium* 1986, **118**:54-67.

459. Wright JR: **Immunoregulatory functions of surfactant proteins**. *Nature reviews Immunology* 2005, **5**(1):58-68.

460. Lohmann-Matthes ML, Steinmuller C, Franke-Ullmann G: **Pulmonary macrophages**. *The European respiratory journal : official journal of the European Society for Clinical Respiratory Physiology* 1994, **7**(9):1678-1689.

461. Trapnell BC, Whitsett JA: **Gm-CSF regulates pulmonary surfactant homeostasis and alveolar macrophage-mediated innate host defense**. *Annual review of physiology* 2002, **64**:775-802.

462. Chen BD, Clark CR, Chou TH: **Granulocyte/macrophage colony-stimulating factor stimulates monocyte and tissue macrophage proliferation and enhances their responsiveness to macrophage colony-stimulating factor**. *Blood* 1988, **71**(4):997-1002.

463. Balbi B, Bason C, Balleari E, Fiasella F, Pesci A, Ghio R, Fabiano F: **Increased bronchoalveolar granulocytes and granulocyte/macrophage colony-stimulating factor during exacerbations of chronic bronchitis**. *The European respiratory journal* 1997, **10**(4):846-850.

464. Tibboel J, Post M: **Characterization Of Elastase-induced Emphysema In Mice: Lung Function**. *American journal of respiratory and critical care medicine* 2010, **181**:A5065.

465. Hu B, Jennings JH, Sonstein J, Floros J, Todt JC, Polak T, Curtis JL: **Resident murine alveolar and peritoneal macrophages differ in adhesion of apoptotic thymocytes**. *American journal of respiratory cell and molecular biology* 2004, **30**(5):687-693.

466. Hou HH, Cheng SL, Liu HT, Yang FZ, Wang HC, Yu CJ: **Elastase induced lung epithelial cell apoptosis and emphysema through placenta growth factor**. *Cell death & disease* 2013, **4**:e793.

467. Poole JA, Gleason AM, Bauer C, West WW, Alexis N, van Rooijen N, Reynolds SJ, Romberger DJ, Kielian TL: **CD11c(+)/CD11b(+) cells are critical for organic dust-elicited murine lung inflammation**. *American journal of respiratory cell and molecular biology* 2012, **47**(5):652-659.

468. Vlahos R, Bozinovski S, Hamilton JA, Anderson GP: **Therapeutic potential of treating chronic obstructive pulmonary disease (COPD) by neutralising granulocyte macrophage-colony stimulating factor (GM-CSF)**. *Pharmacology & therapeutics* 2006, **112**(1):106-115.

469. Fujii T, Hayashi S, Hogg JC, Mukae H, Suwa T, Goto Y, Vincent R, van Eeden SF: **Interaction of alveolar macrophages and airway epithelial cells following exposure to particulate matter produces mediators that stimulate the bone marrow**. *American journal of respiratory cell and molecular biology* 2002, **27**(1):34-41.

470. Qiu C, Li Y, Li M, Li M, Liu X, McSharry C, Xu D: **Anti-interleukin-33 inhibits cigarette smoke-induced lung inflammation in mice**. *Immunology* 2013, **138**(1):76-82.

471. Russell RE, Culpitt SV, DeMatos C, Donnelly L, Smith M, Wiggins J, Barnes PJ: **Release and activity of matrix metalloproteinase-9 and tissue inhibitor of metalloproteinase-1 by alveolar macrophages from patients with chronic obstructive pulmonary disease**. *American journal of respiratory cell and molecular biology* 2002, **26**(5):602-609.

472. Kang MJ, Homer RJ, Gallo A, Lee CG, Crothers KA, Cho SJ, Rochester C, Cain H, Chupp G, Yoon HJ *et al*: **IL-18 is induced and IL-18 receptor alpha plays a critical role in the pathogenesis of cigarette smoke-induced pulmonary emphysema and inflammation**. *Journal of immunology* 2007, **178**(3):1948-1959.

473. Lappalainen U, Whitsett JA, Wert SE, Tichelaar JW, Bry K: **Interleukin-1beta causes pulmonary inflammation, emphysema, and airway remodeling in the adult murine lung**. *American journal of respiratory cell and molecular biology* 2005, **32**(4):311-318.

474. Zhou R, Yazdi AS, Menu P, Tschopp J: **A role for mitochondria in NLRP3 inflammasome activation**. *Nature* 2011, **469**(7329):221-225.

475. Lommatzsch M, Cicko S, Muller T, Lucattelli M, Bratke K, Stoll P, Grimm M, Durk T, Zissel G, Ferrari D *et al*: **Extracellular adenosine triphosphate and chronic obstructive pulmonary disease**. *American journal of respiratory and critical care medicine* 2010, **181**(9):928-934.

476. Shaul ME, Bennett G, Strissel KJ, Greenberg AS, Obin MS: **Dynamic, M2-like remodeling phenotypes of CD11c+ adipose tissue macrophages during high-fat diet--induced obesity in mice**. *Diabetes* 2010, **59**(5):1171-1181.

477. Bystrom J, Evans I, Newson J, Stables M, Toor I, van Rooijen N, Crawford M, Colville-Nash P, Farrow S, Gilroy DW: **Resolution-phase macrophages possess a unique inflammatory phenotype that is controlled by cAMP**. *Blood* 2008, **112**(10):4117-4127.

478. Dalrymple H, Barna BP, Malur A, Malur AG, Kavuru MS, Thomassen MJ: **Alveolar macrophages of GM-CSF knockout mice exhibit mixed M1 and M2 phenotypes**. *BMC immunology* 2013, **14**:41.

479. Hodge S, Matthews G, Mukaro V, Ahern J, Shivam A, Hodge G, Holmes M, Jersmann H, Reynolds PN: **Cigarette smoke-induced changes to alveolar macrophage phenotype and function are improved by treatment with procysteine**. *American journal of respiratory cell and molecular biology* 2011, **44**(5):673-681.

480. Martinez FO, Gordon S: **The M1 and M2 paradigm of macrophage activation: time for reassessment**. *F1000prime reports* 2014, **6**:13.

481. Culpitt SV, Rogers DF, Shah P, De Matos C, Russell RE, Donnelly LE, Barnes PJ: **Impaired inhibition by dexamethasone of cytokine release by alveolar macrophages from patients with chronic obstructive pulmonary disease**. *American journal of respiratory and critical care medicine* 2003, **167**(1):24-31.

482. Kolaczkowska E, Kubes P: **Neutrophil recruitment and function in health and inflammation**. *Nature reviews Immunology* 2013, **13**(3):159-175.

483. Bennett CL, Clausen BE: **DC ablation in mice: promises, pitfalls, and challenges**. *Trends in immunology* 2007, **28**(12):525-531.

484. Probst HC, Tschannen K, Odermatt B, Schwendener R, Zinkernagel RM, Van Den Broek M: **Histological analysis of CD11c-DTR/GFP mice after in vivo depletion of dendritic cells**. *Clinical and experimental immunology* 2005, **141**(3):398-404.

485. Sapoznikov A, Jung S: **Probing in vivo dendritic cell functions by conditional cell ablation**. *Immunology and cell biology* 2008, **86**(5):409-415.

486. Ofulue AF, Ko M: **Effects of depletion of neutrophils or macrophages on development of cigarette smoke-induced emphysema**. *The American journal of physiology* 1999, **277**(1 Pt 1):L97-105.

487. Sica A, Mantovani A: **Macrophage plasticity and polarization: in vivo veritas**. *The Journal of clinical investigation* 2012, **122**(3):787-795.

488. Garofalo RS, Orena SJ, Rafidi K, Torchia AJ, Stock JL, Hildebrandt AL, Coskran T, Black SC, Brees DJ, Wicks JR *et al*: **Severe diabetes, age-dependent loss of adipose tissue, and mild growth deficiency in mice lacking Akt2/PKB beta**. *The Journal of clinical investigation* 2003, **112**(2):197-208.

489. Moreira AP, Hogaboam CM: **Macrophages in allergic asthma: fine-tuning their pro- and anti-inflammatory actions for disease resolution**. *Journal of interferon & cytokine research : the official journal of the International Society for Interferon and Cytokine Research* 2011, **31**(6):485-491.

490. Zaslona Z, Wilhelm J, Cakarova L, Marsh LM, Seeger W, Lohmeyer J, von Wulffen W: **Transcriptome profiling of primary murine monocytes, lung macrophages and lung dendritic cells reveals a distinct expression of genes involved in cell trafficking**. *Respiratory research* 2009, **10**:2.

491. Shay T, Kang J: **Immunological Genome Project and systems immunology**. *Trends in immunology* 2013, **34**(12):602-609.

492. Chaussabel D, Baldwin N: **Democratizing systems immunology with modular transcriptional repertoire analyses**. *Nature reviews Immunology* 2014, **14**(4):271-280.

493. Breuer K, Foroushani AK, Laird MR, Chen C, Sribnaia A, Lo R, Winsor GL, Hancock RE, Brinkman FS, Lynn DJ: **InnateDB: systems biology of innate immunity and beyond--recent updates and continuing curation**. *Nucleic acids research* 2013, **41**(Database issue):D1228-1233.

494. Boggild AK, Krudsood S, Patel SN, Serghides L, Tangpukdee N, Katz K, Wilairatana P, Liles WC, Looareesuwan S, Kain KC: **Use of peroxisome proliferator-activated receptor gamma agonists as adjunctive treatment for *Plasmodium falciparum* malaria: a randomized, double-blind, placebo-controlled trial**. *Clinical infectious diseases : an official publication of the Infectious Diseases Society of America* 2009, **49**(6):841-849.

495. Serghides L, Patel SN, Ayi K, Lu Z, Gowda DC, Liles WC, Kain KC: **Rosiglitazone modulates the innate immune response to *Plasmodium falciparum* infection and improves outcome in experimental cerebral malaria**. *The Journal of infectious diseases* 2009, **199**(10):1536-1545.

496. Olagnier D, Lavergne RA, Meunier E, Lefevre L, Dardenne C, Aubouy A, Benoit-Vical F, Ryffel B, Coste A, Berry A *et al*: **Nrf2, a PPARgamma alternative pathway to promote CD36 expression on inflammatory macrophages: implication for malaria**. *PLoS pathogens* 2011, **7**(9):e1002254.

497. Rowe JA, Claessens A, Corrigan RA, Arman M: **Adhesion of *Plasmodium falciparum*-infected erythrocytes to human cells: molecular mechanisms and therapeutic implications**. *Expert reviews in molecular medicine* 2009, **11**:e16.

498. Ho M, Hoang HL, Lee KM, Liu N, MacRae T, Montes L, Flatt CL, Yipp BG, Berger BJ, Looareesuwan S *et al*: **Ectophosphorylation of CD36 regulates cytoadherence of *Plasmodium falciparum* to microvascular endothelium under flow conditions**. *Infection and immunity* 2005, **73**(12):8179-8187.

499. Dondorp AM, Silamut K, Charunwatthana P, Chuasuwanchai S, Ruangveerayut R, Krintratun S, White NJ, Ho M, Day NP: **Levamisole inhibits sequestration of infected red blood cells in patients with falciparum malaria**. *The Journal of infectious diseases* 2007, **196**(3):460-466.

500. Idell S: **Coagulation, fibrinolysis, and fibrin deposition in acute lung injury**. *Critical care medicine* 2003, **31**(4 Suppl):S213-220.

H.A. Daniel Lagassé

5 N. Rose Street
Baltimore, MD 21224
(617) 549-4257
dlagasse@gmail.com

EDUCATION

2014 **Doctor of Philosophy (PhD)**
Johns Hopkins Bloomberg School of Public Health, Baltimore, MD
W. Harry Feinstone Department of Molecular Microbiology and Immunology
Dissertation: "*Elucidating the function and dynamics of resident and recruited macrophage populations in the lung.*"
Vaccine Science and Policy Certificate

2001 **Bachelor of Arts**
Middlebury College, Middlebury, VT
Molecular Biology and Biochemistry Major

RESEARCH EXPERIENCE

2007 – 2014 **Doctoral Candidate/Student**
Johns Hopkins Bloomberg School of Public Health, Baltimore, MD

Conducted doctoral thesis research in innate immune responses in the lung under the direction of Dr. Alan L. Scott.

- Investigated the role of inflammatory monocytes in limiting malaria-induced lung injury through the clearance of sequestered infected erythrocytes.
  - Examined the dynamics of inflammatory monocyte recruitment and acute lung injury following *Plasmodium* infection.
  - Demonstrated parasite uptake and clearance by activated inflammatory monocytes, not resident lung macrophages using a tdTomato fluorescent transgenic parasite.
  - Identified CCR2-deficient animals have defects in parasite clearance, elevated inflammatory cytokine expression and exacerbated lung injury.
  - Established adoptive transfer of wildtype bone marrow-derived monocytes into CCR2-deficient animals reduces malaria-associated lung damage.

- Elucidated the dynamics of resident lung macrophages during the progression of elastase-induced emphysema.
  - Demonstrated that elastase-mediated lung damage alters the dynamics and activation status of lung macrophages.
  - Revealed that a lung macrophage subpopulation proliferates locally following elastase-induced lung damage using *in vivo* lung-resident phagocytic cell labeling.

Instructed graduate students and post-doctoral fellows to use BD FACSCalibur and FlowJo analysis software.

Trained graduate students in multicolor flow cytometry, intracellular cytokine staining, immunofluorescence microscopy, isolation of primary cells from lungs and bone marrow, mammalian cell culture, molecular biology techniques, and *in vivo* mouse model techniques.

Contributed to NHLBI-funded program project grant "Mechanisms underlying chronic lung pathology"

2002 – 2007 **Senior Research Associate/Research Associate II/Research Associate I**
Archemix Corporation, Cambridge, MA

Therapeutic aptamer discovery and characterization as a member of the Aptamer Discovery group, including *in vitro* selection (SELEX), clone screening and characterization, minimization, and medicinal chemistry.

2005 – 2007 Senior Research Associate
- Discovered highly potent and nuclease resistant anti-NGF and anti-IgE aptamers to advance therapeutic pipeline.

2004 – 2005 Research Associate II
- Discovered and optimized first internal clinical candidate (ARC1779- anti-vWF).
- Participated in the initial ARC1779 IND submission to the FDA. ARC1779 was evaluated in Phase 1 safety (PK/PD) and in Phase 2 for Thrombotic Thrombocytopenia Purpura.
- Optimized aptamers for the anti-IgE and anti-IL-23 programs to advance therapeutic pipeline.

2002 – 2003 Research Associate
- Discovered highly specific anti-gp41 aptamers on the HIV vaccine (CD4 mimic) and HIV fusion inhibitor (anti-gp41) therapeutic programs.

2001-2002 **Research Technician II**
University of Vermont, Burlington, VT
- Characterized a *Salmonella* type III secreted effector (SifA) in a microbial pathogenesis laboratory.

2000 **Research Assistant**
Middlebury College, Middlebury, VT
- Characterized a *Streptococcus mutans* oxidative stress regulatory gene (*per*) in a microbial genetics laboratory.

TECHNICAL SKILLS

Cellular Biology/Cellular Microbiology:
multicolor flow cytometry; intracellular cytokine staining; immunofluorescence microscopy; mammalian cell culture; adoptive transfer of immune cells; subcellular fractionation

Small Mammal Research:
in vivo mouse models; primary cell isolation; intravenous, intraperitoneal, and subcutaneous injections; intranasal/intratracheal aspiration; bronchoalveolar lavage; bone marrow isolation; clodronate-liposome depletions; organ harvest; colony management

Genetic Analysis:
in vitro SELEX; RNA isolation; reverse transcription; PCR; TaqMan qPCR; chromosomal/plasmid DNA isolation; *in vitro* transcription; electroporation/transformation; Southern and Northern blotting

Protein Analysis:
ELISA; Western blotting; dot-blotting; SDS-PAGE; immunoprecipitation; immunoglobulin purification; Biacore 2000

Computational Analysis:
Flowjo; Prism; GenBank database; BioEdit; RNA Structure; Microsoft Office; Adobe Illustrator

TEACHING EXPERIENCE

Fall 2012 & 2013 **Teaching Assistant**
Johns Hopkins Bloomberg School of Public Health, Baltimore, MD
Principles of Immunology I & II
Infection, Immunology and Disease

- Held large group and one-on-one review sessions for 70+ student graduate level courses; grading

Fall 2009 - 2013 **Teaching Assistant**
Johns Hopkins Bloomberg School of Public Health, Baltimore, MD
Topics in Immunology I & II
- Prepared student presenters; facilitated group discussion and detailed analysis of current immunology literature in a journal-club style graduate level course; grading

RESEARCH FELLOWSHIPS AND GRANTS

AAI Predoctoral Trainee Abstract Award Recipient (2011)

Johns Hopkins Malaria Research Institute (JHMRI) Predoctoral Fellow (2010-2011)

The Otis and Calista Causey Fellowship for Immunology Recipient (2008)

Howard Hughes Medical Institute Summer Research Fellow – Middlebury College (Summer 1997, 2000)

Senior Work Fund Recipient - Middlebury College (2000-2001)

PUBLICATIONS

Patents

Aptamers to von Willebrand Factor and their uses as thrombotic disease therapeutics. Diener, J.L., and **Lagassé, H.A.D.** International Patent WO/2006/033854. Published March, 2006.

Nucleic acid ligands specific to immunoglobulin E and their use as atopic disease therapeutics. Cload, S., Diener, J.L., Keene, S.C., Kurz, M., **Lagassé, H.A.D.,** Marsh, H.N., and Sawhney, P. International Patent WO/2005/113813. Published December, 2005.

Aptamers to the human IL-12 cytokine family and their use as autoimmune disease therapeutics. Diener, J.L., Ferguson, A., Hamaguchi, N., Keene, S.C., **Lagassé, H.A.D.**, Sawhney, P., and Thompson, K. International Patent WO/2005/086835. Published September, 2005.

FDA Filings

ARC1779 Investigational New Drug (IND) application. Submitted to FDA.
Nonclinical study report: Affinity and specificity of ARC1779 binding to human vWF.

Peer-reviewed publications

Recruited monocytes are responsible for limiting malaria-induced lung injury through CD36-mediated clearance of sequestered infected erythrocytes. **Lagassé, H.A.D.** Anidi, I.U., Craig, J.M., and Scott A.L. (*in review*)

Inhibition of von Willebrand factor-mediated platelet activation and thrombosis by the anti-von Willebrand factor A1-domain aptamer ARC1779. Diener, J.L., **Lagassé, H.A.D.**, Duerschmeid, D., Merhi, Y., Tanguay, J.F., Hutabarat, R., Gilbert, J., Wagner, D.D., and Schaub, R. *J. Thromb. Haemost.* 2009, 7, 1155-1162.

The role of DNA base excision repair in the pathogenesis of *Salmonella enterica* serovar Typhimurium. Suvarnapunya, A. E., **Lagassé, H.A.D.**, and Stein, M.A. *Mol. Microbiol.* 2003, 48, 549-559.

Reduction and Anticancer Activity of Platinum(IV) Complexes. Choi, S., Filotto, C., Bisanzo, M., Delaney, S., **Lagassé, D.**, Whitworth, J.L., Jusko, A., Li, C., Wood, N.A., Willingham, J., Schwenker, A., and Spaulding, K. *Inorg. Chem.* 1998, 37, 2500-2504.

Abstracts

The dynamics of resident lung macrophage subpopulations following elastase challenge in mice. **Lagassé, H.A.D**., Craig, J.M., Scott, A.L., and Mitzner W. 2014 Annual Meeting of the American Thoracic Society, May 2014, San Diego, CA.

The dynamics and depletion of neutrophils in an elastase model of emphysema. Bradley, C.C., Craig, J.M., Limjunyawong, N., **Lagassé, H.A.D**., Mitzner, W., and Scott, A.L. 2014 Annual Meeting of the American Thoracic Society, May 2014, San Diego, CA.

Lung macrophages control malaria-induced pulmonary inflammation. **Lagassé, H.A.D.** and Scott, A.L. 98th Annual Meeting of the American Association of Immunologists, May 2011, San Francisco, CA.

The role of resident lung macrophages and recruited monocytes in the control of malaria-induced pulmonary inflammation. **Lagassé, H.A.D.** and Scott, A.L. 15th Annual Woods Hole Immunoparasitology Meeting, April 2011, Woods Hole, MA.

Discovery and evaluation of an anti-vWF aptamer for treatment of Acute Coronary Syndrome (ACS). **Lagassé, H.A.D.**, Merlino, P., Gilbert, M., Boomer, R.M., Fraone, J., Lewis, S.D., Makim, A., Benedict, C., Hutabarat, R., McCauley, T., Rottman, J.B., Marsh, H.N., and Diener, J.L. 2nd Annual Meeting of the Oligonucleotide Therapeutics Society, October 2006, New York, NY.

Aptamers that discriminate between IL-23 and IL-12 are specific inhibitors of IL-23 activity in vitro. Thompson, K.M., Ferguson, A., Killough, J., Horwitz, L.R., Sawhney, P., **Lagassé, H.A.D.**, Tang, W., Gilbert, M., Samikkannu, D., Diener, J., Cload, S.T., and Pendergrast, P.S. Drug Discovery Technology World Congress, August 2005, Boston, MA.

Lead optimization of an anti-IgE aptamer that inhibits IgE-mediated histamine release in vitro. Marsh, H.N., Zoltoski, A., Keene, S., Sawhney, P., **Lagasse, D**., Burmeister, P.E., Mills, K., Wang, C., Keefe, A.D., Wilson, C., Kurz, M., Rottman, J.B., Cload, S.T., Zhu, S., Thompson, K., Epstein, D., and Diener, J. Drug Discovery Technology World Congress, August 2005, Boston, MA.

Discovery and evaluation of an anti-vWF aptamer for treatment of Acute Coronary Syndrome (ACS). **Lagassé, H.A.D.**, Merlino, P., Gilbert, M., Killough, J., Mills, K., Boomer, R.M., Lewis, S.D., Makim, A., Benedict, C., McCauley, T., Rottman, J.B., Marsh, H.N., and Diener, J.L. Drug Discovery Technology European Congress, March 2005, London, England.

Cloning and characterization of putative peroxidases (*stpx* and *per*) in *Streptococci*. **Lagassé, D.**, Howard, K., and Spatafora, G.A. 101st American Society of Microbiology General Meeting, May 2001, Orlando, FL

REFERENCES

Available upon request